



**UNIVERSITÉ D'ABOMEY-CALAVI**

**Improvement and comparative assessment of a new  
hydrological modelling approach to catchments in  
Africa and the USA**

**Towards an application to ungauged catchments**

A thesis

*Submitted in fulfilment of the requirements for the degree*

*of*

**Doctor of Philosophy**

*at*

**The University of Abomey-Calavi, BENIN**

*In*

**Climate Change and Water Resources**

*by*

**GABA Olayèmi Ursula Charlène**

*Supervisors:*

**Prof. Abel Afouda** (University of Abomey-Calavi, BENIN)

**Prof. Dr. B. Diekrüger** (University of Bonn, GERMANY)

Institut National de l'Eau, WASCAL-GRP CC & Water Resources

January 2016



**Université d'Abomey-Calavi (UAC)**  
**Institut National de l'Eau (INE)**  
**WASCAL - GRP Climate Change and Water Resources**

No..../...../...../.....

**Improvement and comparative assessment of a new  
hydrological modelling approach to catchments in Africa and  
the USA**

Towards an application to ungauged catchments

A thesis

*Submitted in fulfilment of the requirements for the degree  
of*

**Doctor of Philosophy**

*In*

**Climate Change and Water Resources**

*by*

**GABA Olayèmi Ursula Charlène**

*Supervisors:*

**Prof. Abel Afouda (University of Abomey-Calavi, BENIN)**

**Prof. Dr. B. Diekkrüger (University of Bonn, GERMANY)**

Jury:

President: Prof. AGBOSSOU Euloge

Director: Prof. AFOUDA Abel

Examiner: Prof. DEGAN Gérard

Reviewer: Prof. LAWIN Emmanuel

January 2016

**Improvement and comparative assessment of a  
new hydrological modelling approach to  
catchments in Africa and the USA**

Towards an application to ungauged catchments

## ***DEDICATION***

*To my parents*

*Mr GABA Adimi Prudence*

*and Mrs GABA-ADJAGBA Gilberte*

*for their constant Love and support*

*'The Lord made the earth by his power; by his wisdom He created the world and stretched out the heavens. At his command the waters above the sky roar; he brings clouds from the ends of the earth. He makes lightning flash in the rain and sends the wind from his storeroom.'*

*Jeremiah 51:15-16 (The Holy Bible)*

*'I am a hydrologist. I know very well that my computer model is only a set of logical constructs implemented on some complex electronic hardware but I still think of the variables in the model as representing real water.'*

*Keith Beven, 2008*

## **ACKNOWLEDGEMENTS**

The research presented is this PhD dissertation entitled “Improvement and comparative assessment of a new hydrological modelling approach to catchments in Africa and the USA. Towards an application to ungauged catchments” was conducted at the Institut National de l’Eau (INE) at the University of Abomey-Calavi (UAC) in Bénin in the framework of the West African Science Service Center on Climate Change and Adapted Land Use (WASCAL)- Climate Change and Water Resources. This work was supervised by Professor Abel AFOUDA (University of Abomey-Calavi, Benin) and Professor Bernd DIEKKRÜGER (University of Bonn, Germany). This work was also technically supported by my tutor Dr. Eric Alamou (University of Abomey-Calavi, Benin). The research period extended from September 2012 to December 2015.

The study included an external stay of four months at the Department of Geography at University of Bonn in Germany within the Hydrological Research Group –HRG– under supervision of Professor Bernd DIEKKRÜGER.

This study would not have been possible without the help of a number of people and institutions that I would like to acknowledge here.

First and foremost, praises and thanks to God, the Creator, the Almighty, to whom I owe my very existence. For His showers of blessings throughout my research work to successful completion.

I would like to thank the German Federal Ministry of Education and Research (BMBF) for their financial support without which this thesis would not have been possible. It provided me with a monthly stipend and research funds to conduct the research, as well as enabled me to benefit from the collaboration with German and international scientists.

This research has been funded through the West African Science Service Center on Climate Change and Adapted Land Use (WASCAL). Many thanks to WASCAL headquarters in Accra, Ghana and its staff; to WASCAL in Benin, its Director Pr. Abel AFOUDA, its Coordinator Dr Julien ADOUNKPE and its staff for the assistance they provided us with for administrative and scientific matters.

I would like to express my deep gratitude to Pr. Abel AFOUDA, my supervisor, who guided me through the thesis with the determination of a 'lion'. He always pushed me forward so that I give more than what I thought I could, even in the most difficult moments. I always benefited from his support whenever needed.

I am grateful to Pr. Dr. Bernd DIEKKRÜGER, my co-supervisor; who 'enriched' my work by his questions, answers to my questions, pieces of advice and also through our discussions. He has been able to add to the scientific value of my research. I will not forget to mention that he welcomed me in his Laboratory in Bonn, Germany at the Hydrology Research Group (HRG) where I could work more closely with him but also with the wonderful team of researchers he gave me the opportunity to meet at his Laboratory. I acknowledge all the members of the group and especially Gero SETUP and Dr. Aymar BOSSA.

I would like to thank Dr. Eric Adéchina ALAMOU, my tutor; who guided me through my first steps in this thesis on the application of the Principle of Least in Hydrology. My PhD work is the continuity of his own one. He encouraged me when I needed to be encouraged and helped me through his advice.

I express my gratitude to my WASCAL colleagues especially Mr Jean HOUNKPE, Mr Félicien BADOU, Mrs Alice BONOU/FANDOHAN, Mr Eliézer BIAO and Mr Ganiyu OYERINDE for the help and support they gave me through discussions, giving and attending presentations and also for technical and moral assistance. I am also grateful to Dr. Arnaud ZANNOU and Maxime WUBDA from IRD-Cotonou who helped me in the collection of data.

I address special and warm thanks to my fiancé, Mr Karsène MEMEVEGNI for his unconditional love and his remarkable patience and support; my love and gratitude can hardly be expressed in words. And to his family for their encouragements.

I would like to thank my beloved parents Mr Adimi Prudence GABA and Mrs Gilberte GABA-ADJAGBA to whom this dissertation is dedicated, my brothers Ulrich GABA and Nathan GABA, my sister Marie-Bénédicte GABA, Mr GNANSOUNOU Eyrolles and my nephew GNANSOUNOU Kenzo. They have been a constant source of love, concern, support and strength all these years. I always knew that you believed in me and wanted the best for me.

## **ABSTRACT**

Assessing water resources is still an important issue especially in the context of climatic changes. Although numerous hydrological models exist, new approaches are still under investigation. In this context, we investigate a new modelling approach based on the Physics Principle of Least Action. A first version of a Least Action based hydrological model, in its deterministic version has already given very good results in simulating the Bétérrou catchment in the Ouémé basin, Benin. The thesis presents new hypotheses to go further in the model development with a view of widening its application. The improved version of the model MODHYPMA was applied on 21 subcatchments in Africa, in Bénin, Côte d'Ivoire, Ethiopia; and in the USA. Its performance was compared to two well-known lumped conceptual models, the GR4J and HBV models.

The model was successfully calibrated and validated; it showed a good performance in most catchments. The analysis revealed that the three models have similar performance and timing errors. But in contrary to other models used in this study, MODHYMA is subject to a less loss of performance from calibration to validation. The parameter uncertainties were analysed using the GLUE methodology. It is concluded that model uncertainties are higher during high flows and that uncertainty analysis should include the uncertainty of the discharge data. In order to explore the possible transferability of our model for ungauged basins studies, we then intended to investigate how model parameters could be estimated from the physical catchments characteristics. We relied on statistical methods applied on calibrated model parameters to deduce relationships between parameters and physical catchments characteristics. These relationships were further tested and successfully validated on gauged basins that were considered ungauged.

**Key words.** Rainfall Runoff modelling; Least Action Principle; Uncertainties; Stochastic differential equations; Climate Change; ungauged basins.

# **AMELIORATION ET ÉVALUATION COMPARATIVE D'UNE NOUVELLE APPROCHE DE MODELISATION HYDROLOGIQUE A DES BASSINS EN AFRIQUE ET AUX ETATS-UNIS. VERS UNE APPLICATION AUX BASSINS NON-JAUGÉS**

## **RÉSUMÉ**

L'évaluation des ressources en eau demeure une question importante en particulier dans le contexte du changement climatique. Bien que de nombreux modèles hydrologiques existent, de nouvelles approches sont toujours explorées. Dans ce contexte, nous proposons une nouvelle approche de modélisation basée sur le principe physique de Moindre Action. Une première version du modèle basé sur le principe de Moindre Action, en sa version déterministe a déjà donné de bons résultats dans la simulation du sous-bassin de Bétérou dans le bassin versant de l'Ouémé au Bénin. La présente recherche formule de nouvelles hypothèses afin d'aller plus loin dans le développement du modèle avec pour objectif d'en étendre son application. La version améliorée du modèle MODHYPMA a été appliquée à 21 sous-bassins en Afrique, au Bénin, Côte D'Ivoire, Éthiopie; et aux États Unis. Sa performance a été comparée à celle de deux modèles conceptuels globaux bien connus, GR4J et HBV.

Le modèle a été calibré et validé avec succès; il a montré une bonne performance pour la plupart des bassins. L'analyse montre que les trois modèles ont une performance similaire et des erreurs de décalage. Cependant, contrairement aux autres modèles mis en œuvre au cours de cette étude, MODHYMA subit une moindre perte de performance du calibrage à la validation. L'incertitude des paramètres a été analysée en utilisant la méthodologie GLUE. Nous concluons que l'incertitude du modèle est plus grande pendant la période des hautes eaux et que l'analyse d'incertitudes devrait inclure les incertitudes liées aux données de débit. Afin d'explorer la possible transférabilité de notre modèle aux bassins non-jaugés, nous avons essayé d'investiguer comment les paramètres du modèle pouvaient être estimés à partir des caractéristiques physiques des bassins. Nous nous sommes basés sur des méthodes statistiques appliquées aux paramètres calibrés afin de déduire des relations entre les paramètres et les caractéristiques

physiques des bassins. Ces relations ont été plus tard testées et validées avec succès sur des bassins jaugés mais qui ont été considérés comme non jaugés.

**Mots clefs.** Modélisation Pluie-Débit ; Principe de Moindre Action ; Incertitudes ; Equations différentielles stochastiques ; Changement Climatique; bassins non-jaugés.

## TABLE OF CONTENTS

<b>DEDICATION</b> .....	i
<b>ACKNOWLEDGEMENTS</b> .....	iii
<b>ABSTRACT</b> .....	vi
<b>RÉSUMÉ</b> .....	vii
<b>TABLE OF CONTENTS</b> .....	ix
<b>LIST OF FIGURES</b> .....	xii
<b>LIST OF TABLES</b> .....	xiv
<b>ABBREVIATIONS</b> .....	xvi
1- General Introduction .....	2
1.1- Background and problem statement .....	2
1.2- Research question and objectives.....	6
1.3- Structure of the thesis .....	6
2- River flow generation and hydrological modelling .....	9
2.1- Water cycle and river flow generation.....	9
2.2- Why do we need models?.....	13
2.3- How do we build models? And models classifications.....	15
2.4- The Principle of Least Action (PLA), an old concept but new in hydrological modelling .....	23
2.4.1- Introduction: classical approach of physics-based models .....	23
2.4.2- Action and Principle of Least Action in Physics .....	24
2.4.3- History of the principle.....	26
2.4.4- Application of the PLA in hydrology and the Noether's theorem .....	28
2.4.5- Conclusion: towards the application of the PLA in hydrology .....	30
2.5- Modelling approaches .....	32
2.5.1- The MODHYPMA .....	32
2.5.2- The GR4J model .....	34
2.5.3- The HBV model.....	39
3- Study Areas and Data .....	45
3.1- Geographical overview of Ouémé basin in Benin .....	45
3.1.1- Location .....	45
3.1.2- Climate .....	45
3.1.3- Geology, Geomorphology.....	48

3.1.4-	Soils .....	51
3.1.5-	Land use and land cover.....	51
3.2-	Geographical overview of Comoé River basin at Mbasso (Côte d’Ivoire) .....	55
3.3-	Geographical overview of Sore catchment (Ethiopia) .....	56
3.4-	Geographical overview of Lookout catchment (USA) .....	56
3.5-	Data.....	58
3.5.1-	Discharge data .....	58
3.5.2-	Precipitation data .....	58
3.5.3-	Potential Evapotranspiration (ETP) data .....	60
4-	Application of MODHYPMA.....	64
4.1-	Model calibration approach and Criteria of performance.....	64
4.2-	Model results.....	68
4.3-	Discussion and Conclusion .....	72
5-	Comparison of models .....	81
5.1-	Evaluation of performance .....	81
5.2-	Modelling results .....	81
5.3-	Discussion and Conclusion .....	89
6-	Sensitivity and uncertainty analyses of MODHYPMA.....	91
6.1-	Methodology: sensitivity index and local sensitivity assessment .....	91
6.2-	Results of the sensitivity analysis and discussion .....	92
6.3-	Sampling method for the uncertainty analysis.....	94
6.4-	Results of the uncertainty analysis and discussion.....	96
7-	Towards an application of MODHYPMA to ungauged catchments.....	101
7.1-	Methodology.....	102
7.1.1-	Data and determination of catchments physical characteristics (CPCs)..	102
7.1.2-	Multiple linear regression analysis.....	102
7.2-	Results and discussion .....	104
8-	General conclusion and perspectives.....	115
APPENDIX A.	EQUATIONS OF THE CRITERIA OF PERFORMANCE.....	135
APPENDIX B.	PARAMETER RESPONSE SURFACE FOR EACH PERFORMANCE CRITERION FOR BÉTÉROU (BENIN), 10 083 km <sup>2</sup> .....	137
APPENDIX C.	COMPARED HYDROGRAPHS, FLOW DURATION CURVES AND CRITERIA OF PERFORMANCE FOR MODHYPMA, GR4J & HBV .....	141

APPENDIX D. SENSITIVITY AND UNCERTAINTY ANALYSES RESULTS .....166  
PUBLICATIONS.....178  
PUBLICATION 1.....179  
PUBLICATION 2.....180  
ARTICLE SUBMITTED TO THE *HYDROLOGICAL SCIENCES JOURNAL* .....181

**LIST OF FIGURES**

*Figure 2-1: Precipitation partitioning (From Mujumdar & Nagesh Kumar, 2012)..... 9*

*Figure 2-2: Water cycle from AghaKouchak (2013) ..... 10*

*Figure 2-3: River flow generation pathways..... 13*

*Figure 2-4: A schematic outline of the steps in the modelling process (From Beven, 2012) 15*

*Figure 2-5: Example of a thrown ball (From (Roberts, 2003))...... 25*

*Figure 2-6: Possible paths  $x(t)$ . Picture from Manton (2013) ..... 26*

*Figure 2-7: Schematic structure of GR4J model (Perrin et al. 2003). ..... 35*

*Figure 2-8: Schematic structure of HBV model (Seibert 2005). ..... 40*

*Figure 3-1: Location of sub-catchments of the Ouémé River basin. .... 46*

*Figure 3-2: Climate diagram station Parakou, mean rainfall values for 1961–1990 (from Hiepe (2008))...... 47*

*Figure 3-3: Map of the geology in the Ouémé catchment from (El-Fahem & Kocher, 2008) ..... 49*

*Figure 3-4: Landscape units in Benin (Schönbrodt & Giertz, 2008)..... 50*

*Figure 3-5: Distribution of soil types in Benin from (Giertz & Hiepe, 2008). ..... 52*

*Figure 3-6: Land cover and land use map of the Ouémé catchment with some example pictures. .... 54*

*Figure 3-7: Location of Mbasso catchment (74 900 km<sup>2</sup>) in Comoé basin (Côte d’Ivoire) adapted from (Chantraine & Dufour, 1983) ..... 55*

*Figure 3-8: Location of Sore catchment (1711 km<sup>2</sup>, Ethiopia), DEM, climate and gauging stations from (Kebede et al., 2014). ..... 57*

*Figure 3-9: Location of Lookout catchment (62 km<sup>2</sup>, USA) DEM, climate and gauging stations (Wikipedia). ..... 57*

*Figure 4-1: Box plot of the criteria of performance for MODHYPMA. Crossbar: Median; Circle: Mean; length of box: interquartile range (25th and 75th percentiles); tails: furthest values within the whisker length(length of the interquartile range); Red + sign : Outliers. .... 69*

*Figure 4-2: Application of MODHYPMA to Bétérou catchment (10 083 km<sup>2</sup>) in calibration. .... 73*

*Figure 4-3: Application of MODHYPMA to Bétérou catchment (10 083 km<sup>2</sup>) in validation.74*

*Figure 4-4: Flow duration curves in the Bétérou catchment (10 083 km<sup>2</sup>) in calibration... 75*

*Figure 4-5: Flow duration curves in the Bétérou catchment (10 083 km<sup>2</sup>) in validation. ... 75*

*Figure 4-6: Application of MODHYPMA to Lookout Creek catchment (USA), 62 km<sup>2</sup> in calibration. .... 76*

*Figure 4-7: Application of MODHYPMA to Lookout Creek catchment (USA), 62 km<sup>2</sup> in validation. .... 77*

*Figure 4-8: Flow duration curves in the Lookout Creek catchment (USA), 62 km<sup>2</sup> in calibration. .... 78*

*Figure 4-9: Flow duration curves in the Lookout Creek catchment (USA), 62 km<sup>2</sup> in validation. .... 78*

*Figure 5-1: Compared box plot of the NSE in calibration and validation for the three models (MODHYPMA, GR4J and HBV). Crossbar: Median; Circle: Mean; length of box: interquartile range (25th and 75th percentiles); tails: furthest values within the whisker; Red + sign : Outliers. .... 84*

*Figure 5-2: Application of a) MODHYPMA, b) GR4J and c) HBV to Bétérou catchment (10 083 km<sup>2</sup>) in calibration. .... 86*

*Figure 5-3: Application of a) MODHYPMA, b) GR4J and c) HBV to Bétérou catchment (10 083 km<sup>2</sup>) in validation. .... 87*

*Figure 5-4: Compared flow duration curves in the Bétérou catchment (10 083 km<sup>2</sup>). .... 88*

*Figure 6-1: Sensitivity analysis for MODHYPMA parameters with regard to the total runoff for Bétérou (10 083 km<sup>2</sup>). .... 93*

*Figure 6-2: The dotted plot map of the parameters versus NSE criterion for discharge simulation on Bétérou Catchment (10 083 km<sup>2</sup>). .... 98*

*Figure 6-3: 90% confidence interval of daily runoff due to parameter uncertainty calculated by GLUE method with threshold of 0.6 on Bétérou Catchment (10 083 km<sup>2</sup>). .... 98*

*Figure 7-1: Predicted vs. Calibrated model parameters with the associated 95% confidence interval. .... 109*

*Figure 7-2: Observed and simulated discharge using the regression-based parameter for Donga Pont (586 km<sup>2</sup>) ..... 111*

*Figure 7-3: Observed and simulated discharge using the regression-based parameter for Cote 238 (3058 km<sup>2</sup>) ..... 111*

*Figure 7-4: Observed and simulated discharge using the regression-based parameter for Savè (23486 km<sup>2</sup>), period 1 ..... 112*

*Figure 7-5: Observed and simulated discharge using the regression-based parameter for Savè (23486 km<sup>2</sup>); period 2 ..... 112*

**LIST OF TABLES**

Table 2-1 : Models typology ..... 20

Table 2-2: HBV Model parameters and feasible ranges (From (Seibert and McDonnell 2010)) ..... 43

Table 3-1: List of the Beninese stations for the study..... 59

Table 3-2: List of the other stations for the study. .... 60

Table 4-1: Comparative feaures of Manual-Expert and Automatic calibration (from (Duan *et al.*, 2003))...... 64

Table 4-2: Overview of the results obtained from the model runs..... 70

Table 4-3: Comments about MODHYPMA performance. .... 71

Table 5-1: Overview of the results obtained from the full split sample test calibration-validation for all three models. Calibration was performed on sub-period 1 and validation on sub-period 2 and then calibration on sub-period 2 and validation on sub-period 1. .... 82

Table 6-1:Classification of sensitivity index. .... 92

Table 6-2:Sensitivity indexes computed with regard to the NSE criterion. .... 92

Table 6-3: Results of the Uncertainty Analysis..... 97

Table 7-1: Catchment Physical Features accounted for in this study .....103

Table 7-2: Modelling results and calibrated parameters involved in the multiple regression analysis. ....104

Table 7-3: Physical catchment properties as computed for the sub-catchments . .....106

Table 7-4: Matrix of Correlation between the calibrated parameters vs. CPCs with respect to a non-collinearity condition.....107

Table 7-5: Best parameter model derived from the multiple regression analysis .....107

Table 7-6: Results of the modelling using parameters calculated from the multiple regression analysis for Donga Pont ; Cote 238 and Savè .....110

## LIST OF PHOTOGRAPHS

Photo 1: Partial view of the Source of the Ouémé river in Copargo .....	1
Photo 2: Partial view of the Térou river bridge- Cote 238 station (135 km).....	8
Photo 3: View of the evaporation pan at the synoptic station of Parakou .....	44
Photo 4: Collection of water levels data at Borigourou station (1607 km <sup>2</sup> ) .....	63
Photo 5: Collection of water levels data at Borigourou station (1607 km <sup>2</sup> ) .....	80
Photo 6: Partial view of the Wèwè river (261 km <sup>2</sup> ).....	90
Photo 7: Gauged station of Aguimo (396 km <sup>2</sup> ) .....	100
Photo 8: Partial view of the Térou river nearby Saramanga (135 km).....	114

## ABBREVIATIONS

90PPU	90 percent prediction uncertainties
APB	Absolute Percent Bias
APBIAS	Absolute Percent Bias
ASECNA	Agence pour la Sécurité de la Navigation Aérienne
BMBF	Bundesministerium für Bildung und Forschung/ German Federal Ministry of Education and Research
CPC	Catchments physical characteristics
DEM	Digital elevation model
DG-Eau	the General Water Direction of Benin (Direction Nationale de l'Eau)
ETP	Potential evapotranspiration
GHGs	Greenhouse Gases
GLUE	Generalised Likelihood Uncertainty Estimation
GR4J	Génie Rural à 4 paramètres Journalier
HBV	Hydrologiska byråns vattenavdelning
HRG	Hydrology Research Group
IMPETUS	An Integrated Approach to the Efficient Management of Scarce Water Resources in West Africa
INE	Institut National de l'Eau
INRAB	Institut National de la Recherche Agricole du Bénin
IPCC	The Intergovernmental Panel on Climate Change
IRD	Research Institute for Development (Institut de Recherche pour le Développement)
IWRM	Integrated Water Resources Management
KGE	Kling Gupta Efficiency

MODHYPMA	<u>Modèle Hydrologique</u> basé sur le <u>Principe de Moindre Action</u>
NSE	Nash-Sutcliffe Efficiency
OBEMINES	Office Béninoise des MINES
PB	Percent Bias
PBIAS	Percent Bias
PDE	Partial Differential Equations
PLA	Principle of Least Action
POWER	<b>Planner Oriented</b> evaluative <b>Watershed</b> model for <b>Environmental</b> and socio-economic <b>Responses</b>
PUB	Prediction in Ungauged Basins
R <sup>2</sup>	Coefficient of determination
SRTM	Shuttle Radar Topography Mission
SWAT	Soil Water Assessment Tool
UAC	Université d'Abomey-Calavi
UHP-HRU	Uni- versal Hydrological Program – Hydrological Response Unit is a conceptual semi-distributed model
USA	United States of America
VIF	Variable Inflation Factor
WASCAL	West African Science Service Center on Climate Change and Adapted Land Use
WaSiM	Water Balance Simulation Model
WR <sup>2</sup>	Weighted R <sup>2</sup>
WR <sup>2</sup>	Weighted coefficient of determination
WWAP	United Nations World Water Assessment Programme

## GENERAL INTRODUCTION



**Photo 1: Partial view of the Source of the Ouémé river in Copargo**

## 1- General Introduction

### 1.1- Background and problem statement

It is not to be demonstrated that water is essential for life. It is required not only for drinking, sanitation, hygiene, health but also for agriculture, livestock, fishery, energy, industry, transport, etc... Not to mention that water is essential for ensuring the integrity and sustainability of the Earth's ecosystems (United Nations World Water Assessment Programme (WWAP), 2003). The fact that water is necessary to sustain life is not in dispute. And yet, universal access to water is still unresolved (Gleick, 2003). Its availability is even becoming a more crucial issue. Many reasons can explain this aggravation, among which climate change. Climate change can be defined as a change in the state of the climate that can be identified (e.g. using statistical tests) by changes in the mean and/or the variability of its properties, and that persists for an extended period, typically decades or longer (IPCC, 2007). This persistent change in the climate may be due to natural climatic processes, or to human activities affecting the composition of the atmosphere (mainly the concentrations of Greenhouse Gases called GHGs) or the land use (McCluskey & Qaddumi, 2011).

Because of the very strong connection between global warming and the hydrologic cycle, climate change has a great impact on the availability and the variability of water resources especially in the tropical zone (Afouda *et al.*, 2001, Druyan, 2011). An intensification (or acceleration) of the water cycle should be expected (Huntington, 2006).

We are already facing an important spatial and temporal variability of rainfall. And this has a huge impact on discharges and consequently on water resources. As indicated by Lawin & Afouda (2011), Speth *et al.* (2010) and many others the West African region suffered a decrease of 20% in precipitation during the period 1971 – 1990 in comparison to the period 1950 – 1970, causing a decrease of about 40% in the runoff during the same period over Benin. Water scarcity will

increasingly have the potential to constrain food production growth, with adverse impacts on food security and human well-being (Thornton & Herrero, 2010). The authors emphasize that climate change will exacerbate many of these trends, with direct effects on agricultural yields, water availability, and production risk. Christoph *et al.* (2008) point out that this situation is aggravated by increasing water demand, mainly due to high population growth which finally results in a dramatic reduction of the per capita water availability. All these factors in turn affect the socio-economic development (Aggarwal & Singh, 2010). That is why adaptation is key (Brookes *et al.*, 2010). Appearing as a response, adaptation is defined by the IPCC (2007) as initiatives and measures to reduce the vulnerability of natural and human systems against actual or expected climate change effects. We can add that adaptation contributes to the moderation of harm and possibly exploits beneficial opportunities of climate change. Nevertheless a successful adaptation cannot be achieved without the improvement of water management and the improvement of the knowledge on the water resources.

Therefore it is obvious that the need for a better assessment of water resources is now more crucial in order to implement a sustainable Integrated Water Resources Management (IWRM) and adapt to climate change. This can be done through the use of tools like hydrological models. The idea is supported by Bormann (2005a) who asserts that the prediction of future water fluxes under changing environmental conditions requires the use of hydrological models. Alamou (2011) notes that while researchers need models to improve their scientific knowledge of processes, engineers need them for operational purposes. More importantly, water resource managers require information from models to help decision makers in their task.

Many hydrological models have been applied on Ouémé subcatchments like the conceptual lumped model GR4J reported in Lawin *et al.* (2011), the conceptual distributed model UHP-HRU (Bormann, 2005b, Cornelissen *et al.*, 2013, Giertz *et*

*al.*, 2006, 2012), the semi-distributed model POWER (Braud *et al.*, 2001), the semi-distributed model SWAT (Bossa *et al.*, 2012, Cornelissen *et al.*, 2013), and the distributed model WaSiM (Cornelissen *et al.*, 2013). In contrast to those models, the model based on the Least Action Principle is based on a physics principle which is here applied in hydrology.

The classical physics-based models use the laws of conservation of mass and conservation of momentum and apply them to hydrology to determine equations describing the characteristics of water flow at the scale of the grid or the catchment. Often, equations used to describe processes occurring at the point scale are inadequately used for larger scales. Typically, the classical approach applies the well-known small-scale theories such as Darcy's law, Richards Equation and Saint-Venant equations. As commented by Beven (2012) and many others the validity of Darcy's law falls into a limited range of scales, which are all smaller than the normal element scale of a rainfall-runoff model. The author recalls that a simple averaging from local to catchment scale in the application of the Darcy and Richards equation is physically wrong given the nonlinearity inherent in their formulation and the heterogeneity and complexity of soil properties (Beven, 2012). This opinion is shared by Wheater *et al.* (2013) who gave some examples and argued, in addition, that the parameters may not be measurable at the scales of interest for application. Moreover, because of the lack of relevant theory and supporting data, physics-based hydrological modelling sometimes neglect important processes like macropore flow despite its ubiquity (Wheater *et al.*, 2013). According to McDonnell *et al.* (2007), the difficulty lies in large scales which are characterised by the heterogeneities of the soil, the non-linearity of hydrological processes and their interactions between spatial scales. This results in 'heavily overparameterized' models in which the same final output can be obtained from various parameter values combinations causing a large degree of predictive uncertainty (Beven, 2000). That is why the concept of 'equifinality' has been introduced in hydrology. Despite the reluctance of many

hydrologists to accept this concept, one has to recognize that “there are many acceptable representations (both parameter sets and model structures) that cannot be easily rejected and that should be considered in assessing the uncertainty associated with predictions” (Beven, 2006). Representations depend both on parameter sets and model structures (Beven, 2012). Furthermore, the physically-based distributed models are supposed to allow the a priori determination of models parameters for prediction in ungauged basins but this is not generally the case.

Given all these limitations, wouldn't it be better to approach hydrological systems in a different way from trying to describe all the heterogeneities of the system? Exploring new hydrological theories based on scaling or organizing principles that might underlie the heterogeneity and complexity rather than relying only on theories which try to further prescribe this heterogeneity and describe the resulting process complexity in ever greater detail? Because the more we explore, the more heterogeneous and complex nature appears to be, and the modelling of such complexity will results in more complex models very difficult to implement.

The before mentioned problems and the associated questions were reason for Afouda *et al.* (2004), Afouda & Alamou (2010), Alamou (2011) to initiate a research about the Principle of Least Action and to develop a hydrological model based on this Principle. For management purpose often only total discharge is required, so lumped models are still used and necessary. Therefore a lumped version of the model was proposed. This daily lumped rainfall-runoff model, called MODHYPMA (Modèle Hydrologique basé sur le Principe de Moindre Action) has been applied on Bétérou catchment (about 10 000 km<sup>2</sup>) in the Ouémé basin and has shown very good results (Alamou, 2011). Nevertheless, is this one result sufficient to conclude about the applicability of this model? Can it be considered a promising alternative to the more classical approaches based on Newtonian Physics?

## 1.2- Research question and objectives

These considerations were combined into the following central research question:

*'What is the applicability of optimality principles-based models for water resources estimation and Prediction in Ungauged Basins?'*

And more typically for this study, we intend to test the applicability of MODHYPMA for the evaluation of water resources on the one hand and Prediction in Ungauged Basins on the other hand.

To address this objective a number of specific objectives have been identified:

- To go further in the development of the model and its application to catchments of various sizes (from smaller to larger spatial scale) under various climate conditions ;
- To analyze its performance, to compare the results with two other modelling approaches;
- Then to perform a sensitivity analysis and uncertainty analysis;
- And finally to explore the possible transferability for ungauged basins studies.

## 1.3- Structure of the thesis

This thesis is structured in eight (8) chapters. In **Chapter 1**, the scientific background as well as the research objectives in this study are presented.

**Chapter 2** addresses a description of river flow generation processes and a classification of models. Then the various modelling approaches used in the study are presented with a specific focus on the principle of Least Action, how it has been applied in other disciplines in Physics and how now we intend to implement it in hydrology.

In **Chapter 3**, the study areas which are the Ouémé river basin in Benin with regard to Savè outlet (23 488 km<sup>2</sup>), the Mbasso catchment in Côte d'Ivoire (74 900 km<sup>2</sup>); the Sore catchment in Ethiopia (1711 km<sup>2</sup>); the Léguer catchment

in France; the Lookout catchment in the USA (62 km<sup>2</sup>) are described particularly in terms Climate, Geology, Geomorphology, Soils, Land use and Land cover. Data used in this study are also presented in that section.

**Chapter 4** presents and discusses the results of the analysis of MODHYPMA and then **Chapter 5** presents the comparison of the results from the three models. **Chapter 6** addresses the sensitivity and uncertainty analyses performed for MODHYPMA. **Chapter 7** tests the MODHYPMA for its application to ungauged basins. Finally **Chapter 8** concludes and reports on the perspectives to this study. References and appendices are further presented at last.

# 2

## RIVER FLOW GENERATION AND HYDROLOGICAL MODELLING



Photo 2: Partial view of the Térou river bridge- Cote 238 station (135 km)

## 2- River flow generation and hydrological modelling

### 2.1- Water cycle and river flow generation

The radiant energy coming from the sun is the driving force of the natural circulation of water (Oki & Kanae, 2006). This results in evaporation and transfer of water vapour in the atmosphere. When certain conditions are met, water vapour is transformed again into liquid water (through the condensation process) to form clouds. To the favour of particular atmospheric conditions, this water is precipitated under the form of rain or snow (temperate climates or at very high elevations). In tropical climates, water generally precipitates as rain. After precipitation falls, it is partitioned into different components including: channel flow; overland flow; unsaturated flow; groundwater flow; soil moisture storage; surface storage; infiltration; interception and evapotranspiration (Mujumdar & Nagesh Kumar, 2012). Figure 2-1 shows this partitioning.

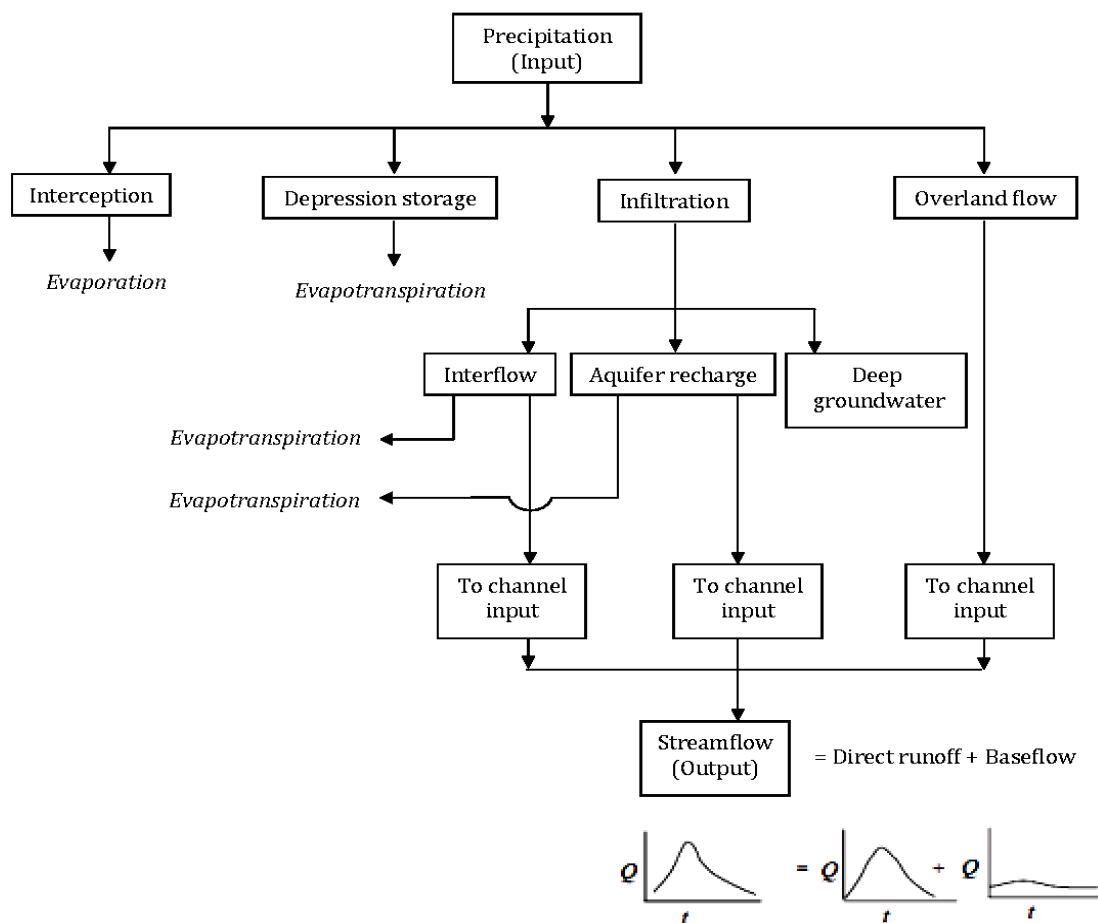


Figure 2-1: Precipitation partitioning (From Mujumdar & Nagesh Kumar, 2012)

When rain falls, one part is intercepted by the vegetation and may return to the air: this is *interception*. The remaining part reaches the ground where a part may be stored in depressions over the surface and may evaporate again (through plant *transpiration* or direct *evaporation*); another portion circulates over the land surface towards rivers (*channel flow* and *overland flow*) by mechanisms called runoff generation pathways and the rest circulates beneath the land (*unsaturated flow*; *groundwater flow*) by *infiltration* and *deep percolation*. All these processes above described are known as the water cycle and are schematized in Figure 2-2.

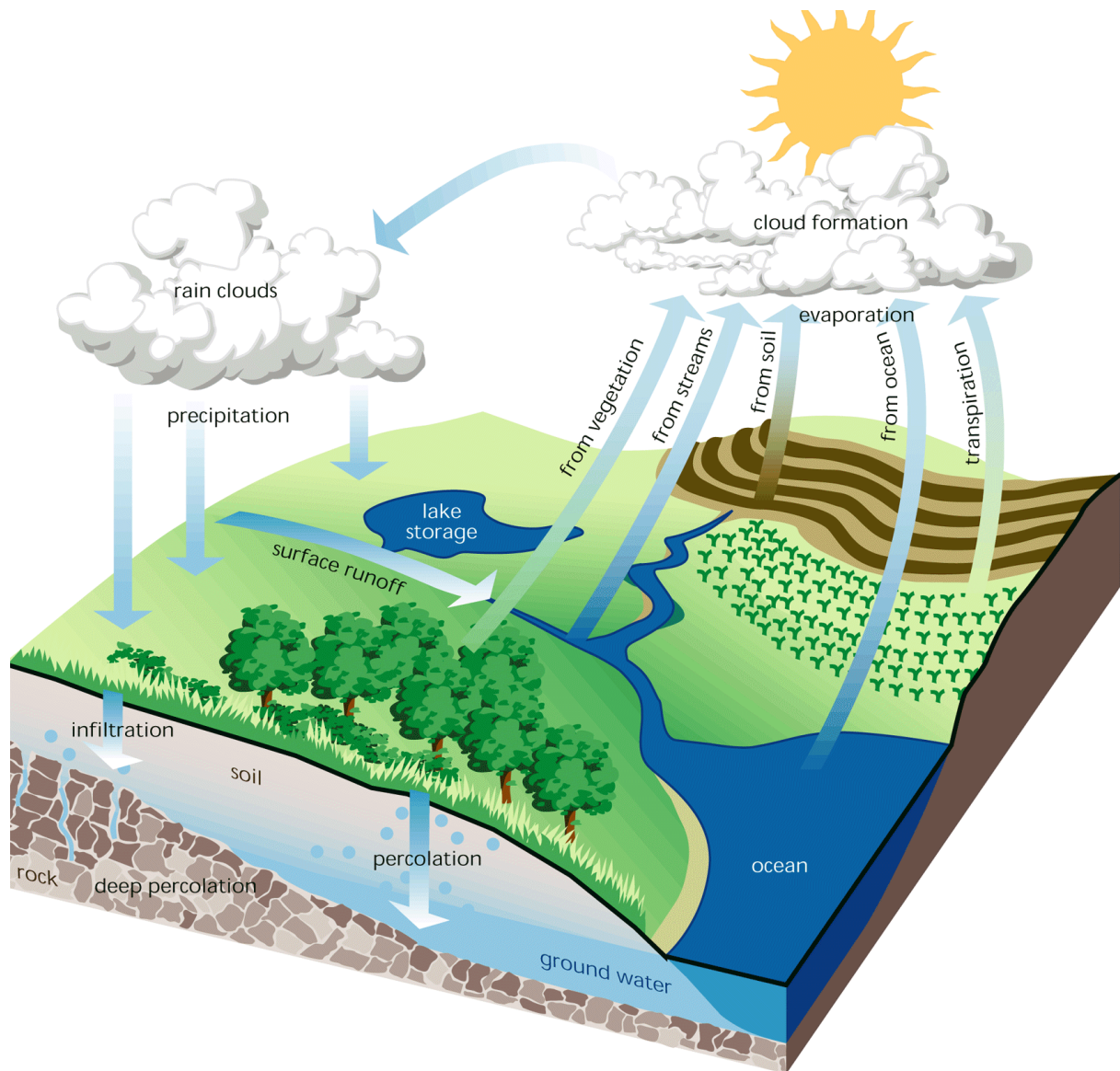


Figure 2-2: Water cycle from AghaKouchak (2013)

The water that falls over a vegetation canopy is partitioned in three (3) separate modes of movement identified by Tabacchi *et al.* (2000): *throughfall*, *stemflow* and *interception loss*. *Throughfall* is the water that falls to the ground either directly, through gaps in the canopy, or indirectly, having dripped off leaves, stems or branches. This mode of movement is controlled by the canopy coverage for an area. *Stemflow* is the rainfall that is intercepted by stems and branches and flows down the tree trunk into the soil. Although this type of flow may be negligible, it can act as a rapid conduit of water sending a significant pulse into the soil water because it occurs from a larger surface (canopy area) to a smaller one (the base of the plant or tree) and it is possible for the water to rapidly enter the soil through flow along roots and other macropores surrounding the root structure (Marin *et al.*, 2000). *Interception loss* in the contrary of the two above described movements is intercepted by the vegetation and returned to the air. It depends both on the density of the vegetation and intensity of the rainfall. Interception losses are said to be usually larger when the precipitation events are of moderate intensity and longer duration, than when they occur in the form of short intense bursts and downpours (Crockford & Richardson, 2000).

The water that falls on the ground flows over the surface and through the soil. As mentioned by Davie (2008), Horton was one of the earliest researchers to work on how overland flow occurs and to express the concept of hillslope hydrology based on the idea that the storm hydrograph is made up of rainfall in excess of the infiltration capacity of the soil. This is what we call *infiltration excess (or Hortonian) overland flow*. Overland flow may also occur on soils with high infiltration capacities. This is the case when the soil becomes saturated. In that case, we speak of *saturation overland flow*. The saturation of the soil may be due to the downslope flow within a hillslope and rain falling on saturated areas and it is more likely to observe this kind of flow in relatively shallow soils overlying an impermeable base and where there are convergent flow lines into the hillslope hollows or in areas immediately adjacent to the stream (Davie, 2008, Shaw *et al.*, 2011). We can also speak of the occurrence of saturated areas where the soil is

not completely saturated. We observe such particularities when the saturation is built up above a soil horizon of lower permeability.

Nevertheless overland flow is not the only type of flows occurring at the catchment scale; we also have *subsurface flow*. It can be defined as the displacement of water through the unsaturated zone. It appears when the lateral hydraulic conductivity is far greater than the vertical conductivity (Uchida *et al.*, 2001). When stored water is displaced to the river by the infiltration of the rainwater we speak of '*translatory or piston flow*'. Another type of subsurface flows is the *return flow* which is actually a component of the saturation overland flow. This return flow is provided by some subsurface water that had been forced back on to the surface through a seepage face. Water that infiltrated the soil on a slope portion of a hill water may flow laterally through the soil and exfiltrate (flow out of the soil) closer to a channel. In very heterogeneous soils, it is possible to observe zones of higher permeability: it is the case of macropores such as cracks, root holes or wormholes. As indicated in the term 'macropores', they are pores that are larger than usual ones: typically with a diameter greater than 3 mm. Their existence in soil matrix gives pathways to subsurface flow to quickly reach the stream because they can transport the bulk of the flow with a minimum contribution of the soil matrix (Blöschl & Sivapalan, 1995). Bunting (1961 quoted by (Shaw *et al.*, 2011)) calls these preferential subsurface pathways as *percolines* and consider that they are a subsurface extension of the dendritic (tree-like) channel network. Nevertheless there is still no general consensus about the evidence of macropores networks.

Groundwater may also contribute to river flow and vice-versa. If there is a connection between the stream bed and groundwater (contact zone) the groundwater may contribute to the streamflow as the water table is high; while when the water table is low the stream may contribute to the groundwater. Base flow is essentially contribution of water from groundwater. Finally the water that reaches the stream is driven to the river through a channel network. The summary is presented in Figure 2-3.

All these processes are part of one continuous cycle that moves water around the globe. They are not mutually exclusive since they might occur in different events in the same catchment, or in the same event in different places on the catchment, depending on the rainfall intensities; prior wetness of the catchment (antecedent conditions); topography of the hillslopes; type, structure and heterogeneity of the soil, regolith and rock; existence of percolines; channel density; etc... (Shaw *et al.*, 2011). The authors noted that land management practices and urbanisation have affected the nature of the river flow generation processes but hopefully in many cases we are only interested in predicting river flow, and do not need to worry too much about the water pathways.

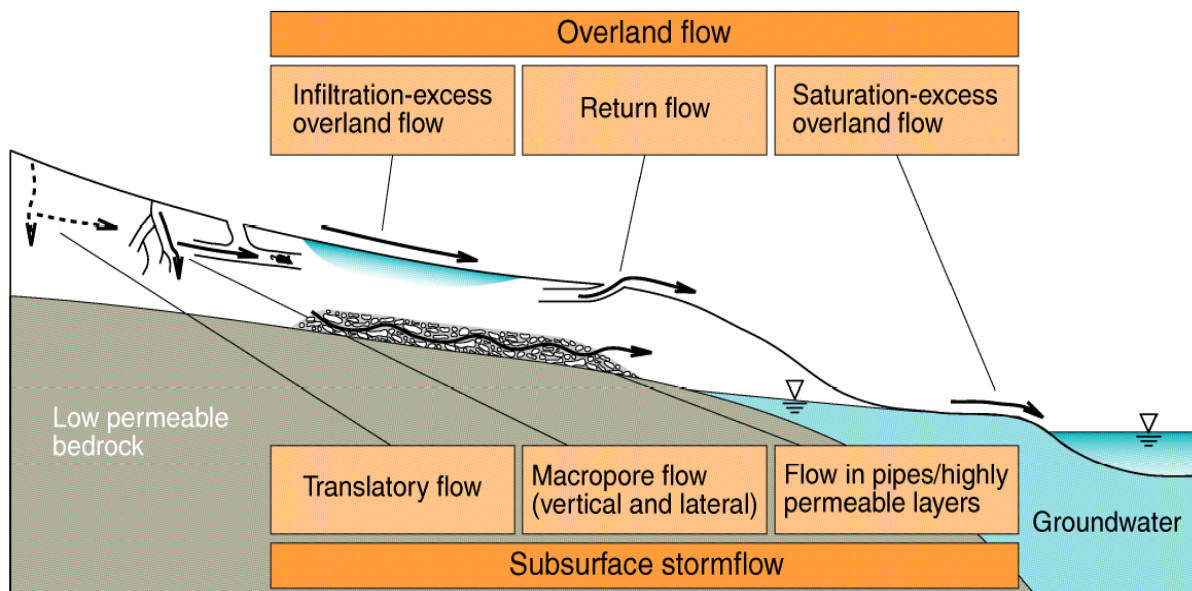


Figure 2-3: River flow generation pathways

### 2.2- Why do we need models?

Models are tools developed in order to represent reality. Mulligan & Wainwright (2004) define them as being abstractions of reality, of the processes of nature. Leconte (2010) sees a model as a set of mathematical equations that represent the state of the catchment and the evolution of the water cycle in relation to specified meteorological conditions. Models are useful both for research and operational purposes. Typically models help in understanding, water resources

planning, flood protection, mitigation of contamination, scenario analysis, prediction, uncertainty analysis, decision making, design, optimization, control, etc. Beven (2012) identifies the limitations of hydrological measurement techniques as the main reason of modelling.

In fact, current techniques do not allow us to measure everything we would like to know about hydrological systems because of the limited range of measurement techniques and the limited range of measurements in space and time. Models also serve as a means of extrapolating from those available measurements in both space and time, particularly to ungauged catchments (where measurements are not available) and into the future (where measurements are not possible) to assess the likely impact of future hydrological, climatic or environmental change and the impact of modern anthropogenic factors on the hydrological system (Beven, 2012, Yu, 2002) or into the past where there are longer periods of rainfall available than there are discharge measurements (Shaw *et al.*, 2011).

These extrapolation and prediction are useful for decision making. In addition to these practical purposes, much rainfall–runoff modelling is also carried out purely for research purposes as a means of formalising knowledge about hydrological systems. Researchers may wish to test a particular representation of the processes controlling how a catchment response works before using a model structure for a wider range of applications (Grayson & Blöschl, 2000).

Furthermore, modelling is needed because it will be costly to sample each field or to monitor each stream segment in a large watershed.

Nevertheless, some authors give a precision which is worth being mentioned here : “Modelling is not an alternative to observation but, under certain circumstances, can be a powerful tool in understanding observations and in developing and testing theory” (Mulligan & Wainwright, 2004).

### 2.3- How do we build models? And models classifications

The 'how' question finds an answer in the 'why' question. In fact, many authors agree to say that a model should necessarily have specific purposes according to which it will be built. This statement is true in the sense that a model is an abstraction of real processes and for a given catchment it may be advisable to adopt different formulations depending on the objectives of the analysis (Brutsaert, 2005). The building of the model will then depend on the processes we would like to represent or to mainly account for. Beven (2012) has defined a schematic outline describing the various steps of a model building (figure 2-4).

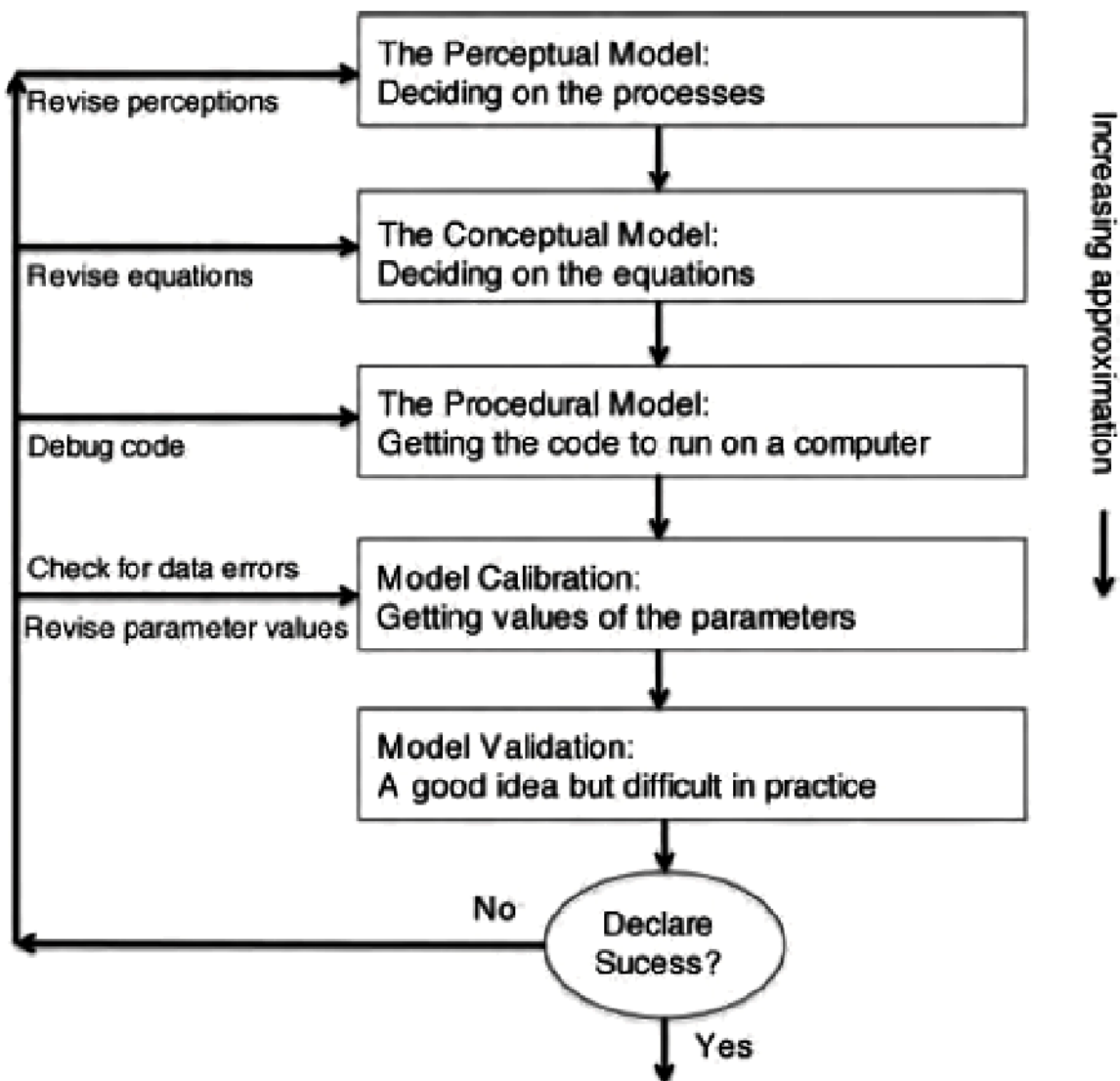


Figure 2-4: A schematic outline of the steps in the modelling process (From Beven, 2012)

The *perceptual model*, which is the summary of our perceptions of how the catchment responds to rainfall under different conditions, is necessarily personal. The mathematical equations describing this perceptual model are referred to as *conceptual model* of the process or processes being considered. The *procedural model* is derived from the equations written in computer language. Model parameters are then estimated, in most cases through *model calibration* so users have to calibrate them against observed data. The application of calibrated parameters on a different period than calibration period allows the *validation process*. At the end of this process, the modelling approach can be said *successful or not*. In case of failure, a revision of each element involved in the model building process may be necessary. These various steps are represented on Figure 2-4.

The 'how' of the model determines how it is classified. There exists a multitude of models. They can be classified according to various criteria. This typology is not exclusive and a given model may be classified in many of these groups (Table 2-1). Models may also be classified in consideration of the Physics or conception on which they have been built. In that case we can cite *empirical models* in which empirical relationships are established between input and output variables; *conceptual models* (among which reservoir models) where the functioning of the catchment is conceptualised but based on empirical relationships and finally *physically based models* in which processes are described on the base of the physical laws of the system.

*Empirical models* describe observed behaviour between variables on the basis of observations alone and do not account for processes. *Conceptual models* are really simple models. Indeed they mainly aim at reflecting the most important aspects of the hydrograph which are that:

- Not all the rainfall in an event becomes streamflow: (a loss function is generally used to account for this aspect);

-There are delays between runoff generation and the hydrograph measured at the outlet of the catchment (a time distribution function is generally used to account for this aspect).

If we consider the purpose of the models, one can distinguish *distributed models* which are elaborated for the purpose of predicting the spatial pattern of flow processes; *lumped models* for the prediction of the hydrograph response without worrying too much about what is happening in space; *semi-distributed models* which may adopt a lumped representation for individual subcatchments: they are in between the two previously mentioned models; and *real-time forecasting models* which are useful for flood forecasting and drought management. Distributed or spatialised models divide the basin in homogeneous entities (grids) while lumped models consider the catchment to be one single spatial unit. Lumped models generally have fewer parameters which can be easily determined from the data. In addition, they present an advantage over physically based models in the sense that the conceptual parameterization in the lumped models is simple and computation is efficient (Yu, 2002). Nevertheless lumped models parameters are often unable to be directly compared with field measurements. Brutsaert (2005) reports that catchment-scale parameters are incapable of accommodating the spatial variability of the input (e.g. rainfall) and of the flow processes (e.g. infiltration and evaporation) and that it is impossible to use this approach to describe the detailed flow paths required in the prediction of pollutant transport or erosion. Despite the shortcomings enumerated above, their usefulness in the prediction of streamflow for certain operational and design purposes is no longer to be demonstrated and they are particularly useful in data-scarce areas.

Many physically based models are distributed and they represent hydrological processes in a physically rigorous manner. Process-based partial differential equations (PDEs) are generally used to describe the spatial variability of hydrological processes. Physically based distributed models are then really helpful in the understanding of hydrological processes. They can also be used to

determine the outflow from headwater catchments when their parameters can be estimated. However physically based models do not produce results that are consistent with observations (Beven, 2012) and the governing parameters of these equations which are supposed to be estimated through measurements are incompatible with the scales used in the models (Yu, 2002). This results in the fact that all parameters cannot be determined a priori using only field measurements but also by calibration. Besides, in most cases these models have a large number of parameters and because PDEs have to be solved numerically the calibration of such models is more complex and requires more computing time. Moreover as commented by Brutsaert (2005), because of the underlying mathematical rigor of the parameterizations of the model components, the limitations of such models may not be fully understood by uninitiated users and they may be applied to situations for which they were not intended. We may also point out the fact that even if distributed models try to describe the processes, certain aspects of the flow that are considered to be less important are still neglected under a number of assumptions. Which means that although distributed models are complex they remain an abstraction of reality. Most of the complexity of physically based model and the parameter scale problems arise from the representations of the subsurface flows, and the inherent lack of observability of subsurface properties (Wheater *et al.*, 2008).

It is interesting to notice that physically based distributed models can be perceived as lumped models in some sense. In fact processes are lumped at the scale of the grid. Actually the main difference between distributed and lumped models is the computational scale. All models are lumped at the scale of the cell or triangle and because the sophistication of modelling techniques is way ahead of the sophistication of measurement techniques, data limitations mean that most distributed models use lumped data (Mulligan & Wainwright, 2004).

To date, hydrologists do not know what is the most appropriate level of model complexity a particular application may require.

*Deterministic* models are opposed to *stochastic* ones. While the former type of models produces only one possible outcome, the latter type might have a distribution of outcomes.

Models can be further subdivided according to the level of process detail and understanding within the model. In that case, it may be termed *black box* or *white box*. Black box models are characterised by the ignorance of users about the processes by which the inputs are transformed to outputs. Nothing is specified by the model builder. In a white box model, all elements of the physical processes transforming input to output are known and specified. Most being actually a mixture of both approaches, they can be termed *grey box models*.

Models typology (except black, white and grey box models) is detailed in Table 2-1.

Table 2-1 : Models typology

Model type	Classification	Characteristics	Strengths	Weaknesses	Examples
<b>Distributed</b>	<i>Purpose</i>	Predicts the spatial pattern of flow processes	Predicts the spatial pattern of flow processes; helpful in the understanding of hydrological processes	Very complex and difficult to be implemented; No superior than lumped models in discharge prediction;	Institute of Hydrology Distributed Model - IHDM
<b>Semi-distributed</b>		The catchment is divided in lumped several spatial units			Kinetic Runoff and Erosion Model KINEROS
<b>Lumped</b>		The catchment is one single spatial unit	Few parameters determined from the data; Simple parameterization; Efficient computation; Particularly useful for certain operational and design purposes and in data-scarce areas	Parameters are unable to be directly compared with field measurements. No consideration of processes. parameters do not accommodate the spatial variability of the input and of the flow processes	The <u>G</u> énie Rural à 4 paramètres Journalier GR4J model; The HBV (Hydrologiska byråns vattenavdelning) model
<b>Real-time forecasting</b>		Flood forecasting and drought management	Helpful in urgent decision making	High level of uncertainty, need of real-time data	

2. River flow generation and Hydrological modelling

Model type	Classification	Characteristics	Strengths	Weaknesses	Examples
<b>Empirical</b>	<b>Functioning</b>	Empirical relationships are established between input and output variables	Simple	None consideration of the system functioning	
<b>Conceptual</b>		The functioning of the catchment is conceptualised but based on empirical relationships	Simple	Equations are not based on physical laws	Soil Water Assessment Tool (SWAT)
<b>Physically based</b>		Use of process-based partial differential equations (PDEs)	Hydrological processes represented in a physically rigorous manner generally in space and time	The scales of measurement for parameters are incompatible with the scales used in the models; results are consistent with observations; the limitations may not be fully understood by uninitiated users	Generalised River Modelling Package-Système Hydrologique Europeen (MIKE-SHE)

2. River flow generation and Hydrological modelling

---

Model type	Classification	Characteristics	Strengths	Weaknesses	Examples
<b>Deterministic</b>	<b>Inputs</b>	Only one possible outcome	-	-	-
<b>Stochastic</b>		A distribution of outcomes	Incorporation of uncertainties in the model	-	Onof and Wheater ((1994a)cited by (Cameron <i>et al.</i> , 2000)) random pulse Bartlett-Lewis gamma model (the RPBLGM)

## 2.4- The Principle of Least Action (PLA), an old concept but new in hydrological modelling

### 2.4.1- Introduction: classical approach of physics-based models

It is accepted that the physical governing laws for water motion at a local scale are well understood since decades (Darcy's law, Richards equation, Saint-Venant Equations). Nevertheless, the usual approach to pass from microphysics of the heterogeneous environment to the physics of the model or the basin by applying the same equations with averaged state variables may pose some problems because they do not take into account the spatial heterogeneity in landscape properties, the inherent nonlinearity of many hydrological processes and the processes interactions at different scales (Alamou, 2011, McDonnell *et al.*, 2007, Wheater *et al.*, 2013). As noted by McDonnell *et al.* (2007) and many others, seeking for macroscale laws that would neither be scale nor place dependent might be an alternative approach.

Most of physics-based models like the Generalised River Modelling Package-Système Hydrologique Europeen (MIKE-SHE) by Refsgaard & Storm (1995), the Representative Elementary Watershed- REW- by Reggiani *et al.* (1998, 1999) or the Physically Based Runoff Production Model: TOPMODEL by (Beven & Kirkby, 1976, 1979) and Beven (1995) use these equations.

The Richards equation describes the soil water flow in the unsaturated zone (Equation 2.1.1).

$$-\frac{\partial q(z,t)}{\partial z} = \frac{\partial}{\partial z} \left[ K(z,t) \frac{\partial \psi(z,t)}{\partial \theta} \frac{\partial \theta(z,t)}{\partial \theta} \right] + \frac{\partial K(z,t)}{\partial \theta} \frac{\partial \theta(z,t)}{\partial z} \quad \text{Eq. 2.1.1}$$

In Equation 2.1.1,  $q$  is the vertical moisture flux;  $\theta$  is the volumetric water content;  $z$  is depth,  $t$  is time;  $K$  is the unsaturated hydraulic conductivity; and  $\psi$  is the hydraulic potential. Numerical methods are generally used to solve this kind of equations; for example the Crank-Nicholson numerical scheme and a finite difference scheme of forward in time and backward in space.

A kinematic wave with a flow-direction algorithm can be used to model the overland flow. Flow in the channel is modelled through channel routing schemes such as the Muskingum–Cunge method.

Darcy's law (1856) expressed in equation 2.1.2 is used in the simulation of the interaction between a stream system and groundwater. The rate of flow of water through a porous medium is proportional to the hydraulic gradient:

$$Q = -K_{\text{sat}} \cdot A \cdot \frac{dh}{dx} \quad \text{Eq.2.1.2}$$

Where  $Q$  is the discharge,  $K_{\text{sat}}$  the hydraulic conductivity,  $A$  the cross-sectional area,  $(dh/dx)$  the hydraulic gradient. The  $h$  term in the hydraulic gradient includes both the elevation and pressure heads.

After presenting the theory of the PLA as it is applied in Physics, we will give the main steps of its evolution through history and then we will address the attempt of application of this principle to hydrology. We will conclude with a small discussion about both approaches.

### *2.4.2- Action and Principle of Least Action in Physics*

Like presented by Roberts (2003), the Physics principle of Least Action is a very simple idea but with far-reaching consequences. This basic idea is that "Nature always finds the most efficient course from one point to another". In other words, the Principle of Least Action says that, in some sense, the true motion also called the physical path is the optimum out of all possible motions (Manton, 2013). In fact, numerous physical situations are expressions of this principle. For instance, the orbits of planets, the path of a thrown ball (See Figure 2.5), the path of a photon of light: they all follow paths of least action to move from a certain point to another. The mathematical definition of this principle requires that we define two types of energy: the kinetic energy  $K$  due to the velocity of the body and the potential energy  $V$ .

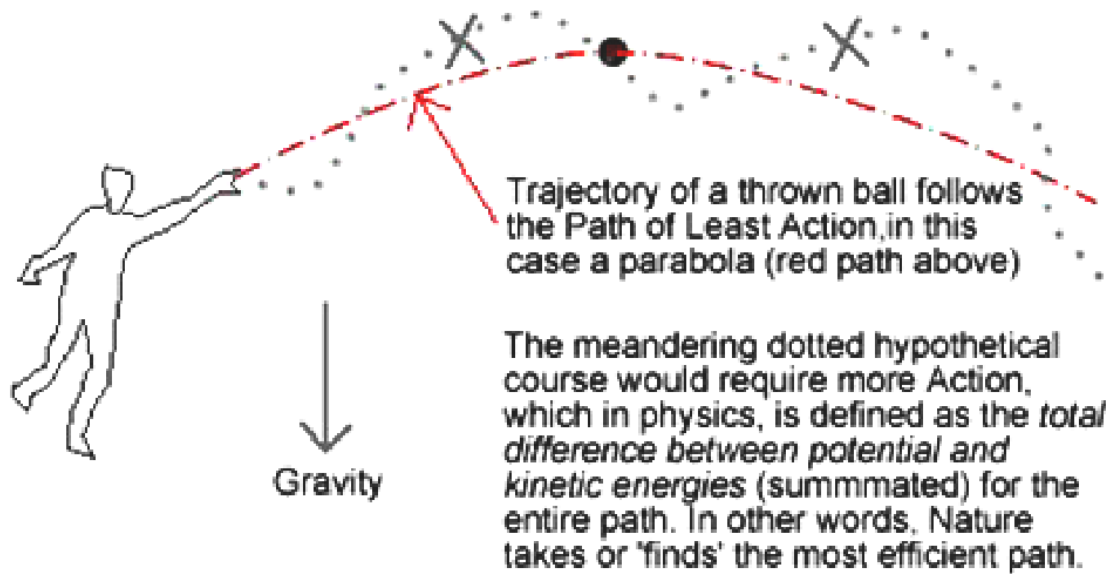


Figure 2-5: Example of a thrown ball (From (Roberts, 2003)).

If  $x(t)$  is a possible path of the body, and  $x(t) = X(t)$  an actual motion between two endpoints  $x_0$  (at time  $t_0$ ) and  $x_1$  (at a later time  $t_1$ ), then we can define the action  $S$  as:

$$S = \int_{t_0}^{t_1} (K - V) dt \quad \text{Eq. 2.2}$$

Called the Hamilton's definition of the action, it is the most commonly used one (Manton, 2013).

Equation 2.2 may be written more shortly using the Lagrangian  $L = K - V$  and then we have:

$$S = \int_{t_0}^{t_1} L dt \quad \text{Eq. 2.3}$$

We can say that the action is the time integral of the Lagrangian.

As clearly explained by Manton (2013), the Principle of Least Action now states that among all the possible paths  $x(t)$  that connect the fixed endpoints, the actual

path taken by the body,  $X(t)$ , is the one that makes the action  $S$  minimal (See Figure 2.6)

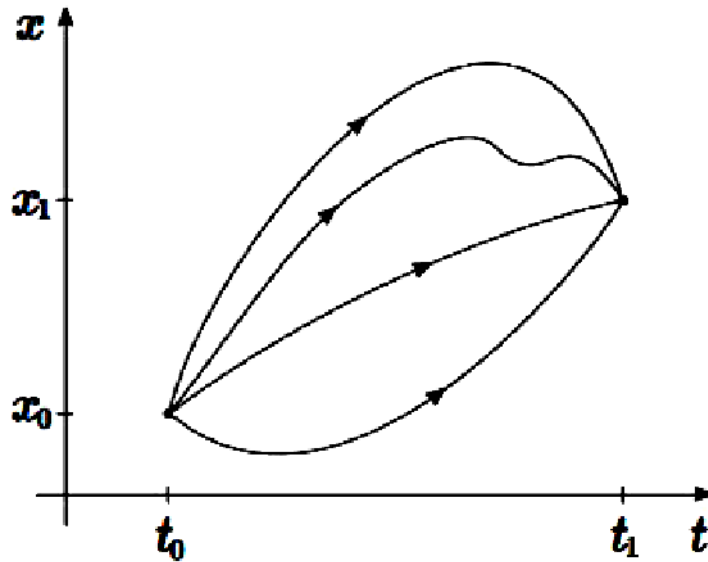


Figure 2-6: Possible paths  $x(t)$ . Picture from Manton (2013)

How do we find this path? One way of applying the Principle of Least Action to a system results in minimising the action  $S$  by the method of calculus of variations. The true path  $X(t)$  then obeys the differential equation obtained.

#### 2.4.3- History of the principle

The principle of least action may be summarised in mainly six (6) names, from the seventeenth (XVIIth) to the twentieth (XXth) century. They are scientists who worked, during these centuries on the statement and the mathematical definition of the principle (Héreau, 2008):

XVIIth century:

- Pierre de Fermat (1601- 1665), French mathematician and physician;

XVIIIth century:

- Pierre-Louis Moreau de Maupertuis (1698- 1759), French mathematician;
- Leonhard Euler (1707- 1783), swiss mathematician;

- Joseph-Louis de Lagrange (1736- 1813), French mathematician;

XIXth century:

- William Hamilton, Irish physician (1805-1865) and Jacobi (1804-1851) admirer and critics of Hamilton.

From Fermat to Hamilton, the principle has been the same principle but the formulations changed.

In 1655, Fermat spoke of “a path that minimizes duration or a length” in the field of light rays; he demonstrated that the light has a different velocity according to the environment.

In 1744, Maupertuis defined the principle of least action for mechanics. Called by Robine (2007), the real father of the principle, he stated the principle as follow: “the path followed by the light ray is the one by which the quantity of action is the smallest”. That is how he introduced for the very first time the concept of action, which measures the “real expenditure of Nature” (Robine, 2007). Meanwhile, Leonhard d’Euler, a contemporary to Maupertuis, has been able to determine the trajectories of bodies using an extremum principle. Since he was in contact with Maupertuis, they worked together in order to verify the validity of this minimum principle in new disciplines of Physics. They validated the principle and Euler in particular, found out a mathematical technique, the calculus of variations to apply it.

In 1788, Lagrange elaborated a new mathematical expression of the action through the “Lagrangian” and expressed the Lagrangian as the algebraic sum of potential and kinetic energies (Léon, 2009). This expression of the action is the one which is most currently used. In fact, Lagrange was in contact with Euler and knew the progress made in the research related to the principle of least action. He simplified the demonstration made by Euler and made clearer the relationship between the least action and the calculus of variations.

From that time on, the principle has been “fertile” in the sense that it has been the starting point for new fields in physics and moreover existing equations have been derived from it (Héreau, 2008, Léon, 2009). For instance, in 1827, Hamilton

developed the Hamiltonian mechanics, followed by Jacobi in 1840. In 1920, De Broglie used it in his quantum theory; in 1916, Hilbert rewrote equations of general relativity. In 1942, Feynman proposed a new formulation in quantum mechanics and found existing results (Robine, 2007).

#### 2.4.4- Application of the PLA in hydrology and the Noether's theorem

If one has to apply this principle to a river network, it will be necessary to define the action of the system and the associated Lagrangian. But before we complete this very important task, we may cast a glance at a theory developed earlier than our model by Rodriguez-Iturbe and co-workers. In fact, Rodríguez-Iturbe *et al.* (1992) and Rodríguez-Iturbe & Rinaldo (1997) developed the idea that the watershed dynamics follows paths that minimise its energy expenditure. They provided evidence for that through the particular case of optimal channel networks. The authors showed by numerical simulations surprising similarities (in the fractal aggregation of their structures and morphology) between optimal channel networks and natural networks (Afouda *et al.*, 2004). Consequently, they postulated three (3) principles of minimum energy expenditure (Rodríguez-Iturbe *et al.*, 1992) as follows:

- a. A river adjusts its channel characteristics toward a state in which the rate of energy dissipation per unit channel area is constant throughout the river network;
- b. Energy expenditure is the same everywhere in the network, when normalized by the area of the channel in which it takes place. This principle makes all channels equally efficient when adjusted for size;
- c. The minimum energy dissipation as a whole is attained by a structure that minimizes the constrained potential energy of the system.

The channel characteristics can be enumerated as the channel pattern, bed configuration, bed slope, cross-section form. These optimality principles stated by Rodriguez-Iturbe and co-workers can find its generalisation in the Principle of

Least Action (Afouda *et al.*, 2004; Alamou, 2011). This gives more strength to the Principle of Least Action.

Now, to apply it we will have to define the action of a drainage network. It has been defined by Afouda *et al.* (2004) as follow:

$$\Lambda[Q] = \int_{\Omega} dX L(X, Q, Q_X) \quad \text{Eq. 2.4}$$

Where  $L(\cdot)$  is the Lagrangian,  $Q(X)$  is the discharge and  $X$  stands for time and space coordinates. As we said in the previous sections, applying the method of calculus of variations to the action gives the following equation which is known as the **Euler-Lagrange equation** (eq.2.5):

$$\frac{\partial L}{\partial Q} - \frac{\partial}{\partial X} \left( \frac{\partial L}{\partial Q_X} \right) = 0 \quad \text{Eq. 2.5}$$

We now write  $L$  as the algebraic sum of potential and kinetic energies where  $\nu$  is a parameter of nonlinearity:

$$L = -\frac{1}{2} \left[ Q^{2\nu} + \left( \frac{\partial Q}{\partial X} \right)^2 \right] \quad \text{Eq. 2.6}$$

From equations 2.5 and 2.6, Afouda *et al.* (2004) derived the generalised evolution equation:

$$\frac{\partial}{\partial X} \left[ \frac{\partial Q}{\partial X} \right] = \nu Q^{2\nu-1} \quad \text{Eq. 2.7}$$

Arguing that the action of a system is minimum is equivalent to say that it exhibits a symmetry. A continuous symmetry may be defined as any infinitesimal transformation of the generalized coordinates, of the associated velocities, and possibly of the time variable  $t$ , that leaves the value of the Action unaffected (Nicolis, 2011). A more general principle, called Noether's theorem (1918) states that whenever a physical system exhibits a continuous symmetry of the Action, there is an associated conservation law. This theorem has been proved by the German mathematician Emmy Noether and relates symmetries to conservation

laws (Bauman, 2012). And in particular the following symmetries, the translation in space, the translation in time, and eventually the rotation through a fixed angle are associated respectively to the conservation of momentum; the conservation of energy and to the conservation of the angular momentum (Arovas, 2012, Hanc *et al.*, 2004, Nicolis, 2011).

### 2.4.5- Conclusion: towards the application of the PLA in hydrology

The principle of least action belongs to the group of what we call optimisation principles. As reminded by Manton (2013), they play a fundamental role in many areas of physical science. This principle is in fact applied in ray optics where the laws of reflection and refraction may be derived from it, in electromagnetism, in particle physics, etc. Hanc *et al.* (2003) add that one can use this principle in Relativity if the correct form for the action is found. Manton (2013) explains also that a profound understanding of the dynamics of bodies comes from the Principle of Least Action. And points out the fact that from this principle derive all three Newton's laws of motion and as a corollary the equations of motion. That means that both classical and new approaches in hydrology modelling are based on the same principle of least action. But Afouda *et al.* (2004) insist on the idea that the explicit use of the PLA allows one to avoid the introduction of *ah doc* hypotheses (like in the case of the solution of the Saint-Venant equations) and leads to a model representing simultaneously both rainfall transformation and runoff processes. Moreover Alamou (2011) notes that even though the formulation based on the least action principle has the same physical content as the Newton's equations, it constitutes another point of view, leading to concepts that are more general and powerful. The PLA introduces an optimality principle which is not the case for other traditionally used approaches. This theory brings a new understanding of hydrological systems. Many authors recognise the importance to look at hydrology from that point of view. Developing new hydrological theories based on scaling is one of the science themes (Theme 5) identified in the framework of the PUB Science strategy at the end of the 2003-

2012 IAHS Decade on Predictions in Ungauged Basins (PUB) (Sivapalan *et al.*, 2012). McDonnell *et al.* (2007) express the need to move beyond the practice of explicitly characterizing or prescribing landscape heterogeneity in models and in this way reproduce process complexity. Instead, they propose the exploration of the set of organizing principles that might underlie the heterogeneity and complexity as one of the new avenues for research in watershed science. The Principle of Least Action has many advantages over classical approaches. The underlying physics of physically based distributed models has generally been derived from small scale, mainly laboratory-based, process observations. Consequently, the processes may not apply under field conditions and at field scales of interest. The spatial aggregation from small scale to a larger one is not able to reproduce field scale processes because of the great heterogeneity of the soils. Moreover although the parameters may be measurable at small scale, they may not be measurable at the scales of interest for application (Wheater *et al.*, 2013). It is demonstrated that the dominant modes of process response cannot be specified a priori. As explained in above sections, classical approaches use averaging methods to pass from the microscopic scale to the macroscopic scale without accounting for the heterogeneities of the soil and the non-linearity of the processes while the PLA may be applied at all scales. Moreover while classical physically based approaches apply at the catchment scale laws that govern water motion at a local scale, the PLA approach considers a more correct approach (at least theoretically) in the sense that PLA is valid at the local as well as the catchment scale. Therefore the PLA based model has the advantage of incorporating an optimality principle which leads to a minimum number of parameters if compared with known hydrological models. Further, with the PLA, we may derive a single differential equation, which when solved analytically, leads to well-known equations of recession curves for the case of no-rain (Alamou, 2011). When uncertainties (as a random function) are added to this, the deterministic ordinary equation is transformed into a stochastic differential equation from which the probability of the output can be derived (Biao *et al.*,

2015). The mathematical formulation of the PLA is simpler (concept of energy rather than force and the use of any coordinates). Léon (2009) observes that all the interest of the PLA lies in the fact that it allows one to derive fundamental laws just by knowing the Lagrangian of a system. Feynman *et al.*(1964) comment that this principle has a practical utility and may lead to excellent numerical results. Nevertheless, Manton (2013) mentions possible disadvantages. The first one is mainly related to the method of calculus. As we discussed above, the standard method by which one derives the equation of motion is the calculus of variations, which is not elementary calculus. The second one is about the physics. The equation of motion derived from the PLA has no friction term meaning that the energy is conserved. This is actually good at a theoretical level but when friction is present in the motion, it needs to be added separately. Neuenschwander *et al.* (2006) agree on the idea. This may be an important aspect to account for in the improvement of the theoretical development of the model.

## 2.5- Modelling approaches

### 2.5.1- The MODHYPMA

The application of the Least Action Principle results in the following differential equation (Eq. 2.8) (Alamou, 2011).

$$\left| \frac{dQ}{dt} + \frac{\nu}{\lambda} Q^{(2\nu-1)} = \frac{X(t)}{\lambda} q(t) \right. \quad \text{Eq. 2.8}$$

Where  $Q$  [ $\text{mm.d}^{-1}$ ] represents the discharge,  $t$  [s] the time,  $q$  [mm] the net rainfall. While  $\nu$  expresses the non-linearity of the physical phenomenon of water flow,  $\lambda$  is a macroscopic parameter which describes properties related to the geomorphology and pedology of the catchment.  $X$  describes the state (dry or wet) of the basin (Alamou, 2011).  $\nu$  and  $\lambda$  are the model parameters. In definitive,  $\nu$  and  $\lambda$  are physical parameters (they describe the physical structure of the system) and  $X$  is a process variable (it is related to the order of magnitude of the processes).

The numerical solution of the differential equation gives the expression of the discharge.

$$Q_t - Q_{t-1} + \frac{\nu}{\lambda} Q_{t-1}^{(2\nu-1)} = X_t \frac{q_{t-1}}{\lambda} \quad \text{Eq. 2.9}$$

From equation (2.9),  $Q_t$  may be derived as follow (2.10)

$$Q_t = Q_{t-1} - \frac{\nu}{\lambda} Q_{t-1}^{(2\nu-1)} + X_t \frac{q_{t-1}}{\lambda} \quad \text{Eq. 2.10}$$

Where  $Q_t$  = discharge at the outlet at the time  $t$

$Q_{t-1}$  = discharge at the outlet at the time  $t - 1$

$X_t$  describes the state of the basin at the time  $t$

$q_{t-1}$  = net rainfall of the time  $t - 1$  (= precipitation-ETP if precipitation > ETP)

A daily time step has been chosen because of data availability and because the response time of natural basins of average size in tropical areas is about one day (Alamou, 2011).

Parameters  $\nu$  and  $\lambda$  are considered as constants and have been estimated from observed discharges during the recession period where  $q_{t-1} = 0$ . In this case, Equation (2.10) reduces to:

$$Q_t - Q_{t-1} = -\frac{\nu}{\lambda} Q_{t-1}^{(2\nu-1)} \quad \text{Eq. 2.11}$$

For the computation of the state of the soil, three new important assumptions were made:

- First,

***“From day  $t-1$  to day  $t$ , the state  $X$  of the soil changes and  $X_t$  depends on  $X_{t-1}$ ”***

- Second,

***“The state of the soil is modified by the occurrence or not of the precipitation”***

$X_t$  is a function of  $X_{t-1}$  and  $q_t$ .

$$q_t = P - ETP; \quad \text{If } P < ETP \text{ then } q_t = 0 \quad \text{Eq. 2.12}$$

$$\text{If } q_t = 0, \quad X_t = X_{t-1} - \frac{\nu}{\lambda} X_{t-1} \quad \text{If not,} \quad X_t = X_{t-1} + \frac{\nu}{\lambda} q_t^{(2\nu-1)} \quad \text{Eq. 2.13}$$

Equations 2.10; 2.12 and 2.13 give respectively the formulas for the discharge, the net rainfall, and the state of the wetness of the catchment.

- Third,

***“The state of the soil  $X_t$  is equal to zero as long as it is smaller than a threshold value  $TX$ ”***

In other words,

$$\text{If } X_t < TX, \quad X_t = 0 \quad \text{Eq. 2.14}$$

In semi-arid and sub-humid areas a certain amount of rainfall is required before discharge starts. In order to account for this amount, a new parameter  $TX$  has been introduced as a threshold. The amount depends on catchment properties like geology, topography, land use.  $TX$  is obtained by calibration.

### 2.5.2- The GR4J model

GR4J (Perrin *et al.*, 2003) stands for modèle du Génie Rural à 4 paramètres Journalier. It is a 4-parameter conceptual model which works with two (2) storage reservoirs.

All four parameters are real numbers.  $x_1$  and  $x_3$  are positive,  $x_4$  is greater than 0.5 and  $x_2$  can be either positive, zero or negative. The schematic description of the model is given in Figure 2-7:

- $x_1$  : maximum capacity of the production store (mm)
- $x_2$  : groundwater exchange coefficient (mm)
- $x_3$  : one day ahead maximum capacity of the routing store (mm)
- $x_4$  : time base of unit hydrograph UH1 (days).

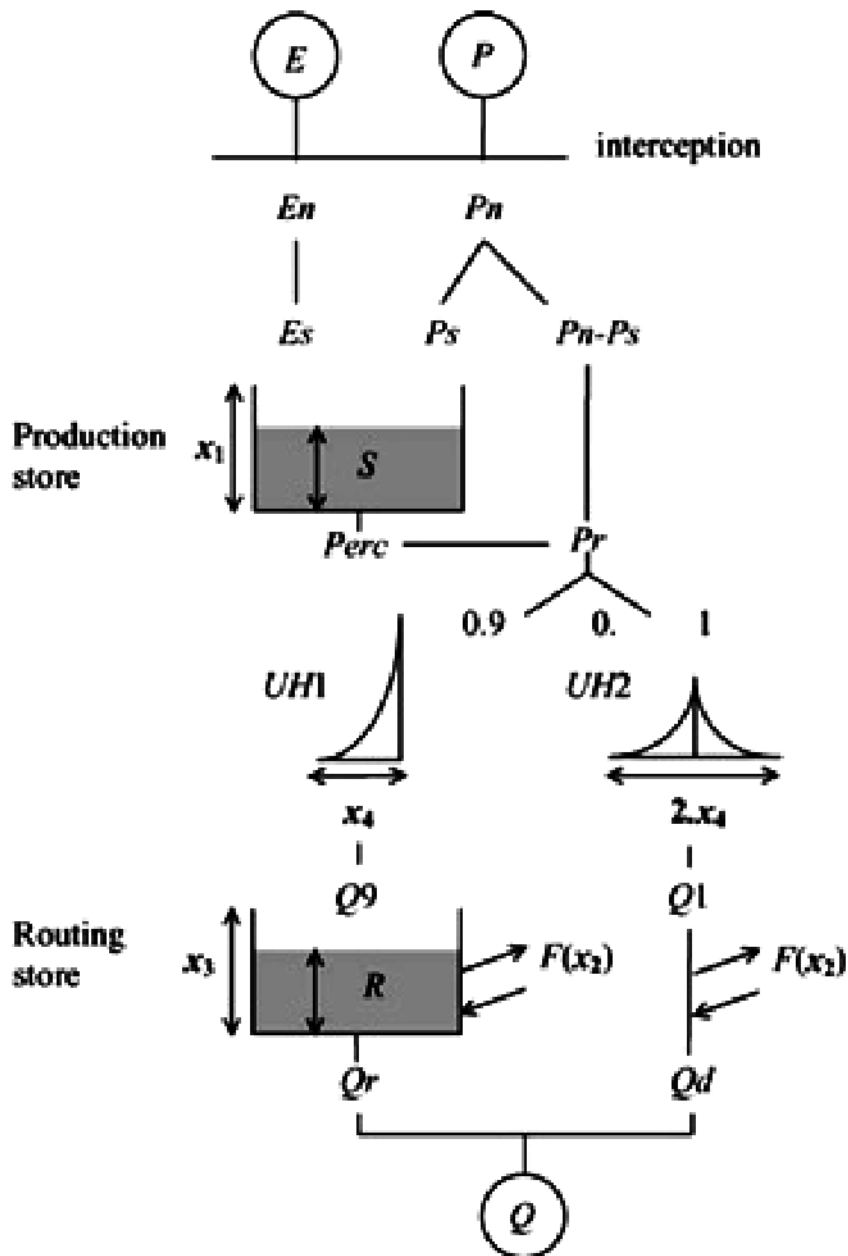


Figure 2-7: Schematic structure of GR4J model (Perrin et al. 2003).

The inputs are the precipitation  $P$  [mm] and evapotranspiration  $E$  [mm].  $E$  can be a long-term average value, which means that the same  $PE$  series is repeated every year. The first step is the computation of the net rainfall and the potential evapotranspiration ( $PE$ ).  $E$  is subtracted from  $P$  and either a net rainfall  $P_n$  or a net evapotranspiration capacity  $E_n$  is determined (Equations 2.15 and 2.16).

$$\left| \text{If } P \geq E, \text{ then } P_n = P - E \text{ and } E_n = 0 \right.$$

$$\text{Eq. 2.15}$$

$$\text{Otherwise } P_n = 0 \text{ and } E_n = E - P \quad \text{Eq. 2.16}$$

The second step is the computation of the Production (SMA) store. When,  $P_n$  is different from zero a part  $P_s$  of  $P_n$  fills the production store according to Equation 2.16.  $x_1$  [mm] is the maximum capacity of the SMA store.

$$P_s = \frac{x_1 \left(1 - \left(\frac{S}{x_1}\right)^2\right) \tanh\left(\frac{P_n}{x_1}\right)}{1 + \frac{S}{x_1} \tanh\left(\frac{P_n}{x_1}\right)} \quad \text{Eq. 2.16}$$

In the other case, when  $E_n$  is different from zero, an actual evaporation rate is determined as a function of the level in the production store to calculate the quantity  $E_s$  of water that will evaporate from the store. It is obtained by  $E_s$  (Equation 2.17).

$$E_s = \frac{S \left(2 - \frac{S}{x_1}\right) \tanh\left(\frac{E_n}{x_1}\right)}{1 + \left(1 - \frac{S}{x_1}\right) \tanh\left(\frac{E_n}{x_1}\right)} \quad \text{Eq. 2.17}$$

The level  $S$  of the store is modified according to Equation 2.18;  $x_1$  being the threshold. Some water is percolated from the store (Equation 2.19).  $Perc$  is always lower than  $S$ .  $Perc$  is deduced from  $S$  and the final expression of  $S$  is indicated in (Equation 2.20).

$$S = S - E_s + P_s \quad \text{Eq. 2.18}$$

$$Perc = S \left\{ 1 - \left[ 1 + \left( \frac{4 S}{9 x_1} \right)^4 \right]^{-1/4} \right\} \quad \text{Eq. 2.19}$$

$$S = S - Perc \quad \text{Eq. 2.20}$$

The third step is the linear routing with unit hydrographs.  $Pr$  is the total input of the routing functions (Equation 2.21).

$$Pr = Perc + (Pn - Ps) \quad \text{Eq. 2.21}$$

This water  $Pr$  is divided into two flow components:

- 90% : routed by a unit hydrograph UH1 and then a non-linear routing store ;
- 10% : routed by a single unit hydrograph UH2.

The unit hydrographs UH1 and UH2 allow to simulate the time lag between the rainfall event and the resulting streamflow peak. UH1 has a time base of  $x_4$  days whereas UH2 has a time base of  $2x_4$  days.  $x_4$  can take real values and is greater than 0.5 day.

The discrete forms of the unit hydrographs UH1 and UH2 have respectively  $n$  and  $m$  ordinates where  $n$  and  $m$  are the smallest integers exceeding  $x_4$  and  $2x_4$ ; respectively. The ordinates of the unit hydrographs are obtained from the corresponding S-curves (cumulative proportion of the input with time) denoted by SH1 and SH2, respectively. SH1 is defined along time  $t$  by equations 2.22 to 2.28.

$$\text{For } t \leq 0, SH1(t) = 0 \quad \text{Eq. 2.22}$$

$$\text{For } 0 \leq t \leq x_4, \quad SH1(t) = \left(\frac{t}{x_4}\right)^{5/2} \quad \text{Eq. 2.23}$$

$$\text{For } t \geq x_4, SH1(t) = 1 \quad \text{Eq. 2.24}$$

$$\text{For } t \leq 0, SH2(t) = 0 \quad \text{Eq. 2.25}$$

$$\text{For } 0 \leq t \leq x_4, \quad SH2(t) = \frac{1}{2} \left(\frac{t}{x_4}\right)^{5/2} \quad \text{Eq. 2.26}$$

$$\text{For } x_4 < t < 2x_4, \quad SH2(t) = 1 - \frac{1}{2} \left(2 - \frac{t}{x_4}\right)^{5/2} \quad \text{Eq. 2.27}$$

$$\text{For } t \geq 2x_4, \quad SH2(t) = 1 \quad \text{Eq. 2.28}$$

UH1 and UH2 ordinates are then calculated by Equations 2.29 and 2.30 (j is an integer):

$$UH1(j) = SH1(j) - SH1(j - 1) \quad \text{Eq. 2.29}$$

$$UH2(j) = SH2(j) - SH2(j - 1) \quad \text{Eq. 2.30}$$

The fourth step is the computation of the catchment water exchange. F is the groundwater exchange term equation 2.31. It is calculated with R the level in the routing store. x3 its 'reference' capacity and x2 the water exchange coefficient. The signe of X2 depends on the water flux. When water is imported x2 is positive, when water is exported x2 is negative and when there is no water exchange x2 is equal to zero.

$$F = x_2 \left( \frac{R}{x_3} \right)^{7/2} \quad \text{Eq. 2.31}$$

In absolute value, F cannot be greater than x2: x2 represents the maximum quantity of water that can be added (or released) to (from) each model flow component when the routing store level equals x3.

The fifth step is the computation of the non-linear routing store. The output Q9 of UH1 and F are added to the routing store. R is updated (equation 2.32).

$$R = \max(0; R + Q9 + F) \quad \text{Eq. 2.32}$$

The expression of the outflow Qr of the reservoir is given by Equation 2.33.

$$Q_r = R \left\{ 1 - \left[ 1 + \left( \frac{R}{x_3} \right)^4 \right]^{-1/4} \right\} \quad \text{Eq. 2.33}$$

Qr is always lower than R, the level in the reservoir (See Equation 2.34)

$$R = R - Q_r \quad \text{Eq. 2.34}$$

The sixth step is the computation of the total streamflow. The flow component  $Q_d$  is given by Equation 2.35. Finally the total streamflow is the sum of  $Q_r$  and  $Q_d$  (Equation 2.36).

$$Q_d = \max(0; Q_1 + F) \quad \text{Eq. 2.35}$$

$$Q = Q_r + Q_d \quad \text{Eq. 2.36}$$

### 2.5.3- The HBV model

The HBV (Hydrologiska byråns vattenavdelning) model is a conceptual model. It has fifteen (15) parameters (See Table 2-2). Discharge is simulated at a daily time step. The input variables are daily rainfall, temperature and potential evaporation or long-term averages of monthly potential evaporation. Figure 2-8 shows the structure of the model. The model consists of different routines: snow, soil and routing. A threshold temperature, **TT** [°C] is defined. When temperature is above this threshold precipitation is simulated to be rain, otherwise precipitation is simulated to be snow. Snow is multiplied by a snowfall correction factor, **SFCF** [-]. Snowmelt  $M$  [mm d<sup>-1</sup>] is computed by a degree-day method using the degree-day factor **CFMAX** (mm d<sup>-1</sup> °C<sup>-1</sup>) which compensates for systematic errors in the snowfall measurements and evaporation from the snowpack in the model (the latter is not simulated explicitly) (See equation 2.37).

$$melt = M = CFMAX (T(t) - TT) \quad \text{Eq. 2.37}$$

Meltwater and rainfall is retained within the snowpack until it exceeds a certain fraction, **CWH** [-], of the water equivalent of the snow.

When temperatures drop below **TT**, Liquid water within the snowpack refreezes.

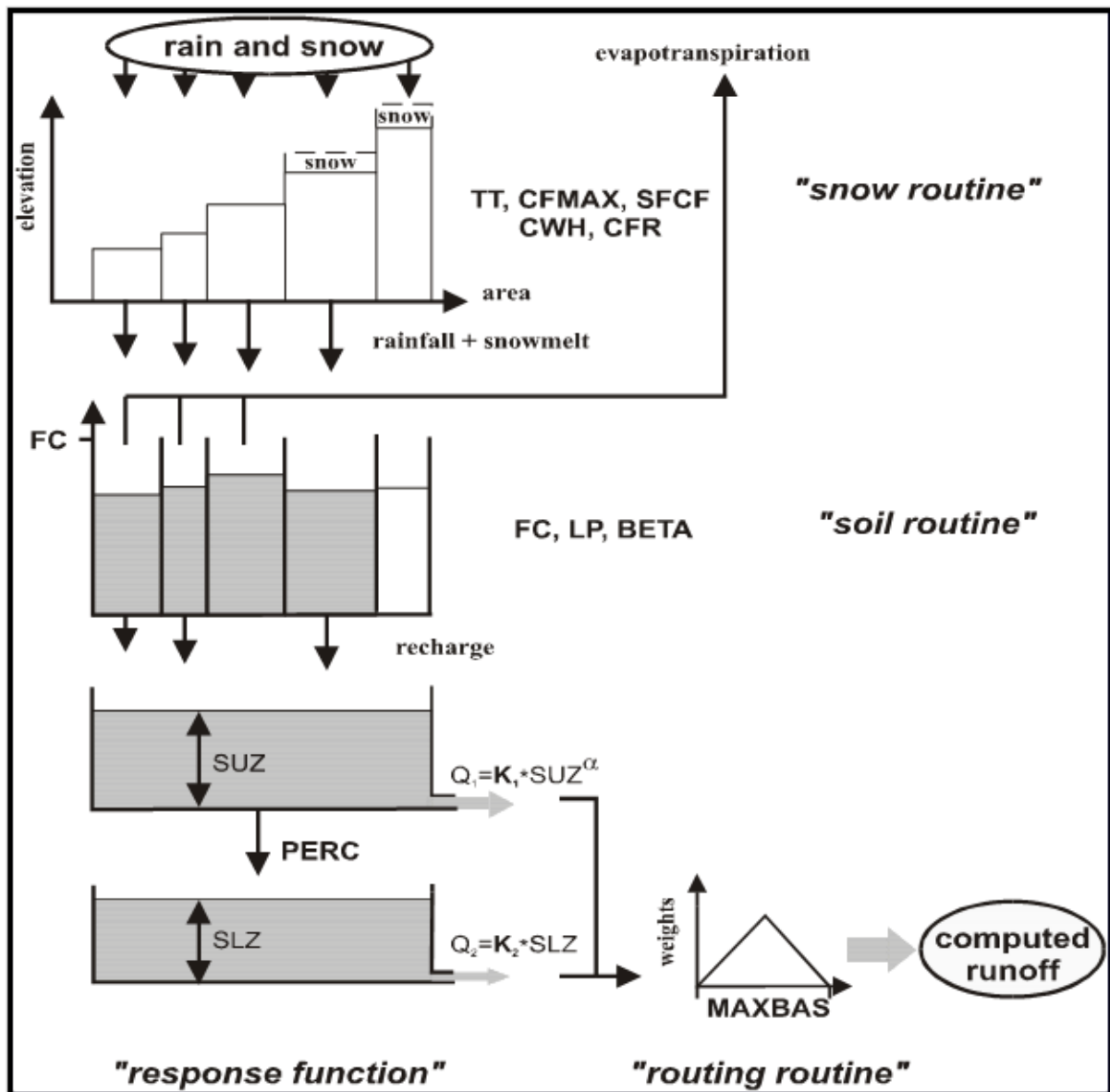


Figure 2-8: Schematic structure of HBV model (Seibert 2005).

The amount of refreezing liquid water within the snow pack,  $R$  ( $\text{mm d}^{-1}$ ) is computed using a refreezing coefficient,  $CFR$  (-) (See equation 2.38).

$$\text{refreezing} = R = CFR \cdot CFMAX (TT - T(t)) \quad \text{Eq. 2.38}$$

The amount of rainfall and snowmelt ( $P$ ) is divided into groundwater recharge and water filling the soil box. The partition is a function of the ratio between

current water content of the soil box ( $SM$  [mm]) and its maximum value ( $FC$  [mm]) (See equation 2.39).

$$\frac{recharge}{P(t)} = \left(\frac{SM(t)}{FC}\right)^{BETA} \quad \text{Eq. 2.39}$$

Actual evaporation from the soil box equals the potential evaporation if  $SM/FC$  is above  $LP$  [-] while a linear reduction is used when  $SM/FC$  is below  $LP$  (See equation 2.40).

$$E_{act} = E_{pot} \min\left(\frac{SM(t)}{FC \cdot LP}, 1\right) \quad \text{Eq. 2.40}$$

Groundwater recharge is added to the upper groundwater box ( $SUZ$  [mm]).  $PERC$  [mm d<sup>-1</sup>] defines the maximum percolation rate from the upper to the lower groundwater box ( $SLZ$  [mm]). Runoff from the groundwater boxes is computed as the sum of two or three linear outflow equations depending on whether  $SUZ$  is above a threshold value,  $UZL$  [mm], or not (See equation 2.41).

$$Q_{GW}(t) = K_2 SLZ + K_1 SUZ + K_0 \max(SUZ - UZL, 0) \quad \text{Eq. 2.41}$$

This runoff is finally transformed by a triangular weighting function defined by the parameter  $MAXBAS$  (See equation 2.42) to give the simulated runoff [mm d<sup>-1</sup>].

$$Q_{sim}(t) = \sum_{i=1}^{MAXBAS} c(i) Q_{GW}(t - i + 1)$$

$$\text{where } c(i) = \int_{i-1}^i \frac{2}{MAXBAS} - \left|u - \frac{MAXBAS}{2}\right| \cdot \frac{4}{MAXBAS^2} du \quad \text{Eq. 2.42}$$

If different elevation zones are used the changes precipitation and temperature with elevation are calculated using the two parameters PCALT [%/100 m] and TCALT [°C / 100 m] (See equation 2.43 and 2.44).

$$P(h) = P_0 \cdot \left( 1 + \frac{PCALT(h - h_0)}{10\,000} \right) \quad \text{Eq. 2.43}$$

$$T(h) = T_0 \cdot \left( 1 + \frac{TCALT(h - h_0)}{100} \right) \quad \text{Eq. 2.44}$$

The long-term mean of the potential evaporation,  $E_{pot}$ , M for a certain day of the year can be corrected to its value at day  $t$ ,  $E_{pot}(t)$ , by using the deviations of the temperature,  $T(t)$ , from its long-term mean,  $T_M$ , and a correction factor, **CET** [°C-1] (See equation 2.45).

$$E_{pot}(t) = (1 + c_{ET}(T(t) - T_M)) \cdot E_{pot,M} \text{ but } 0 \leq E_{pot}(t) \leq 2 E_{pot,M} \quad \text{Eq. 2.45}$$

As noted by Seibert & McDonnell (2010) the parameters in the HBV model each have a physical meaning, but they are not measurable since they represent effective values at the catchment scale.

In the current study we did not use various elevation zones. We used daily potential evaporation.

**Table 2-2: HBV Model parameters and feasible ranges (From (Seibert and McDonnell 2010))**

Parameter	Explanation	Unit	Lower bound	Upper bound
<b><i>Snow routine</i></b>				
TT	Threshold temperature	°C	-1.5	2.5
CFMAX	Degree-day factor	mm d <sup>-1</sup> °C <sup>-1</sup>	1	10
SFCF	Snowfall correction factor*	-	0.5	1.2
CWH	Water holding capacity	-	0	0.2
CFR	Refreezing coefficient	-	0	0.1
<b><i>Soil routine</i></b>				
FC	Maximum of storage in the soil	mm	50	500
LP	Threshold for reduction of evaporation	-	0.3	1
BETA	Shape coefficient	-	1	6
CET	Factor for correction of long-term evaporation rates based on temperature	-	0	0.3
<b><i>Response routine</i></b>				
K <sub>0</sub>	Recession coefficient (upper storage)	d <sup>-1</sup>	0.1	0.5
K <sub>1</sub>	Recession coefficient (upper storage)	d <sup>-1</sup>	0.05	0.3
K <sub>2</sub>	Recession coefficient (lower storage)	d <sup>-1</sup>	0.003	0.1
UZL	Threshold for the P <sub>K0</sub> -outflow	mm	0	50
PERC	Maximal flow from upper to lower box	mm d <sup>-1</sup>	0	4
MAXBAS	Routing, length of weighting function	d	1	7

## STUDY AREAS AND DATA



Photo 3: View of the evaporation pan at the synoptic station of Parakou

### 3- Study Areas and Data

Our study was carried out on twenty one (21) catchments in Benin, Côte D'Ivoire, Ethiopia, and the USA. By applying MODHYPMA under various hydro-meteorological conditions, we expect to come out with sounder results that could be easily generalized.

#### 3.1- Geographical overview of Ouémé basin in Benin

##### 3.1.1- Location

Seventeen (17) of these catchments are located in Benin in West Africa. Our study area is the Ouémé river basin in Benin with regard to Savè outlet (23 488 km<sup>2</sup>). The Ouémé River basin covers more than the half of Bénin's area. It is located in central Bénin between 8°-10° N and 1°30'-2°45' E in the departments of Donga and Borgou (Judex & Thamm, 2008). The figure 3-1 shows in (A) the location of Benin in Africa, in (B) the map of Bénin with the Ouémé basin (in blue colour) and more specifically the Ouémé river basin with regard to Savè outlet in scratch. In (C) we have the various subcatchments. As precised by Hiepe (2008), the Ouémé river basin is delimited by a small ridge to the East, the Atacora Mountains to the West, and low mountain ranges to the North, which serve as a divide to the Niger catchment. The river Ouémé takes its source in the classified forest of Tanéka in the town of Copargo (Tossa & Tonouhewa, 2009).

##### 3.1.2- Climate

Benin belongs to the tropical sub-saharan region with a wet and dry climate (Bossa, 2012). This sub-humid tropical climate is largely controlled by the West African monsoon circulation. During the course of a year, Benin is alternatively affected by a relatively cool and humid monsoon air mass originating from the Gulf of Guinea, and the hot, dry, and dusty Saharan air mass (Fink *et al.*, 2010). The dry season is characterised by these northeasterly Harmattan winds (Volker & Tim, 2008).

### 3. Study areas and data

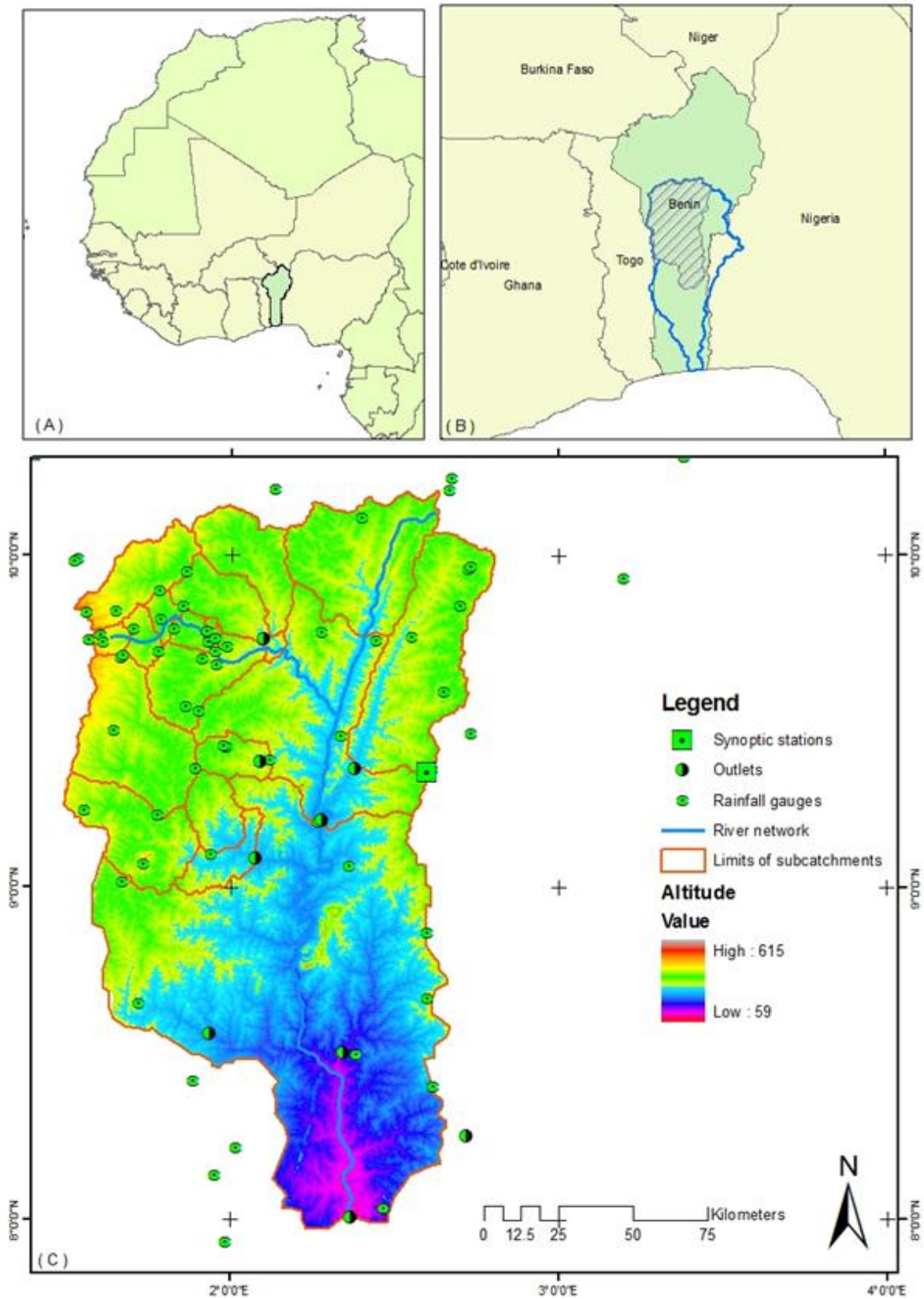


Figure 3-1: Location of sub-catchments of the Ouémé River basin.

The seasonal northward and southward movement of the ITCZ (the Inter-Tropical Convergence Zone) determines the ‘modality’ of rainfall in West Africa (Lebel & Ali, 2009).

In the north of Benin, climate is unimodal with a single rainy season lasting typically from April to October while in the south the bimodal annual rain distribution can be separated into a strong rainy season from mid-February to early August, and a weaker one from mid-August to November (Diederich & Simmer, 2008). The mean annual precipitation (1960 – 2010) at Bétérou is 1204 mm and at Savè 1098 mm (Avahounlin *et al.*, 2013). The mean annual temperature at Parakou station is 26.8°C (Mulindabigwi *et al.*, 2008).

As illustrated on the climate diagram of the Parakou station (Figure 3.2), the highest rainfall totals occur in August and September, whereas the highest temperatures are recorded in March and April, at the beginning of the rainy season (Hiepe, 2008).

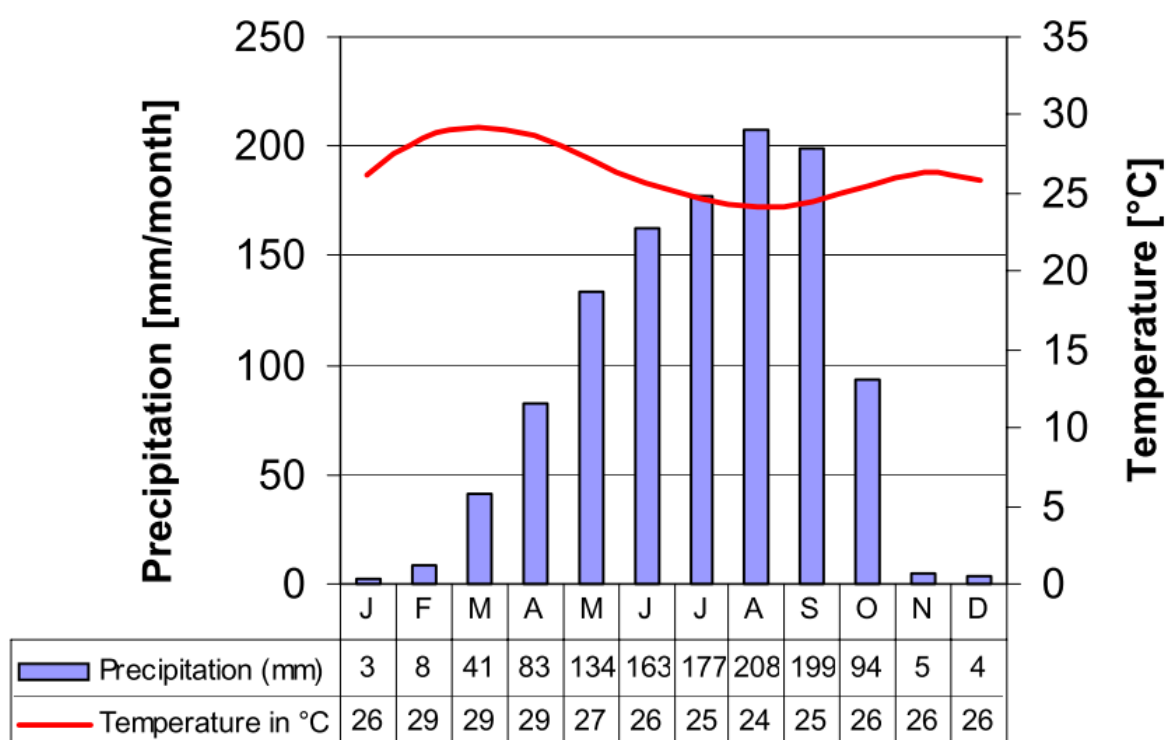


Figure 3-2: Climate diagram station Parakou, mean rainfall values for 1961–1990 (from Hiepe (2008)).

#### 3.1.3- Geology, Geomorphology

The geology of Benin is composed of two major structures which are the remetamorphised Precambrian crystalline basement located in Central Benin and three sedimentary basins, located in North (Kandi basin and Precambrian Volta basin) and South Benin (Coastal basin) (Schönbrodt & Giertz, 2008). The first also known as the Dahomeyides or the Benino-Nigerian shield consists predominantly of complex migmatites, granulites and gneisses including less abundant mica shists, quartzites and amphibolites (Reichert *et al.*, 2010). Lateritic consolidated soil layers, granites and alterites are also present. The sedimentary basins occupy only 20% of Benin. The superposition of different tectonic phases is shown by the existence of intense fracturing and major faults of many kilometres length (e.g., the NNE-SSW trending Kandi fault); ultramylonite bands accompany many of the faults (El-Fahem & Kocher, 2008). See figure 3-3.

The geomorphology of Benin is closely linked to its geologic structure (Schönbrodt & Giertz, 2008). Geomorphology is flat on the sedimentary plateaus while the altitude is much higher on the crystalline basement. Figure 3-4 shows the landscape units in Benin. As observed by Menz (2010), the topographic relief in Benin is generally low, varying only a few meters from the coastal plain northwest to the Atacora mountain range, with the country's highest elevation point at Mt. Sokbaro (658 meters asl).

Hilly plateaus are the main characteristic of the Coastal and Kandi Basins while the Volta Basin is characterized by seasonally flooded plains. In Central Benin, the Dahomeyen peneplain which covers the major part of the country (Le Barbé *et al.*, 1993) is framed by the sedimentary basins (Schönbrodt & Giertz, 2008).

Various configurations of land surfaces may be observed on this crystalline basement (Reichert *et al.*, 2010):

- slight undulations (Parakou Plateau or Kouande-Pehonco peneplains);
- strong fractures (Pira peneplain) ;
- typical seasonally waterlogged linear depressions such 'inland valleys' ;
- scattered inselbergs (Nikki peneplain).

### 3. Study areas and data

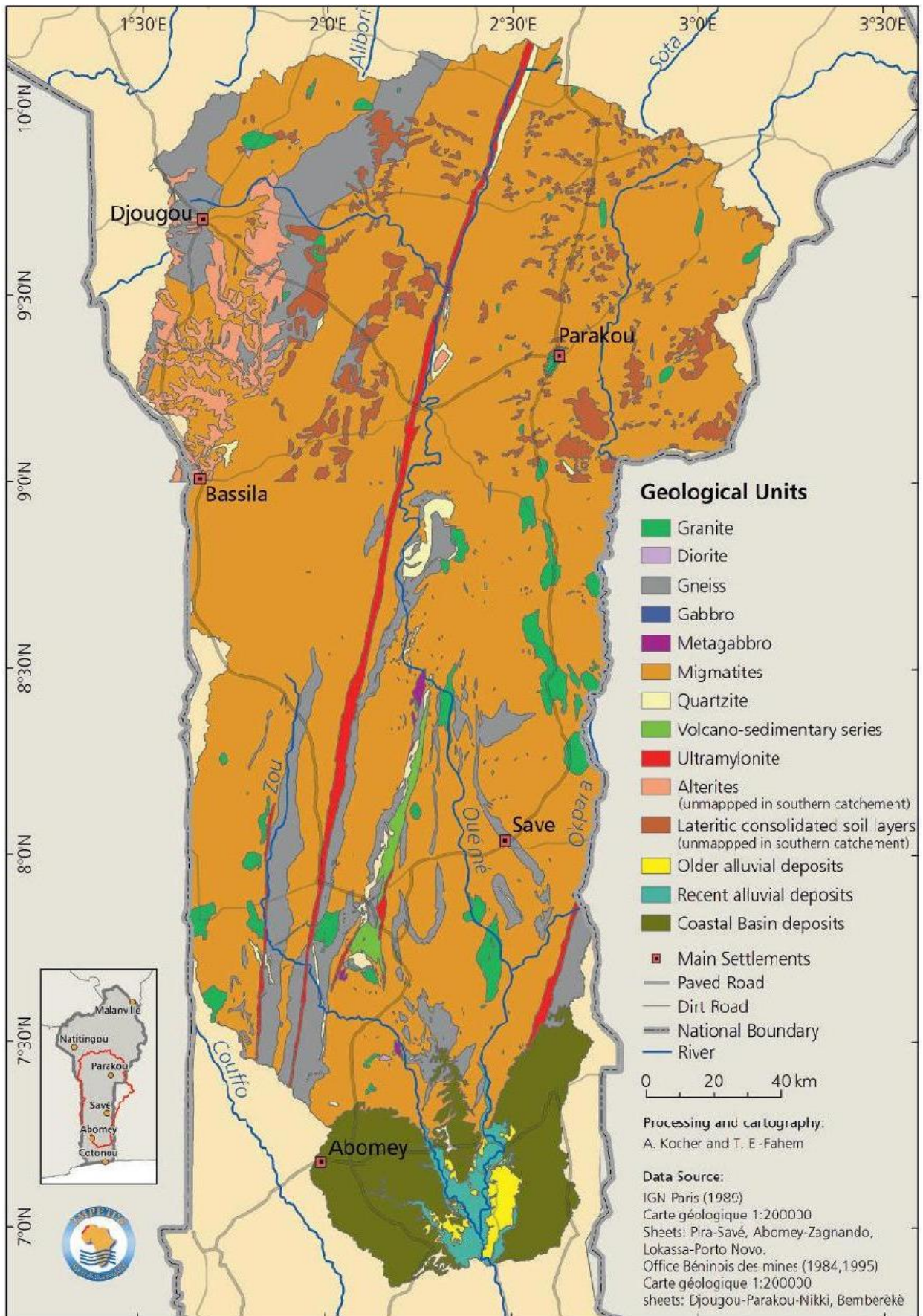


Figure 3-3: Map of the geology in the Ouémé catchment from (El-Fahem & Kocher, 2008)

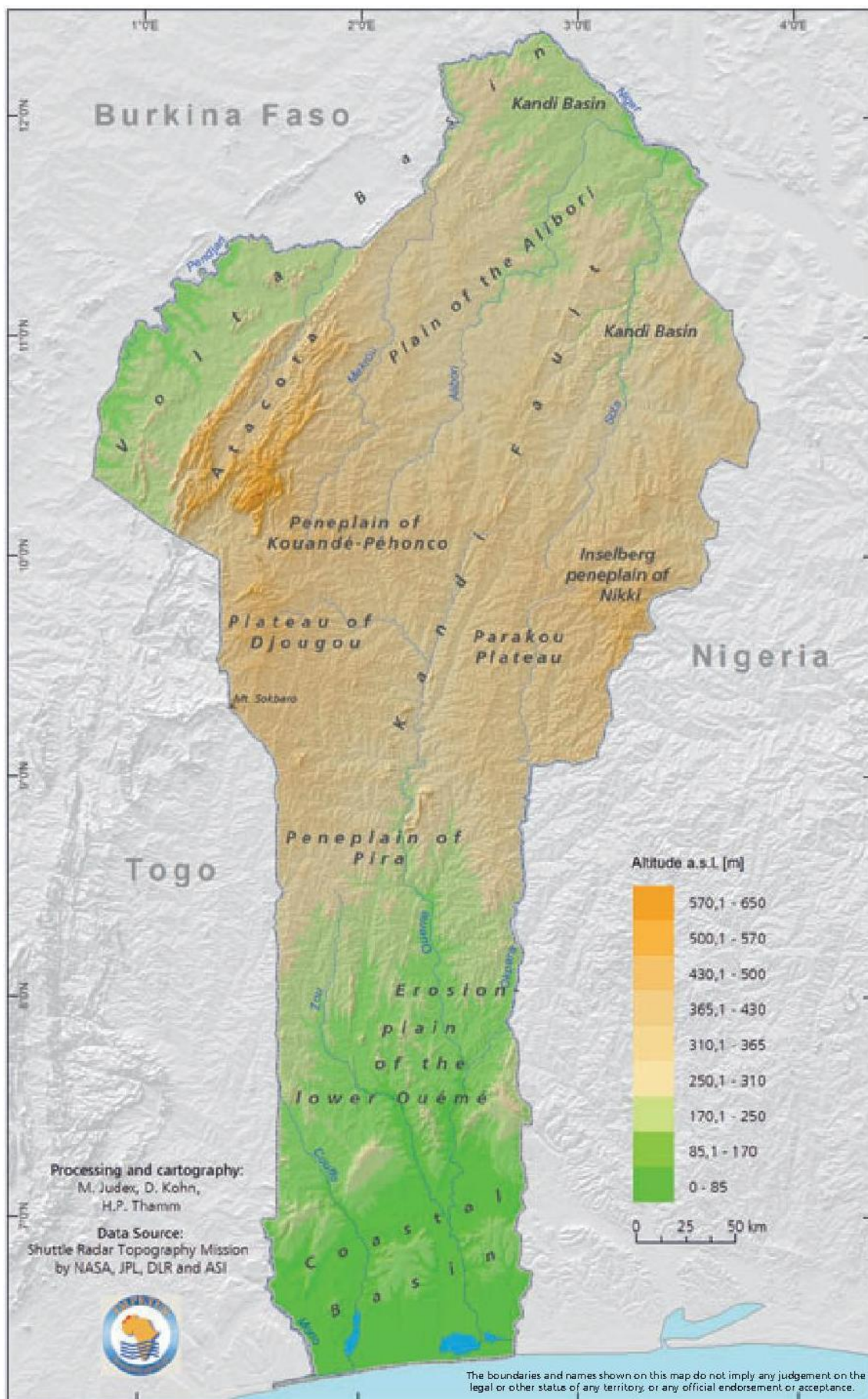


Figure 3-4: Landscape units in Benin (Schönbrodt & Giertz, 2008)

#### 3.1.4- Soils

Although small scale variability of the soils is very high, we can distinguish fersialitic soils (*sols ferrugineux tropicaux*) with high gravel contents on the crystalline basement, while ferralitic and hydromorphic soils prevail in the sedimentary basins in the south of Benin (Giertz & Hiepe, 2008). The soil map (figure 3-5) provides detailed information about the large scale distribution of soils in Benin.

The regional differentiation of soils in Benin roughly corresponds to the large geomorphological units: fersialitic soils on the crystalline basement are characterized by clay translocation and iron segregation (ferruginous tropical soils with concretions), which lead to a clear horizon differentiation (Gaiser *et al.*, 2010). Nevertheless, Richard (2012) notes that soils are not too much diversified and that this means that the geologic origin of soils does not impact much their pedologic nature.

Crusted and lateritic soils are characteristic for the region, causing a significant portion of lateral flow components, surface runoff and interflow (Bormann, 2005a).

#### 3.1.5- Land use and land cover

The Ouémé catchment landscape forms a mosaic of forest islands, gallery forest, savannah, woodlands, agricultural lands, pastures and mosaics of cropland and bush fallow, plantation with *Parkia*, Cashew and palm trees (Bossa, 2012).

However, the dominant land use observed is the small-scale agriculture (Thamm & Judex, 2008). Annual crops like maize, cassava, yam, millet, sorghum, cotton can be found (Sintondji, 2005). In the upper part of the catchment, small-scale agricultural production systems with variable fallow cycles are predominant (Judex *et al.*, 2008).

### 3. Study areas and data

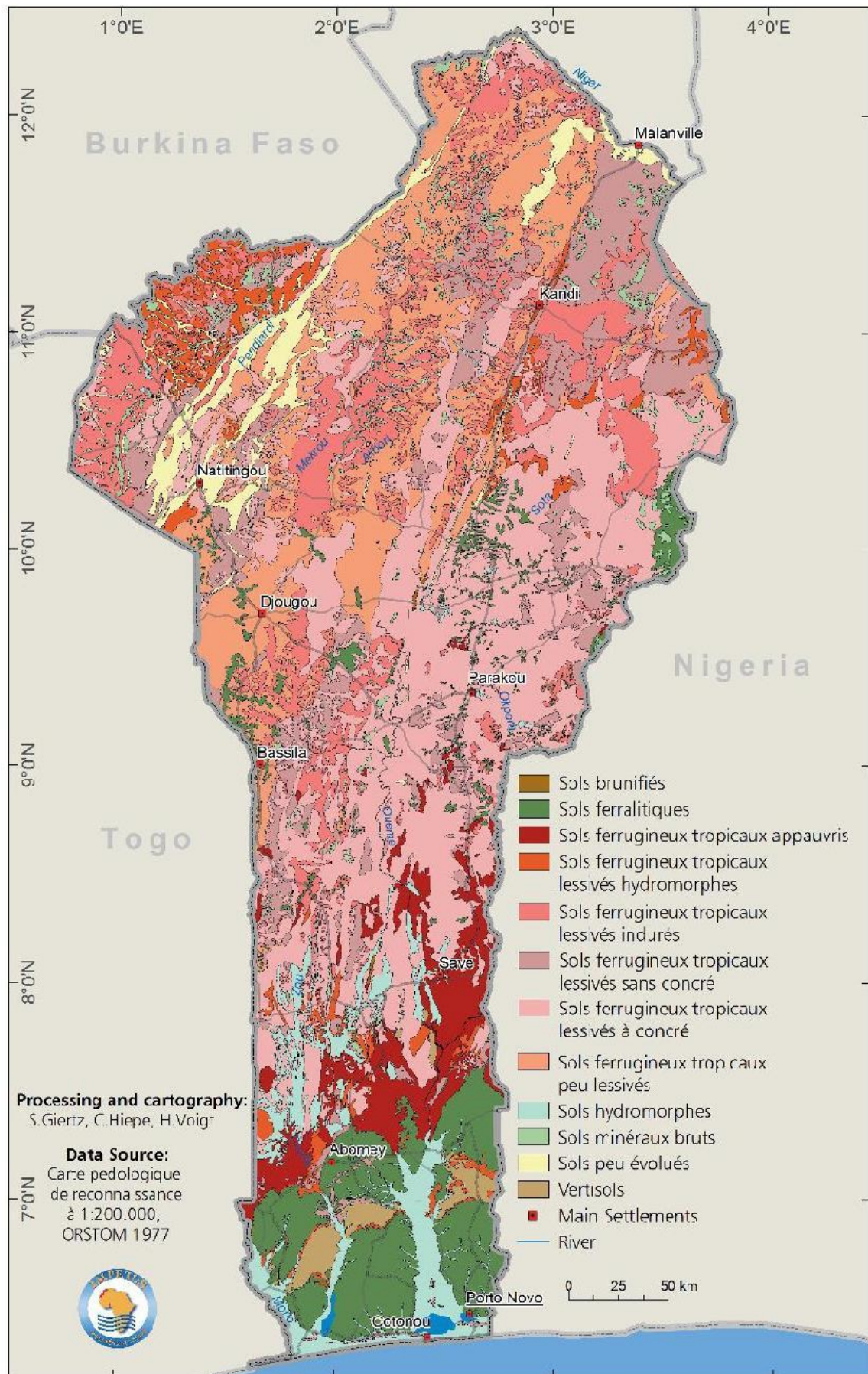


Figure 3-5: Distribution of soil types in Benin from (Giertz & Hiepe, 2008).

The Kandi fault zone is a morphological ridge without settlements and mostly situated in a forest reservation area (El-fahem, 2008). Land use and land cover patterns depend on the local density of the population (Thamm & Judex, 2008):

- Northern part: old settlement areas with high population density like in Parakou and Djougou. Some vast protected state-owned forest areas (*forêt classée*) can be found between Djougou and Parakou, such as the *Forêt de l'Ouémé Supérieur* and the *Forêt de Wari-Marou*. Nevertheless, forests are decreasing due to increasing shortage of cropland because of high population density. Agricultural products are first intended for subsistence but also for sale on regional markets.

- the middle of the catchment between 8° and 9° north latitude: because of the high population growth, the rate of deforestation is also high in the region. The land use patterns are a mixture of fields, fallows, and patches of forest.

- The south of the catchment is characterized by large plantations and intensive agricultural land use. In contrary to the north, dense forests remain (e.g., *Forêt de Locoli*, *Forêt de Lama*).

Figure 3-5 gives an overview of the land use/land cover of the Ouémé catchment. Generally forest is decreasing due to agricultural expansion (Giertz *et al.*, 2006). Together with the gathering of firewood, production of charcoal, selective cutting of valuable trees and uncontrolled bush fire, expansion of agriculture is the reason for that (Sintondji, 2005).

### 3. Study areas and data

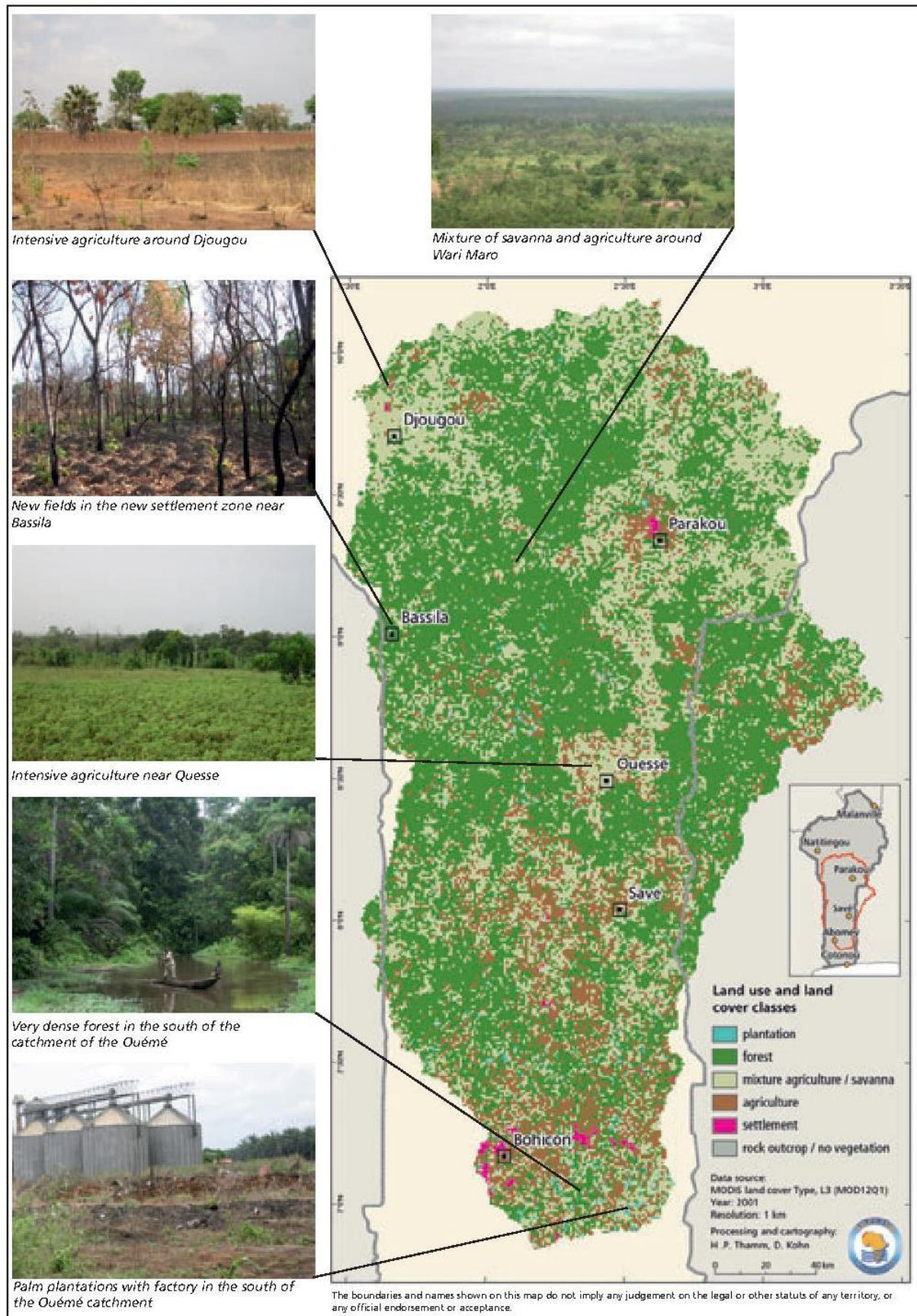


Figure 3-6: Land cover and land use map of the Ouémé catchment with some example pictures.

### 3.2- Geographical overview of Comoé River basin at Mbasso (Côte d'Ivoire)

Located in West Africa, Mbasso catchment (74 900 km<sup>2</sup>) belongs to the Comoé River basin (78 000 km<sup>2</sup>) of which it covers more than 95 % of area (Figure 3-7). Mbasso (Longitude: -3.5°; Latitude: 6.1°) is located in the south of Côte d'Ivoire (Boyer *et al.*, 2006). The Comoé River is the longest river of Côte d'Ivoire (1160 km) and covers four (4) countries: Côte d'Ivoire, Ghana, Burkina Faso and Mali. Altitudes are relatively low and vary from 731 m to 50 m decreasing southwards (Boyer *et al.*, 2006). The geology is characterized by three (3) main formations.

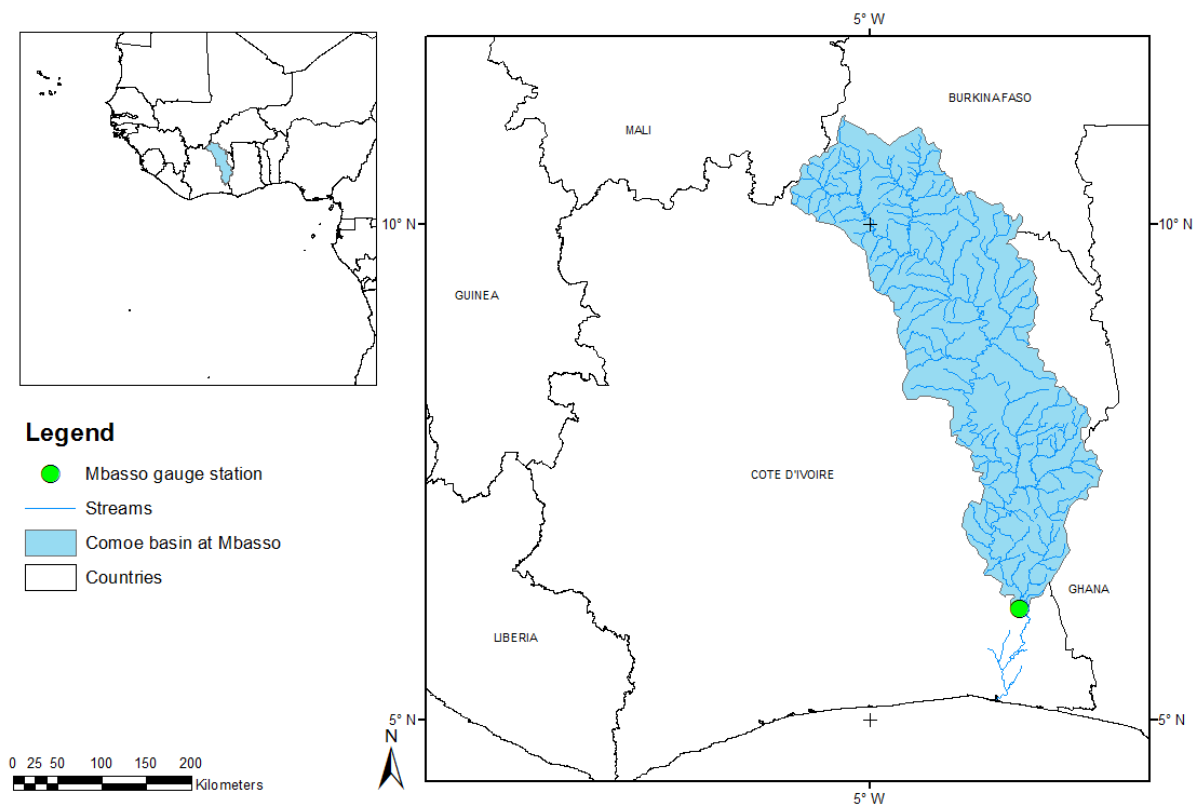


Figure 3-7: Location of Mbasso catchment (74 900 km<sup>2</sup>) in Comoé basin (Côte d'Ivoire) adapted from (Chantraine & Dufour, 1983)

First, a Precambrian platform which consists of Birimian complex and granitoid in the northern and central part of the catchment. Second, Tertiary and Mesozoic era represented in the south by sandy shale. Third, quaternary era composed of sedimentary layers and located in the south. Luvisols, Cambisols, Fluvisols, Acrisols and Ferrasols are the main soils found in the basin (Boyer *et al.*, 2006).

The catchment is divided in three (3) climatic zones: 1) the transitional tropical climate in the north (Zone III); 2) the transitional equatorial climate in the center (Zone II) and 3) the equatorial climate in the south (Zone I). The minimum average temperature recorded at Bobo Dioulasso is 18.8 °C (in January) and the maximum average temperature recorded is 37.2 °C (in February). Average annual precipitation ranges from 1250 to 1700 mm in Zone I, from 1100 to 1600 mm in Zone II and from 1500 to 2500 mm in Zone III. Two (2) main types of vegetation can be found in the catchment: savannah in the north and dense forest in the south with intermediary vegetation. Land use is mainly dominated by agriculture.

#### 3.3- Geographical overview of Sore catchment (Ethiopia)

With an area of 1711 km<sup>2</sup> the Sore catchment is located in the highland region of the Baro-Akobo basin in Ethiopia between 8°21' and 7°49' latitude and 35°31' and 35°57' longitude (Kebede *et al.*, 2014). The elevation of the Sore catchment varies from 2661m to 1547 m and the highest elevation ranges are located east and south. The elevation decreases towards the north and north-west (Figure 3-8) (Kebede *et al.*, 2014). The annual rainfall belongs to the interval [1804-2020] mm. The monthly maximum temperature is between 24°C and 28°C, and the monthly minimum temperature is between 12°C and 14°C. Flow data used for this study were recorded near the town of Mettu.

#### 3.4- Geographical overview of Lookout catchment (USA)

The Lookout catchment is located within the HJ Andrews Experimental Forest (HJA) in the central western Cascade Mountains of Oregon, USA (44.2°N, 122.2°W) (Seibert & McDonnell, 2010).

### 3. Study areas and data

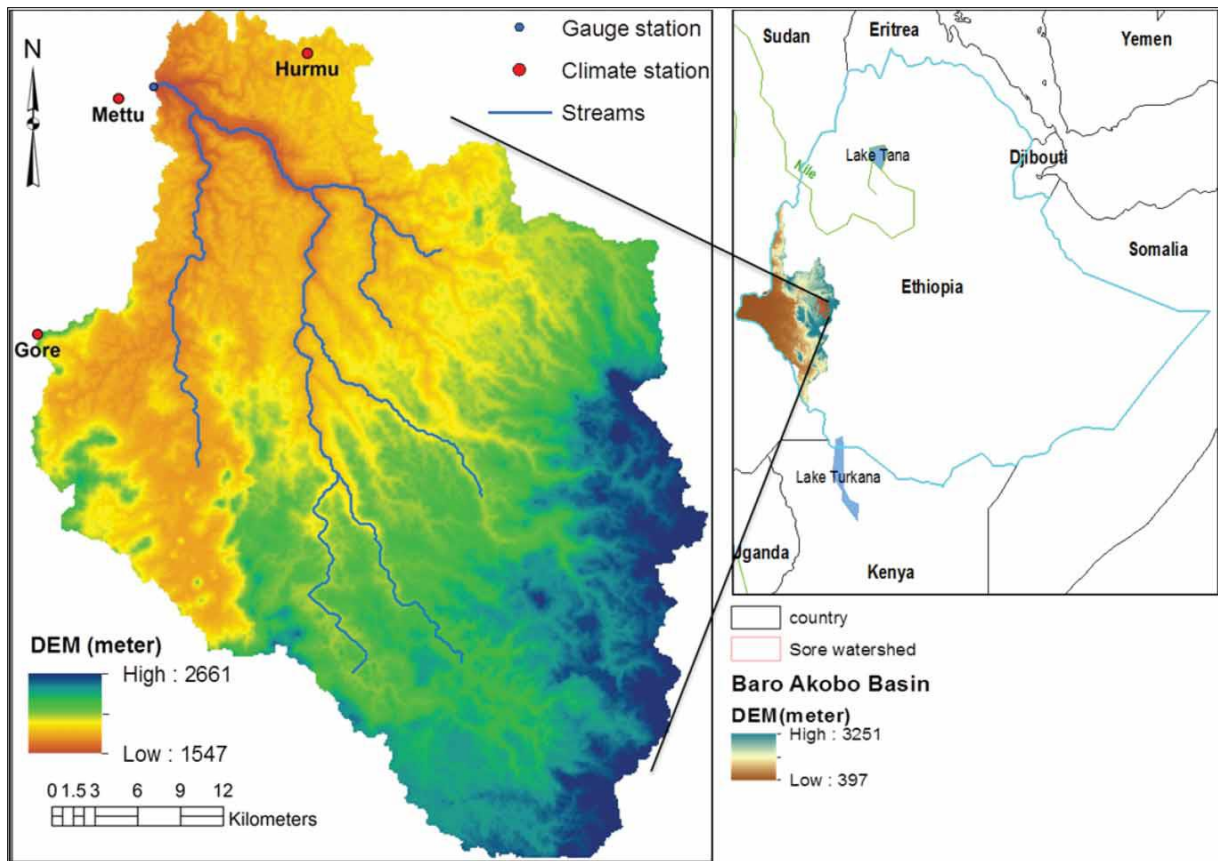


Figure 3-8: Location of Sore catchment (1711 km<sup>2</sup>, Ethiopia), DEM, climate and gauging stations from (Kebede et al., 2014).

With an area of 62 km<sup>2</sup> at the outlet of LOOK, the main drainage within the HJA is Lookout Creek. Elevations range from about 450 to 1600 m (Figure 3-9).

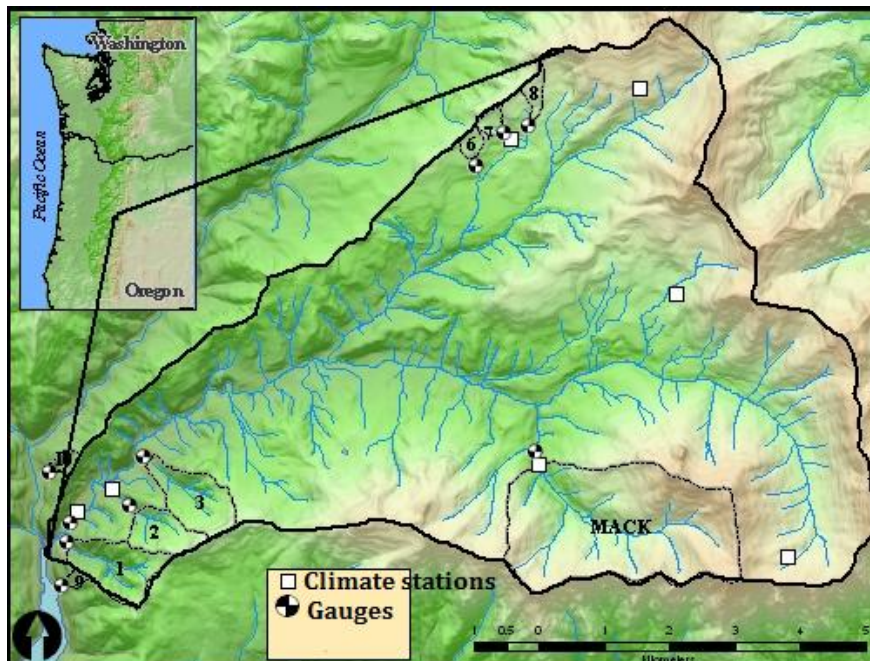


Figure 3-9: Location of Lookout catchment (62 km<sup>2</sup>, USA) DEM, climate and gauging stations (Wikipedia).

The long-term mean annual precipitation varies from about 2300 mm at lower elevations to 3550 mm at upper elevations. Most of the precipitation (about 80%) falls between November and April, typically during long-duration frontal storms of low to moderate intensity (Seibert & McDonnell, 2010).

#### 3.5- Data

##### *3.5.1-Discharge data*

Tables 2-1 and 2-2 give detailed information on the size, location (longitude and latitude) and average discharge of the outlets or stations retained for our work. The catchments are ranked according to increasing area. Daily discharges at the outlets of the catchments were used.

The discharge data were provided by DG-Eau, the General Water Direction of Benin. The annual averaged discharge were estimated from these data while the location data were taken from the Impetus Atlas (Giertz 2008).

The discharge data of Lookout, Le Léguer, Sore and Mbasso were obtained from the respective sources indicated table 2-2.

##### *3.5.2-Precipitation data*

Defined as release of water from the atmosphere to reach the surface of the earth, precipitation is the major input of water to a river catchment area (Davie, 2008). Given that, it is important that it is measured with much accuracy. And yet, this is a very difficult challenge in practice considering the highly variable character of precipitation over the area of a catchment. And it varies as well as spatially, temporally and even in intensity. The variations are mainly influenced by the weather patterns of the region but other factors such as topography and altitude can also cause major variations.

Because the original data from rainfall gauges are punctual, they needed to be spatialized over the catchment before being used as input data in our lumped models. The punctual rainfall data were provided by ASECNA, the national

meteorological catchment but also those located outside and geographically close to the catchment limits.

**Table 3-1: List of the Beninese stations for the study.**

	Stations	River	Area (km <sup>2</sup> )	Longitude	Latitude	Q annual average (m <sup>3</sup> s <sup>-1</sup> )
1	Bokpérou	Donga	32	1.93	9.77	] 0.01, 0.5[
2	Kolokondé	Donga	105	1.69	9.75	]0, 2[
3	Wèwè	Wèwè	261	2.0	9.38	]1,5[
4	Koua	Donga	292	1.77	9.78	]1, 7[
5	Aguimo	Aguimo	396	2.02	9.13	]0.5, 5[
6	Nekété	Donga	409	1.83	9.81	]1,6[
7	Tébou	Ouémé	515	1.87	9.96	]2, 7[
8	Donga Pont	Donga	587	1.95	9.71	]6,12[
9	Sani	Sani	745	2.12	9.76	]8, 25[
10	Donga-Affon	Donga	1308	2.10	9.73	]2, 4[
11	Saramanga	Térou	1360	1.82	9.23	]5, 15[
12	Bori-Gourou	Ouémé	1607	2.40	9.76	]2, 15[
13	Barérou	Yérou Maro	2134	2.37	9.35	]4, 15[
14	Cote238	Térou	3060	2.08	9.08	]10, 45[
15	Aval-Sani	Ouémé	3279	2.15	9.73	]10, 30[
16	Bétérou	Ouémé	10083	2.27	9.2	]25, 100[
17	Savè	Ouémé	23491	2.42	8.0	]60, 210[

Then they were spatialized by the geostatistical method called Kriging. This method is based on the use of the variogram which is a 2-Dimensionnal function that characterizes the spatial correlation of a data set. An experimental variogram is firstly obtained by the treatment of observed values. A variogram model is then calculated by fitting to the experimental points. The variogram model is chosen from a set of mathematical functions that describe spatial relationships.

In our case, for each catchment of the Ouémé River basin, a variogram model was calculated for each year from the daily precipitation. The data of a given year were interpolated by using the variogram model of this particular year. Each

### 3. Study areas and data

catchment was discretized into spatial square grids of dimensions 2km x 2km. The daily precipitation was estimated for each grid and then averaged over the catchment. The variograms were computed with the programming tool IDL 6.1 (Research Systems, 2004) and data were spatialised with the software Surfer 8 (Golden Software Inc., 2002).

**Table 3-2: List of the other stations for the study.**

	Catchment	Station	Country	Size (km <sup>2</sup> )	Longitude	Latitude	Q annual average (m <sup>3</sup> s <sup>-1</sup> )	Source of data
1	Lookout Creek	LOOK	USA	62	122.2	44.2	3	(Seibert & McDonnell, 2010)
2	Le Léguer	Belle-Isle-en-Terre	FRANCE	260	3.4	48.5	4	GR4J sample file (Perrin <i>et al.</i> , 2003)
3	Sore	Mettu	ETHIOPIA	1 711	35	8	45	(Kebede <i>et al.</i> , 2014)
4	Mbasso	Mbasso	COTE D'IVOIRE	74 900	-3.5	6.1	111	(Boyer <i>et al.</i> , 2006)

The spatialized precipitation data of Lookout, Le Léguer, Sore and Mbasso were obtained from the respective sources indicated table 2-2.

#### 3.5.3-Potential Evapotranspiration (ETP) data

The evaporation of water is a crucial process in hydrology and climate (Grayson & Blöschl, 2000). Indeed, two main factors determine the importance of evaporation which are the available energy and the amount of water present. These two factors are both dependant on the climate of a particular region.

The first driver which is the available energy is the balance between solar and terrestrial radiation: the net radiation. Energy is required so that to convert liquid water into gaseous water vapour. The second driver, water is present as water bodies (lakes, streams or the oceans), moisture in the soil or water for plants (transpiration through opening or closing of stomata in the leaf). Water availability interacts with plant ecophysiology and controls vegetation functioning (Fatichi *et al.*, 2015) and then transpiration.

Many other factors influence evaporation: the temperature at the evaporating surface and that of the ambient air, the vapour pressure of the existing water vapour in the air. It is also important to mention the wind speed which plays an important role in the evaporation process in the sense that the replacement of saturated air by drier air enables the air to absorb more water vapour.

Both evaporation from an open surface and from a vegetated surface are affected by these factors, but in the latter case, evaporation depends also on the presence of negative pressure potential within the soil (Shaw *et al.*, 2011) .

Evaporation from a land surface comprises the evaporation of liquid water from precipitation collected on the land surface, from wetted soils and the transpiration of water by plants. This is called evapotranspiration. One can distinguish two types of evapotranspiration, the potential one and the actual one. Potential evapotranspiration (ETP) can be defined as the evapotranspiration that would occur if the water supply were unlimited (Weiß & Menzel, 2008) while actual evaporation ( $E_t$ ) is that which actually occurs (i.e. if there is not much available water actual will be less than potential but if there is enough water actual is equal potential) (Davie, 2008).

We generally assume the evapotranspiration to be relatively conservative over an area, so that a measurement at one site will give a good estimate of the flux over a larger area. However this assumption is good when the energy inputs are a limitation to the rates of actual evapotranspiration; this assumption may be bad when rates of actual evapotranspiration are limited by water availability like for example in the dry season. At the catchment or landscape scale, the *complementary concept*, introduced by Bouchet (1963 cited by (Shaw *et al.*, 2011)), states that there is a feedback mechanism whereby changes in actual evapotranspiration  $E_t$  over the area alter the temperature and humidity of the over-passing air which in turn changes ETP.

However, in our study because of data availability, we applied the closest synoptic stations measurements to the catchments. That would be interesting to apply this concept in further studies.

In our modelling approach we used the Daily Potential Evapotranspiration (ETP) of the area that was computed by ASECNA, the national meteorological services using the Penman-Monteith formula. This formula is based on a combination of energy balance and mass transfer equations. As recalled by Grayson & Blöschl (2000) it is the most fundamental equation available to examine the evaporation process (See Equation 3.1):

$$ETP = \frac{s \cdot (R_n - G) + \rho \cdot c_p \cdot D / r_a}{s + \gamma \cdot (1 + r_c / r_a)} \quad \text{Eq.3.1}$$

Where  $s$  is the slope of the saturation specific humidity versus temperature relation;  $\rho$  is density of air;  $c_p$  is specific heat of air;  $\gamma$  is  $c_p/L$  where  $L$  is latent heat of vaporisation,  $D$  is saturation deficit or saturation minus actual specific humidity,  $r_a$  is aerodynamic resistance, and  $r_c$  is stomatal resistance.

The values were computed for the synoptic stations of Parakou and Savè. The values of ETP were attributed to the different catchments according to the geographical closeness.

The Potential Evapotranspiration (ETP) data of Lookout, Le Léguer, Sore and Mbasso were obtained from the respective sources indicated Table 2-2.

# APPLICATION OF MODHYPMA



Photo 4: Collection of water levels data at Borigourou station (1607 km<sup>2</sup>)

## 4- Application of MODHYPMA

### 4.1- Model calibration approach and Criteria of performance

Addressing the assessment of model performance requires the definition of a procedure. In the first step the values of model parameters need to be estimated. They cannot be generally measured on the field. And when they are, single values obtained from point measurements are not representative of a much larger spatial unit or the whole catchment because of the heterogeneity in space and non-stationarity in time (Beven, 2008). Calibration is then necessary to get model parameters. For that purpose, model outputs are compared to observations. The model result is expected to closely match the observations. In order to obtain the best fit, an optimum parameters set is generally searched. This optimization may be done according to a manual (by the modeller) or automatic approach (by some computerised optimisation algorithm). Table 4-1 gives an overview of the main comparative features between these two approaches.

**Table 4-1: Comparative feaures of Manual-Expert and Automatic calibration (from (Duan *et al.*, 2003)).**

<b>Manual calibration</b>	<b>Automatic Calibration</b>
User knowledge and expertise	Speed and power of computer
Subjective (realistic)	Objective (statistics)
Complicated and highly labour intensive	Computer intensive
Time consuming	Time saving
Excellent results	Results may not be acceptable

Automatic calibration relies on a computer algorithm which performs numerous trials of the model. This approach is objective; in fact one or several objective functions are to be optimized while the computer explores the parameter space. In contrast, the main particularity of manual approach is that it is based on human judgment without having recourse to a computer algorithm. The user

adjusts the parameters interactively in successive model runs (Wheater *et al.*, 2008). Although this approach is time consuming, it allows the user to integrate different signals (peaks, recessions, low flows,...) at once. At some point both approaches can be combined somehow. This is what we did in the present research.

In order to decide on the 'best fit', the modeller needs to rely on performance criteria whatever the calibration approach chosen. There exist in the literature numerous criteria which may be used to evaluate the goodness-of-fit of a model. Nevertheless, none of them is able on its own to perform ideally (Krause *et al.*, 2005). Depending on the purpose of the modelling task, low flow, high flow, total discharge or other aspects are important. This requires adapted calibration strategies and adapted model quality measures. Many authors acknowledge the use of multiple evaluation techniques and consider it as an integral part of the ideal model calibration procedure (Moriasi *et al.*, 2007, Wagener *et al.*, 2001). As commented by Gupta *et al.* (2009), the calibration process is a multi-objective problem as we seek, for example, at matching the overall volume of flow, flow variability but also fitting the timing and shape of the hydrograph. Besides, Beven (2012) defined similar requirements for a rainfall-runoff model and insists that the visual inspection of plots of observed and predicted variables is indispensable. In fact, it is recommended to have recourse to both qualitative and quantitative criteria because both numerical criteria and visual analysis allow for capturing distinct aspects of model performance (Ritter & Muñoz-Carpena, 2013). Biondi *et al.* (2012) also argue that in spite of the large number of existing goodness-of-fit metrics, visual inspection is still very important as it allows the analysis of temporal dynamics and error occurrence patterns.

Due to the fact that one numerical criterion cannot catch all the information about the quality of the model (Stanislaw, 1998), various criteria must be used. Indeed, it is crucial that calibration methodologies should extract as much information as possible from available data (Duan *et al.*, 2003). Wheeler *et al.* (2008) claim that more information can be extracted from available data if various objective

functions are used. We have chosen eight numerical criteria of which the Nash-Sutcliffe efficiency (NSE) calculated on flows, the NSE calculated on root squared transformed flows, the NSE calculated on log transformed flows, the Kling Gupta Efficiency KGE (Gupta *et al.*, 2009), the Percent Bias (PBIAS) and the Absolute Percent Bias (APBIAS), The weighted coefficient of determination -WR<sup>2</sup> (Krause *et al.*, 2005) and the coefficient of determination (R<sup>2</sup>). The Nash-Sutcliffe criterion is largely used in hydrology but is criticised because it tends to strongly overestimate larger values in a time series whereas lower values are neglected (Krause *et al.*, 2005). The NSE calculated on root squared transformed flows is said to be more suitable for an all-purpose model (Pushpalatha *et al.*, 2012). In the calculation of the NSE calculated on log transformed flows, it is needed to add a small constant (here one-twentieth was chosen) to the discharge values before applying the Logarithm function. The Kling Gupta Efficiency KGE is derived from the NSE and is said to more account for the linear correlation, the bias and the variability of flow (Gupta *et al.* 2009, Kling *et al.* 2012). The weighted coefficient of determination (WR<sup>2</sup>) allows to correct the insensitivity of the R<sup>2</sup> to additive and proportional differences between model predictions and measured data. WR<sup>2</sup> is weighted with the value of the gradient **b** of the regression on which R<sup>2</sup> is based. Equation 4.1 gives the expression of WR<sup>2</sup>. For further details concerning this criterion refer to Krause *et al.* (2005).

$$WR^2 = \begin{cases} |b| \cdot R^2 & \text{for } b \leq 1 \\ |b|^{-1} \cdot R^2 & \text{for } b > 1 \end{cases} \quad \text{Eq. 4.1}$$

The equations of the rest of the criteria of performance are given in Appendix A. The selection of a large number of evaluation criteria (eight) is also motivated by the purpose of the study which is the assessment of a very new modelling approach. In fact, we are interested to see how the various criteria would evolve. From the literature cited above it is clear that only a combination of quality measures would provide a comprehensive assessment of model quality although single quality measures are correlated.

#### 4. Application of MODHYPMA

---

In terms of visual analysis, we applied two commonly used graphical techniques namely the hydrographs and percent exceedance probability curves which are said to be particularly relevant (Moriassi *et al.*, 2007).

For the calibration of MODHYPMA, the model was run over the whole parameter space by defining discrete increments on each parameter range and the parameter response surface for each performance criterion was drawn. The calibrated parameter set was chosen according to the following calibration scheme:

- (a) elimination of all parameter sets which give  $NSE < 0.5$ ;
- (b) among the remaining parameter sets, elimination of those who have Nash LOG Q and Nash RQ  $< 0.4$ ;
- (c) among the remaining parameter sets, elimination of those who have a PBIAS  $> 15\%$ ; generally at this stage the remaining goodness-of-fit statistics are acceptable;
- (d) at this step, there are only few parameter sets left; their hydrographs are analyzed and the “best” fit is chosen considering the timing, high and low flows, the recession curve.

We consider the simulation to be accepted if the  $NSE > 0.5$  and if we obtain a fairly good graphical fit. The latter part is subjective but this is inevitable if the recommendations of Beven (2012) and others are considered.

When model results are compared to observations, Beven (2012) insists that the data should contain enough information to support the robust optimisation of the parameter values. In the opposite side the data might contain inconsistencies (disinformative data). The various periods of simulation were chosen according to the existence and quality of the data. In addition, for a given catchment we tried to choose both dry and wet years. The shortness of some series is justified by the data quality and availability. On many catchments data collection equipment were installed very recently. The percentage of missing data per year

is sometimes very high (more than 50 %). Given the shortness of the series, data were duplicated to serve as warm-up data. We also checked for obvious inconsistencies.

#### 4.2- Model results

The results from MODHYPMA model were good. As we can see from the box plot (Figure 4-1) the interquartile range is roughly [0.6-0.8] for the NSE criterion, [0.7-0.9] for the Nash Root criterion, [0.6-0.85] for the Nash Log criterion, [0.6-0.8] for the KGE, [(-0.15)-0.15] for the Percent Bias, [0.3-0.5] for the Absolute Percent Bias, [0.4-0.7] for the Weighted  $R^2$  and [0.65-0.8] for the  $R^2$ . For the plotting of (Figure 4-1), we used both calibration and validation data. Generally, we noticed small loss of performance from calibration to validation and in some cases, the performance is even better in the validation period. Detailed values of performance criteria are given in Table 4-2.

Comments about the performance of the model on the various tested catchments are presented in Table 4-3. We can see from the table that MODHYPMA was not sufficient for Sore (1711 km<sup>2</sup>) in the calibration period; for Aguimo (402 km<sup>2</sup>) and Mbasso (74900 km<sup>2</sup>) in the validation period; for Bokpéro (32 km<sup>2</sup>), Kolokondé (105 km<sup>2</sup>), Wèwè (261 km<sup>2</sup>) and Tébou (515 km<sup>2</sup>) for the calibration and the validation periods.

For all runs, we can say that the beginning of the season is globally well simulated but sometimes underestimated. The recession curve is very well simulated. Low flows seem to be overestimated. Middle flows are well represented. MODHYPMA tends to underestimate the highest flows. The model is subject to some timing errors.

4. Application of MODHYPMA

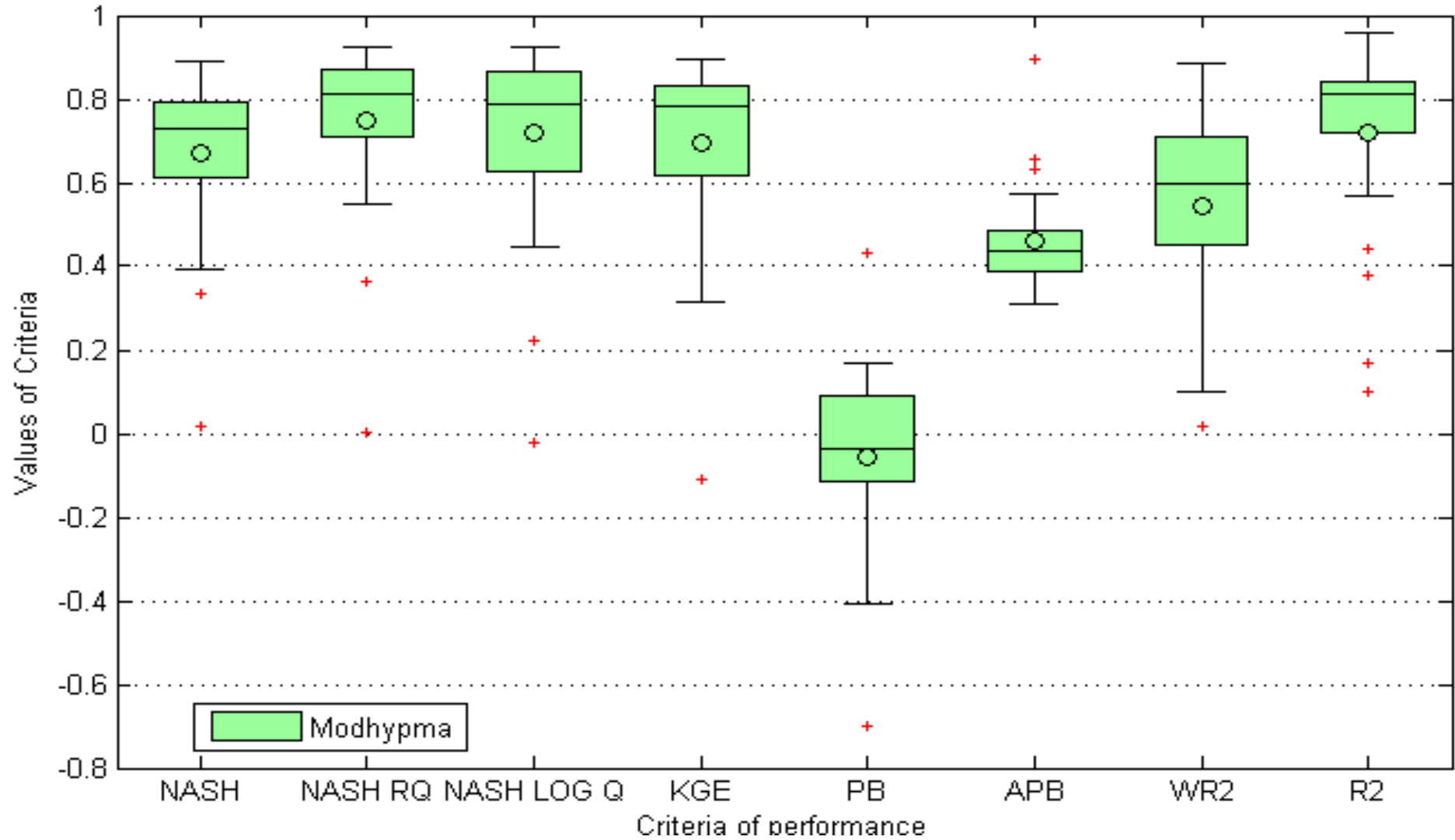


Figure 4-1: Box plot of the criteria of performance for MODHYPMA. Crossbar: Median; Circle: Mean; length of box: interquartile range (25th and 75th percentiles); tails: furthest values within the whisker length (length of the interquartile range); Red + sign : Outliers.

#### 4. Application of MODHYPMA

Table 4-2: Overview of the results obtained from the model runs.

N°	1	2	3	4	5	6	7	8	9	10	11	12	13	14	15	16	17
<b>Stations</b>	Look out	Le Léguer	Koua	Agui mo	Neké té	Donga Pont	Sani	Donga-Affon	Sara-manga	Bori-Gourou	Sore	Barérou	Cote 238	Aval-Sani	Bétérou	Savè	Mba sso
<b>Country</b>	USA	FRANCE	BE NIN	BE NIN	BE NIN	BE NIN	BENIN	BENIN	BE NIN	BENIN	ETHI OPIA	BENIN	BE NIN	BE NIN	BE NIN	BENIN	CI
<b>Cal.period</b>	1978-1987	1991-1992	2002-2004	2000-2001	2002-2003	1999	2004-2005	1999&2001	2001-2002	2000-2002	1990-1993	2001 & 2005	2001-2001	2001-2002	1998-2003	1996-99/02-03	1979-1987
<b>Val.period</b>	1988-1998	-	2004-2006	2004-2005	2004	2001	-	2005	2005	2003-2005	1994-1997	-	2005	2003&2005	2004-6/8-10	2004-2009	1992-1998
<b>Area (km<sup>2</sup>)</b>	62	260	292	396	409	587	745	1 308	1 360	1 607	1 711	2 134	3 060	3 279	10 083	23 491	74 900
$\nu$	1.38	1.72	1.27	1.05	0.95	1.25	1.00	1.20	1.09	0.92	1.30	1.08	1.04	1.01	0.99	1.03	1.00
$\lambda$	29	5	11	13	5	11	15	14	10	13	30	15	13	10	16	12	20
TX	0.00	0.00	0.95	0.40	0.00	0.80	0.00	0.37	0.30	0.12	0.00	0.30	0.17	0.00	0.10	0.20	0.00
NSE CAL	0.72	0.61	0.78	0.75	0.77	0.67	0.80	0.78	0.79	0.84	0.48	0.83	0.83	0.72	0.89	0.84	0.60
NSE VAL	0.65	-	0.80	0.02	0.60	0.80	-	0.61	0.57	0.73	0.78	-	0.73	0.81	0.76	0.72	0.43
NRQ CAL	0.74	0.55	0.75	0.70	0.87	0.81	0.76	0.90	0.84	0.81	0.68	0.87	0.92	0.84	0.92	0.90	0.71
NRQ VAL	0.71	-	0.74	0.00	0.66	0.87	-	0.79	0.82	0.80	0.83	-	0.85	0.88	0.87	0.77	0.62
NLQ CAL	0.75	0.45	0.67	0.47	0.82	0.86	0.53	0.89	0.82	0.58	0.79	0.87	0.92	0.82	0.91	0.89	0.70
NLQ VAL	0.78	-	0.73	-0.02	0.53	0.79	-	0.83	0.92	0.63	0.80	-	0.82	0.90	0.90	0.73	0.68
KGE CAL	0.85	0.62	0.62	0.83	0.81	0.77	0.82	0.72	0.83	0.88	0.33	0.80	0.79	0.77	0.86	0.90	0.63
KGE VAL	0.81	-	0.71	-0.11	0.69	0.84	-	0.48	0.75	0.57	0.82	-	0.78	0.82	0.64	0.83	0.32
PB CAL	-0.05	-0.08	0.36	-0.11	0.45	0.01	0.00	-0.11	0.11	0.09	-0.41	-0.06	-0.02	0.09	0.01	0.05	-0.17
PB VAL	-0.04	-	0.23	-0.70	-0.16	0.13	-	0.43	-0.11	-0.26	-0.03	-	-0.12	0.14	-0.20	0.09	-0.36
APB CAL	0.39	0.46	0.62	0.47	0.44	0.51	0.34	0.39	0.43	0.41	0.48	0.43	0.33	0.48	0.31	0.34	0.57
APB VAL	0.43	-	0.62	0.90	0.69	0.46	-	0.54	0.52	0.44	0.36	-	0.42	0.40	0.39	0.46	0.65
WR <sup>2</sup> CAL	0.68	0.31	0.82	0.65	0.57	0.47	0.77	0.56	0.68	0.80	0.36	0.46	0.62	0.61	0.77	0.77	0.49
WR <sup>2</sup> VAL	0.56	-	0.82	0.02	0.31	0.71	-	0.71	0.45	0.44	0.66	-	0.56	0.73	0.60	0.89	0.13
R <sup>2</sup> CAL	0.82	0.57	0.83	0.76	0.76	0.67	0.82	0.81	0.81	0.85	0.86	0.60	0.83	0.84	0.93	0.87	0.84
R <sup>2</sup> VAL	0.72	-	0.88	0.10	0.64	0.81	-	0.80	0.61	0.73	0.86	-	0.74	0.76	0.92	0.96	0.38

#### 4. Application of MODHYPMA

**Table 4-3: Comments about MODHYPMA performance.**

N°	Stations	Country	Area (km <sup>2</sup> )	Model Performance		Comments
				Calibration	Validation	
1	Bokpérou	BENIN	32	Not sufficient		The model is not able to catch the dynamics of the flow
2	Lookout	USA	62	Sufficient		Good timing but slight underestimation of highest peaks
3	Kolokondé	BENIN	105	Not sufficient		Systematic and important underestimation of flows
4	Le Léguer	FRANCE	260	Sufficient		Acceptable simulation but some middle and high flows are underestimated and some low flows are overestimated
5	Wèwè	BENIN	261	Not sufficient		Systematic and important underestimation of flows
6	Koua	BENIN	292	Sufficient		Good timing, peaks well simulated but slight underestimation of the flows of the beginning of season
7	Aguimo	BENIN	396	Sufficient	Not sufficient	Systematic and important underestimation of flows
8	Nekété	BENIN	409	Sufficient		Good timing but underestimation of peaks
9	Tébou	BENIN	515	Not sufficient		Good timing but large underestimation of peaks
10	Donga Pont	BENIN	587	Sufficient		Middle flows well simulated but underestimation of some peaks
11	Sani	BENIN	745	Sufficient		Good timing, peaks well simulated
12	Donga-Affon	BENIN	1308	Sufficient		Good timing but underestimation of highest peaks
13	Saramanga	BENIN	1360	Sufficient		Highest peaks not well simulated
14	Bori-Gourou	BENIN	1607	Sufficient		Highest peaks not well simulated
15	Sore	ETHIOPIA	1711	Sufficient	Not sufficient	Good timing and simulation of flows. In calibration peaks are underestimated
16	Barérou	BENIN	2134	Sufficient		Good timing but underestimation of some highest peaks
17	Cote238	BENIN	3060	Sufficient		Good timing but underestimation of some highest peaks
18	Aval-Sani	BENIN	3279	Sufficient		Good timing but underestimation of some highest peaks
19	Bétérou	BENIN	10083	Sufficient		Good timing but underestimation of some highest peaks
20	Savè	BENIN	23491	Sufficient		Good timing but underestimation of some highest peaks
21	Mbasso	CI	74900	Sufficient	Not sufficient	Good timing but underestimation of some highest peaks

The observed and simulated hydrographs of Bétérou catchment (10 083 km<sup>2</sup>) in calibration and validation are shown respectively in Figures 4-2 and 4-3. The observed and simulated flow duration curves of the same catchment (10 083

km<sup>2</sup>) in calibration and validation are provided respectively in figures 4-4 and 4-5. The beginning of the season is quite well simulated apart from some slight underestimations. The timing is good and the recession flows well simulated. Nonetheless some highest peaks are underestimated especially in validation. These observations are confirmed by the flow duration curves where the blue curve is under the red one when the probability of exceedance is less than 0.1. In Appendix B are presented the parameter response surface for each criterion for Bétérou catchment.

As well the observed and simulated hydrographs of Lookout catchment (62 km<sup>2</sup>) in calibration and validation are shown respectively in Figures 4-6 and 4-7. The observed and simulated flow duration curves of the same catchment (62 km<sup>2</sup>) in calibration and validation are provided respectively in Figures 4-8 and 4-9. The timing is quite good. Some highest peaks in calibration are underestimated. The flow duration curves match almost perfectly.

#### 4.3- Discussion and Conclusion

The limited applicability of the model to Bokpérou (32 km<sup>2</sup>) can be explained by the fact that a daily time step may be longer than the storm response time of the catchment and a finer time resolution may be necessary in order to better model the dynamics of the discharge but also the peaks of the hydrographs (Beven, 2012). The study conducted by Varado *et al.* (2006) on the Donga upstream catchments (particularly Ara and Bokpérou) confirms this. MODHYPMA was not sufficient for some catchments with concentration time lower than 1 day namely Wèwè and Kolokondé. Data quality may be questioned. Nevertheless, the model has to be improved. Further research could be the reassessment of hypotheses underlying computations; the development towards a semi-distributed version in order to better represent the spatial variability of the processes. Furthermore, the fact that the model is spatially lumped is usually a source of errors in the prediction of the hydrograph peaks. Actually, the spatial distribution and intensity of the storms is not accounted for (Kitanidis & Bras, 1980).

#### 4. Application of MODHYPMA

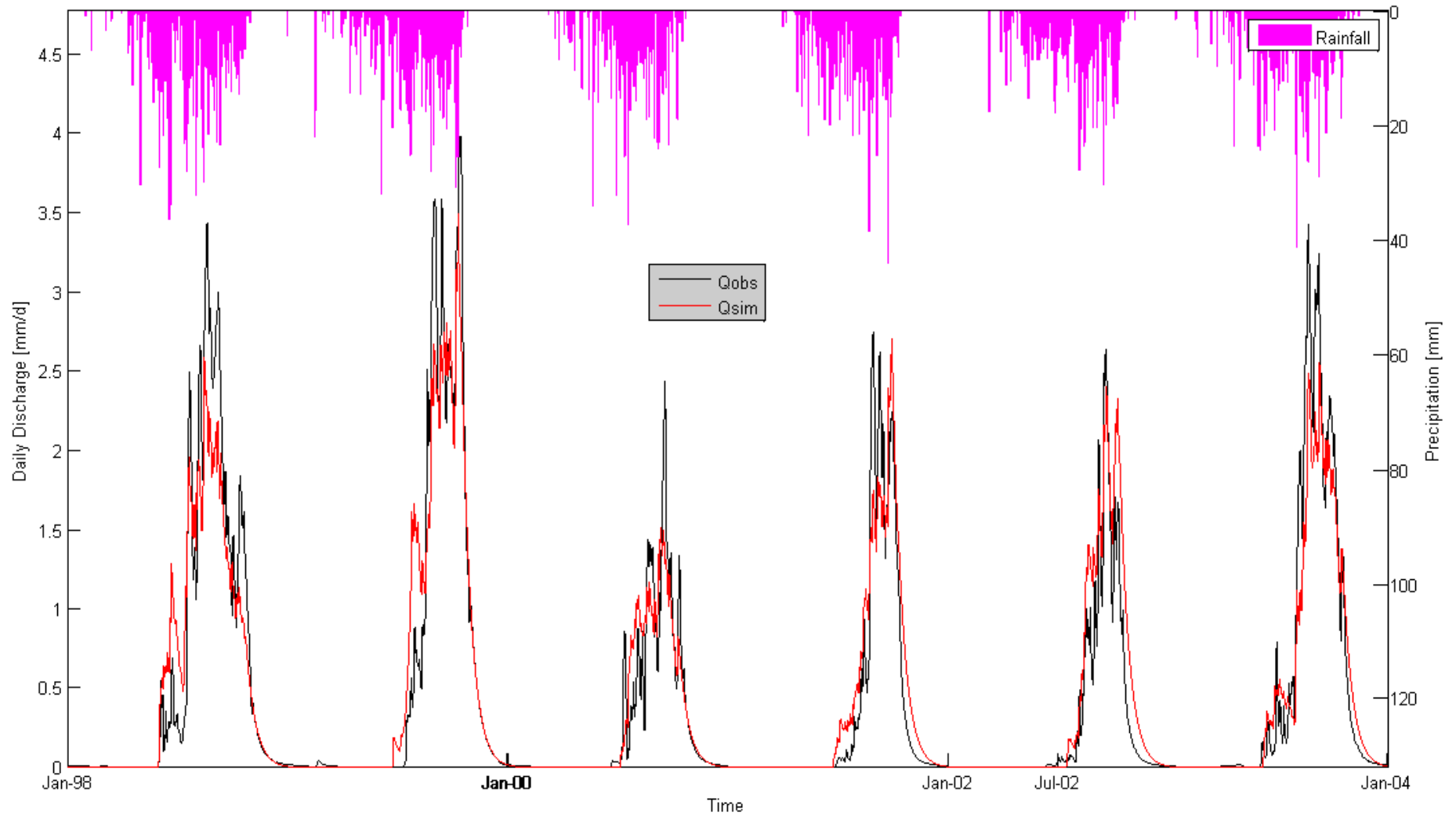


Figure 4-2: Application of MODHYPMA to Bétérou catchment (10 083 km<sup>2</sup>) in calibration.

#### 4. Application of MODHYPMA

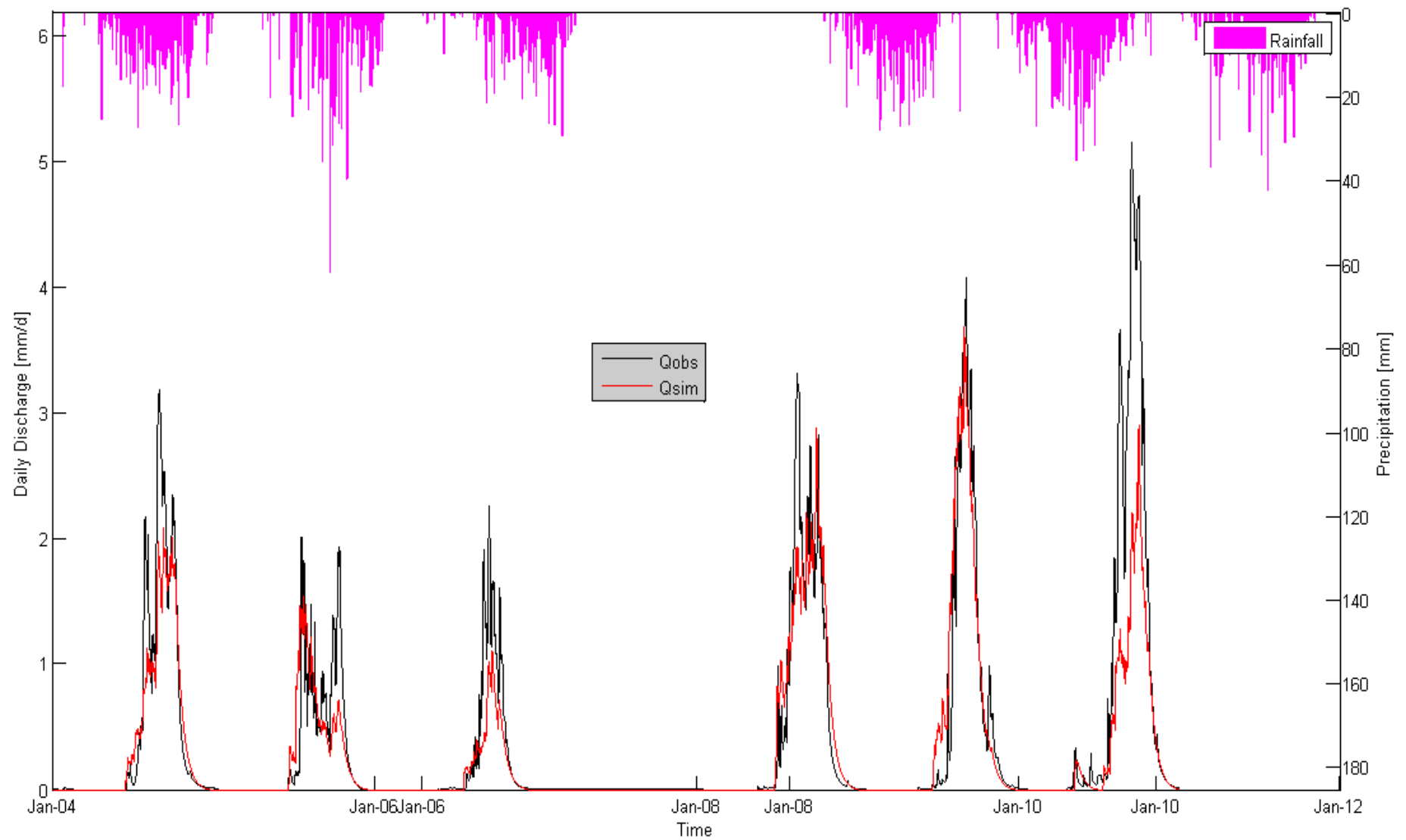


Figure 4-3: Application of MODHYPMA to Bétérou catchment (10 083 km<sup>2</sup>) in validation.

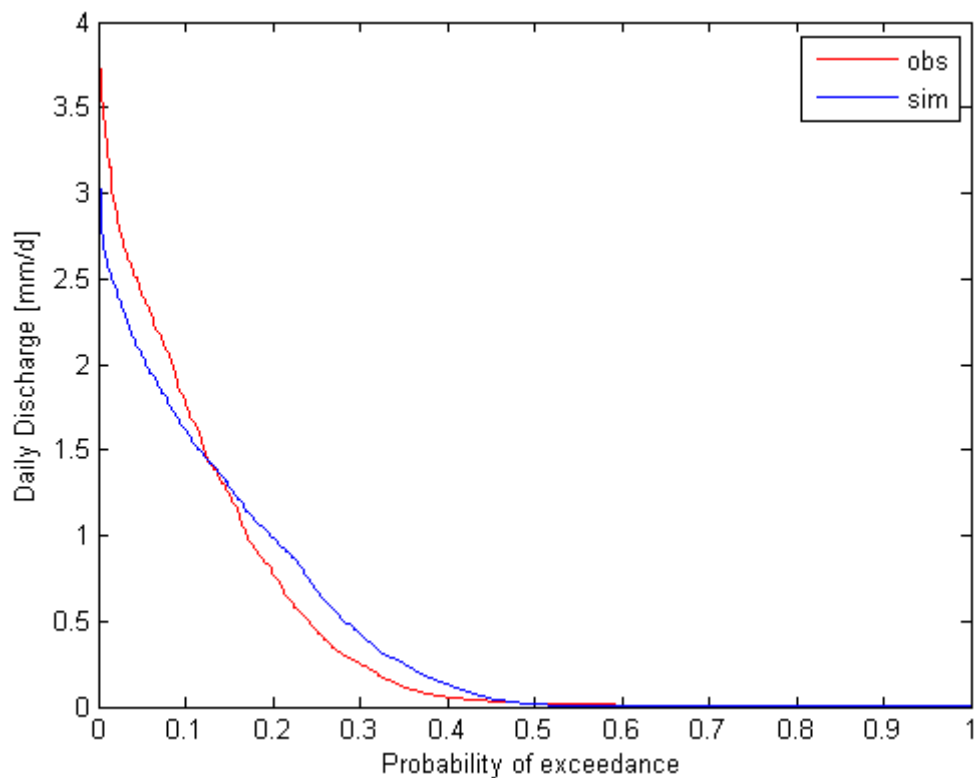


Figure 4-4: Flow duration curves in the Bétérou catchment (10 083 km<sup>2</sup>) in calibration.

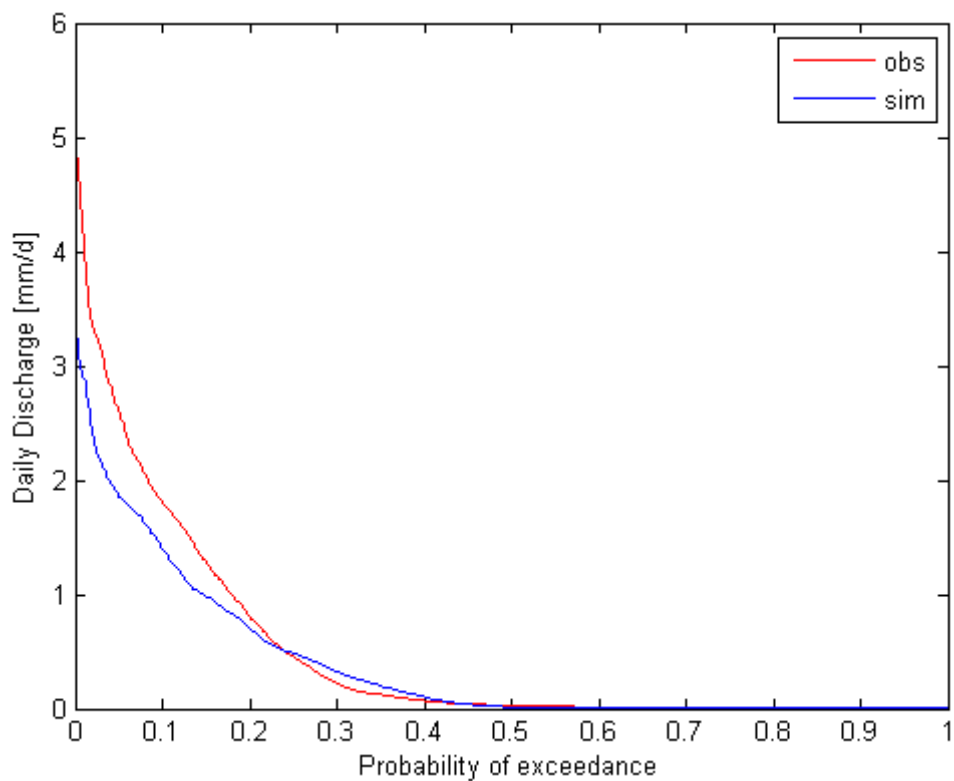


Figure 4-5: Flow duration curves in the Bétérou catchment (10 083 km<sup>2</sup>) in validation.

#### 4. Application of MODHYPMA

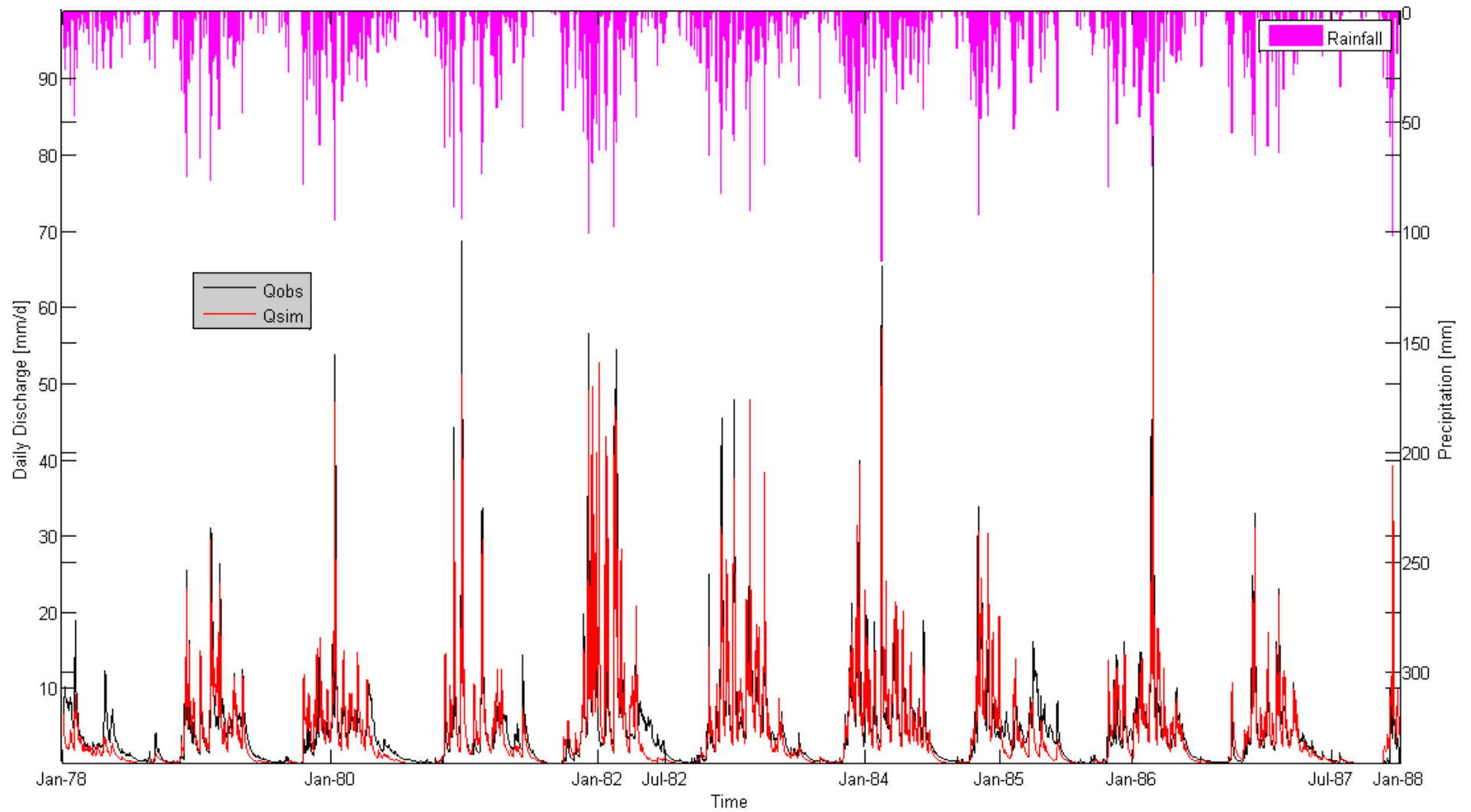


Figure 4-6: Application of MODHYPMA to Lookout Creek catchment (USA), 62 km<sup>2</sup> in calibration.

#### 4. Application of MODHYPMA

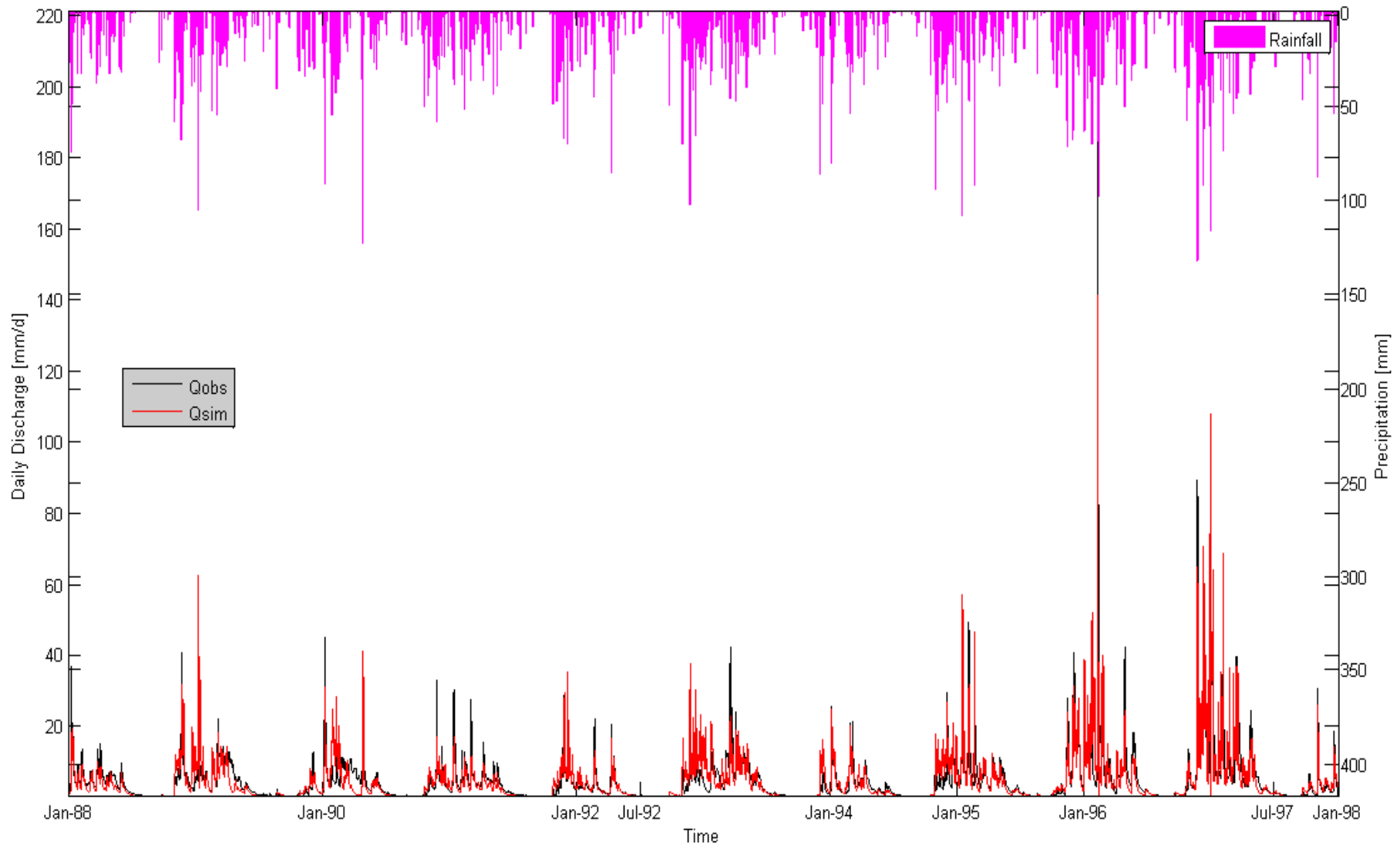


Figure 4-7: Application of MODHYPMA to Lookout Creek catchment (USA), 62 km<sup>2</sup> in validation.

#### 4. Application of MODHYPMA

---

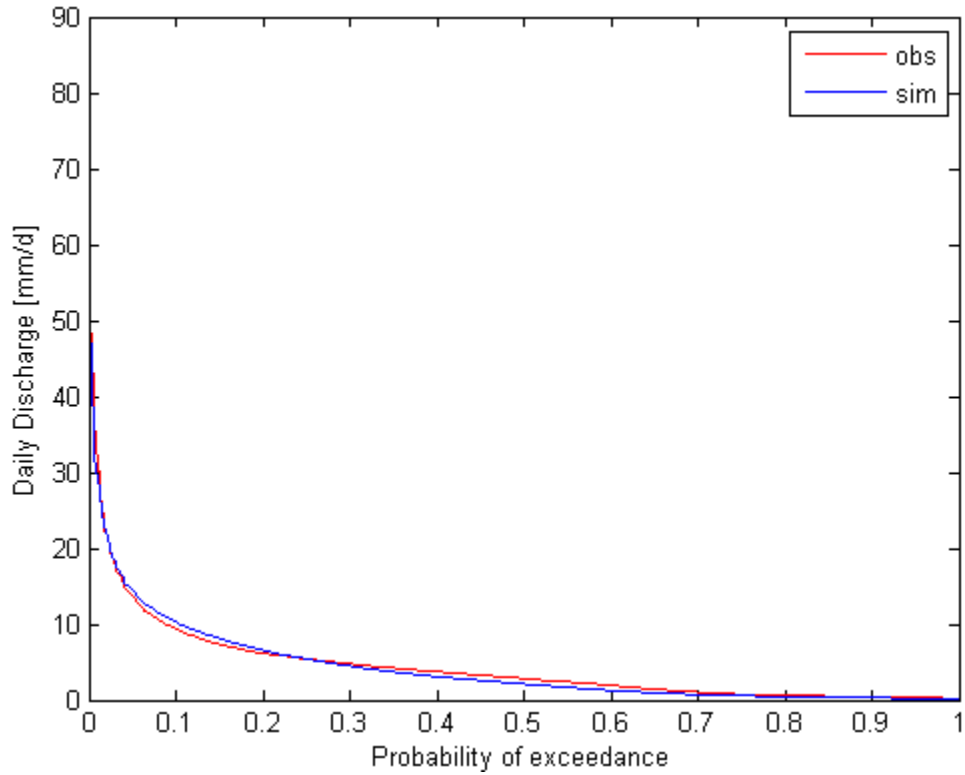


Figure 4-8: Flow duration curves in the Lookout Creek catchment (USA), 62 km<sup>2</sup> in calibration.

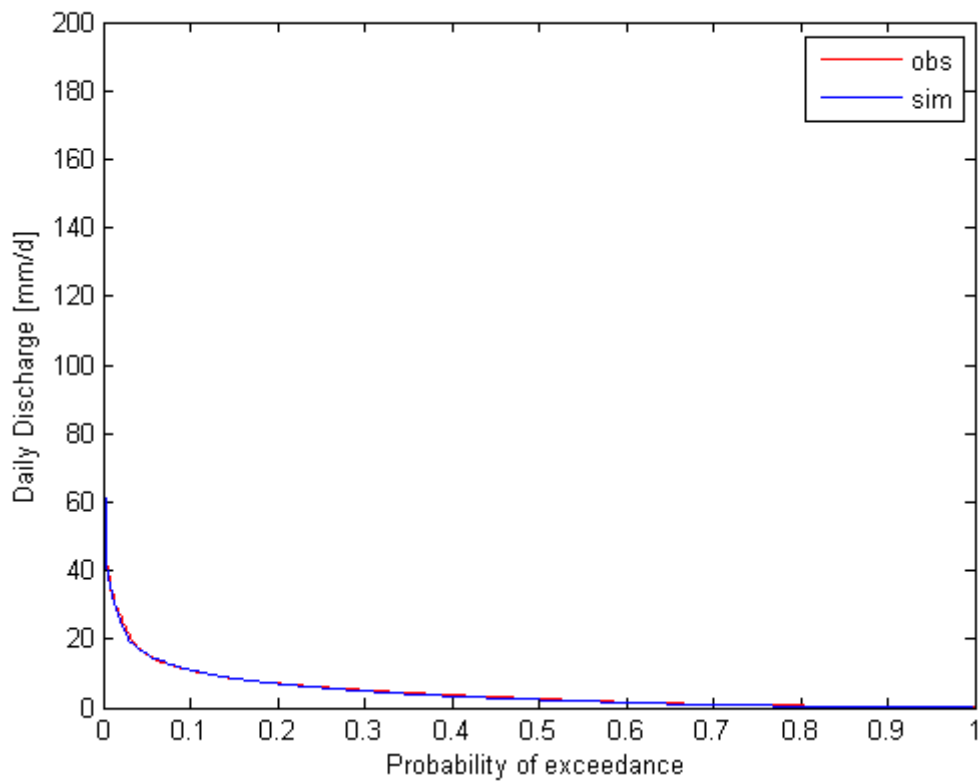


Figure 4-9: Flow duration curves in the Lookout Creek catchment (USA), 62 km<sup>2</sup> in validation.

#### 4. Application of MODHYPMA

---

The simulation of the Aguimo catchment (396 km<sup>2</sup>) in Benin was not satisfactory. The values of the discharge were underestimated and the model was able to estimate only a little part of the lowest flows. This behaviour may be explained by two main reasons. First, the quality of the discharge data may be pointed out. In fact, the number of gaugings realised on Aguimo river is not only limited but also spatially ill-distributed and available only for the low flows (Zannou, 2011). Secondly the successful application of other models like UHP-HRU (Giertz *et al.*, 2006) on this catchment suggests that our model was not able to capture the spatio-temporal dynamics of the hydrological processes.

On the Sore catchment (1 711 km<sup>2</sup>) in Ethiopia, MODHYPMA underestimates the discharge for the calibration period while the validation is good. The behaviour of the model makes sense when we analyse the Potential Evapotranspiration as its cumulated value in calibration period is much greater than in validation period. Over the calibration period (1990-1993) the mean annual ETP is 1548 mm while over the validation period (1994-1997) the mean annual ETP is 1328 mm which gives a difference of 220 mm.

In the modelling of the Mbasso catchment (74 900 km<sup>2</sup>) in Côte d'Ivoire the model shows a general underestimation of the discharge. Although the NSE criterion of the simulation in the calibration period is acceptable, the hydrograph reveal a slight underestimation. This general trend to an underestimation may find an explanation in the fact that two years of the calibration period (1983 and 1984) are very dry years constraining the models to work like in extreme dry conditions.

To this point we may conclude on a good performance and acceptability of MODHYPMA. From the criteria given by Janssen and Heuberger (1995) on how to assess a calibrated model, we may say 1) the model is able to reproduce the system behaviour; 2) the model is suitable for water resources assessment; 3) the model is 'robust' for the data set. Nevertheless, the model needs to be further improved and tested on more and longer data sets; the calibration method should be improved and additional modelling of relevant processes is needed.

# COMPARISON OF MODELS

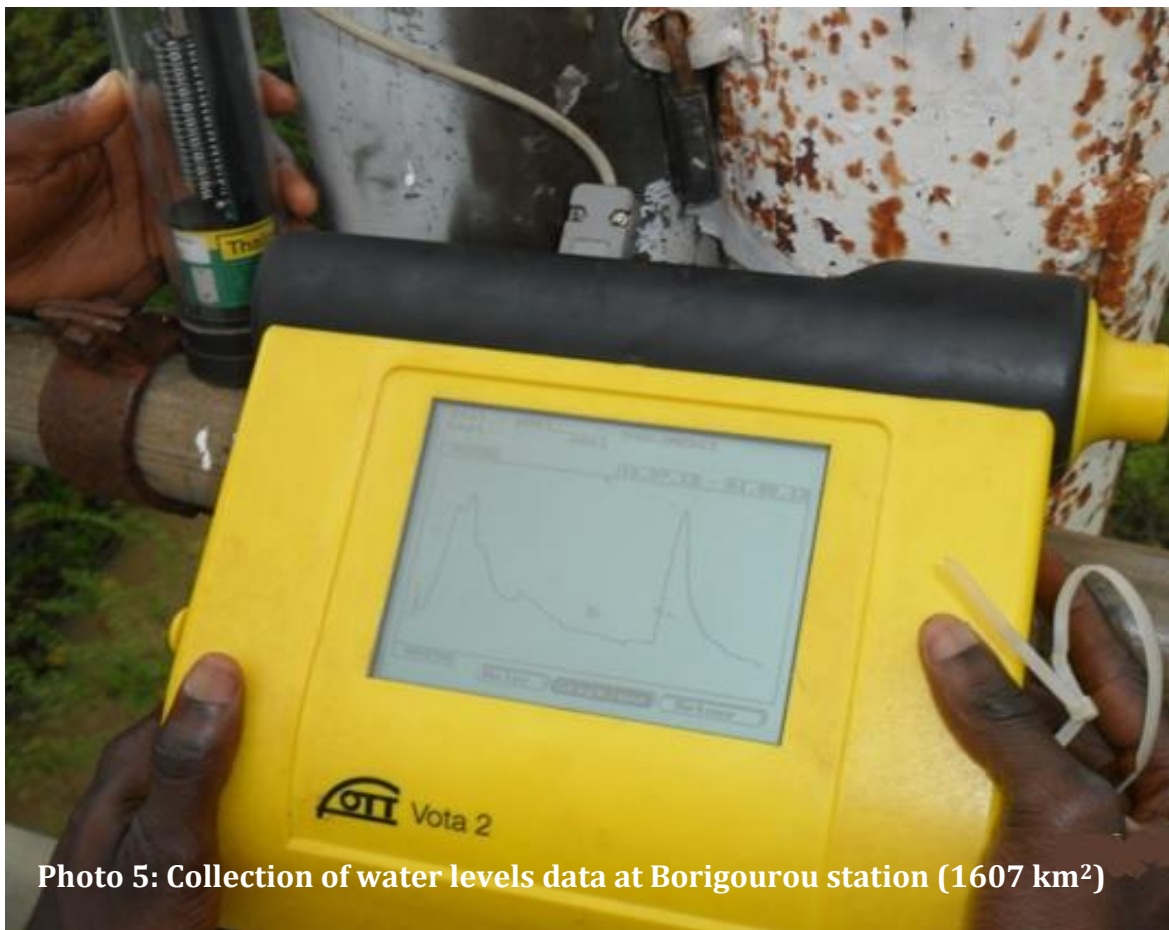


Photo 5: Collection of water levels data at Borigourou station (1607 km<sup>2</sup>)

## 5- Comparison of models

### 5.1- Evaluation of performance

In contrary to the previous section, the assessment of the models was based on only one numerical criterion because we are comparing models. We have chosen to use the Nash-Sutcliffe efficiency (NSE) calculated on flows as the comparison criterion. We chose this criterion because it is by far the most used criterion in the assessment of hydrological models performance.

In terms of visual analysis, like previously we applied two commonly used graphical techniques namely the hydrographs and percent exceedance probability curves which are said to be particularly relevant (Moriassi *et al.*, 2007).

For the simulation of the three models, we used exactly the same input data. We consider the simulation to be accepted if the  $NSE > 0.5$  and if we obtain a fairly good graphical fit. For the three models, NSE was optimized. Because data sets are not always very long, calibration and validation were performed in full split sample test in which the model was calibrated for one period and validated for another followed by the calibration of the second period and validation using the first period. Mean NSE values for calibration and validation periods were computed.

### 5.2- Modelling results

Results of the runs of the three (3) models are given in Table 5-1 for the full split sample tests. For calibration, the NSE ranges from 0.13 to 0.89 for MODHYPMA, from 0.31 to 0.94 for GR4J and from 0.175 to 0.91 for HBV. For validation, the NSE ranges from -0.46 to 0.845 for MODHYPMA, from -0.53 to 0.83 for GR4J and from -0.485 to 0.82 for HBV. Figure 5-1 shows the compared box plots of the mean NSE for the three models for the calibration and validation periods. The results from MODHYPMA model were good.

## 5. Comparison of models

**Table 5-1: Overview of the results obtained from the full split sample test calibration-validation for all three models. Calibration was performed on sub-period 1 and validation on sub-period 2 and then calibration on sub-period 2 and validation on sub-period 1.**

NB	STATIONS	COUNTRY	AREA (km <sup>2</sup> )	Sub-period 1	$\nu$	$\lambda$	TX	CAL - VAL	MOD HYPMA	GR4J	HBV
				Sub-period 2						NSE	NSE
1	<b>BOKPÉROU</b>	BENIN	32	2002-2003	0.85	20	0.00	MEAN NSE CAL	<b>0.132</b>	<b>0.310</b>	<b>0.175</b>
				2004-2005	0.99	12	0.20	MEAN NSE VAL	<b>-0.460</b>	<b>-0.010</b>	<b>-0.485</b>
2	<b>LOOKOUT</b>	USA	62	1978-1987	1.37	32	0.00	MEAN NSE CAL	<b>0.720</b>	<b>0.790</b>	<b>0.820</b>
				1988-1997	1.35	31	0.00	MEAN NSE VAL	<b>0.715</b>	<b>0.755</b>	<b>0.795</b>
3	<b>KOLOKONDÉ</b>	BENIN	105	2002-2003	1.28	13	0.50	MEAN NSE CAL	<b>0.475</b>	<b>0.830</b>	<b>0.800</b>
				2004-2005	1.17	11	0.00	MEAN NSE VAL	<b>0.380</b>	<b>0.775</b>	<b>0.710</b>
4	<b>WÈWÈ</b>	BENIN	261	2000-2002	1.10	11	0.20	MEAN NSE CAL	<b>0.490</b>	<b>0.640</b>	<b>0.640</b>
				2004-2005	1.16	15	0.30	MEAN NSE VAL	<b>0.480</b>	<b>0.615</b>	<b>0.595</b>
5	<b>KOUA</b>	BENIN	292	2002-2003	1.27	11	1.40	MEAN NSE CAL	<b>0.810</b>	<b>0.890</b>	<b>0.845</b>
				2004-2005	1.27	11	0.95	MEAN NSE VAL	<b>0.770</b>	<b>0.790</b>	<b>0.740</b>
6	<b>AGUIMO</b>	BENIN	396	2000-2001	1.07	21	0.25	MEAN NSE CAL	<b>0.505</b>	<b>0.475</b>	<b>0.425</b>
				2004-2005	1.00	21	0.10	MEAN NSE VAL	<b>0.395</b>	<b>0.340</b>	<b>0.075</b>
7	<b>NÉKÉTÉ</b>	BENIN	409	2002-2003	0.97	5	0.05	MEAN NSE CAL	<b>0.810</b>	<b>0.875</b>	<b>0.805</b>
				2004	0.96	10	0.15	MEAN NSE VAL	<b>0.665</b>	<b>0.820</b>	<b>0.570</b>
8	<b>TÉBOU</b>	BENIN	515	1998-1999	1.49	40	1.00	MEAN NSE CAL	<b>0.755</b>	<b>0.795</b>	<b>0.665</b>
				2004-2005	1.31	18	1.00	MEAN NSE VAL	<b>0.655</b>	<b>0.670</b>	<b>0.445</b>
9	<b>DONGA PONT</b>	BENIN	586	1999	1.28	17	1.00	MEAN NSE CAL	<b>0.790</b>	<b>0.780</b>	<b>0.830</b>
				2001	1.21	10	0.80	MEAN NSE VAL	<b>0.745</b>	<b>0.710</b>	<b>0.670</b>
10	<b>SANI</b>	BENIN	745	2004	1.01	19	0.00	MEAN NSE CAL	<b>0.890</b>	<b>0.810</b>	<b>0.660</b>
				2005	1.02	27	0.00	MEAN NSE VAL	<b>0.820</b>	<b>0.800</b>	<b>0.585</b>
11	<b>DONGA AFFON</b>	BENIN	1 308	1999&2001	0.18	13	0.35	MEAN NSE CAL	<b>0.790</b>	<b>0.875</b>	<b>0.810</b>
				2005	1.07	10	0.20	MEAN NSE VAL	<b>0.685</b>	<b>0.650</b>	<b>0.547</b>
12	<b>SARAMANGA</b>	BENIN	1 378	2001-2002	1.09	13	0.25	MEAN NSE CAL	<b>0.775</b>	<b>0.840</b>	<b>0.785</b>
				2005	1.19	24	0.50	MEAN NSE VAL	<b>0.715</b>	<b>0.735</b>	<b>0.760</b>

5. Comparison of models

NB	STATIONS	COUNTRY	AREA (km <sup>2</sup> )	Sub-period 1	$\nu$	$\lambda$	TX	CAL - VAL	MOD HYPMA	GR4J	HBV
				Sub-period 2						NSE	NSE
13	<b>BORIGOUROU</b>	BENIN	1 607	2000-2002	0.93	14	0.15	MEAN NSE CAL	<b>0.845</b>	<b>0.835</b>	<b>0.805</b>
				2003-2005	1.04	20	0.25	MEAN NSE VAL	<b>0.675</b>	<b>0.605</b>	<b>0.710</b>
14	<b>SORE</b>	ETHIOPIA	1 711	1990-1993	1.62	65	0.00	MEAN NSE CAL	<b>0.695</b>	<b>0.745</b>	<b>0.795</b>
				1994-1997	1.08	14	0.00	MEAN NSE VAL	<b>0.430</b>	<b>0.310</b>	<b>0.620</b>
15	<b>BARÉROU</b>	BENIN	2 162	2001	1.15	18	0.50	MEAN NSE CAL	<b>0.885</b>	<b>0.940</b>	<b>0.910</b>
				2005	1.20	21	0.60	MEAN NSE VAL	<b>0.845</b>	<b>0.780</b>	<b>0.710</b>
16	<b>COTE238</b>	BENIN	3 133	2001-2002	1.04	13	0.17	MEAN NSE CAL	<b>0.835</b>	<b>0.875</b>	<b>0.835</b>
				2005	1.11	20	0.30	MEAN NSE VAL	<b>0.760</b>	<b>0.830</b>	<b>0.820</b>
17	<b>AVAL SANI</b>	BENIN	3 283	2001-2002	1.07	9	0.40	MEAN NSE CAL	<b>0.800</b>	<b>0.855</b>	<b>0.820</b>
				2003&2005	1.00	10	0.15	MEAN NSE VAL	<b>0.700</b>	<b>0.790</b>	<b>0.575</b>
18	<b>BÉTÉROU</b>	BENIN	10 326	1998-2003	1.01	16	0.15	MEAN NSE CAL	<b>0.845</b>	<b>0.860</b>	<b>0.845</b>
				2004-2006/2008-2010	1.05	16	0.15	MEAN NSE VAL	<b>0.815</b>	<b>0.680</b>	<b>0.785</b>
19	<b>MBASSO</b>	COTE D'IVOIRE	74 900	1979-1987	1.05	26	0.00	MEAN NSE CAL	<b>0.570</b>	<b>0.470</b>	<b>0.695</b>
				1992-1998	1.09	25	0.00	MEAN NSE VAL	<b>0.530</b>	<b>-0.530</b>	<b>0.475</b>
20	<b>SAVÈ</b>	BENIN	23 488	1996-1999/2002-2003	1.08	17	0.25	MEAN NSE CAL	<b>0.820</b>	<b>0.825</b>	<b>0.825</b>
				2004-2009	1.00	13	0.15	MEAN NSE VAL	<b>0.780</b>	<b>0.635</b>	<b>0.780</b>

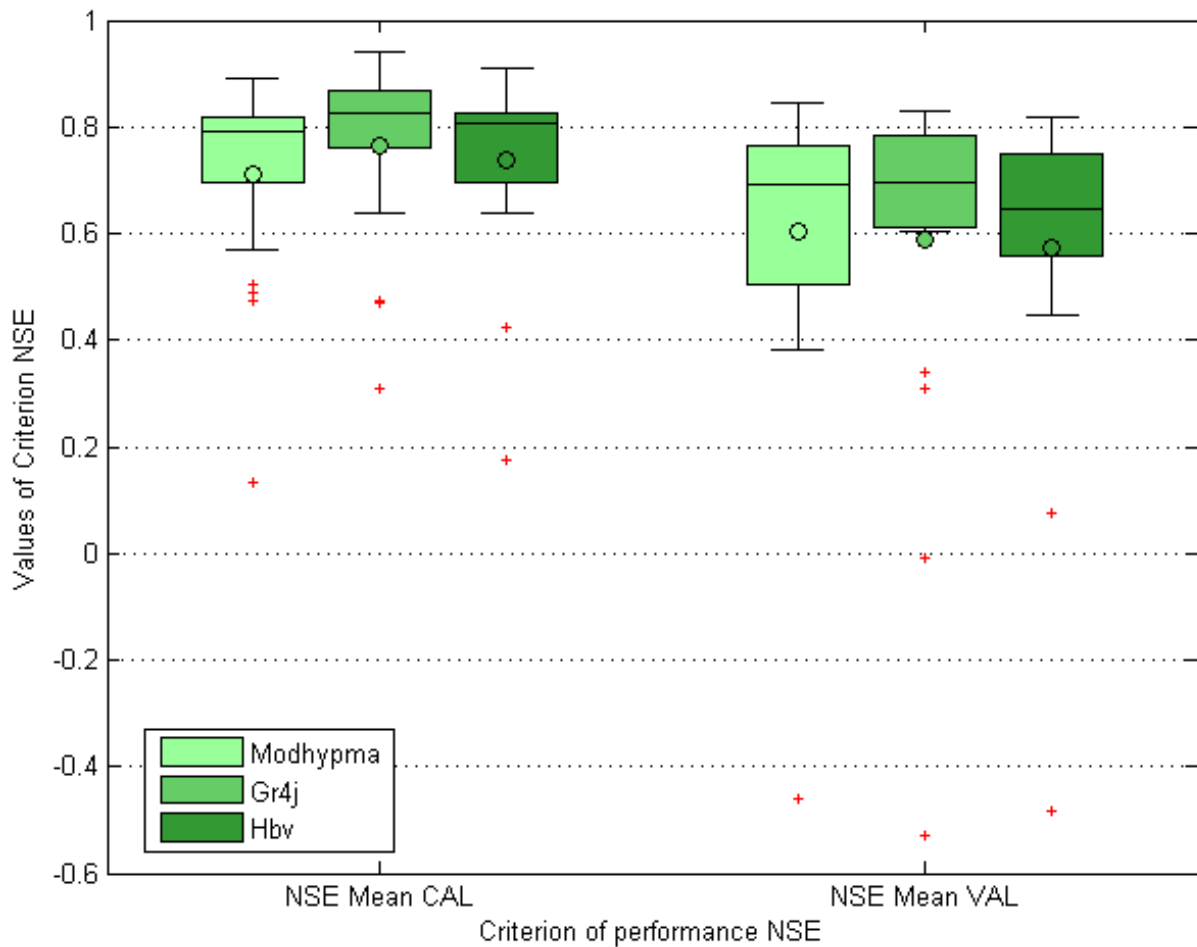


Figure 5-1: Compared box plot of the NSE in calibration and validation for the three models (MODHYPMA, GR4J and HBV). Crossbar: Median; Circle: Mean; length of box: interquartile range (25th and 75th percentiles); tails: furthest values within the whisker; Red + sign : Outliers.

As we can see from the box plot (Figure 5-1) for MODHYPMA the interquartile range is roughly [0.7-0.85] for the calibration period and [0.5-0.75] for the validation period. For GR4J model, the interquartile range is roughly [0.75-0.9] for the calibration period and [0.6-0.75] for the validation period. For HBV model, the interquartile range is roughly [0.7-0.85] for the calibration period and [0.55-0.7] for the validation period.

In the calibration period, as shown in the box plot, the median for GR4J is greater than 0.8 while for the two other models the value is about 0.80. In the validation period, the median for MODHYPMA and GR4J is around 0.7 while it is around 0.65 for HBV.

In the calibration period, as shown in the box plot, the mean for GR4J is around 0.75 while for the two other models the value is between 0.70 and 0.75. In the

validation period, the mean for MODHYPMA is around 0.6 while it is comprised between 0.5 and 0.6 for HBV and GR4J.

All three models failed in the simulation of Bokpéroù (32 km<sup>2</sup>). Taking a NSE of 0.5 as a threshold, MODHYPMA was not sufficient for Sore (1711 km<sup>2</sup>) and Aguimo (402 km<sup>2</sup>) in the validation and for Wèwè (261 km<sup>2</sup>) and Kolokondé (105 km<sup>2</sup>) for the calibration and the validation period. GR4J was sufficient for Sore (1711 km<sup>2</sup>) in validation, for Mbasso (74 900 km<sup>2</sup>) and Aguimo (402 km<sup>2</sup>). HBV was not sufficient for Mbasso (74 900 km<sup>2</sup>) and Tébou (515 km<sup>2</sup>).

When considering all catchments except Bokpéroù, in calibration the best performance was attained by MODHYPMA for 3 catchments, by GR4J for 11 catchments and by HBV for 5 catchments. In validation the best performance was attained by MODHYPMA for 7 catchments, by GR4J for 7 catchments and by HBV for 5 catchments. As a conclusion, we can say that in the calibration period GR4J presented a greater performance compared to other models which showed similar performance. In the validation period, MODHYPMA and GR4J revealed similar performance while HBV showed a lower performance. Overall, GR4J showed a higher performance but as HBV, it showed an important drop in model performance from calibration to validation. This loss of performances was relatively small for MODHYPMA showing a similar quality for the calibration and the validation periods.

The observed hydrographs of Bétérou (10 083 km<sup>2</sup>) compared to the simulated ones in calibration and validation are shown in figures 5-2 and 5-3 together with the flow duration curves in Figure 5-4. The first graph shows the result from MODHYPMA, the second the result from GR4J and the third is the result of HBV. The compared hydrographs and flow duration curves of the three models for the other catchments are shown in Appendix C.

## 5. Comparison of models

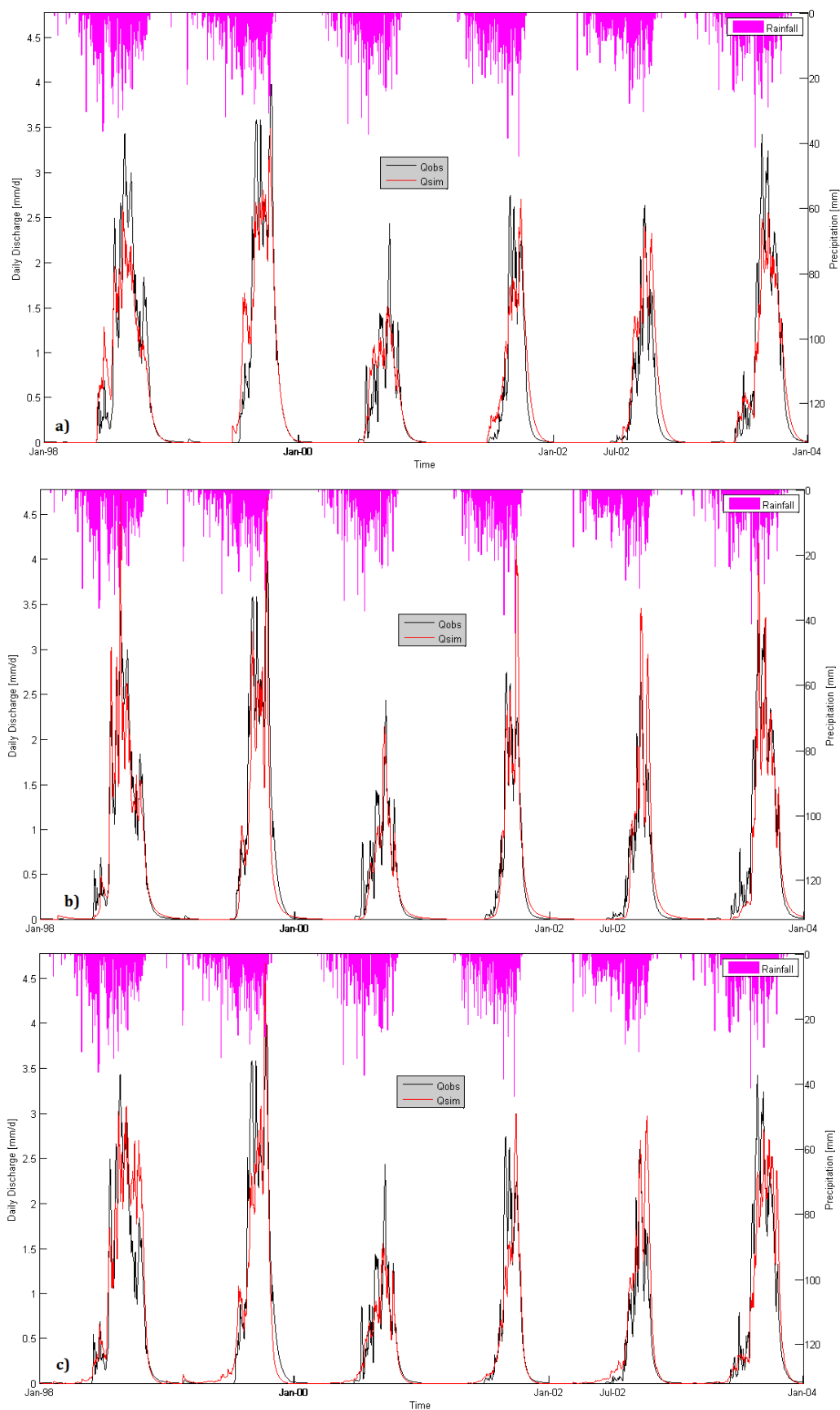


Figure 5-2: Application of a) MODHYPMA, b) GR4J and c) HBV to Bétérou catchment (10 083 km<sup>2</sup>) in calibration.

## 5. Comparison of models

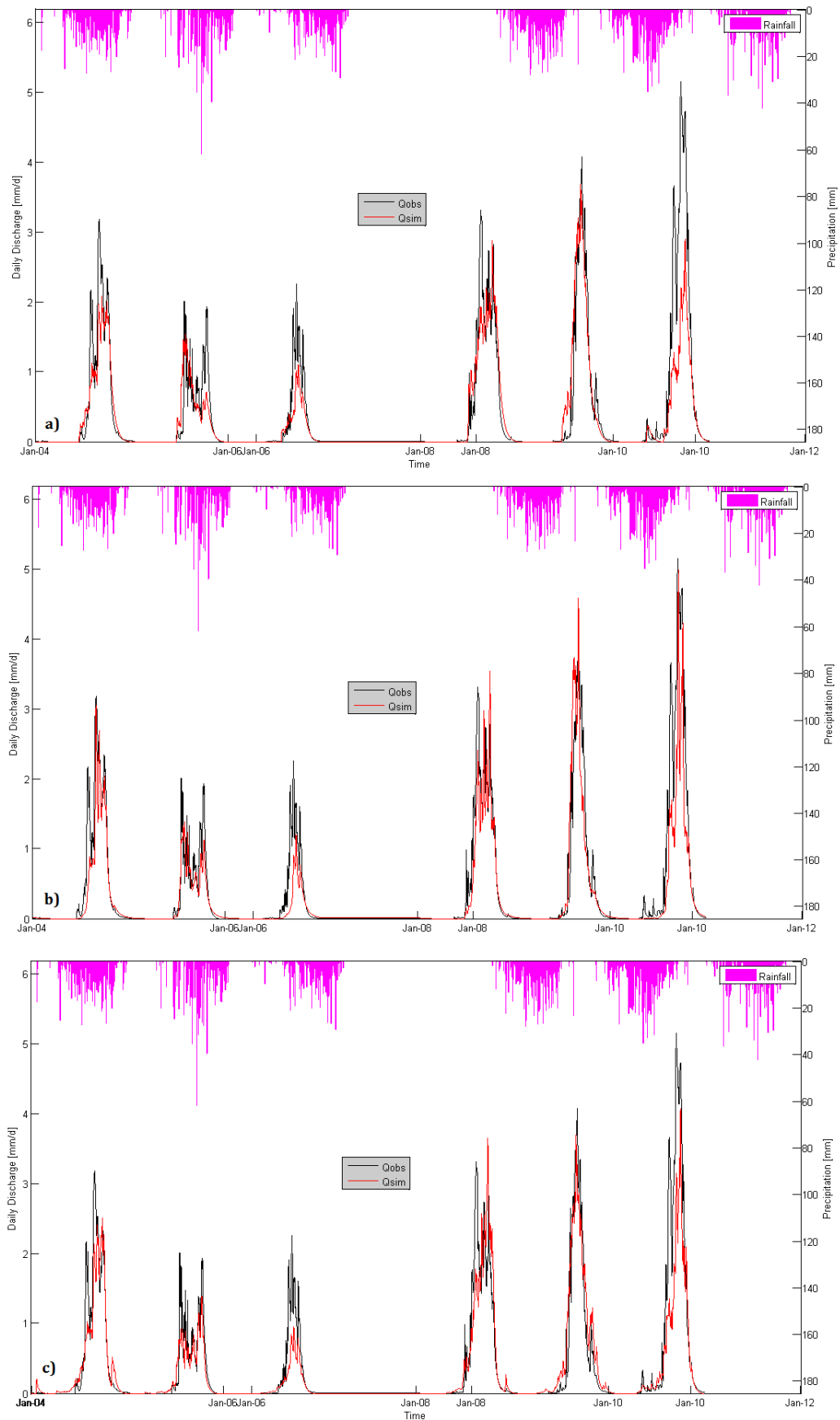


Figure 5-3: Application of a) MODHYPMA, b) GR4J and c) HBV to Bétérou catchment (10 083 km<sup>2</sup>) in validation.

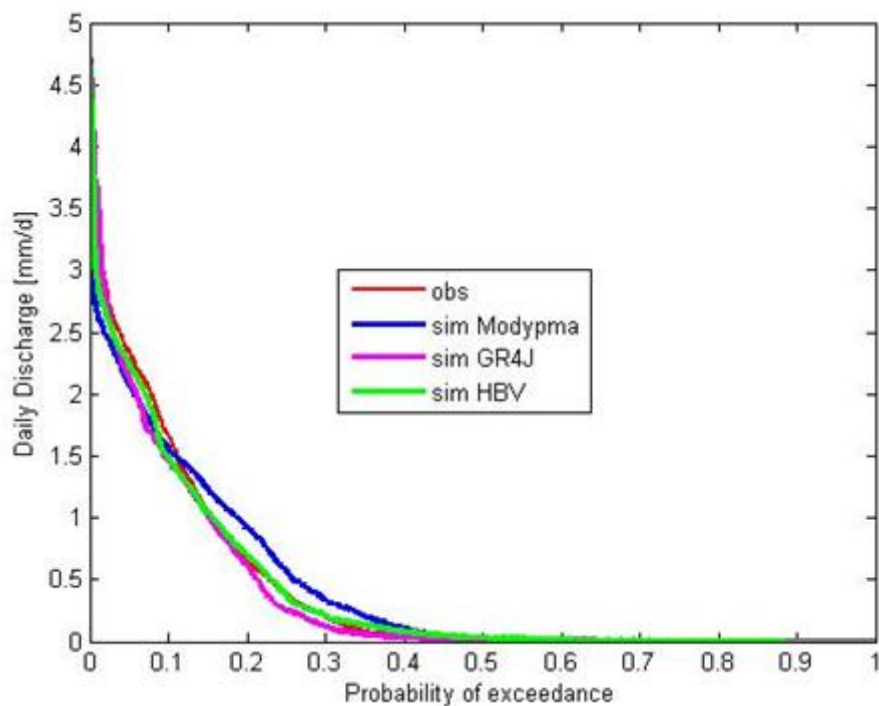


Figure 5-4: Compared flow duration curves in the Bétérou catchment (10 083 km<sup>2</sup>).

From the analysis of the hydrographs and the flow duration curves, we conclude that globally at the beginning of the season, the three models have a good fit; MODHYPMA sometimes overestimates this part of the hydrograph while GR4J shows a systematic underestimation and HBV a systematic overestimation.

The recession curve is very well simulated by MODHYPMA, well modelled by GR4J and HBV. MODHYPMA tends to overestimate the low flows while they are quite well reproduced by GR4J and slightly overestimated by HBV. Middle flows are well represented by all the three evaluated models. High flows are quite well simulated by GR4J but some peaks are overestimated. MODHYPMA underestimates the highest flows. HBV has an intermediate behaviour. All models are subject to timing errors.

The models were not sufficient on some catchments Aguiamo (409 km<sup>2</sup>) in Benin, Sore (1 711 km<sup>2</sup>) in Ethiopia, Mbasso (74 900 km<sup>2</sup>) in Côte d'Ivoire.

### 5.3- Discussion and Conclusion

The limited applicability of all models to Bokpéro (32 km<sup>2</sup>) has been explained in the previous section.

Reasons for the unsatisfactory simulation of the Aguimo catchment (396 km<sup>2</sup>) in Benin for all three models were suggested in the previous chapter. On the Sore catchment (1 711 km<sup>2</sup>) in Ethiopia, MODHYPMA underestimates the discharge for the calibration period while the validation is good. For GR4J and HBV models, the discharge is globally overestimated during the validation period. This curious behaviour of the three models has been analysed and Potential Evapotranspiration values were used to explain it (See Chapter 4).

In the modelling of the Mbasso catchment (74 900 km<sup>2</sup>) in Côte d'Ivoire all three models show a general underestimation of the discharge. Although the NSE criterion of MODHYPMA and the HBV model simulations in the calibration period are acceptable, the hydrographs reveal a slight underestimation. Climate conditions were the reason evoked to explain this fact (See Chapter 4).

As a conclusion, it can be said that MODHYMA performs as well as the other models with the difference that from calibration to validation MODHYMA is subject to a less loss of performance. If these results could be further confirmed by other studies or using different comparison approaches, this would suggest that MODHYMA does not try just to fit perfectly to the data but try to capture the physical information that is available in the data. Consequently it would be a better candidate for climate change impacts assessments.

It is important to mention that in this study, we relied only on the NSE criterion for the comparison of the models, more sophisticated or robust comparison approaches could be elaborated. Various approaches could be constructed in function of the modelling purpose.

# SENSITIVITY AND UNCERTAINTY ANALYSES OF MODHYPMA



Photo 6: Partial view of the Wèwè river (261 km<sup>2</sup>)

## 6- Sensitivity and uncertainty analyses of MODHYPMA

### 6.1- Methodology: sensitivity index and local sensitivity assessment

The magnitude of the effect of parameters on model output is known as the sensitivity of a model to its parameters (Wainwright & Mulligan, 2004). As defined by Moriasi *et al.* (2007) the sensitivity analysis is a process through which we evaluate the rate of change in the model output (discharge) with respect to changes in model inputs (parameters). In our study, we analysed the sensitivity of one parameter at a time with respect to the percent change in total runoff. We chose a local sensitivity approach i.e. for each parameter the sensitivities were evaluated in the immediate region of the identified optimum parameter set after the calibration of model while the other parameter is kept unaltered (Beven, 2012, Wainwright & Mulligan, 2004).

For that we calculated a sensitivity index  $S_i$  defined as follow (Eq. 6.1):

$$S_i = \frac{P_{10} - M_{10}}{B} \quad \text{Eq. 6.1}$$

$P_{10}$  = result of the simulation (NSE) with model calibrated parameter 10% increased

$M_{10}$  = result of the simulation (NSE) with model calibrated parameter 10% decreased

$B$  = result of the baseline simulation (NSE).

Table 6-1 shows the classification of sensitivity according to the value of the index computed.

We also computed the index with 100% change in model calibrated parameters but this time with regard to the total runoff. The associated change was plotted.

**Table 6-1: Classification of sensitivity index.**

Class	Index	Sensitivity
I	<0.05	Low
II	0.05-0.2	Medium
III	0.2-1.0	High
IV	>1.0	Very high

### 6.2- Results of the sensitivity analysis and discussion

The computed values of the sensitivity index  $S_i$  are shown in table 6-2. Parameter  $v$  has a very high to high sensitivity. Parameter  $\lambda$  has a medium to low sensitivity while parameter TX has a low sensitivity.

**Table 6-2: Sensitivity indexes computed with regard to the NSE criterion.**

No	Stations	Country	Area (km <sup>2</sup> )	Sensitivity index $S_i$		
				$v$	$\lambda$	TX
1	Lookout	USA	62	-2.09	0.08	0.00
2	Le Léguer	FRANCE	260	-5.04	0.06	0.00
3	Koua	BENIN	292	-0.79	0.01	0.02
4	Nekété	BENIN	409	0.07	-0.02	0.00
5	Donga Pont	BENIN	587	-0.51	0.08	0.01
6	Sani	BENIN	745	-0.92	0.13	0.00
7	Donga-Affon	BENIN	1308	0.005	0.10	0.01
8	Saramanga	BENIN	1360	0.48	0.00	0.01
9	Bori-Gourou	BENIN	1607	-0.14	0.04	0.02
10	Sore	ETHIOPIA	1711	0.65	-0.09	0.00
11	Barérou	BENIN	2134	0.56	0.07	0.07
12	Cote238	BENIN	3060	0.29	-0.03	0.01
13	Aval-Sani	BENIN	3279	-0.05	-0.02	0.00
14	Bétérou	BENIN	10083	0.06	-0.01	0.00
15	Savè	BENIN	23491	-0.45	0.06	0.01

Legend=

High and very high	Medium	Low
--------------------	--------	-----

Figure 6-1 shows the results of the sensitivity analysis with regard to the total runoff for Bétérou catchment. As can be seen from the plot, a decrease in the optimum value of  $v$  (first plot) does not induce much change in total runoff as it is

the case for an increase in the optimum value of  $\nu$  (increase in total runoff > 1000 %). A decrease in the optimum value of  $\lambda$  (second plot) induces an important change in total runoff (increase up to 100 %) while an increase in the optimum value of  $\lambda$  induces a decrease in total runoff (50 %). Changes in the optimum value of TX slightly affect total runoff. Parameter  $\nu$  appears to be the most sensitive parameter.

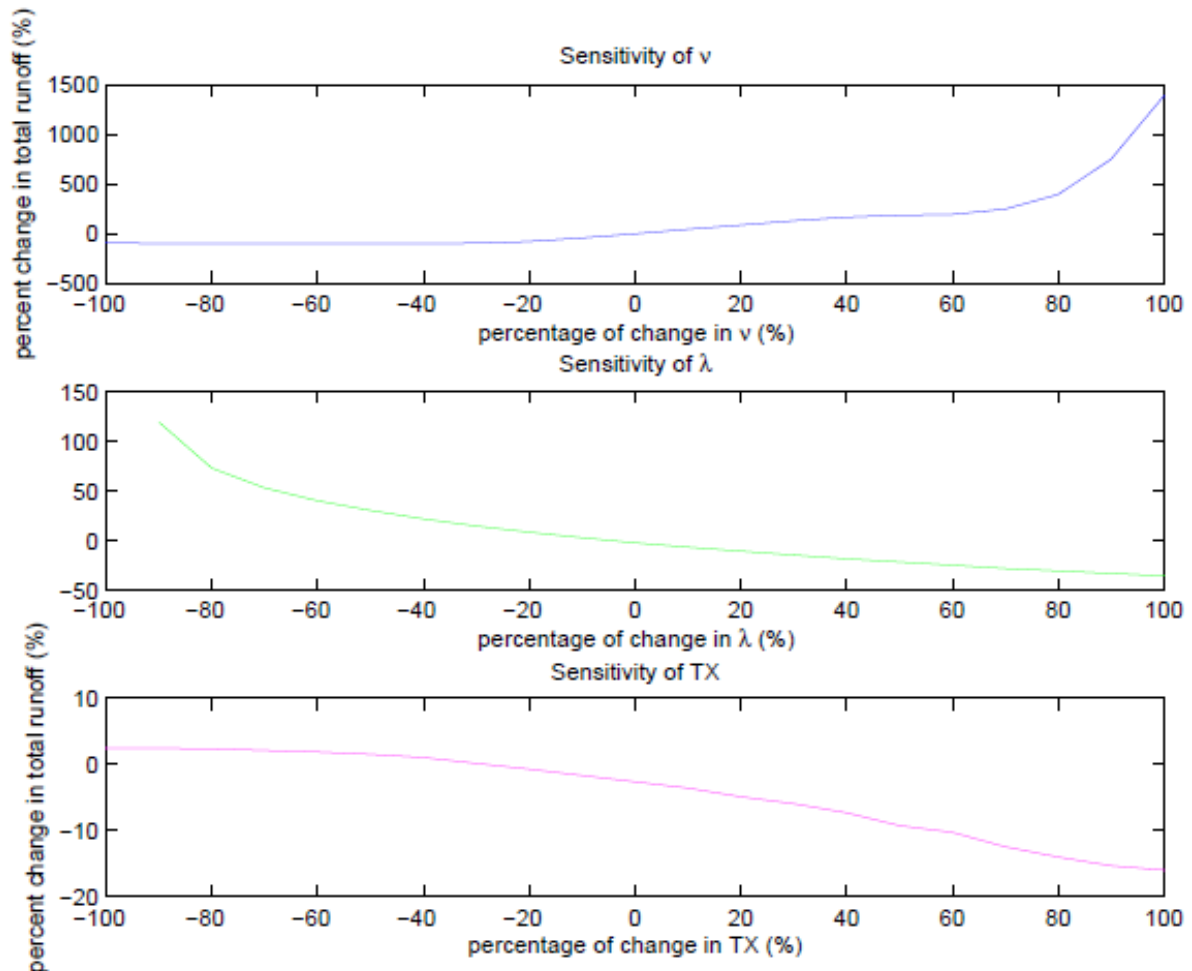


Figure 6-1: Sensitivity analysis for MODHYPMA parameters with regard to the total runoff for Bétérrou (10 083 km<sup>2</sup>).

The local sensitivity analysis revealed that  $\nu$  has a high sensitivity,  $\lambda$  a medium to low sensitivity and TX a low sensitivity. These results imply that the parameter  $\nu$  must be estimated with more attention. Indeed, it will contribute to a larger part of the calibrated model uncertainties.

The analysis of the hydrographs and the calibration of model parameters allow us to conclude that  $v$  should not be considered as a constant. In fact, the dominant process is not the same all along the year. We noticed that slightly changes of  $v$  result in better simulation of particular parts of the observed hydrograph (beginning of the season, rainy season, recession). We recommend that the hypothesis about  $v$  being constant should be reassessed.

### 6.3- Sampling method for the uncertainty analysis

Uncertainty in hydrology is not only epistemic (lack of exhaustive knowledge about processes) but also due to the inherent randomness of these processes. Uncertainty may be defined as the confidence we have about what we “know” and the aim of the uncertainty analysis is to study how the uncertainties propagate to model outputs (Brown & Heuvelink, 2005). Uncertainty originates from model inputs, from the model (through its parameters, structure and solutions) and from observations. Although “model parameters are not inherently uncertain because they do not refer to real, measurable quantities” (Brown & Heuvelink, 2005), we considered in this study only the parameters uncertainty. Parameters sets were sampled over the whole parameter space. The uncertainty of the parameters has been assessed with the GLUE -Generalized Likelihood Uncertainty Estimation- methodology (Beven & Binley, 1992) with the use of the Gluewin software (Ratto & Saltelli, 2001). The basic idea behind GLUE is that basing on watershed data at our disposal, the result of calibration should not be a single set of parameters but instead a family of plausible parameters sets which are used to generate uncertain streamflow forecasts (Duan *et al.*, 2003).

The sets of model parameters used for the parameter uncertainty analysis were generated with the Simlab Software (Giglioli & Saltelli, 2008). We chose a uniform distribution and the Latin Hypercube as the sampling method. For the GLUE analysis to be efficient, the parameters space should be well sampled. Latin hypercube is a stratified sampling method as its purpose is to achieve a better coverage of the sample space of the model parameters with less samples.

Therefore this method appears to be more efficient in the estimation of the output statistics than random sampling (Sintondji, 2005).

In order to achieve this objective and still reduce the number of runs, this method was selected. In GLUE, it is assumed that many sets of parameter values can be considered equally likely as simulators of the catchment (Beven & Binley, 1992). However it mustn't be forgotten that model performance is assessed through quality measures. Thus, Abbaspour (2008) points out a very important point when he looks at the non-uniqueness problem from the point of view of objective function. As a matter of fact, the assessment of the performance of a model may considerably vary depending on the criterion used. This is why it is important to mention which criterion we chose as objective function. The NSE criterion was chosen as the likelihood function since it is widely used in hydrological modelling. Although GLUE is widely used, it is in the same time much criticized. That is why we think it is worth discussing, in short, the controversy about this methodology. As a matter of fact, many authors like Clark *et al.* (2011) have questioned the choice of (or the way of combining) the likelihood measures as well as the choice of the rejection threshold (behavioural vs non-behavioural). The authors argued that as we are within a more formal application of Bayesian principles, this choice should be objective. In particular, Jin *et al.* (2010) in their study used two values of threshold and came out with the conclusion that both the width of the confidence interval and the percentage coverage of the observation values are sensitive to the choice of these threshold values. GLUE is also blamed for not attempting to make a distinction between data and model errors neither to allow for a better model diagnostic where each modelling hypothesis could be tested with scrutiny (Clark *et al.*, 2011, 2012). As to Beven *et al.* (2012) and Beven and Binley (2014), first, a formal Bayesian statistical approach is not necessarily more objective than GLUE; second, science is still looking for (an) appropriate likelihood measure(s) i.e that would properly reflect(s) the information content in a set of input and evaluation data; third, without knowing the various sources of uncertainty (aleatory and epistemic) it is impossible to separate out their

impacts in the modelling process; fourth, unless we can considerably reduce uncertainties in observations by greatly improved observational techniques, it will be very difficult to separate model errors from data errors. In short, one of main challenges in hydrological modelling remains the reduction of the epistemic errors in input and output data (Beven & Binley, 2014).

A number of runs were generated for each catchment. Behavioural sets were obtained by applying a threshold of 0.60 (NSE).

#### 6.4- Results of the uncertainty analysis and discussion

While for the calibration of MODHYPMA, the model was run over the whole parameter space by defining discrete increments on each parameter range (and the parameter response surface for each performance criterion was drawn); for the uncertainty analysis of MODHYPMA, the model was run only with parameters sets derived using the Latin Hypercube approach (stratified sampling). Analysing uncertainty requires the definition of behavioural simulations. The results of the analysis are summarised in Table 6-3. We performed between 200 and 700 runs per catchment. The behavioural runs obtained in final were by far very few; they range between 20 and 389.

For Bétérou catchment for example, 400 runs were generated. We got 258 behavioural sets with the threshold of 0.65 (NSE). Figure 6-2 presents how the NSE criterion varies in function of the parameter values. On x-axis are the values taken by the parameter and on y-axis are the values of performance. Parameter  $v$  appears to be the primary source of uncertainty as it shows the highest sensitivity. This result had already been confirmed by the sensitivity analysis. However, the dotted plot of  $\lambda$  reveals that the model is not completely insensitive to this second parameter but not much sensitive to TX. The arrows indicate the parameter values which give the best NSE value. The 90 Percent Prediction Uncertainty (90PPU) has been calculated at the 5% and 95% levels with the behavioural simulations and plotted in Figure 6-3.

6. Sensitivity and Uncertainty analyses of MODHYPMA

**Table 6-3: Results of the Uncertainty Analysis.**

	CATCHMENT	NU	LAMBDA	TX	RUNS	BEHAVIOURAL RUNS	P-FACTOR	R-FACTOR
<b>1</b>	DONGA AFFON	[0.90 - 1.2]	[5 - 30]	[0 - 0.4]	700	229	0.78	0.29
<b>2</b>	BETEROU	[0.95 - 1.27]	[8 - 30]	[0.1 - 0.4]	700	368	0.60	0.58
<b>3</b>	LOOKOUT	[1.16 - 1.6]	[12 - 100]	0	400	123	0.58	0.38
<b>4</b>	AVAL SANI	[0.95 - 1.15]	[5 - 25]	[0.05 - 0.2]	500	283	0.55	0.36
<b>5</b>	LE LEGUER	[1.6 - 1.81]	[32 - 80]	[0 - 0.1]	200	20	0.19	0.18
<b>6</b>	BAREROU	[0.95 - 1.20]	[5 - 30]	[0.2 - 0.4]	300	110	0.33	0.48
<b>7</b>	BORIGOUROU	[0.75 - 1.05]	[5 - 30]	[0.05 - 0.2]	700	231	0.36	0.53
<b>8</b>	COTE 238	[0.9 - 1.2]	[5 - 30]	[0.05 - 0.4]	700	389	0.43	0.56
<b>9</b>	DONGA PONT	[1.1 - 1.5]	[10 - 40]	[0.5 - 1]	200	109	0.41	0.30
<b>10</b>	SORE	[0.9 - 1.5]	[8 - 50]	[0.05 - 0.5]	700	358	0.70	0.51
<b>11</b>	NEKETE	[0.75 - 1.15]	[5 - 30]	[0 - 0.05]	400	174	0.43	0.37
<b>12</b>	SANI	[0.95 - 1.20]	[10 - 30]	0	300	138	0.45	0.55
<b>13</b>	SARAMANGA	[0.95 - 1.3]	[5 - 30]	[0.05 - 0.4]	700	331	0.44	0.53
<b>14</b>	SAVE	[0.9 - 1.2]	[6 - 30]	[0.1 - 0.5]	700	360	0.60	0.54

## 6. Sensitivity and Uncertainty analyses of MODHYPMA

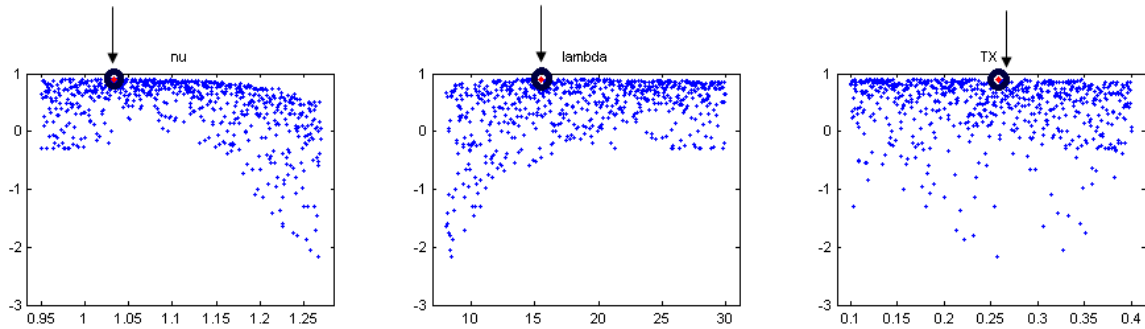


Figure 6-2: The dot plot map of the parameters versus NSE criterion for discharge simulation on Bétéroü Catchment (10 083 km<sup>2</sup>).

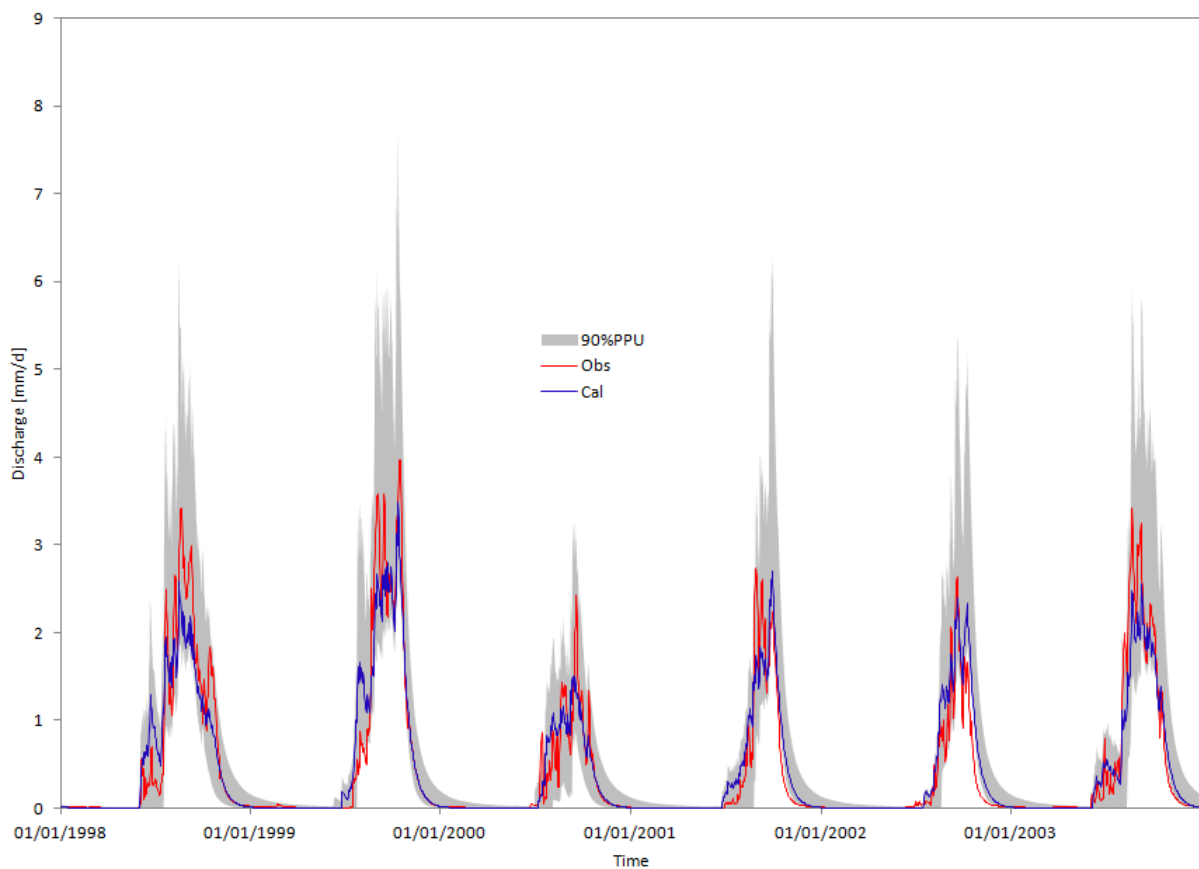


Figure 6-3: 90% confidence interval of daily runoff due to parameter uncertainty calculated by GLUE method with threshold of 0.6 on Bétéroü Catchment (10 083 km<sup>2</sup>).

Figures showing the dot plots of the parameters and the 90PPU for the rest of the catchments are presented in Appendix D. We can notice that the uncertainty band is larger during the high flows but computed as relative uncertainty; uncertainty is similar for low and high flows. The p-factor which is the percentage of observations covered by the 90PPU is 0.53 for Bétéroü. The r-factor is the

relative width of the 90% uncertainty band. The p-factor is expected to be as close as possible to 1 while the r-factor is expected to be very small (close to zero). Table 6-3 presents the r and p- factors calculated for the catchments. The p-factor is generally good but we have very low values like 0.33. The r-factor is generally good, the highest value is 0.55.

The r-factor is 0.48 and 0.24 respectively for Bétérrou and Donga Affon. Although the r-factor is very good, the p-factor is a little bit low, illustrating the fact that the model could not totally simulate the flow processes. However, one has to remember that there are other sources of uncertainties and it is generally accepted that measured data (discharge as well as boundary conditions) are inherently uncertain (Beven & Binley, 2014, Moriasi *et al.*, 2007, Yu, 2002).

This result suggests that further study must be carried out including the uncertainty of the discharge data. The equifinality thesis incorporated in GLUE analysis raises the question of the identifiability and transferability of model parameters ( e.g. Shen *et al.*, 2012). Next chapter will focus on this aspect in the context of application of MODHYPMA to ungauged catchments. Some gauged catchments will be considered as ungauged and will be further tested with linear regression relationships derived from calibrated catchments. With the small width of the uncertainty band, we may expect good results. The introduction of the parameter TX led to the improvement of the modelling of a number of catchments. However, the increase in model performance causes decreasing identifiability due to a greater parameter interaction, and therefore increasing parameter uncertainty (Wagener *et al.*, 2001).

# 7

## TOWARDS AN APPLICATION OF MODHYPMA TO UNGAUGED CATCHMENTS



Photo 7: Gauged station of Aguimo (396 km<sup>2</sup>)

## 7- Towards an application of MODHYPMA to ungauged catchments

As clearly recognised by many authors among which Beven (2012), Brutsaert (2005), Shaw *et al.* (2011), one of the objectives of the modelling exercise is to predict catchments responses where we do not have data i.e. the ungauged or data-poor basins. For such an approach, it is required that hydrographs should be predicted from other information within that catchment or from other catchments (Parajka *et al.*, 2013). Model parameters can be identified by using basin characteristics rather than calibrations (Tianqi *et al.*, 2007). Prediction in Ungauged Basins is still an important challenge to Hydrology. Although physically-based distributed models are supposed to allow the a priori determination of parameters for ungauged basins, it is not actually the case. Moreover in a context of limited availability of data, such approaches are really valuable.

Apart from climatic conditions or spatial and temporal rainfall distribution, the hydrological processes and runoff occurring over a catchment are influenced by various other factors among which are the physical features such as:

- the catchment morphology and the arrangement of the river network (shape, size, elevation, drainage density ,... );
- the catchment physical properties (soils types, vegetation, land use, geology, ...)

According to MODHYPMA design, the parameters are related to the properties of runoff and to the physical features of the catchment. More specifically,  $v$  expresses the non-linearity of the physical phenomenon of water flow,  $\lambda$  is a macroscopic parameter which describes properties related to the geomorphology and pedology of the catchment and  $TX$  accounts for the amount of rainfall required before discharge starts (this is specific to semi-arid and sub-humid areas). These parameters are estimated by calibration and this is why we worked on establishing, through statistical methods, relationships between model parameters and catchment features. Similar studies have been carried out on the Ouémé river basin (see (Bossa & Diekkrüger, 2012)) and gave good results.

## 7.1- Methodology

### 7.1.1- Data and determination of catchments physical characteristics (CPCs)

Additional data was used for this study. Among which are the digital elevation model (DEM) with a resolution of 90 m, SRTM; the soil data and land use data from IMPETUS (Christoph *et al.*, 2008) and INRAB (Institut National de la Recherche Agricole du Bénin; (Bossa & Diekkrüger, 2012)); Geology data from OBEMINES (Office Béninoise des MINES). The DEM was used to delineate the catchments and determine rivers networks. The various layers of geology, soils and land use were superimposed to the shapefiles of the catchments. A number of physical properties were selected (Table 7-1) and from the above mentioned data.

The selection of catchments for this analysis was done according to two main criteria. In fact, after calibration of MODHYPMA (performed in above section 4) and analysis of uncertainty (performed in above section 6) p-factor and r-factor were analysed. Only catchments that showed a p-factor greater than 50% and an r-factor inferior to 0.5 were considered. In other words, the calibrated parameter sets used in the approach were derived from catchments where more than 50% of the measurements were captured by the 90% prediction uncertainty, and where the ratio of average distance between 5 and 95 percentiles of the cumulative distribution of the simulated variable and the standard deviation of the corresponding measured variable was less than 0.5. In total ten (10) catchments were kept. Their CPCs (Table 7-1) were calculated from the data.

### 7.1.2- Multiple linear regression analysis

SPSS software, a statistical analysis tool was used for the determination of the regression equations. Before implementing the correlation between CPCs and calibrated parameters, colinearity among CPCs has been checked. This was done through the comparison of the Variable Inflation Factor (VIF) to a given threshold (see equations 7.1 and 7.2).

**Table 7-1: Catchment Physical Features accounted for in this study**

Catchment Physical Properties	Description
Catchment area	The catchment is the surface that receives rainfall and produces runoff
Length of longest flow path	Distance from the catchment's outlet to the most distant source on the catchment boundary
Hypsometric integral	Describes the distribution of elevation across the catchment area.
Mean elevation	Average elevation of the catchment from SRTM DEM
Average slope of catchment	Calculated from digital elevation model SRTM DEM pixel by pixel
Drainage density	Total stream length by unit surface
Basin shape	Gravelius index $K_G$ : the ratio of catchment perimeter to the perimeter of the circle with the same area as the catchment. It is close to 1 for a catchment with an almost circular shape and greater than 1 when the catchment has an elongated shape.
	Elongation ratio: the ratio of length of longest drainage to diameter of a circle with the same area
Land cover (%)	Forest, grassland, cropland, savannah, ..
Soil (%)	Lixisols, leptosols, vertisols, ..
Geology (%)	Migmatite, granite, alterite, ..

We consider there is an inflation and then colinearity if the value of the VIF is greater than the given threshold. In the current study 10 was chosen as the threshold value.

$$VIF = 1/(1 - r_{ij}^2) \quad \text{Eq.7.1}$$

$$Y' = \beta_0 + \beta_1 X_1 + \beta_2 X_2 + \beta_3 X_3 + \dots + \beta_n X_n \quad \text{Eq.7.2}$$

Where  $r_{ij}^2$  is the colinearity coefficient,  $\beta_1, \beta_2, \dots, \beta_n$  are regression coefficients ;  $X_1, X_2, X_3, \dots, X_n$  are independant variables (here catchments characteristics),  $Y'$  is the dependant variable (here model parameter) and  $\beta_0$  is an intercept of the regression line.

If CPC1 and CPC2 show an inflation, one of the two is removed from the list in order to solve collinearity problems. In definitive, from an initial list of 23 CPCs, only 20 were kept for the regression analysis. A correlation matrix has been computed with the calibrated model parameters. CPCs which showed the highest correlation values (typically greater than 0.7) for a given parameter are selected for a multiple linear regression form, using the statistical analysis tool SPSS. Each model input parameter is explained by one or many catchment properties. The validation criteria were the coefficients of determination and Fisher probabilities.

## 7.2- Results and discussion

### Modelling results and calibrated parameters values

The catchments range from 750 to 10 080 km<sup>2</sup>. The model was calibrated and validated in section 4. Table 7-2 gives the values of performance criteria as well as the values of the calibrated parameters for catchments involved in the analysis. As commented above, model performance is good. The NSE, NSE Root and KGE are greater than 0.7 for all catchments; the NSE Log of Sani catchment is a bit low (0.53).

**Table 7-2: Modelling results and calibrated parameters involved in the multiple regression analysis.**

Nº	1	2	3	4	5	6	7	
<b>Stations</b>	Sani	Donga-Affon	Sara-manga	Bori-Gourou	Barérou	Aval-Sani	Bétérou	
<b>Country</b>	BENIN	BENIN	BENIN	BENIN	BENIN	BENIN	BENIN	
<b>Cal.period</b>	2004-2005	1999&2001	2001-2002	2000-2002	2001 & 2005	2001-2002	1998-2003	
<b>Val.period</b>	-	2005	2005	2003-2005	-	2003&2005	2004-6/8-10	
<b>Area (km<sup>2</sup>)</b>	745	1308	1360	1607	2134	3279	10083	
	v	1.00	1.20	1.09	0.92	1.08	1.01	0.99
	λ	15	14	10	13	15	10	16
	TX	0.00	0.37	0.30	0.12	0.30	0.00	0.10
	NSE CAL	0.80	0.78	0.79	0.84	0.83	0.72	0.89
	NSE VAL	-	0.61	0.57	0.73	-	0.81	0.76
	NRQ CAL	0.76	0.90	0.84	0.81	0.87	0.84	0.92
	NRQ VAL	-	0.79	0.82	0.80	-	0.88	0.87
	NLQ CAL	0.53	0.89	0.82	0.58	0.87	0.82	0.91
	NLQ VAL	-	0.83	0.92	0.63	-	0.90	0.90
	KGE CAL	0.82	0.72	0.83	0.88	0.80	0.77	0.86
	KGE VAL	-	0.48	0.75	0.57	-	0.82	0.64
	PB CAL	0.00	-0.11	0.11	0.09	-0.06	0.09	0.01
	PB VAL	-	0.43	-0.11	-0.26	-	0.14	-0.20
	APB CAL	0.34	0.39	0.43	0.41	0.43	0.48	0.31
	APB VAL	-	0.54	0.52	0.44	-	0.40	0.39
	WR <sup>2</sup> CAL	0.77	0.56	0.68	0.80	0.46	0.61	0.77
	WR <sup>2</sup> VAL	-	0.71	0.45	0.44	-	0.73	0.60
	R <sup>2</sup> CAL	0.82	0.81	0.81	0.85	0.60	0.84	0.93
	R <sup>2</sup> VAL	-	0.80	0.61	0.73	-	0.76	0.92

The percent bias does not exceed 10% and the maximum absolute percent bias is of 55%. The weighted R<sup>2</sup> presents generally good values in spite of some low

values in validation (0.44). Here in this study, we adopted a particular calibration approach that implies more or less subjectivity, it could be good to establish a well defined calibration procedure that will give the same result whoever the user. However this approach should depend on the objectives of the modelling.

### **Catchment Physical Characteristics (CPCs)**

Table 7-3 presents the results of the computation of the catchment features. Certain features do not show much variation. It is the case for the drainage density, the average slope of catchment, the Gravelius  $K_G$  Index and the elongation ratio. In contrary, the geological features units a great disparity. In tables 7-4 and 7-5 are respectively presented the matrix of correlation between the calibrated parameters and the CPCs (with respect to a non-colinearity condition) and the best parameter model derived from the multiple regression analysis.

In table 7-4, highest correlations are highlighted (put in bold and underlined). After the analysis of these specific CPCs, parameters equations have been derived. The models with the best coefficient of determination  $R^2$  and Fisher probability have been kept.

When analyzing more closely these equations, we can say that the computed parameter models reflect the theoretical background of the model parameters. The parameter  $v$ , for example expresses the non-linearity of the physical phenomenon of water flow. This parameter is correlated with the percentage of crop land and the elongation ratio. Depending on the density and nature of vegetation or land use, some water is intercepted and does not contribute to the flow. Catchment shape influences the form of the hydrograph.

7. Towards an application of MODHYPMA to ungauged catchments

Table 7-3: Physical catchment properties as computed for the sub-catchments .

Catchment Characteristics	Donga Pont	Sani	Donga-Affon	Saramanga	Bori-Gourou	Barérou	Cote238	Aval-Sani	Bétérou	Savè
Area (km <sup>2</sup> )	586.68	741.80	1307.29	1359.50	1620.38	2127.33	3058.83	3286.81	10076.97	23486.15
Drainage density (km/ km <sup>2</sup> )	0.16	0.17	0.19	0.14	0.17	0.19	0.16	0.18	0.19	0.18
Hypsometric integral	0.41	0.48	0.40	0.41	0.44	0.47	0.34	0.35	0.30	0.55
Elevation mean	395.90	376.13	380.60	402.76	357.19	346.71	376.76	382.82	354.96	317.68
Average slope of catchment	2.63	2.27	2.52	2.51	2.37	2.42	2.69	2.46	2.50	2.76
Gravelius K <sub>c</sub> Index	2.03	2.11	1.99	1.90	1.95	2.05	1.99	1.90	1.95	2.16
Elongation ratio	2.41	2.10	2.19	1.96	1.56	2.12	2.16	1.81	1.95	2.40
Crop land (%)	47.98	10.39	44.65	22.01	17.36	31.58	14.27	32.09	25.74	23.28
Forest (%)	1.53	2.82	2.55	6.28	2.42	3.19	8.41	2.65	2.96	7.54
Grass land (%)	0.00	0.00	0.01	0.00	1.17	0.02	0.45	0.02	0.66	0.91
Residential (%)	0.41	0.02	0.24	0.42	0.12	1.26	0.21	0.16	0.47	0.28
Luvisol (%)	2.09	0.10	56.75	69.27	72.34	11.66	51.37	38.15	45.32	54.85
Alisol (%)	96.96	82.41	34.31	29.93	18.25	85.05	45.54	48.66	46.65	31.15
Plinthosol (%)	0.45	14.94	0.37	0.01	6.30	2.78	1.41	11.60	5.70	2.98
Gleysol (%)	0.00	0.00	8.35	0.00	0.00	0.00	0.00	0.00	0.00	1.81
Alterites (%)	12.19	0.00	22.97	41.46	0.00	0.00	26.42	9.73	3.32	5.04
Gneiss (%)	40.90	22.04	32.38	22.08	13.51	0.01	10.47	35.51	15.15	11.01
Granite (%)	0.10	3.24	1.83	0.00	0.40	0.60	0.00	2.77	1.15	1.96
Migmatites (%)	45.67	63.10	37.24	36.24	69.94	91.46	57.16	45.50	68.76	73.49
Lateritic consolidated soil layers (%)	0.09	11.57	4.86	0.00	5.73	7.92	5.14	5.95	8.20	4.82

**Table 7-4: Matrix of Correlation between the calibrated parameters vs. CPCs with respect to a non-collinearity condition**

Physical Catchment Characteristics	$\nu$	$\lambda$	Xt
Area (km <sup>2</sup> )	-0.28	0.37	-0.25
Drainage density (km/ km <sup>2</sup> )	0.07	0.58	-0.06
Hypsometric integral	0.04	0.10	0.15
Elevmean	0.38	<b>-0.73</b>	0.10
Average slope of catchment	0.57	-0.28	0.58
Gravelius KG Index	0.04	<b>0.71</b>	-0.10
Elongation ratio	<b>0.77</b>	0.40	0.45
Crop land (%)	<b>0.74</b>	-0.06	0.59
Forest (%)	0.25	-0.50	0.39
Grass land (%)	-0.69	0.21	-0.24
Residential (%)	0.28	0.28	0.52
Alisol (%)	0.04	0.47	-0.20
Plinthosol (%)	-0.62	0.08	<b>-0.93</b>
Gleysol (%)	<b>0.77</b>	0.13	0.58
Alterites (%)	0.60	-0.62	0.56
Gneiss (%)	0.27	-0.52	-0.20
Granite (%)	-0.02	0.10	<b>-0.60</b>
Migmatites (%)	-0.44	0.64	-0.15
Lateritic consolidated soil layers (%)	-0.37	<b>0.73</b>	-0.56

**Table 7-5: Best parameter model derived from the multiple regression analysis**

Parameters	Equations	R <sup>2</sup>	Fisher p
$\nu$	0.46+0.004(% Crop land)+0.024 (Elongation ratio)	0.83	0.03
$\lambda$	7.38-0.067 (Mean elevation) + 15.55 (K <sub>G</sub> index)	0.75	0.064
<b>TX</b>	0.3+0.04 (% Granite)-0.032 (% Plinthosol)	0.9	0.008

For example, for a given rainfall, low discharge values will be observed at the outlet for an elongated catchment because a long period of time is needed to propagate the flow. In contrast, a catchment with a shape like a fan will be subject to very high discharge values in shorter periods of time.

The parameter  $\lambda$  is a macroscopic parameter which describes properties related to the geomorphology and pedology of the catchment. This parameter is correlated with the mean elevation and the  $K_G$  index. These CPCs are important features in the definition of the catchment morphology. The features do not change over time. This would mean that parameter  $\lambda$  has a constant value over time for a given catchment. This is more or less consistent with theoretical considerations. But it is not exactly the case in practice. Nevertheless this result (about model parameter) is acceptable so far as the local sensitivity of  $\lambda$  is low.

The parameter  $TX$  accounts for the amount of rainfall that is required before discharge starts (this is specific to semi-arid and sub-humid areas). This parameter is correlated with the percentage of granite and Plinthosol. The geology of the substratum influences not only groundwater flow but also surface flow. The substratum permeability has a role to play in the starting and rising of flow, on its volume and on the contribution to low river flow by groundwater. Moreover, the soil type influences the rate of flow rising as well as its volume.

Correlations between calibrated and predicted model parameters with associated 95% confidence interval are presented in Figure 7-1. Coefficients of determination are all greater than 0.7 and Fisher probabilities inferior to 5% .

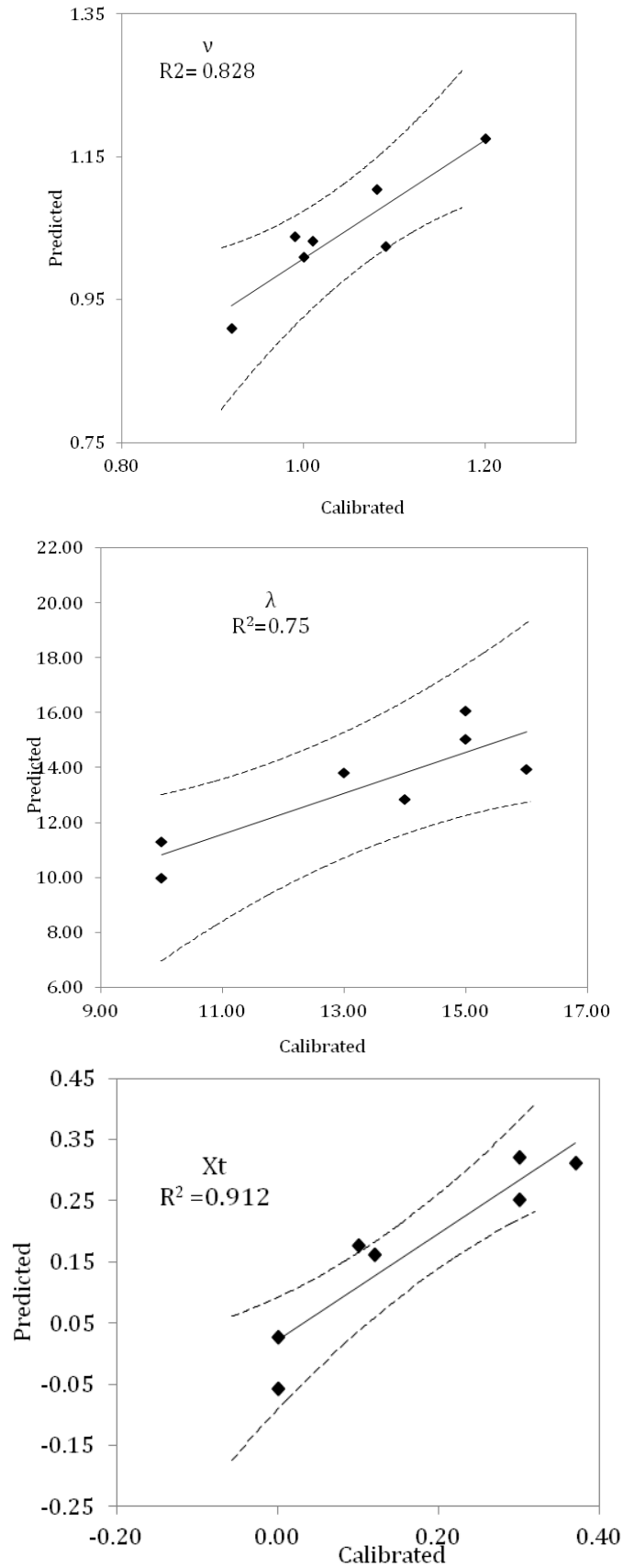


Figure 7-1: Predicted vs. Calibrated model parameters with the associated 95% confidence interval.

### Validation of parameters models on ungauged basins

For three catchments (Donga Pont; Cote 238 and Savè) not used for the regression, we computed the parameters from the equations established in table 7-5. Table 7-6 gives the results of application of these parameters to the various catchments. The results are good. NSE for the three catchments is greater than 0.7 The PBIAS is less than 30%. The maximum APBIAS is 65%. The  $WR^2$  present good values although we have a low value for Donga Pont.

Figures 7-2 to 7-5 show the observed and simulated discharge using the regression-based parameter for the three catchments.

**Table 7-6: Results of the modelling using parameters calculated from the multiple regression analysis for Donga Pont ; Cote 238 and Savè**

Nº	1	2	3	
<b>Stations</b>	Donga Pont	Cote 238	Savè	Savè
<b>Country</b>	BENIN	BENIN	BENIN	BENIN
<b>Period</b>	1999/2001	2001-2/2005	CAL=1996-2004	CAL=2004-2010
<b>Area (km<sup>2</sup>)</b>	587	3060	23491	23491
<b>v</b>	1.23	1.04	1.13	1.13
<b>λ</b>	12.56	13.00	19.73	19.73
<b>TX</b>	0.29	0.26	0.29	0.29
<b>NSE</b>	0.71	0.71	0.86	0.67
<b>NRQ</b>	0.72	0.75	0.87	0.72
<b>NLQ</b>	0.56	0.67	0.76	0.61
<b>KGE</b>	0.67	0.61	0.83	0.70
<b>PB</b>	0.22	-0.28	0.15	0.26
<b>APB</b>	0.65	0.44	0.38	0.53
<b>WR<sup>2</sup></b>	0.54	0.37	0.78	0.87
<b>R<sup>2</sup></b>	0.78	0.56	0.87	0.93

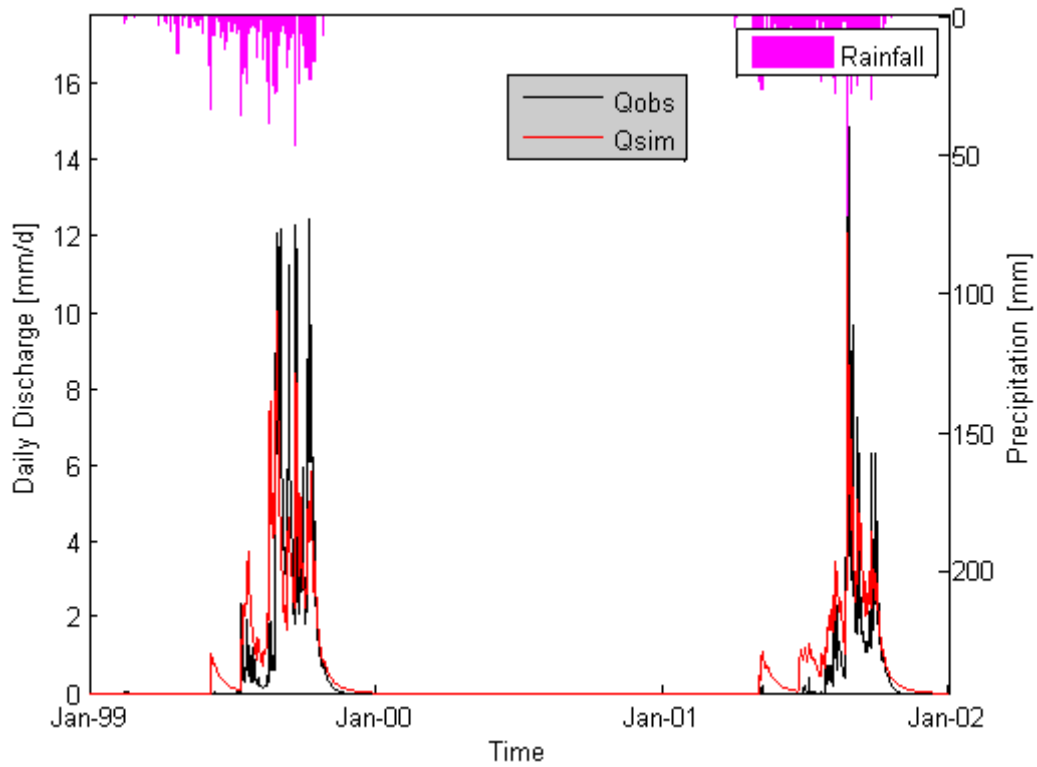


Figure 7-2: Observed and simulated discharge using the regression-based parameter for Donga Pont (586 km<sup>2</sup>)

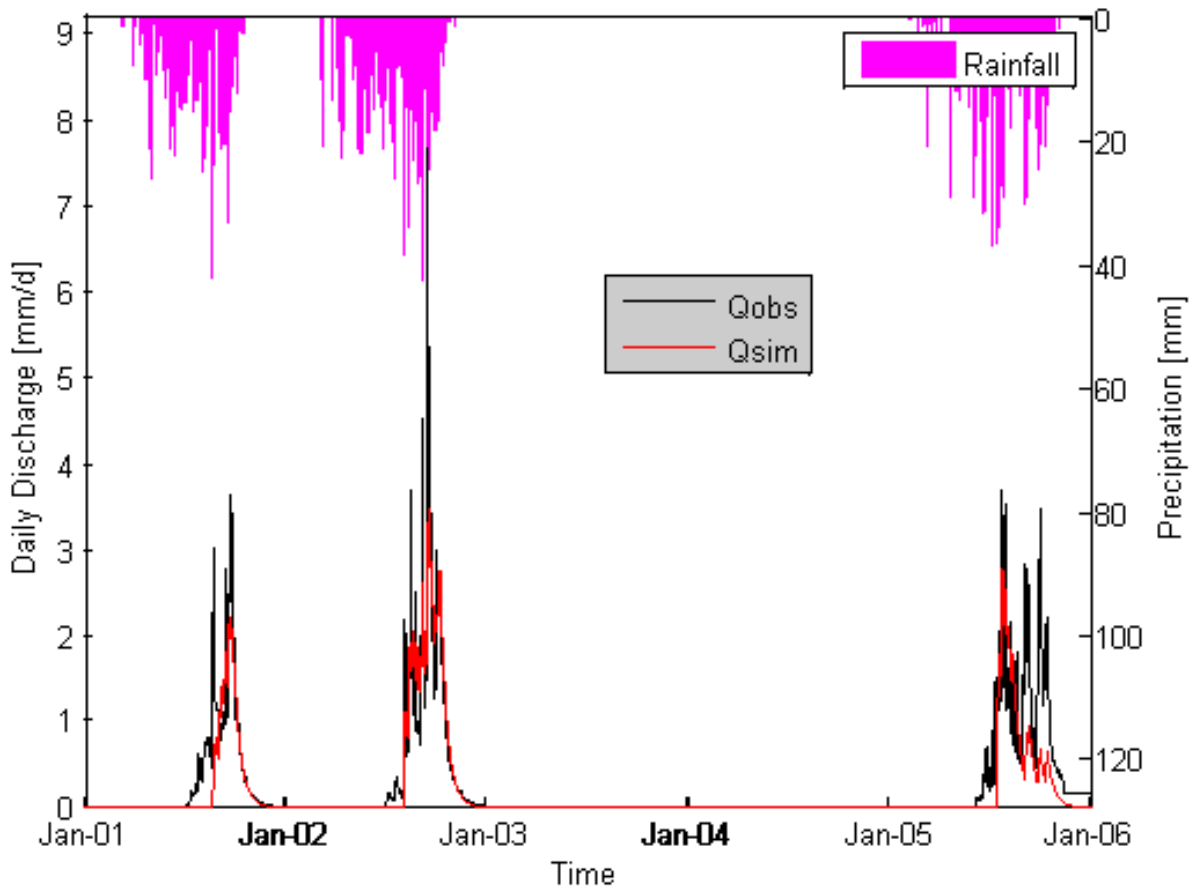


Figure 7-3: Observed and simulated discharge using the regression-based parameter for Cote 238 (3058 km<sup>2</sup>)

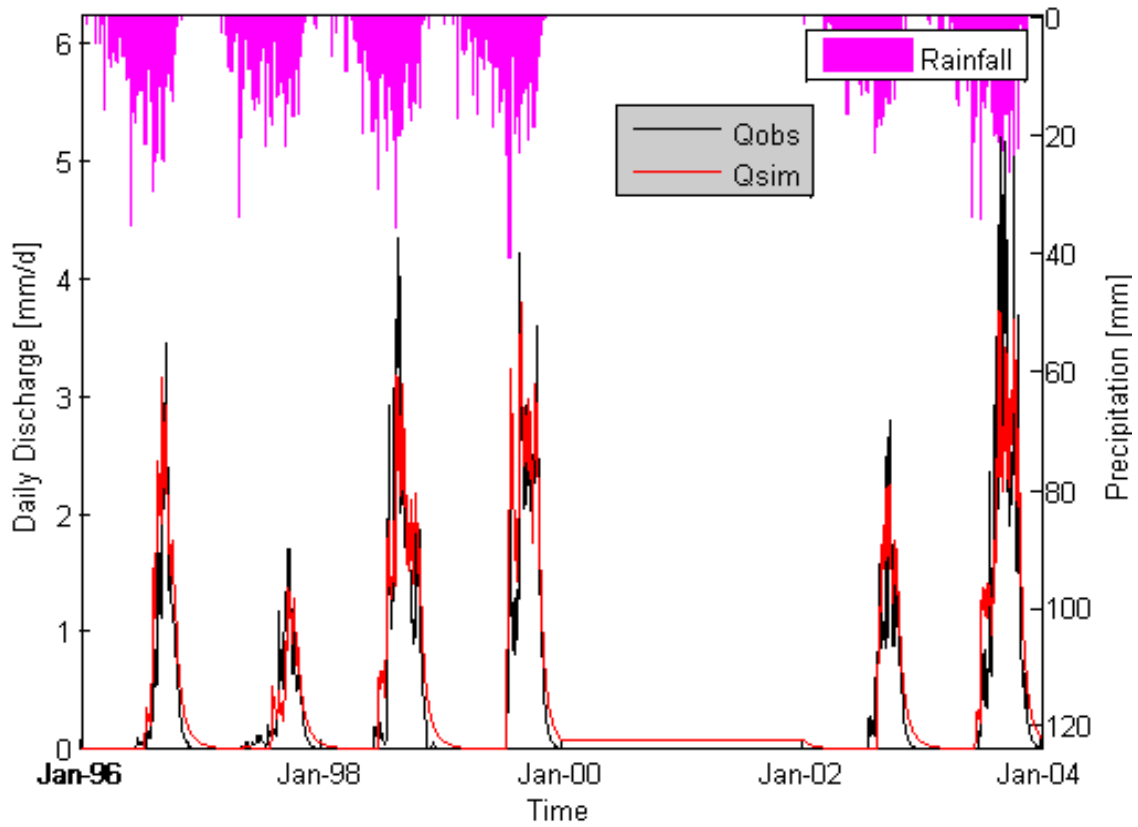


Figure 7-4: Observed and simulated discharge using the regression-based parameter for Savè (23486 km<sup>2</sup>), period 1

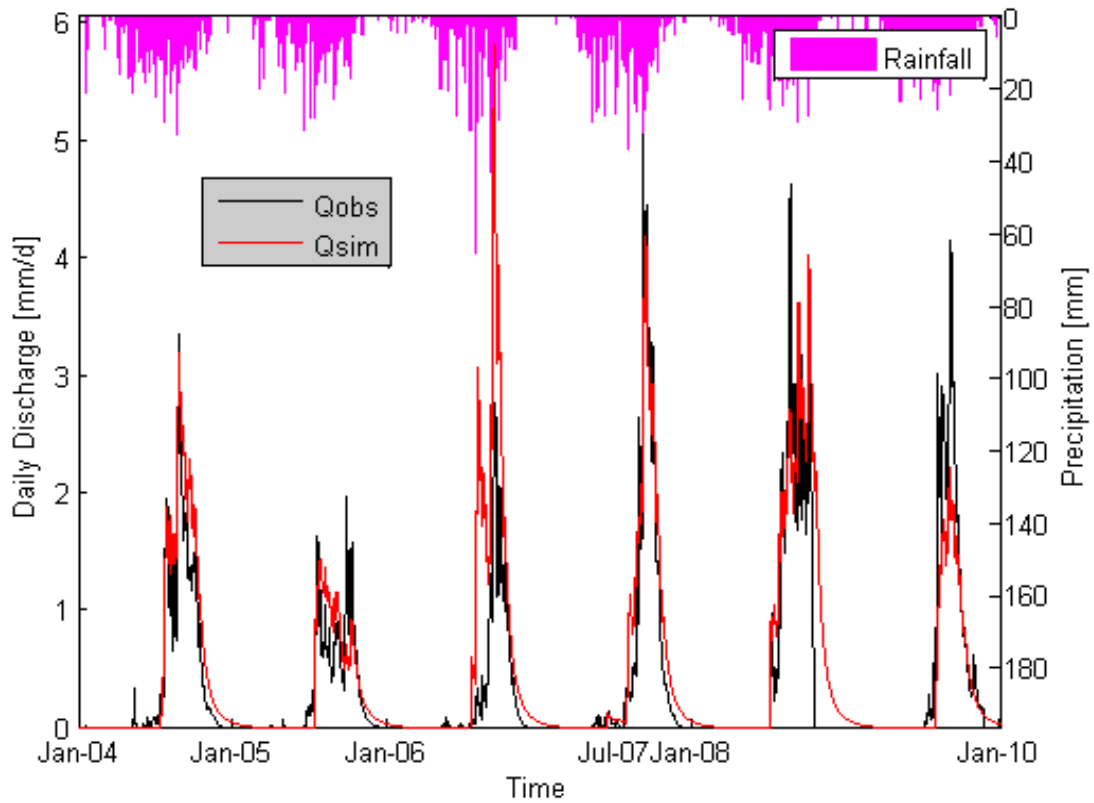


Figure 7-5: Observed and simulated discharge using the regression-based parameter for Savè (23486 km<sup>2</sup>); period 2

The objective of this chapter was to explore the possible transferability of MODHYPMA for ungauged basins studies. After determining the physical features of the catchments, they were correlated with the model calibrated parameters. The best parameter models were derived from a multiple regression analysis. The computed parameter models show a link with the theoretical background of the model parameters. These parameter models were validated by applying them on gauged catchments that were considered ungauged. Satisfying results were obtained leading to the conclusion that MODHYPMA can be used for PUB.

Nevertheless, further steps can be taken, in fact this study can be extended to the analysis of how these parameters could evolve or be estimated in a context of climate change impacts assessment more specifically for land use change impacts assessment. In that case, parameter  $v$  seems to be the most decisive factor. The impact of land use change on catchments that have been affected by an important change in land use patterns in the last 30 years could be investigated. This kind of studies could lead to the assessment of future land use change (land use scenarii) impacts on runoff.

The estimation of uncertainties associated with these predictions (in Ungauged Basins) should also be carried out. More sub-catchments of Ouémé basin could be further tested (using the derived parameters equations) for validation or improvement.

Finally, our regionalization results could be compared to results from other models.

## GENERAL CONCLUSION AND PERSPECTIVES



Photo 8: Partial view of the Téro river nearby Saramanga (135 km)

## 8- General conclusion and perspectives

The assessment of water resources is becoming a greater challenge in a context of climatic change. New modelling approaches are being explored in order to bring a different understanding of the catchment functioning that would lead to better theories and numerical results. Instead of relying only on complex overparametrized models that try to prescribe all the heterogeneities of the hydrological system, we propose to the use of simpler models that have the advantages to have less parameters and are applicable at all scales. This study presented the case of a model based on an optimal principle: the Principle of Least Action (PLA).

This model was firstly formulated in 2004 and the theoretical bases were elaborated. Studies are being conducted on the topic and the main objective of the present work was to advance in the development of the model based on the PLA and to evaluate it. The evaluation was done through its application on a large range of catchments in terms of drainage areas and climates; its comparison to two other models and the analysis of sensitivity and uncertainties. Given the parsimony of the model, another objective was to further apply the model for the prediction of the hydrology of ungauged catchments which is one of the major challenges to hydrologists (Wheater *et al.*, 2008).

The first part of this dissertation was dedicated to a brief recall of the river flow generation pathways as well as the hydrological processes that are involved. The importance of hydrological models and how they are built was also addressed. The modelling approaches used in this work and the geographical overview of the study areas were later presented.

As far as the first objective is concerned i.e. to go further in the development of the model, we proposed a new parameter TX that was introduced to account for the amount of rainfall is required before discharge starts. This being a particular

feature of semi-arid and sub-humid areas. Besides, the coding of the model was improved in order to perform an automatic calibration and to generate a large number of runs for the uncertainty analysis.

Regarding the second objective which was the assessment of the model, we first applied it to catchments of various sizes (from smaller to larger spatial scale) under various climate conditions. In fact, twenty (20) catchments in Africa (Benin, Côte D'Ivoire, Ethiopia) and USA were selected. Their areas range from 32 to 74,900 km<sup>2</sup>. Eight criteria of performance were used among which the NSE, the Percent Bias (PB) and the Weighted R<sup>2</sup> for the model calibration. MODHYPMA was successfully applied to most catchments but showed also some insufficiencies. From the results displayed as a box plot, we can say that the interquartile range was roughly [0.6-0.8] for the NSE criterion, [0.7-0.9] for the Nash Root criterion, [0.6-0.85] for the Nash Log criterion, [0.6-0.8] for the KGE, [(-0.15)-0.15] for the Percent Bias, [0.3-0.5] for the Absolute Percent Bias, [0.4-0.7] for the Weighted R<sup>2</sup> and [0.65-0.8] for the R<sup>2</sup>. From the hydrographs and flow duration curves, for all runs, we can say that the beginning of the season was globally well simulated but sometimes underestimated. The recession curve was very well simulated. Low flows were overestimated. Middle flows were well represented. MODHYPMA tended to underestimate the highest flows. The model was subject to some timing errors. Data quality, the concentration time lower than 1 day for some catchments and the inability of the current version of the model to reproduce some particular processes were the main reasons pointed out to justify model insufficiencies.

Still for the second objective, we secondly compared the results of MODHYPMA to those of two well-known models namely GR4J and HBV.

Here only the NSE was used as criterion of performance for the comparison of the results. The calibration and validation of the models were performed in full split sample test: calibration based on one period and validation on another period followed by the calibration on the second period and validation using the first

period. The mean NSE values for calibration and validation periods were then computed. The three models gave globally good results on most catchments but revealed also some insufficiencies. From the results displayed as a compared box plot, we can say that for MODHYPMA the interquartile range was roughly [0.7-0.85] for the calibration period and [0.5-0.75] for the validation period. For GR4J model, the interquartile range was roughly [0.75-0.9] for the calibration period and [0.6-0.75] for the validation period. For HBV model, the interquartile range was roughly [0.7-0.85] for the calibration period and [0.55-0.7] for the validation period. The main conclusions of this section were that in the calibration period GR4J presented a greater performance compared to other models which showed similar performance. In the validation period, MODHYPMA and GR4J revealed similar performance while HBV showed a lower performance. Overall, GR4J showed a higher performance but as HBV, it showed an important drop in model performance from calibration to validation. This loss of performances was relatively small for MODHYPMA showing a similar quality for the calibration and the validation periods.

From the hydrographs and flow duration curves, for all runs, we can say that globally at the beginning of the season, the three models had a good fit; MODHYPMA sometimes overestimated this part of the hydrograph while GR4J showed a systematic underestimation and HBV a systematic overestimation.

The recession curve was very well simulated by MODHYPMA, well modelled by GR4J and HBV. MODHYPMA tended to overestimate the low flows while they were quite well reproduced by GR4J and slightly overestimated by HBV. Middle flows were well represented by all the three evaluated models. High flows were quite well simulated by GR4J but some peaks were overestimated. MODHYPMA underestimated the highest flows. HBV had an intermediate behaviour. All models were subject to timing errors.

Data quality, the concentration time lower than 1 day for some catchments and the inability of the models to reproduce some particular processes were the main reasons raised explain model insufficiencies.

The results show that the objective had been achieved. In fact, the model, with a daily time step, has been successfully applied to a certain range of catchments. Nevertheless, we do not recommend its application to catchments with response time lower than one day. That means that MODHYPMA still needs to be improved.

The third objective of this thesis was the analysis of the sensitivity of MODHYMA's parameters. A local sensitivity analysis was performed: a sensitivity index  $S_i$  was calculated using the results of the simulation (NSE) with model calibrated parameter 10% increased, 10% decreased and the baseline simulation. The results allowed us to conclude that the parameter  $v$  had a high sensitivity; the parameter  $\lambda$  had a medium to low sensitivity and the parameter TX had a low sensitivity. These results implied that the parameter  $v$  would contribute to a larger part of the calibrated model uncertainties. Besides, the analysis of the hydrographs and the calibration of model parameters led us to propose the hypothesis of  $v$  being a constant should be reassessed.

The second part of the third objective was to perform an uncertainty analysis of MODHYMA. Only parameters uncertainty was analyzed using the GLUE - Generalized Likelihood Uncertainty Estimation- methodology. A uniform distribution as well as the Latin Hypercube as the sampling method were chosen. For each catchment, we generated a number of runs and a threshold of 0.60 (NSE) was applied to select behavioural sets. Simlab and Gluewin softwares were used for the purpose of the uncertainty analysis. We performed between 200 and 700 runs per catchment. The behavioural runs obtained in final were by far very few; they range between 20 and 389. For all catchments, the dot plots of the parameters were realized and the 90PPU were plotted. Parameter  $v$  appeared to be the primary source of uncertainty confirming the result obtained after the sensitivity analysis. Good values were reached for p and r-factors. Values of p-factor ranged from 0.33 to 0.78 while values of r-factor ranged from 0.29 to 0.58.

The fourth objective of this research was the application of MODHYPMA for PUB. We relied on statistical methods and the use of the physical features of the various catchments. After correlating these features with the model calibrated parameters, the best parameter models were derived from a multiple regression analysis. The computed parameter models reflected the theoretical background of the model parameters. In fact, the parameter  $\nu$ , which expresses the non-linearity of the physical phenomenon of water flow was correlated with the percentage of crop land and the elongation ratio. The parameter  $\lambda$  which is a macroscopic parameter describing properties related to the geomorphology and pedology of the catchment was correlated with the mean elevation and the  $K_G$  index. And the parameter  $TX$  which accounts for the amount of rainfall that is required before discharge starts (specificly to semi-arid and sub-humid areas) was correlated with the percentage of granite and Plinthosol. Correlations between calibrated and predicted model parameters with associated 95% confidence interval were presented. Coefficients of determination were all greater than 0.7 and Fisher probabilities inferior to 5%. These parameter models were validated by applying them on gauged catchments that were considered ungauged. Satisfying results ( $NSE > 0.67$ ) were obtained leading to the conclusion that MODHYPMA can be used for PUB.

The global objective of the study had been fulfilled; nevertheless there are still challenges left. One future challenge in the model development is to further work on the model theoretical aspects. A number of assumptions have to be reconsidered. Like pointed out before further research could be the reassessment of hypotheses underlying computations like for example the hypothesis about the parameter  $\nu$  being constant; the development towards a semi-distributed/finer time step version in order to better represent the spatial variability of the processes and improve the simulation of the peak flows. And for the particular

case of small catchments, smaller time-step (hourly) data may be used when available. There is also a need to search for better quality data (if possible). Shaw *et al.* (2011) draw attention on the quality of the input data, they comment that we should not expect a model perform better than we can define the inputs. The quality of the input data is consequently an important aspect about model assessment. Additionally Duan *et al.* (2003) recall that because parameter estimates are data dependent, adequate data are needed for estimation.

We should consider the use of the actual evapotranspiration rather than the potential one and an additional module may be added in order to compute it from relevant input data that would be provided from meteorological stations. Attribution of evapotranspiration to each basin has to be further analysed.

Rainfall data may be extended to satellite data so as to make a comparison between results (from ground data and from satellite data). It is relevant to notify here that in very small catchments there is generally not enough rainfall measurements and the extrapolation of data from further rainfall stations may be an important source of uncertainty.

It would be also very important to incorporate the uncertainty from the observed data (discharge, precipitation, ...) and boundary conditions in the model assessment. The evaluation and quantification of uncertainties associated with river flow measurements is already the scope of many studies (See for example the study conducted by (McMillan *et al.*, 2010)). The comparison of models could be extended to the uncertainty analysis of GR4J and HBV. Moreover the uncertainty analysis could be performed using other criteria than the NSE. Some weighted schemes could be adopted in order to improve the selection of behavioural simulations.

Calibration/validation procedure has to be improved. It would be of great importance to build a well-structured and systematic calibration approach supported by useful guidelines and automated techniques such as the Shuffled Complex Evolution Algorithm (SCE-UA), or the Multi-objective Optimisation Algorithm (MOCOM). The analysis revealed that MODHYPMA could be a good

candidate for climate change impacts assessments as well as impacts of land use changes; more sophisticated or robust comparison approaches could be elaborated and more data sets tested. This should be the object of future research.

The parsimony of this model is also a great advantage conferring it a notable simplicity. This simple structure, more suitable for regionalisation purposes (Wagener *et al.*, 2001) allowed us the extension of our work to ungauged basins.

The derived parameter equations reflect the theoretical background of the model parameters. They could be improved or validated using more sub-catchments of Ouémé basin along with the estimation of uncertainties. Moreover, the regionalization results could be compared to results from other models.

The application of the PLA is rather new in hydrology. This principle has brought new breakthroughs and progress in many areas in physics. We expect the same in the field of hydrology; in particular in addressing the issue of passing from the point scale to the basin scale in physics-based modelling. Besides, because they require less data, lumped models are sometimes preferred over distributed ones in the situations of little data. As commented above, the model has yet to be improved but has shown its applicability under various climatic conditions. There is still the need to apply it on more basins in other regions and under other climate conditions.

## References

- Abbaspour, K. C. (2008) SWAT-CUP2: SWAT Calibration and Uncertainty Programs - A User Manual, 95. Duebendorf, Switzerland: Department of Systems Analysis, Integrated Assessment and Modelling (SIAM), Eawag, Swiss Federal Institute of Aquatic Science and Technology,. Retrieved from [http://swat.tamu.edu/media/114860/usermanual\\_swatcup.pdf](http://swat.tamu.edu/media/114860/usermanual_swatcup.pdf).
- Afouda, A. & Alamou, A. E. (2010) Modèle hydrologique basé sur le Principe de Moindre Action (MODHYPMA). *Ann. des Sci. Agron. du Bénin* **13**(1), 23–45.
- Afouda, A., Bouchez, J.-M., Braud, I., Cazenave, F., Depraetere, C., Dessay, N., Diedhiou, A., et al. (2001) Variabilité climatique et variabilité hydrologique en Afrique de l'Ouest : Un système couplé. *Atelier sur le Couplage des modèles atmosphériques Hydrol.*, 1–5. Toulouse, France.
- Afouda, A., Lawin, A. E. & Lebel, T. (2004) A stochastic streamflow model based on a minimum energy expenditure concept. *Contemp. Probl. Math. Phys.*, 153–169. Catholic University of Louvain: Belgium.
- Aggarwal, P. K. & Singh, A. K. (2010) Implications of Global Climatic Change on Water and Food Security. In: *Global Change: Impacts on Water and food Security Water Resources Development and Management* (C. Ringler, A. K. Biswas & S. Cline, eds.), 49–63. Berlin, Heidelberg: Springer Berlin Heidelberg. doi:10.1007/978-3-642-04615-5
- AghaKouchak, A. (2013) Integrated Water Cycle Analysis, 54pp. University of California, Irvine,USA.
- Alamou, A. E. (2011) *Application du Principe de Moindre Action à la Modélisation Pluie-débit*. Thesis (PhD). Université d'Abomey-Calavi, Benin. 231p.
- Arovas, D. (2012) Noether ' s Theorem, 1–19. California, San Diego: University of California San Diego, Department of Physics. Retrieved from <http://www.physics.ucsd.edu/students/courses/fall2010/physics110a/LECTURES/CH07.pdf>
- Avahounlin, R. F., Lawin, A. E., Alamou, A. E., Chabi, A. & Afouda, A. (2013) Analyse Fréquentielle des Séries de Pluies et Débits Maximaux de L ' Ouémé et Estimation des Débits de Pointe. *Eur. J. Sci. Res.* **107**(3), 355–369. Retrieved from <http://www.europeanjournalofscientificresearch.com>
- Barbé, L. Le, Alé, G., Millet, B., Texier, H., Borel, Y. & Gualde, R. (1993) *Les ressources en eaux superficielles de la République du Bénin*. Paris: Editions de l'ORSTOM. 540p

- Bauman, D. (2012) Symmetries and Conservation Laws, Vol. 87, 87–91. Cambridge, UK: Department of Applied Mathematics and Theoretical Physics, Cambridge University. Retrieved from <http://www.damtp.cam.ac.uk/user/db275/concepts/Symmetry.pdf>
- Beven, K. (1995) TOPMODEL. In: *Computer models of watershed hydrology* (V. P. Singh, ed.). Littleton, Colorado: Water Resources Publications. Retrieved from <https://books.google.bj/books?id=8XfuAAAAMAAJ>
- Beven, K. (2000) Uniqueness of place and process representations in hydrological modelling. *Hydrol. Earth Syst. Sci.* **4**(2), 203–213. Retrieved from <http://hal.archives-ouvertes.fr/hal-00304594>
- Beven, K. (2006) A manifesto for the equifinality thesis. *J. Hydrol.* **320**, 18–36. doi:10.1016/j.jhydrol.2005.07.007
- Beven, K. (2008) *Environmental Modelling: An Uncertain Future?* London: Routledge.
- Beven, K. (2012) *Rainfall-Runoff Modelling*, 2nd ed. Chichester, UK: John Wiley & Sons, Ltd. doi:10.1002/9781119951001
- Beven, K. & Binley, A. (1992) The Future of Distributed Models: Model Calibration and Uncertainty Prediction. *Hydrol. Process.* **6**, 279–298. Retrieved from <http://www.mobilehealthcaretoday.com/blogs/mhct-blog/2011/03/the-future-of-distributed-healthcare.aspx>
- Beven, K. & Binley, A. (2014) GLUE: 20 years on. *Hydrol. Process.* **28**(24), 5897–5918. doi:10.1002/hyp.10082
- Beven, K. & Kirkby, M. J. (1976) Toward a Simple Physically Based Variable Contributing Area of Catchment Hydrology. Working Paper No. 154, School of Geography, University of Leeds, UK.
- Beven, K. & Kirkby, M. J. (1979) A physically based, variable contributing area model of basin hydrology / Un modèle à base physique de zone d'appel variable de l'hydrologie du bassin versant. *Hydrol. Sci. Bull.* **24**(1), 43–69. doi:10.1080/02626667909491834
- Beven, K., Smith, P., Westerberg, I. & Freer, J. (2012) Comment on 'Pursuing the method of multiple working hypotheses for hydrological modeling' by P. Clark et al. *Water Resour. Res.* **48**(11), 1–16. doi:10.1029/2012WR012282
- Biao, E. I., Gaba, C., Alamou, A. E. & Afouda, A. (2015) Influence of the uncertainties related to the Random Component of Rainfall Inflow in the

- Ouémé River Basin ( Benin , West Africa ). *Int. J. Curr. Eng. Technol.* **5**(3), 1618–1629.
- Biondi, D., Freni, G., Iacobellis, V., Mascaro, G. & Montanari, A. (2012) Validation of hydrological models : Conceptual basis , methodological approaches and a proposal for a code of practice. *Phys. Chem. Earth* **42-44**, 70–76. Elsevier Ltd. doi:10.1016/j.pce.2011.07.037
- Blöschl, G. & Sivapalan, M. (1995) Scale issues in hydrological modelling : A review. *Hydrol. Process.* **9**, 251–290.
- Bormann, H. (2005) Evaluation of hydrological models for scenario analyses : signal-to-noise-ratio between scenario effects and model uncertainty Upper Ouémé catchment. *Adv. Geosci.* **5**, 43–48.
- Bormann, H. (2005) Regional hydrological modelling in Benin (West Africa): Uncertainty issues versus scenarios of expected future environmental change. *Phys. Chem. Earth* **30**, 472–484. doi:10.1016/j.pce.2005.07.002
- Bossa, Y. A. (2012) *Multi-scale modeling of sediment and nutrient flow dynamics in the Ouémé catchment ( Benin ) - towards an assessment of global change effects on soil degradation and water quality*. Thesis (PhD). University of Bonn, Germany. 130p.
- Bossa, Y. A. & Diekkrüger, B. (2012) Estimating scale effects of catchment properties on modeling soil and water degradation in Benin ( West Africa ). *Sixth Bienn. Int. Congr. Environ. Model. Softw. (iEMSs), Manag. Resour. a Ltd. Planet.* Leipzig, Germany (in press).
- Bossa, Y. A., Diekkrüger, B., Igué, a. M. & Gaiser, T. (2012) Analyzing the effects of different soil databases on modeling of hydrological processes and sediment yield in Benin (West Africa). *Geoderma* **173-174**, 61–74. Elsevier B.V. doi:10.1016/j.geoderma.2012.01.012
- Boyer, J. F., Dieulin, C., Rouche, N., Cres, A., Servat, E., Paturel, J. E. & Mahé, G. (2006) SIEREM an environmental information system for water resources. 5th World FRIEND Conference. In: *Climate Variability and Change--hydrological Impacts* IAHS publication, 19–25. La Havana - Cuba: IAHS Publication 308.
- Braud, I., Varado, N., Galle, S., Haverkamp, R., Lebel, T. & Reggiani, P. (2001) Modélisation hydrologique du bassin versant de l’Ouémé à l’aide du modèle POWER. Grenoble, France.

- Brookes, J. D., Ainger, C. M., Howe, C., Norton, J. W. & Schladow, G. (2010) Water and climate change: challenges for the 21st century. *J. Water Clim. Chang.* **01**(1), 1. doi:10.2166/wcc.2010.100
- Brown, J. & Heuvelink, G. B. M. (2005) Assessing Uncertainty Propagation Through Physically based Models of Soil Water Flow and Solute Transport. *Encycl. Hydrol. Sci.* John Wiley & Sons, Ltd.
- Brutsaert, W. (2005) *Hydrology – An Introduction*, 1st ed. New York: Cambridge University Press. doi:http://dx.doi.org/10.1017/CBO9780511808470
- Cameron, D., Beven, K. & Tawn, J. (2000) An evaluation of three stochastic rainfall models. *J. Hydrol.* **228**(1-2), 130–149. doi:10.1016/S0022-1694(00)00143-8
- Christoph, M., Fink, A., Diekkrüger, B., Giertz, S., Reichert, B. & Speth, P. (2008) IMPETUS : Implementing HELP in the Upper Ouémé basin. *Water SA* **34**(4), 481–489 (HELP Special Issue). Retrieved from [http://www.wrc.org.za/publications\\_watersa\\_sa\\_help\\_sp\\_edition.htm](http://www.wrc.org.za/publications_watersa_sa_help_sp_edition.htm)
- Clark, M. P., Kavetski, D. & Fenicia, F. (2011) Pursuing the method of multiple working hypotheses for hydrological modeling. *Water Resour. Res.* **47**(9), n/a–n/a. doi:10.1029/2010WR009827
- Clark, M. P., Kavetski, D. & Fenicia, F. (2012) Reply to comment by K. Beven et al. on ‘Pursuing the method of multiple working hypotheses for hydrological modeling’. *Water Resour. Res.* **48**(11), 1–7. doi:10.1029/2012WR012547
- Cornelissen, T., Diekkrüger, B. & Giertz, S. (2013) A comparison of hydrological models for assessing the impact of land use and climate change on discharge in a tropical catchment. *J. Hydrol.* **498**, 221–236. Elsevier B.V. doi:10.1016/j.jhydrol.2013.06.016
- Crockford, R. H. & Richardson, D. P. (2000) Partitioning of rainfall into throughfall, stemflow and interception: effect of forest type, ground cover and climate. *Hydrol. Process.* **14**(16-17), 2903–2920. John Wiley & Sons, Ltd. doi:10.1002/1099-1085(200011/12)14:16/17<2903::AID-HYP126>3.0.CO;2-6
- Davie, T. (2008) *Fundamentals of Hydrology*. (J. Gerrard, Ed.), Second. Oxon: Routledge.
- Diederich, M. & Simmer, C. (2008) Observations of Past and Present Rainfall in Benin. In: *IMPETUS Atlas Benin Research Results 2000 – 2007* (M. Judex & H.-P. Thamm, eds.), 3rd ed., 144. Bonn, Germany.

- Druyan, L. M. (2011) Studies of 21st-century precipitation trends over West Africa. *Int. J. Climatol.* **31**, 1415–1424. doi:10.1002/joc.2180
- Duan, Q., Gupta, H. V., Sorooshian, S., Rousseau, A. N. & Turcotte, R. (Eds.). (2003) *Calibration of Watersheds Models*. Washington DC: American Geophysical Union.
- El-fahem, T. (2008) *Hydrogeological conceptualisation of a tropical river catchment in a crystalline basement area and transfer into a numerical groundwater flow model - Case study for the Upper Ouémé catchment in Benin*. Thesis (PhD). University of Bonn, Germany. 156p.
- El-Fahem, T. & Kocher, A. (2008) Geology of the Ouémé Catchment. In: *IMPETUS Atlas Benin Research Results 2000 – 2007* (M. Judex & H.-P. Thamm, eds.), 3rd ed., 144. Bonn, Germany.
- Fatichi, S., Pappas, C. & Ivanov, V. Y. (2015) Modeling plant–water interactions: an ecohydrological overview from the cell to the global scale. *WIREs Water*. doi:10.1002/wat2.1125
- Feynman, R., Leighton, R. & Sands, M. (1964) The Principle of Least Action. In: *The Feynman lectures on Physics, Volume 2* (Addison-Wesley, ed.), 2nd ed., 1–14. Reading, MA.
- Fink, A. H., Paeth, H., Ermert, V., Pohle, S. & Diederich, M. (2010) Meteorological processes influencing the weather and climate of Benin. In: *Impacts of Global Change on the Hydrological Cycle in West and Northwest Africa* (P. Speth, M. Christoph & B. Dieckkrüger, eds.), 692p. Heidelberg, Germany: Springer.
- Gaiser, T., Goldbach, H., Giertz, S., Hiepe, C. & Klose, A. (2010) Soils. In: *Impacts of Global Change on the Hydrological Cycle in West and Northwest Africa* (P. Speth, M. Christoph & B. Dieckkrüger, eds.), 692p. Heidelberg, Germany: Springer.
- Giertz, S. (2008) Gauged sub-catchments of the Ouémé River. (M. Judex & H.-P. Thamm, Eds.) *IMPETUS Atlas Benin. Research Results 2000 – 2007*. Bonn, Germany. Retrieved from <http://www.impetus.uni-koeln.de/en/impetus-atlas>
- Giertz, S., Dieckkrüger, B. & Höllermann, B. (2012) Impact of global change on water resources in the Ouémé catchment, Benin. In: *River Basins and Change* (J. J. Bogardi, J. Leentvaar & H. Nachtnebel, eds.), 206. Global Water System Project.

- Giertz, S., Diekkrüger, B., Jaeger, A. & Schopp, M. (2006) An interdisciplinary scenario analysis to assess the water availability and water consumption in the Upper Ouémé catchment in Benin. *Adv. Geosci.* **9**, 3–13.
- Giertz, S. & Hiepe, C. (2008) Soil Map of Benin. In: *IMPETUS Atlas Benin Research Results 2000 – 2007* (M. Judex & H.-P. Thamm, eds.), 3rd ed., 144. Bonn, Germany.
- Giglioli, N. & Saltelli, A. (2008) SimLab 2.2 Software for Sensitivity and Uncertainty Analysis, tool for sound modelling. Ispra, Italy: Joint Research Centre, European Commission Institute for Systems Informatics and Safety.
- Gleick, P. H. (2003) Global freshwater resources: Soft-Path solutions for the 21st century. *Science (80-. )*. **302**, 1524–1528. doi:10.1126/science.1089967
- Golden Software Inc., C. (2002) Surfer (R)-version 8.01.
- Grayson, R. & Blöschl, G. (Eds.). (2000) *Spatial Patterns in Catchment Hydrology. Observations and Modelling*, 1st ed., Vol. 1. Cambridge, UK: Cambridge University Press. doi:10.2136/vzj2002.0202
- Gupta, H. V., Kling, H., Yilmaz, K. K. & Martinez, G. F. (2009) Decomposition of the mean squared error and NSE performance criteria: Implications for improving hydrological modelling. *J. Hydrol.* **377**(1-2), 80–91. Elsevier B.V. doi:10.1016/j.jhydrol.2009.08.003
- Hanc, J., Tuleja, S. & Hancova, M. (2003) Simple derivation of Newtonian mechanics from the principle of least action. *Am. J. Phys.* **71**(4), 386–391. doi:10.1119/1.1528915
- Hanc, J., Tuleja, S. & Hancova, M. (2004) Symmetries and conservation laws: Consequences of Noether's theorem. *Am. J. Phys.* **72**(4), 428–435. doi:10.1119/1.1591764
- Héreau, F. (2008) Le principe de moindre action. Reims: Laboratoire de Mathématiques Université de Reims.
- Hiepe, C. (2008) *Soil degradation by water erosion in a sub-humid West-African catchment : a modelling approach considering land use and climate change in Benin*. Thesis (PhD). University of Bonn, Germany. 335p.
- Huntington, T. G. (2006) Evidence for intensification of the global water cycle: Review and synthesis. *J. Hydrol.* **319**(1-4), 83–95. doi:10.1016/j.jhydrol.2005.07.003

- IPCC. (2007) Summary for Policymakers. In: *Climate Change 2007: The Physical Science Basis. Contribution of Working Group I to the Fourth Assessment Report of the Intergovernmental Panel on Climate Change* (S. Solomon, D. Qin, M. Manning, Z. Chen, M. Marquis, K. B. Averyt, M. Tignor, et al., eds.), 1–18. Cambridge University Press, UK.
- Janssen, P. H. M. & Heuberger, P. S. C. (1995) Calibration of process-oriented models. *Ecol. Modell.* **83**, 55–66.
- Jin, X., Xu, C.-Y., Zhang, Q. & Singh, V. P. (2010) Parameter and modeling uncertainty simulated by GLUE and a formal Bayesian method for a conceptual hydrological model. *J. Hydrol.* **383**(3-4), 147–155. Elsevier B.V. doi:10.1016/j.jhydrol.2009.12.028
- Judex, M. & Thamm, H.-P. (2008) *IMPETUS Atlas Benin Research Results 2000 – 2007*. (M. Judex & H.-P. Thamm, Eds.), 3rd ed. Bonn, Germany. Retrieved from <http://www.impetus.uni-koeln.de/en/impetus-atlas>
- Judex, M., Thamm, H.-P. & Menz, G. (2008) Land Use and Land Cover in Central Benin. In: *IMPETUS Atlas Benin Research Results 2000 – 2007* (M. Judex & H.-P. Thamm, eds.), 3rd ed., 144. Bonn, Germany: IMPETUS Project.
- Kebede, A., Diekkrüger, B. & Moges, S. A. (2014) Comparative study of a physically based distributed hydrological model versus a conceptual hydrological model for assessment of climate change response in the Upper Nile, Baro-Akobo basin: a case study of the Sore watershed, Ethiopia. *Int. J. River Basin Manag.* 1–20. doi:10.1080/15715124.2014.917315
- Kitanidis, P. & Bras, R. L. (1980) Real-Time Forecasting with a conceptual Hydrologic model. 2-Applications and results. *Water Resour. Res.* **16**(6), 1034–1044.
- Kling, H., Fuchs, M. & Paulin, M. (2012) Runoff conditions in the upper Danube basin under an ensemble of climate change scenarios. *J. Hydrol.* **424-425**, 264–277. Elsevier B.V. doi:10.1016/j.jhydrol.2012.01.011
- Krause, P., Boyle, D. & Bäse, F. (2005) Comparison of different efficiency criteria for hydrological model assessment. *Adv. Geosci.* (5), 89–97. Retrieved from <http://www.adv-geosci.net/5/89/2005/adgeo-5-89-2005.html>
- Lawin, A. E. & Afouda, A. (2011) Analyse de la Variabilité du Régime Pluviométrique dans la Région Agricole d'Ina au Bénin. *Eur. J. Sci. Res.* **50**(3), 425–439. Retrieved from <http://www.eurojournals.com/ejsr.htm>
- Lawin, A. E., Vissin, W. E., Sintondji, L., Gohoungossou, A., Vodounou, J.-B., Zannou, A. B. Y., Akognongbe, A., et al. (2011) Contribution du Projet Ouémé-2025 à

l'étude de la dynamique et de la disponibilité des ressources en eau du bassin de l'Ouémé: Résultats préliminaires. Cotonou, Benin.

Lebel, T. & Ali, A. (2009) Recent trends in the Central and Western Sahel rainfall regime (1990–2007). *J. Hydrol.* **375**(1-2), 52–64. Elsevier B.V. doi:10.1016/j.jhydrol.2008.11.030

Leconte, R. (2010) Introduction à la modélisation de l'eau. École de technologie supérieure (Québec).

Léon, J. (2009) L'action et le Principe de moindre action. Retrieved from jac\_leon.perso.neuf.fr/principe\_moins\_action.html

Manton, N. S. (2013) The Principle of Least Action in Dynamics, 1–25. Cambridge, UK: DAMTP, Centre for Mathematical Sciences, University of Cambridge.

Marin, C. T., Bouten, W. & Sevink, J. (2000) Gross rainfall and its partitioning into throughfall, stemflow and evaporation of intercepted water in four forest ecosystems in western Amazonia. *J. Hydrol.* **237**(1–2), 40–57. doi:http://dx.doi.org/10.1016/S0022-1694(00)00301-2

McCluskey, A. & Qaddumi, H. (2011) *Water And Climate Change.Synthesis Of The Science*. Colorado and Washington: World Bank.

McDonnell, J. J., Sivapalan, M., Vaché, K., Dunn, S., Grant, G., Haggerty, R., Hinz, C., et al. (2007) Moving beyond heterogeneity and process complexity: A new vision for watershed hydrology. *Water Resour. Res.* **43**(7), 1–6. doi:10.1029/2006WR005467

McMillan, H., Freer, J., Pappenberger, F., Krueger, T. & Clark, M. (2010) Impacts of uncertain river flow data on rainfall-runoff model calibration and discharge predictions. *Hydrol. Process.* **1284**(March), n/a–n/a. doi:10.1002/hyp.7587

Menz, G. (2010) Topography and natural regions. In: *Impacts of Global Change on the Hydrological Cycle in West and Northwest Africa* (P. Speth, M. Christoph & B. Diekkrüger, eds.), 692p. Heidelberg, Germany: Springer.

Moriasi, D. N., Arnold, J. G., Liew, M. W. Van, Bingner, R. L., Harmel, R. D. & Veith, T. L. (2007) Model evaluation guidelines for systematic quantification of accuracy in watershed simulations. *Am. Soc. Agric. Biol. Eng.* **50**(3), 885–900.

Mujumdar, P. P. & Nagesh Kumar, D. (2012) *Floods in a Changing Climate: Hydrologic Modeling*, 2nd ed. Cambridge, UK: Cambridge University Press. doi:10.1017/CB09781139088428

- Mulindabigwi, V., Giertz, S., Hadjer, K., Heldmann, M. & Judex, M. (2008) The Upper Ouémé Catchment. In: *IMPETUS Atlas Benin Research Results 2000 – 2007* (M. Judex & H.-P. Thamm, eds.), 3rd ed., 144. Bonn, Germany.
- Mulligan, M. & Wainwright, J. (2004) Modelling and Model Building. In: *Environmental Modelling. Finding Simplicity in Complexity* (J. Wainwright & M. Mulligan, eds.), 7–73. Chichester, UK: John Wiley & Sons, Ltd. doi:10.1002/9781118351475
- Neuenschwander, D. E., Taylor, E. F. & Tuleja, S. (2006) Action: Forcing Energy to Predict Motion. *Phys. Teach.* **44**(3), 146–152. doi:10.1119/1.2173320
- Nicolis, A. (2011) The Noether theorem, 1–5. New York: Columbia University. Retrieved from [http://phys.columbia.edu/~nicolis/NewFiles/Noether\\_theorem.pdf](http://phys.columbia.edu/~nicolis/NewFiles/Noether_theorem.pdf)
- Oki, T. & Kanae, S. (2006) Global Hydrological Cycles and World Water Resources. *Sci.* **313** (5790 ), 1068–1072. doi:10.1126/science.1128845
- Parajka, J., Viglione, a., Rogger, M., Salinas, J. L., Sivapalan, M. & Blöschl, G. (2013) Comparative assessment of predictions in ungauged basins-Part 1: Runoff-hydrograph studies. *Hydrol. Earth Syst. Sci.* **17**, 1783–1795. doi:10.5194/hess-17-1783-2013
- Perrin, C., Michel, C. & Andréassian, V. (2003) Improvement of a parsimonious model for streamflow simulation. *J. Hydrol.* **279**, 275–289. doi:10.1016/S0022-1694(03)00225-7
- Pushpalatha, R., Perrin, C., Moine, N. Le & Andréassian, V. (2012) A review of efficiency criteria suitable for evaluating low-flow simulations. *J. Hydrol.* **420-421**, 171–182. Elsevier B.V. doi:10.1016/j.jhydrol.2011.11.055
- Ratto, M. & Saltelli, A. (2001) Model assessment in integrated procedures for environmental impact evaluation : software prototypes. IMPACT Project.
- Refsgaard, J. C. & Storm, B. (1995) MIKE SHE. In: *Computer models of watershed hydrology* (V. P. Singh, ed.), pp 809–846. Littleton, Colorado: Water Resources Publications. Retrieved from <https://books.google.bj/books?id=8XfuAAAAMAAJ>
- Reggiani, P., Hassanizadeh, S. M., Sivapalan, M. & Gray, W. G. (1999) A unifying framework for watershed thermodynamics: Constitutive relationships. *Adv. Water Resour.* **23**(1), 15–39. doi:10.1016/S0309-1708(99)00005-6
- Reggiani, P., Sivapalan, M. & Hassanizadeh, S. M. (1998) A unifying framework for watershed thermodynamics: balance equations for mass, momentum, energy

- and entropy, and the second law of thermodynamics. *Adv. Water Resour.* **22**(4), 367–398. Elsevier.
- Reichert, B., Klose, S. & Kocher, A. (2010) Geology. In: *Impacts of Global Change on the Hydrological Cycle in West and Northwest Africa* (P. Speth, M. Christoph & B. Diekkrüger, eds.), 692p. Heidelberg, Germany: Springer.
- Research Systems, C. (2004) IDL (Interactive Data Language)- version 6.1. Research Systems.
- Richard, A. (2012) Caractérisation de la variabilité spatiale des propriétés hydrodynamiques des sols de l'Ouémé supérieur (Bénin) : Rapport d'analyse, 37p. Cotonou, Benin: Laboratoire d'Hydraulique et de Maitrise de l'Eau (LHME).
- Ritter, A. & Muñoz-Carpena, R. (2013) Performance evaluation of hydrological models: Statistical significance for reducing subjectivity in goodness-of-fit assessments. *J. Hydrol.* **480**, 33–45. Elsevier B.V. doi:10.1016/j.jhydrol.2012.12.004
- Roberts, W. (2003) It all adds up - the principle of Least Action. Retrieved from [http://www.principlesofnature.net/principle\\_of\\_least\\_action.htm](http://www.principlesofnature.net/principle_of_least_action.htm)
- Robine, F. (2007) Entre mathématiques et métaphysique : une histoire du principe de moindre action. *Le Princ. moindre action*, 1–41. Paris: Département de Physique de l'École Polytechnique et l'École Normale Supérieure. Retrieved from [http://softs.polytechnique.fr/departements/physique/colloques/pdf/2007/Robine\\_Florence\\_X-ENS-UPS2007.pdf](http://softs.polytechnique.fr/departements/physique/colloques/pdf/2007/Robine_Florence_X-ENS-UPS2007.pdf)
- Rodríguez-Iturbe, I. & Rinaldo, A. (1997) *Fractal River Basins: Chance and Self-Organization*. Cambridge, UK: Cambridge University Press. Retrieved from [http://books.google.com/books?id=\\_xjhtl7zeB8C&pgis=1](http://books.google.com/books?id=_xjhtl7zeB8C&pgis=1)
- Rodríguez-Iturbe, I., Rinaldo, A., Rigon, R., Bras, R. L., Marani, A. & Ijász-Vásquez, E. (1992) Energy Dissipation, Runoff Production, and the Three-Dimensional Structure of River Basins. *Water Resour. Res.* **28**(4), 1095–1103.
- Schönbrodt, S. & Giertz, S. (2008) Geomorphology of Benin. In: *IMPETUS Atlas Benin Research Results 2000 – 2007* (M. Judex & H.-P. Thamm, eds.), 3rd ed., 144. Bonn, Germany.
- Seibert, J. & McDonnell, J. J. (2010) Land-cover impacts on streamflow: a change-detection modelling approach that incorporates parameter uncertainty. *Hydrol. Sci. J.* **55**(3), 316–332. doi:10.1080/02626661003683264

- Shaw, E. M., Beven, K., Chappell, N. A. & Lamb, R. (2011) *Hydrology in Practice*. (E. M. Shaw, K. Beven, N. A. Chappell & R. Lamb, Eds.), Fourth Edi. Oxon: Spon Press.
- Shen, Z. Y., Chen, L. & Chen, T. (2012) Analysis of parameter uncertainty in hydrological and sediment modeling using GLUE method: a case study of SWAT model applied to Three Gorges Reservoir Region, China. *Hydrol. Earth Syst. Sci.* **16**(1), 121–132. doi:10.5194/hess-16-121-2012
- Sintondji, L. O. (2005) *Modelling the rainfall-runoff process in the Upper Ouémé catchment ( Terou in Bénin Republic ) in a context of global change : extrapolation from the local to the regional scale*. Thesis (PhD). Rheinischen Friedrich-Wilhelms-Universität Bonn, Germany. 205 p.
- Sivapalan, M., Takeuchi, K., Franks, S. W., Gupta, V. K., Karambiri, H., Lakshmi, V., Liang, X., et al. (2012) IAHS Decade on Predictions in Ungauged Basins ( PUB ), 2003 – 2012 : Shaping an exciting future for the hydrological sciences. *Hydrol. Sci. J.* **48**(6), 857–880. doi:10.1623/hysj.48.6.857.51421
- Speth, P., Christoph, M. & Diekkrüger, B. (2010) *Impacts of Global Change on the Hydrological Cycle in West Africa and Northwest Africa*. (P. Speth, M. Christoph & B. Diekkrüger, Eds.). Cologne and Bonn, Germany: Springer. doi:10.1007/978-3-642-12957-5
- Stanislaw, W. (1998) The interdependence and applicability of some statistical quality measures for hydrological models. *J. Hydrol.* **206**, 98–103.
- Tabacchi, E., Lambs, L., Guilloy, H., Planty-Tabacchi, A.-M., Muller, E. & Décamps, H. (2000) Impacts of riparian vegetation on hydrological processes. *Hydrol. Process.* **14**(16-17), 2959–2976. doi:10.1002/1099-1085(200011/12)14
- Thamm, H.-P. & Judex, M. (2008) Land Use in the Ouémé Catchment. In: *IMPETUS Atlas Benin Research Results 2000 – 2007* (M. Judex & H.-P. Thamm, eds.), 3rd ed., 144. Bonn, Germany.
- Thornton, P. K. & Herrero, M. (2010) *The Inter-Linkages Between Rapid Growth In Livestock Production, Climate Change, And The Impacts On Water Resources, Land Use, And Deforestation*. The World Bank. doi:10.1596/1813-9450-5178
- Tianqi, A. O., Yoshitani, J., Takeuchi, K., Fukami, K., Mutsuura, T. & Ishidaira, H. (2007) Toward the application of the physically based distributed hydrological model BTOPMC to ungauged basins. *Predict. Ungauged Basins PUB Kick-off*, 20–22. Brasilia: IASH Publications.
- Tossa, A. A. Y. & Tonouhewa, A. (2009) Profil du bassin de l’Ouémé et caractérisation des sites pilotes (analyse des données). Rapport Final, 64p.

- Cotonou, Benin: Projet de renforcement des capacités nationales de suivi des ressources en eau axe sur la gestion de l'eau agricole.
- Uchida, T., Kosugi, K. & Mizuyama, T. (2001) Effects of pipeflow on hydrological process and its relation to landslide: a review of pipeflow studies in forested headwater catchments. *Hydrol. Process.* **15**(11), 2151–2174. John Wiley & Sons, Ltd. doi:10.1002/hyp.281
- United Nations World Water Assessment Programme (WWAP). (2003) The United Nations World Water Development Report: Water for People, Water for Life. Barcelona. doi:92-3-103881-8
- Varado, N., Braud, I., Galle, S., Lay, M. Le, Séguis, L., Kamagate, B. & Depraetere, C. (2006) Multi-criteria assessment of the Representative Elementary Watershed approach on the Donga catchment (Benin) using a downward approach of model complexity. *Hydrol. Earth Syst. Sci.* **10**(3), 427–442. doi:10.5194/hess-10-427-2006
- Volker, E. & Tim, B. (2008) The Climate 7 of Benin (1961 to 1990). In: *IMPETUS Atlas Benin Research Results 2000 – 2007* (M. Judex & H.-P. Thamm, eds.), 3rd ed., 144. Bonn, Germany.
- Wagner, T., Boyle, D. P., Lees, M. J., Wheeler, H. S., Gupta, H. V. & Sorooshian, S. (2001) A framework for development and application of hydrological models. *Hydrol. Earth Syst. Sci.* **5**(September 2000), 13–26. doi:10.5194/hess-5-13-2001
- Wainwright, J. & Mulligan, M. (2004) *Environmental Modelling. Finding Simplicity in Complexity*. (J. Wainwright & M. Mulligan, Eds.). Chichester, UK: John Wiley & Sons, Ltd. doi:10.1002/9781118351475
- Wei, M. & Menzel, L. (2008) A global comparison of four potential evapotranspiration equations and their relevance to stream flow modelling in semi-arid environments. *Adv. Geosci.* **18**, 15–23.
- Wheeler, H., McIntyre, N., Bulygina, N., Fraser, C. & Jackson, B. (2013) Prediction in ungauged basins – the challenge of catchment non-stationarity. *Putt. Predict. Ungauged Basins into Pract.* (J. W. Pomeroy, P. H. Whitfield & C. Spence, eds.), 1–384. Canmore, Alberta: Canadian Water Resources Association.
- Wheeler, H. S., McIntyre, N. & Wagner, T. (2008) Calibration, uncertainty, and regional analysis of conceptual rainfall-runoff models. In: *Hydrological Modelling in Arid and Semi-Arid Areas* (H. S. Wheeler, S. Sorooshian & K. D. Sharma, eds.), 99–111. UK: Cambridge University Press.

Yu, Z. (2002) *Hydrology. Modeling and Prediction*. Las Vegas.  
doi:10.1006/rwas.2002.0172

Zannou, A. B. Y. (2011) *Analyse et Modélisation du Cycle Hydrologique Continental pour la Gestion Intégrée des Ressources en Eau au Bénin Cas du Bassin de l'Ouémé à Bétérou*. Thesis (PhD). Université d'Abomey-Calavi (UAC), Benin. 315p.

## APPENDIXES

## APPENDIX A. EQUATIONS OF THE CRITERIA OF PERFORMANCE

$S_i$  is the simulated discharge for each time step, and  $O_i$  is the observed value.  $N$  is the total number of values within the time period of analysis.

1) Percent Bias (PB) %

$$P.B. = \frac{\sum_{i=1}^N (S_i - O_i)}{\sum_{i=1}^N O_i} \cdot (100)$$

2) Absolute Percent Bias (APB) %

$$A.B.P. = \frac{\sum_{i=1}^N |S_i - O_i|}{\sum_{i=1}^N O_i} \cdot (100)$$

3) Coefficient of Efficiency (CE) or Nash-Sutcliffe (Ns)

$$CE = \frac{\sum_{i=1}^N (S_i - O_i)^2}{\sum_{i=1}^N (O_i - \bar{O})^2}$$

4) Coefficient of Efficiency (CE) or Nash-Sutcliffe (**NSE Log**) calculated with the logarithmic values of the observed and simulated discharges. In order to avoid having to calculate the ln of zero, the fortieth of the observed mean is added to the values:

$$CE (\ln Q) = \frac{\sum_{i=1}^N [\ln(S_i + \bar{O}/40) - \ln(O_i + \bar{O}/40)]^2}{\sum_{i=1}^N [\ln(O_i + \bar{O}/40) - \ln(\bar{O} + \bar{O}/40)]^2}$$

- 5) Coefficient of Efficiency (CE) or Nash-Sutcliffe (**Ns squared root**) calculated with the squared root values of the observed and simulated discharges.:

$$CE (\sqrt{Q}) = \frac{\sum_{i=1}^N (\sqrt{S_i} - \sqrt{O_i})^2}{\sum_{i=1}^N (\sqrt{O_i} - \sqrt{\overline{O}})^2}$$

- 6) Kling-Gupta Efficiency (KGE):

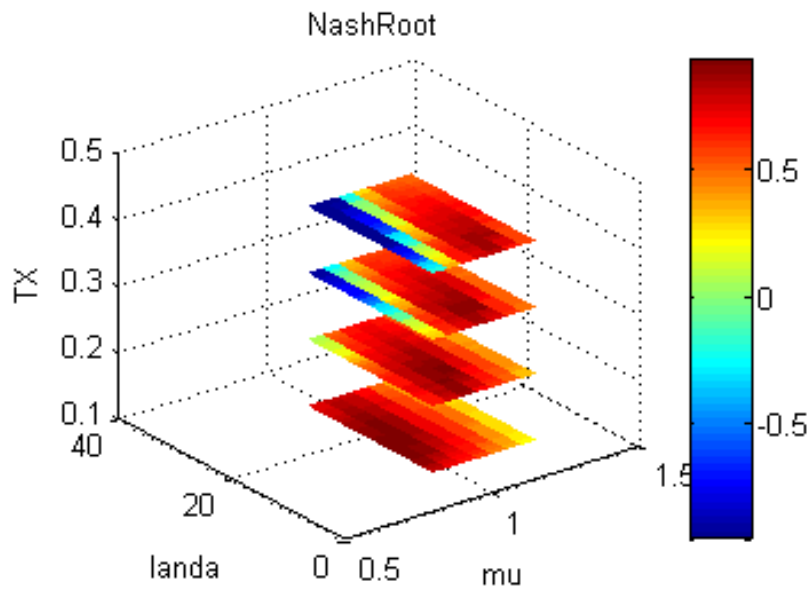
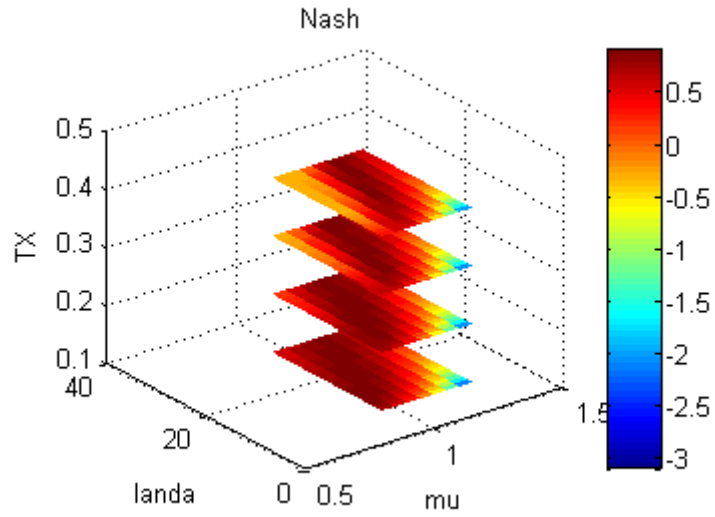
r=linear correlation coefficient between observed and simulated;

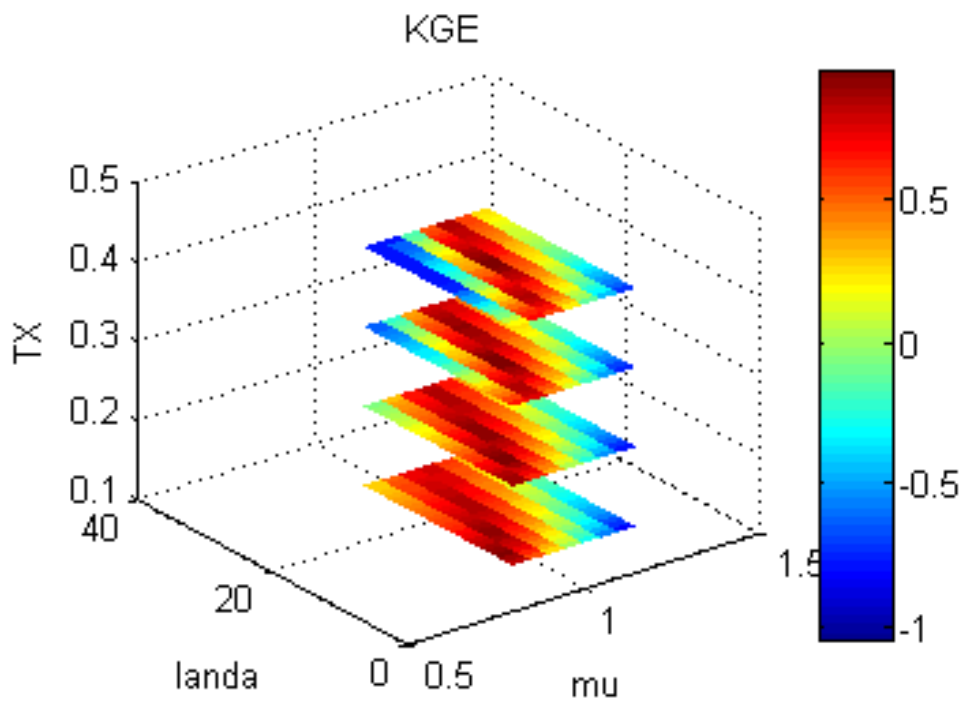
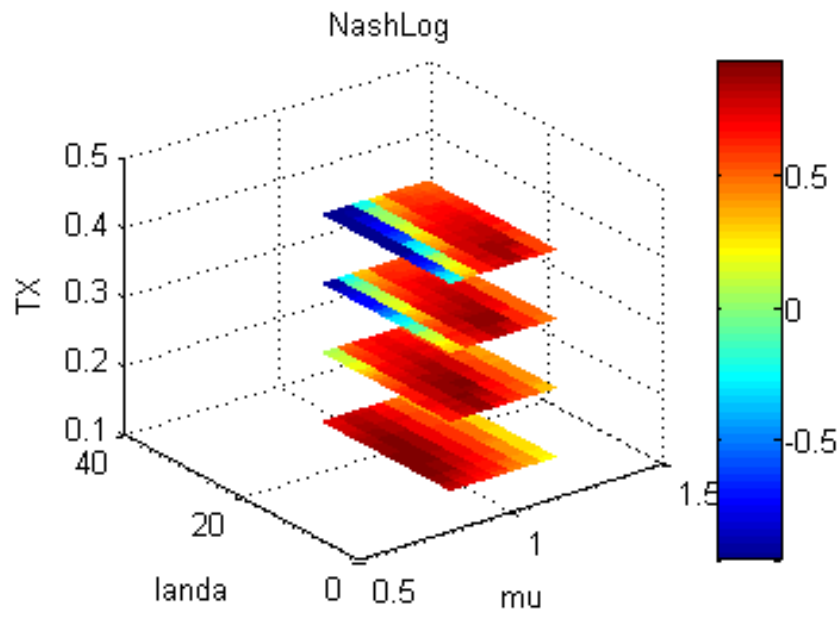
$\alpha$  = (standard deviation of simulated)/ (standard deviation of observed)

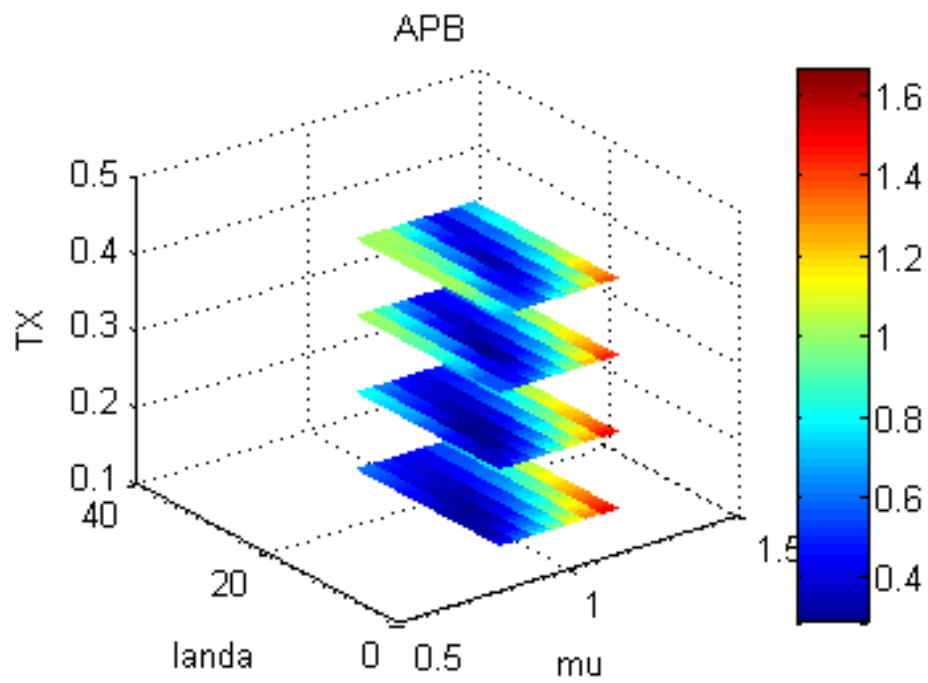
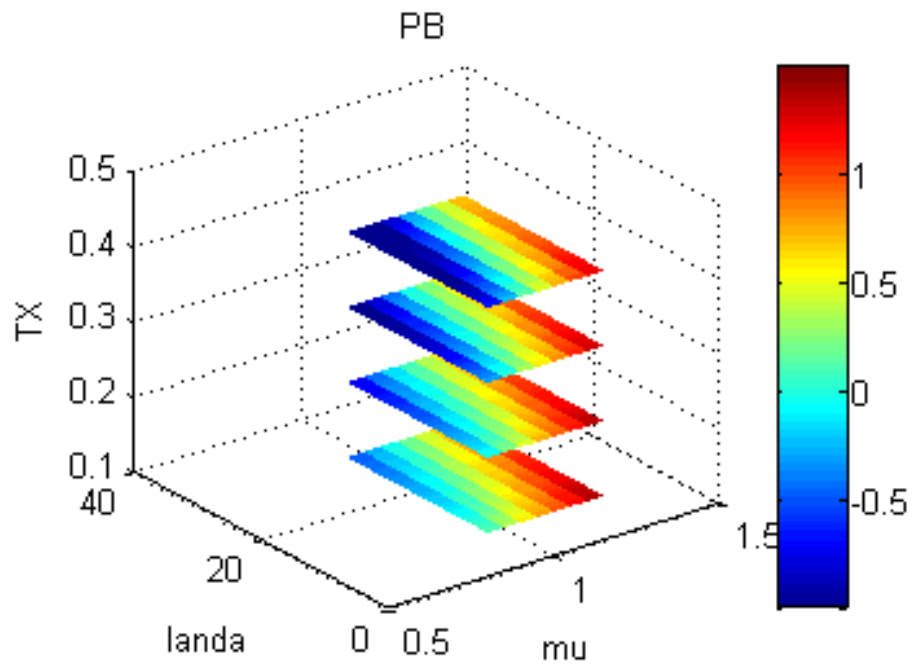
$\beta$ = ratio (mean simulated)/ (mean observed)

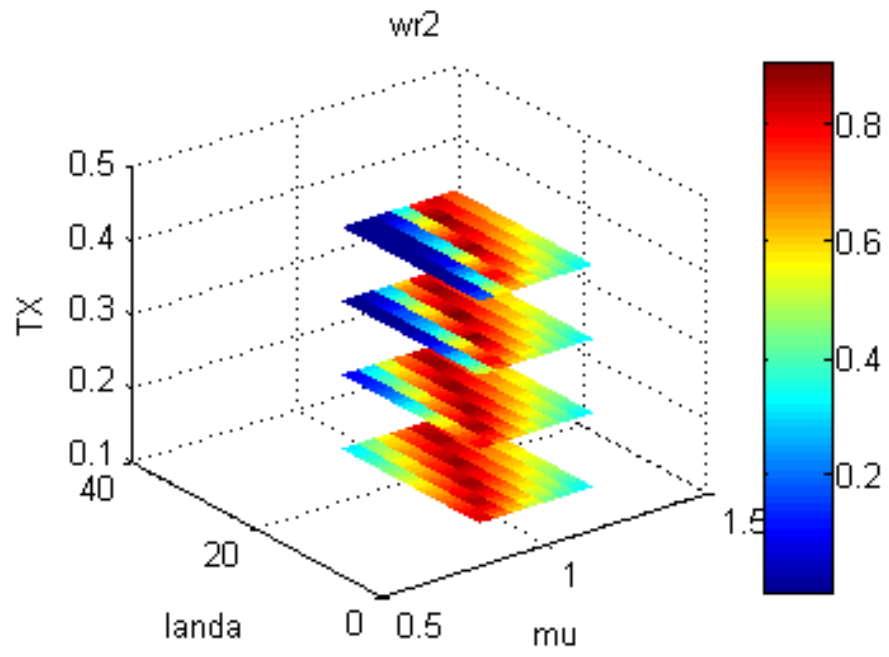
$$KGE = 1 - \sqrt{(r - 1)^2 + (\alpha - 1)^2 + (\beta - 1)^2}$$

**APPENDIX B. PARAMETER RESPONSE SURFACE FOR EACH PERFORMANCE CRITERION FOR BÉTÉROU (BENIN), 10 083 km<sup>2</sup>.**









## APPENDIX C. COMPARED HYDROGRAPHS, FLOW DURATION CURVES AND CRITERIA OF PERFORMANCE FOR MODHYPMA, GR4J & HBV

<i>Fig.C- 1: Compared hydrographs, flow duration curves and criteria of performance for MODHYPMA, GR4J &amp; HBV: Calibration of Lookout Creek catchment (USA), 62 km<sup>2</sup>. .....</i>	143
<i>Fig.C- 2: Compared hydrographs, flow duration curves and criteria of performance for MODHYPMA, GR4J &amp; HBV: Validation of Lookout Creek catchment (USA), 62 km<sup>2</sup>. .....</i>	144
<i>Fig.C- 3: Compared hydrographs, flow duration curves and criteria of performance for MODHYPMA, GR4J &amp; HBV: Calibration of Le Léguer catchment (FRANCE), 260 km<sup>2</sup>. .....</i>	145
<i>Fig.C- 4: Compared hydrographs, flow duration curves and criteria of performance for MODHYPMA, GR4J &amp; HBV: Calibration of Aguimo catchment (BENIN), 396 km<sup>2</sup>. .....</i>	146
<i>Fig.C- 5: Compared hydrographs, flow duration curves and criteria of performance for MODHYPMA, GR4J &amp; HBV: Validation of Aguimo catchment (BENIN), 396 km<sup>2</sup>. .....</i>	147
<i>Fig.C- 6: Compared hydrographs, flow duration curves and criteria of performance for MODHYPMA, GR4J &amp; HBV: Calibration of Donga Pont catchment (BENIN), 587 km<sup>2</sup>. .....</i>	148
<i>Fig.C- 7: Compared hydrographs, flow duration curves and criteria of performance for MODHYPMA, GR4J &amp; HBV: Validation of Donga Pont catchment (BENIN), 587 km<sup>2</sup>. .....</i>	149
<i>Fig.C- 8: Compared hydrographs, flow duration curves and criteria of performance for MODHYPMA, GR4J &amp; HBV: Calibration of Sani catchment (BENIN), 745 km<sup>2</sup>. .....</i>	150
<i>Fig.C- 9: Compared hydrographs, flow duration curves and criteria of performance for MODHYPMA, GR4J &amp; HBV: Calibration of Donga Affon catchment (BENIN), 1 308 km<sup>2</sup> ...</i>	151
<i>Fig.C- 10: Compared hydrographs, flow duration curves and criteria of performance for MODHYPMA, GR4J &amp; HBV: Validation of Donga Affon catchment (BENIN), 1 308 km<sup>2</sup>. .....</i>	152
<i>Fig.C- 11: Compared hydrographs, flow duration curves and criteria of performance for MODHYPMA, GR4J &amp; HBV: Calibration of Saramanga catchment (BENIN), 1 360 km<sup>2</sup>. ....</i>	153
<i>Fig.C- 12: Compared hydrographs, flow duration curves and criteria of performance for MODHYPMA, GR4J &amp; HBV: Validation of Saramanga catchment (BENIN), 1 360 km<sup>2</sup>. .....</i>	154
<i>Fig.C- 13: Compared hydrographs, flow duration curves and criteria of performance for MODHYPMA, GR4J &amp; HBV: Calibration of Sore catchment (BENIN), 1 711 km<sup>2</sup>. .....</i>	155
<i>Fig.C- 14: Compared hydrographs, flow duration curves and criteria of performance for MODHYPMA, GR4J &amp; HBV: Validation of Sore catchment (ETHIOPIA), 1 711 km<sup>2</sup>. .....</i>	156
<i>Fig.C- 15: Compared hydrographs, flow duration curves and criteria of performance for MODHYPMA, GR4J &amp; HBV: Calibration of Barérou catchment (BENIN), 2 134 km<sup>2</sup>. .....</i>	157
<i>Fig.C- 16: Compared hydrographs, flow duration curves and criteria of performance for MODHYPMA, GR4J &amp; HBV: Calibration of Côte 238 catchment (BENIN), 3 060 km<sup>2</sup>. .....</i>	158
<i>Fig.C- 17: Compared hydrographs, flow duration curves and criteria of performance for MODHYPMA, GR4J &amp; HBV: Validation of Côte 238 catchment (BENIN), 3 060 km<sup>2</sup>. .....</i>	159
<i>Fig.C- 18: Compared hydrographs, flow duration curves and criteria of performance for MODHYPMA, GR4J &amp; HBV: Calibration of Aval Sani catchment (BENIN), 3 279 km<sup>2</sup>. .....</i>	160
<i>Fig.C- 19: Compared hydrographs, flow duration curves and criteria of performance for MODHYPMA, GR4J &amp; HBV: Validation of Aval Sani catchment (BENIN), 3 279 km<sup>2</sup>. .....</i>	161
<i>Fig.C- 20: Compared hydrographs, flow duration curves and criteria of performance for MODHYPMA, GR4J &amp; HBV: Calibration of Savè catchment (BENIN), 23 491 km<sup>2</sup>. .....</i>	162

*Fig.C- 21: Compared hydrographs, flow duration curves and criteria of performance for MODHYPMA, GR4J & HBV: Validation of Savè catchment (BENIN), 23 491 km<sup>2</sup>. .....163*

*Fig.C- 22: Compared hydrographs, flow duration curves and criteria of performance for MODHYPMA, GR4J & HBV: Calibration of Mbasso catchment (CÔTE D'IVOIRE), 74 900 km<sup>2</sup>.  
.....164*

*Fig.C- 23: Compared hydrographs, flow duration curves and criteria of performance for MODHYPMA, GR4J & HBV: Validation of Mbasso catchment (CÔTE D'IVOIRE), 74 900 km<sup>2</sup>.  
.....165*

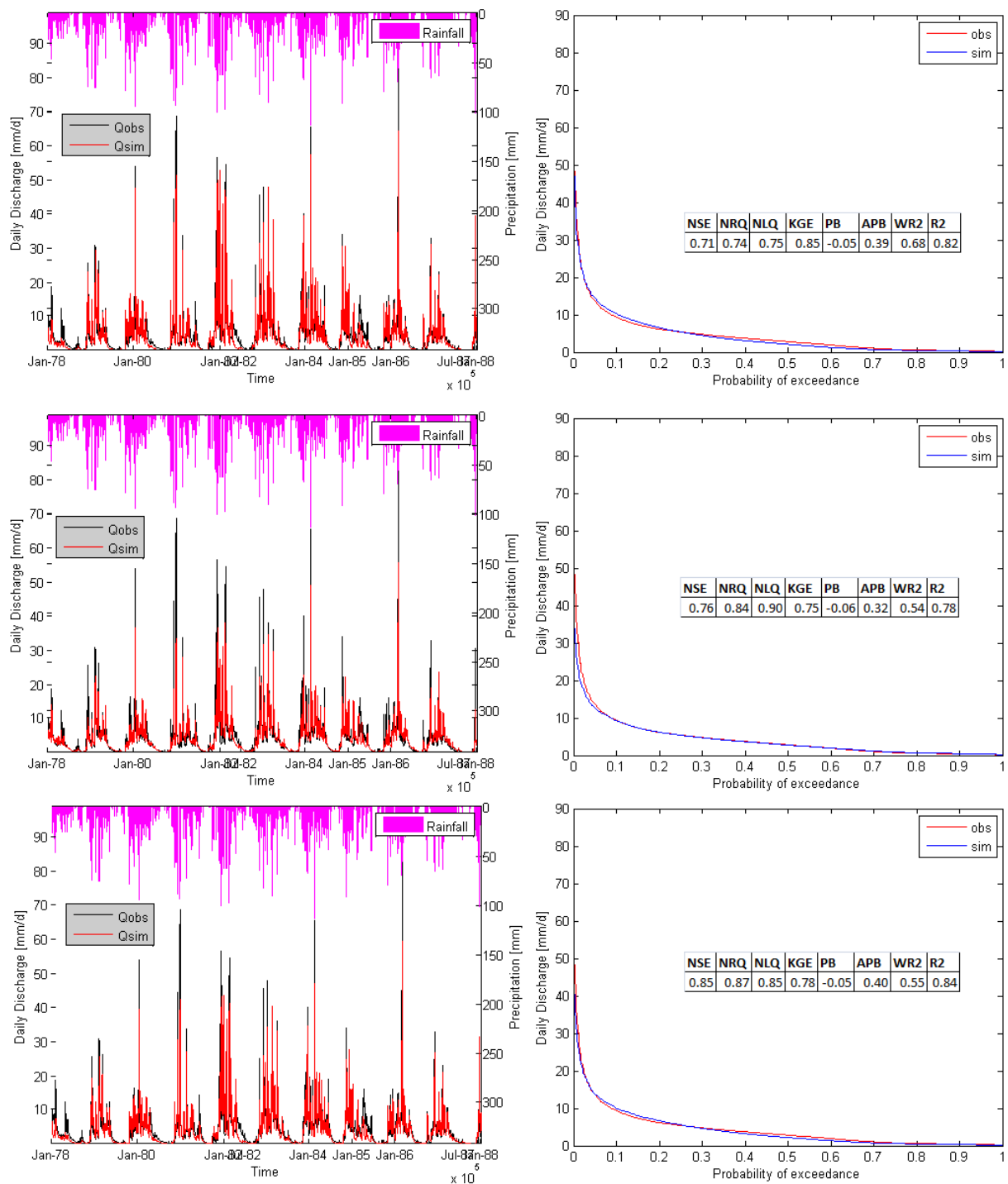


Fig.C- 1: Compared hydrographs, flow duration curves and criteria of performance for MODHYPMA, GR4J & HBV: Calibration of Lookout Creek catchment (USA), 62 km<sup>2</sup>.

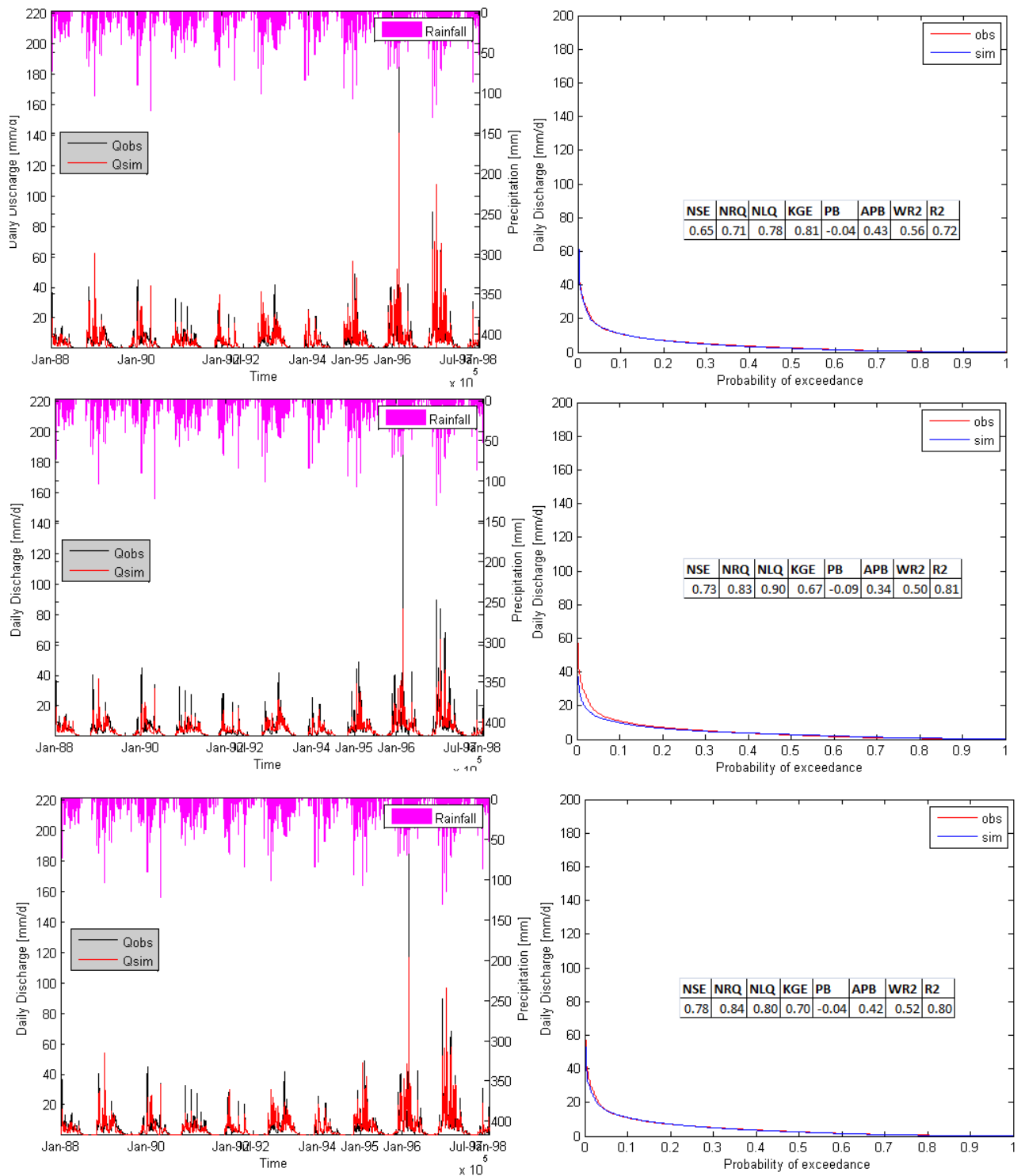


Fig.C- 2: Compared hydrographs, flow duration curves and criteria of performance for MODHYPMA, GR4J & HBV: Validation of Lookout Creek catchment (USA), 62 km<sup>2</sup>.

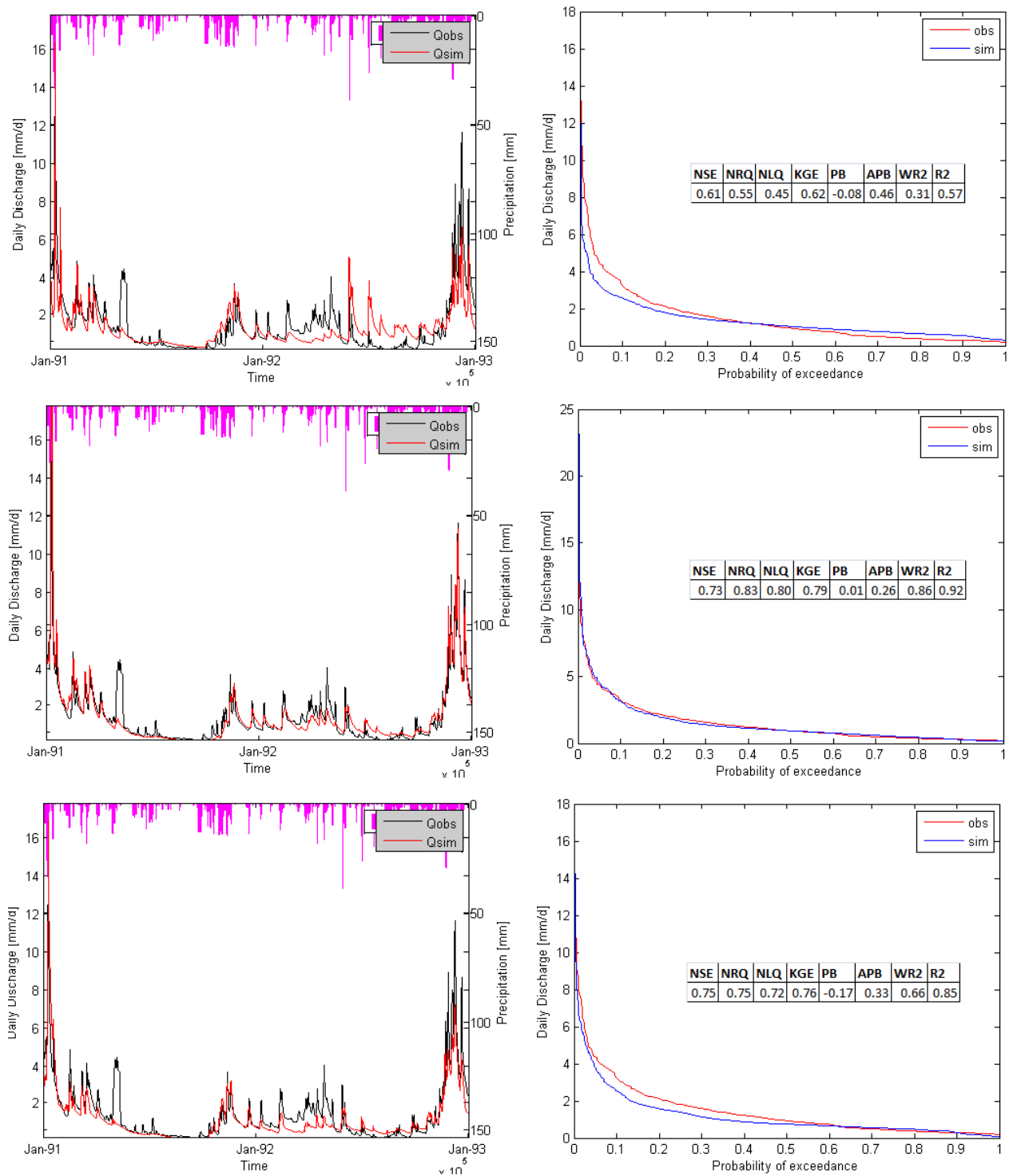


Fig.C- 3: Compared hydrographs, flow duration curves and criteria of performance for MODHYPMA, GR4J & HBV: Calibration of Le Léguer catchment (FRANCE), 260 km<sup>2</sup>.

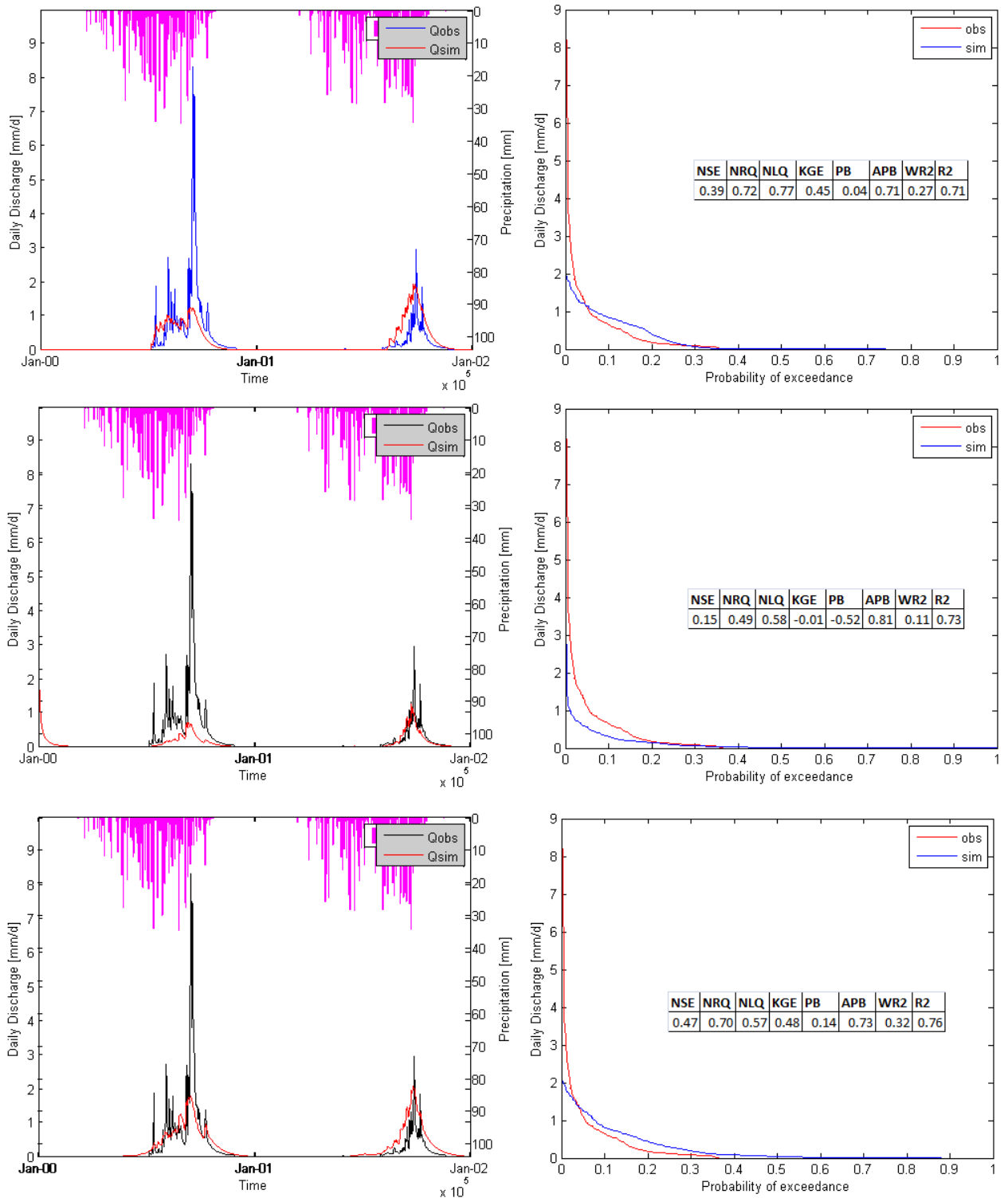


Fig.C- 4: Compared hydrographs, flow duration curves and criteria of performance for MODHYPMMA, GR4] & HBV: Calibration of Aquimo catchment (BENIN), 396 km<sup>2</sup>.

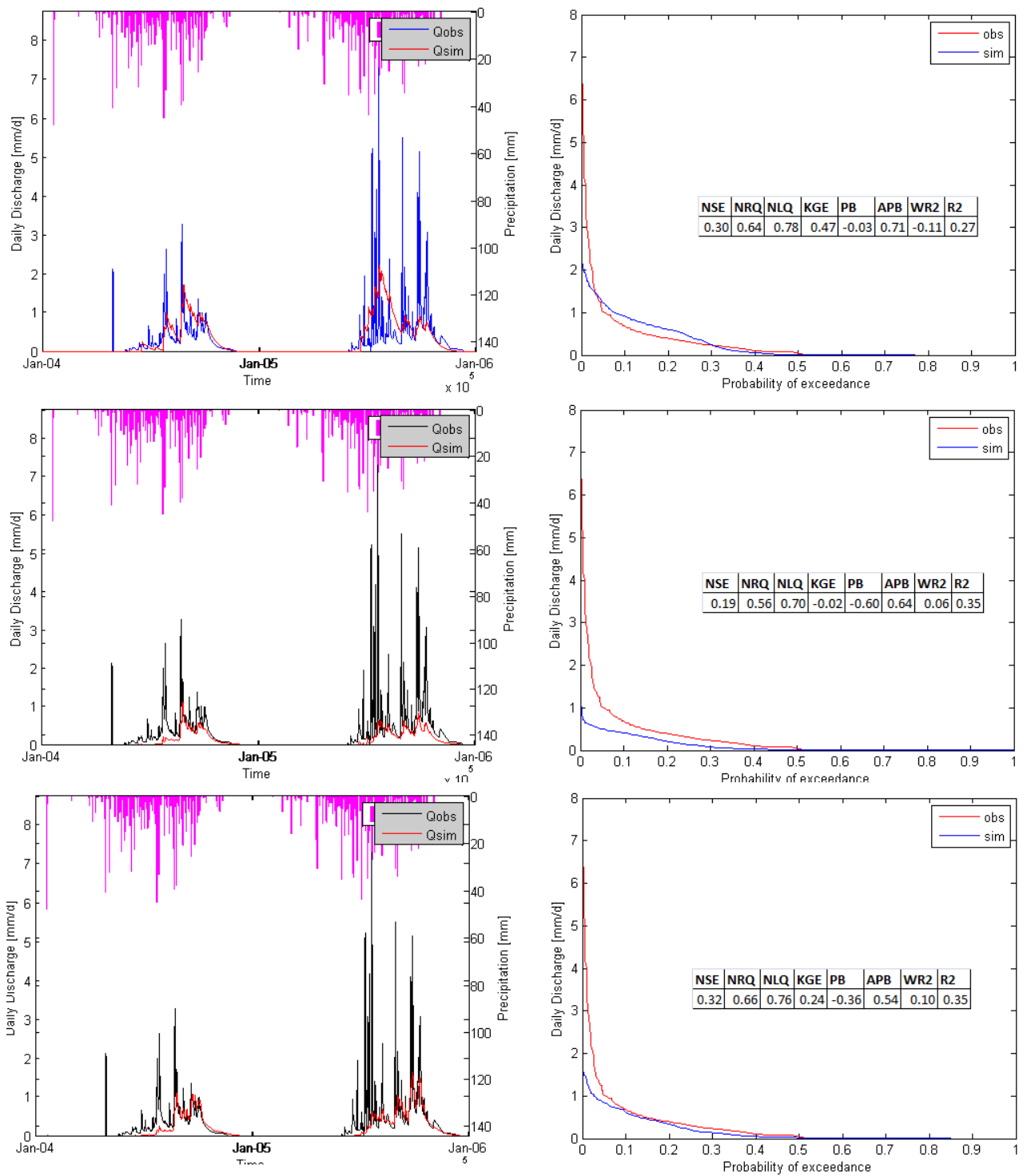


Fig.C- 5: Compared hydrographs, flow duration curves and criteria of performance for MODHYPMA, GR4J & HBV: Validation of Aguimo catchment (BENIN), 396 km<sup>2</sup>.

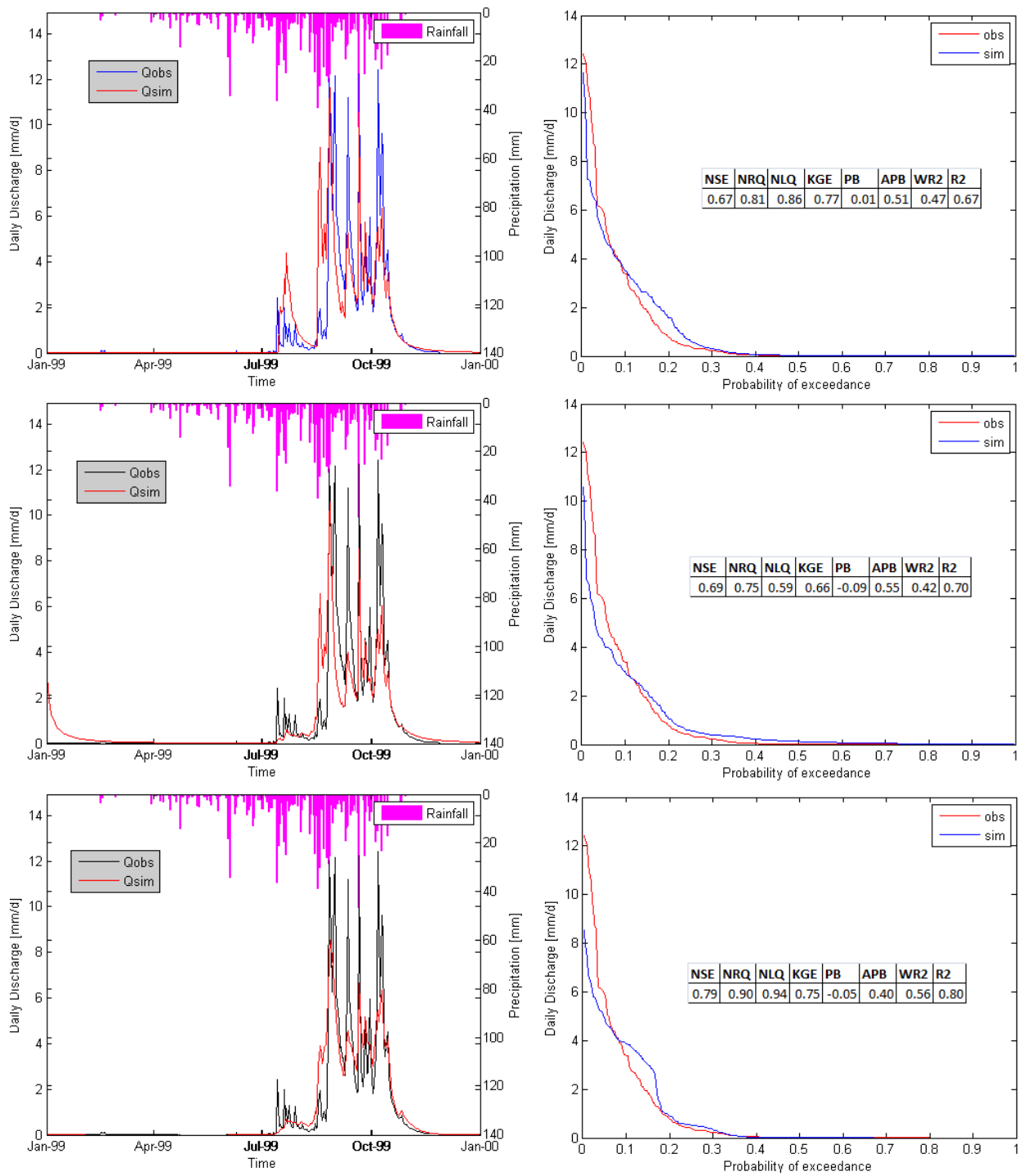


Fig.C- 6: Compared hydrographs, flow duration curves and criteria of performance for MODHYPMA, GR4J & HBV: Calibration of Donga Pont catchment (BENIN), 587 km<sup>2</sup>.

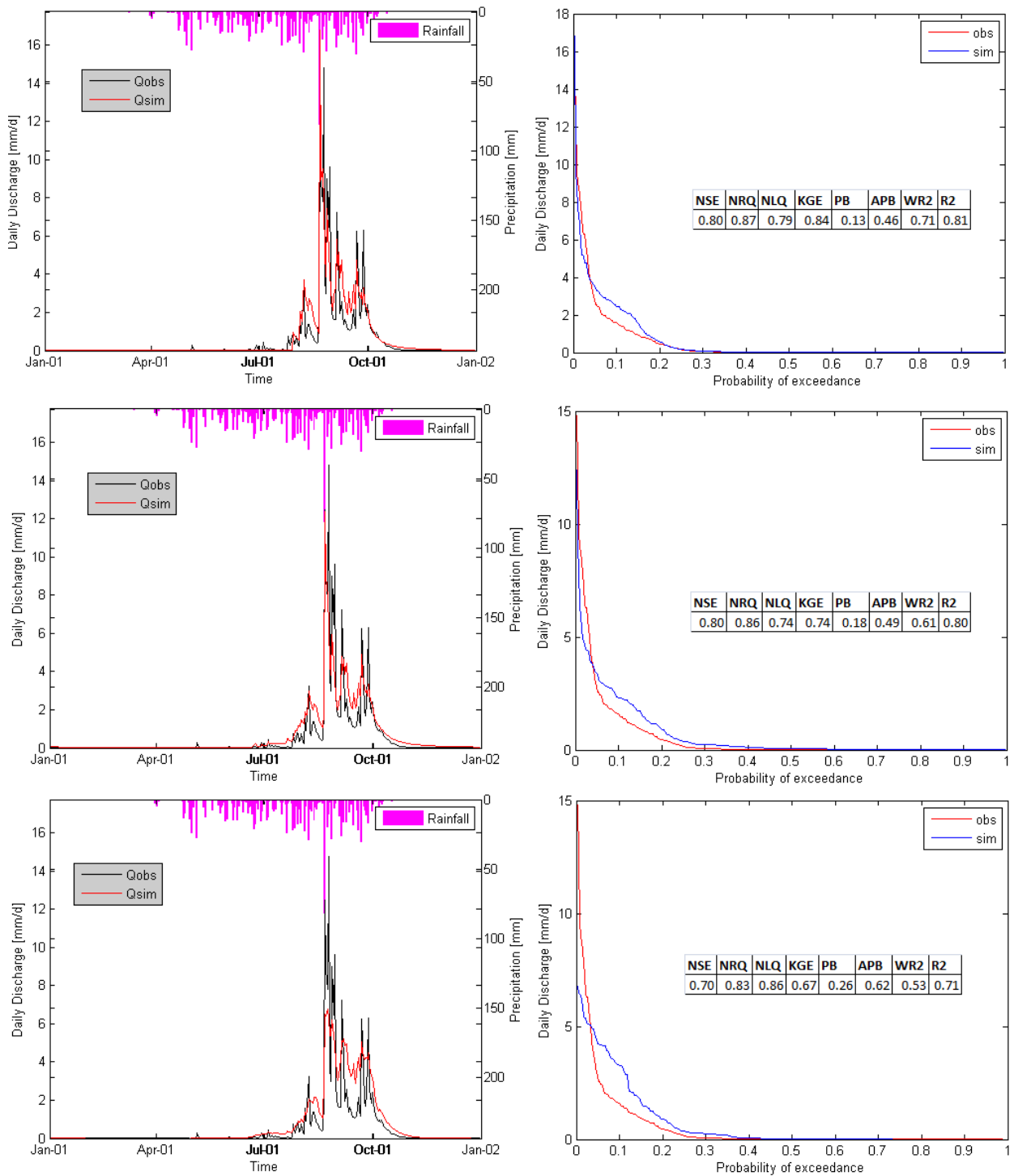


Fig.C- 7: Compared hydrographs, flow duration curves and criteria of performance for MODHYPMA, GR4J & HBV: Validation of Donga Pont catchment (BENIN), 587 km<sup>2</sup>.

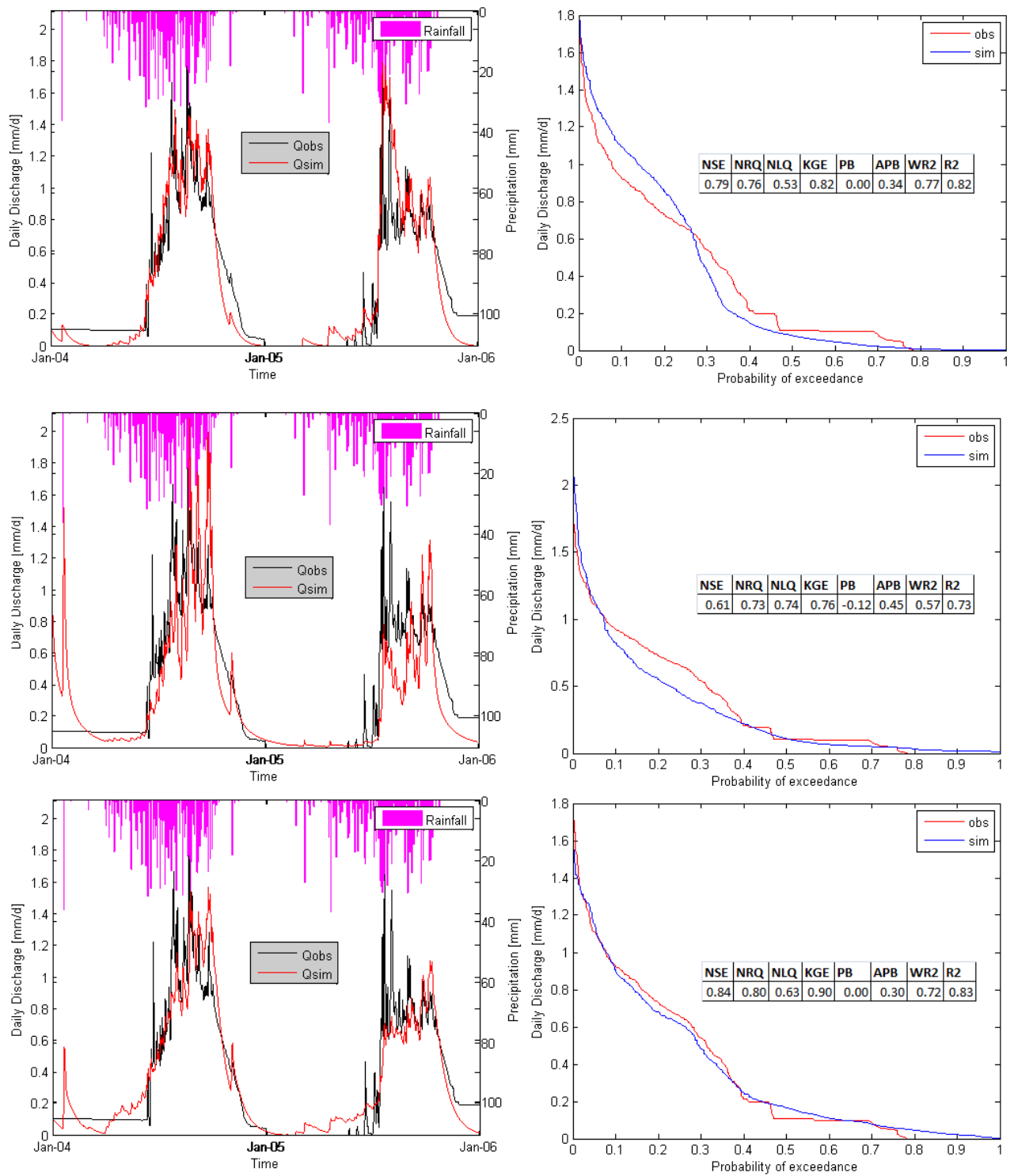


Fig.C- 8: Compared hydrographs, flow duration curves and criteria of performance for MODHYPMA, GR4J & HBV: Calibration of Sani catchment (BENIN), 745 km<sup>2</sup>.

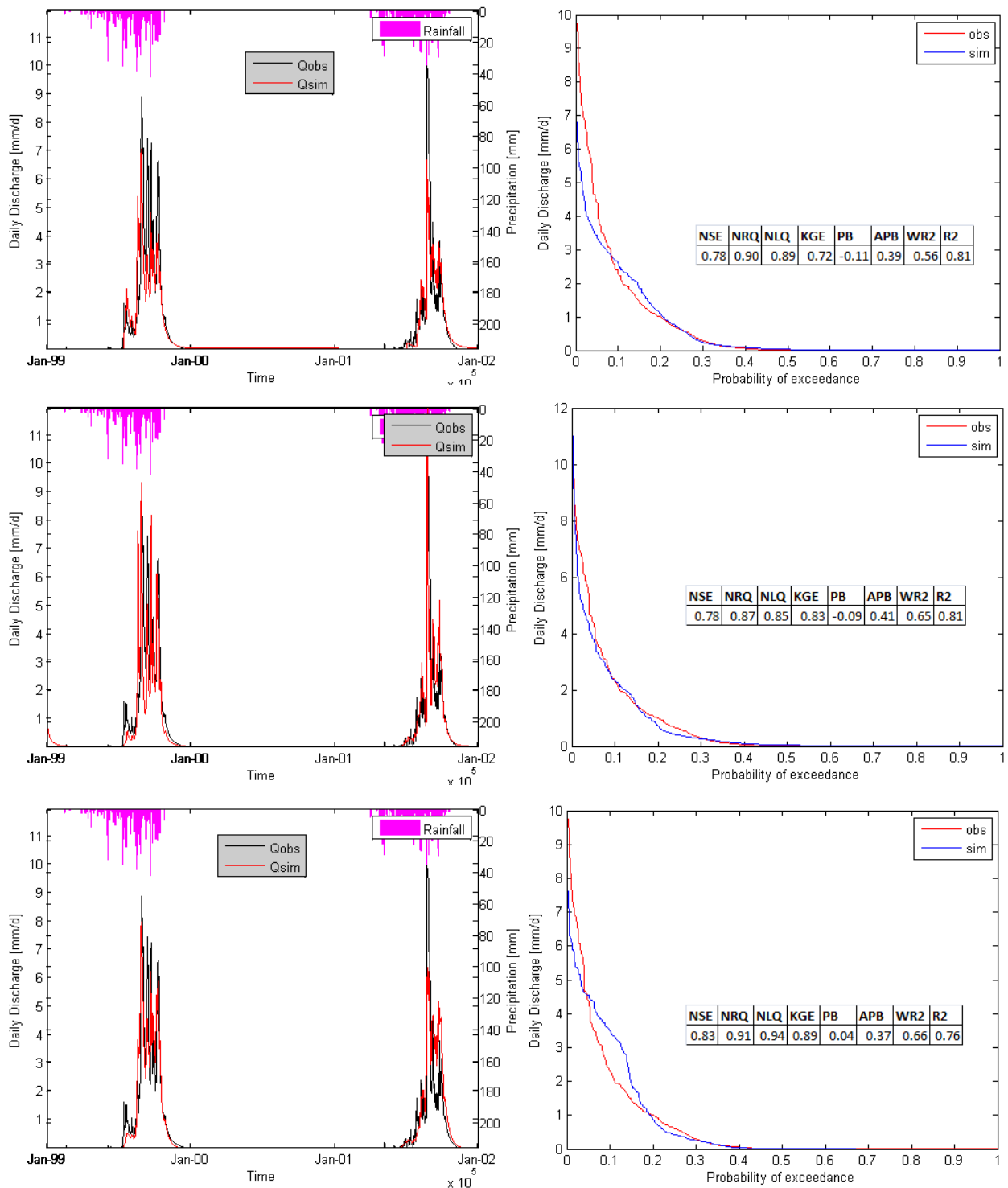


Fig.C- 9: Compared hydrographs, flow duration curves and criteria of performance for MODHYPMA, GR4J & HBV: Calibration of Donga Affon catchment (BENIN), 1 308 km<sup>2</sup>.

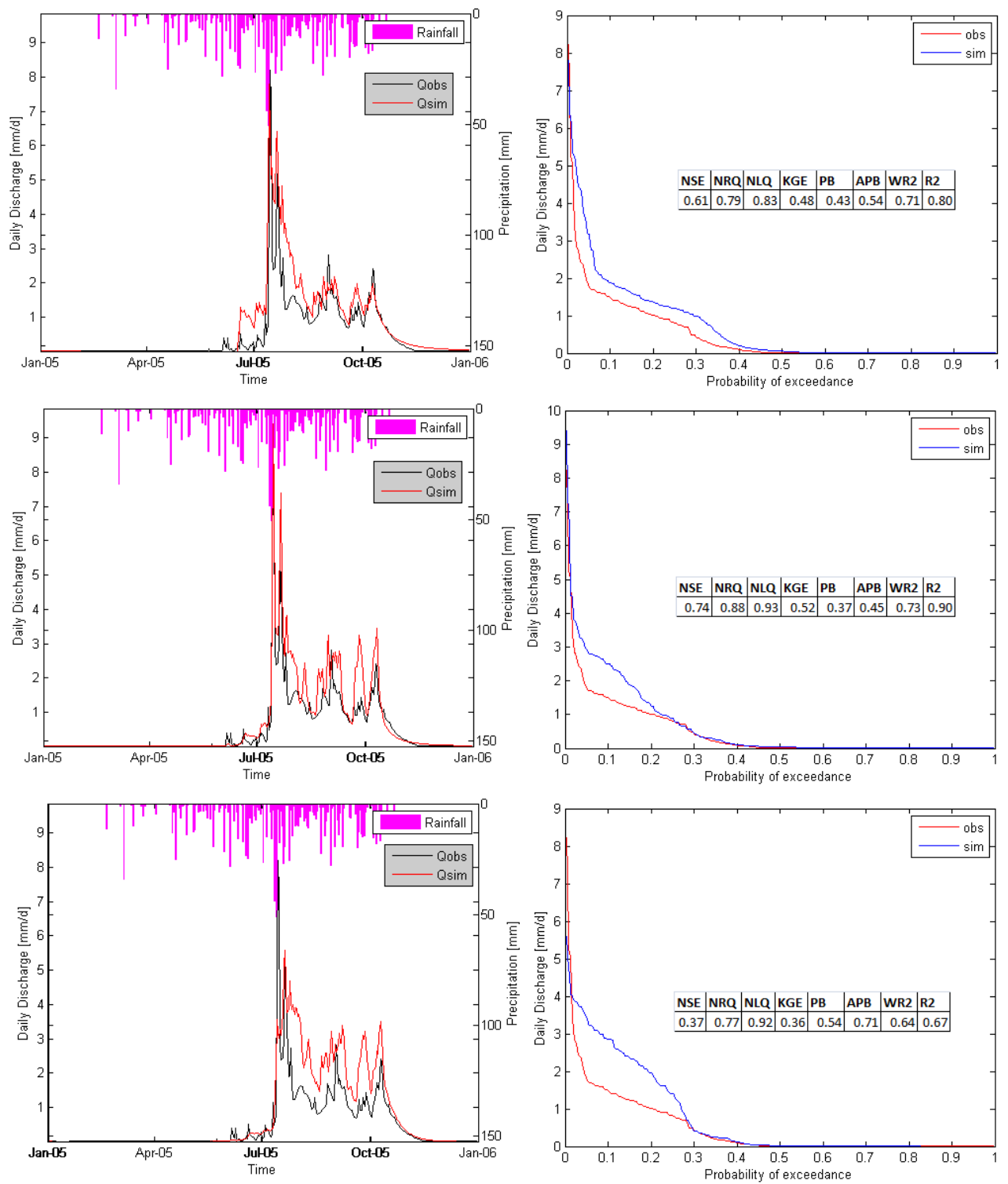


Fig.C- 10: Compared hydrographs, flow duration curves and criteria of performance for MODHYPMA, GR4J & HBV: Validation of Donga Affon catchment (BENIN), 1 308 km<sup>2</sup>.

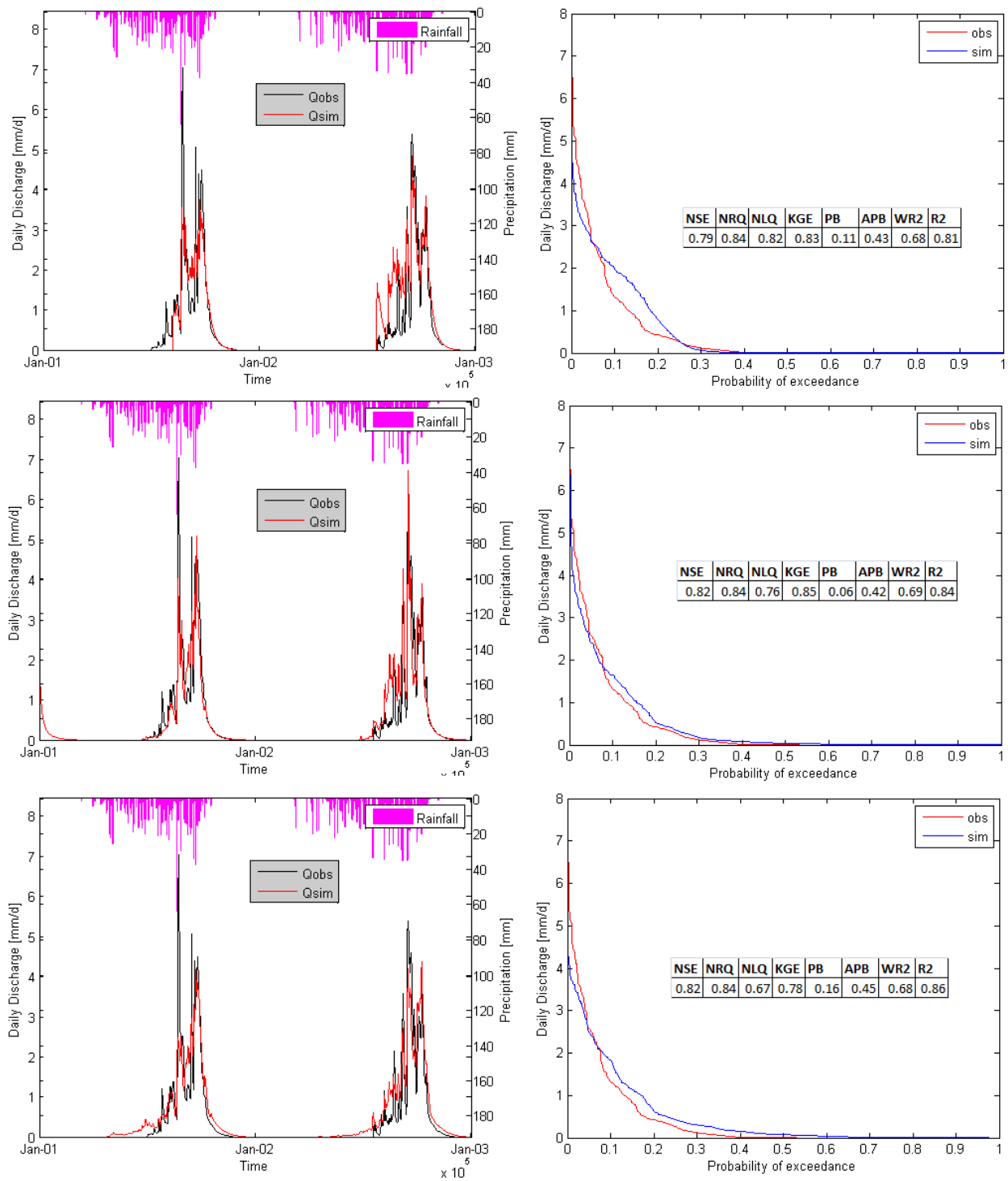


Fig.C- 11: Compared hydrographs, flow duration curves and criteria of performance for MODHYPMA, GR4J & HBV: Calibration of Saramanga catchment (BENIN), 1 360 km<sup>2</sup>.

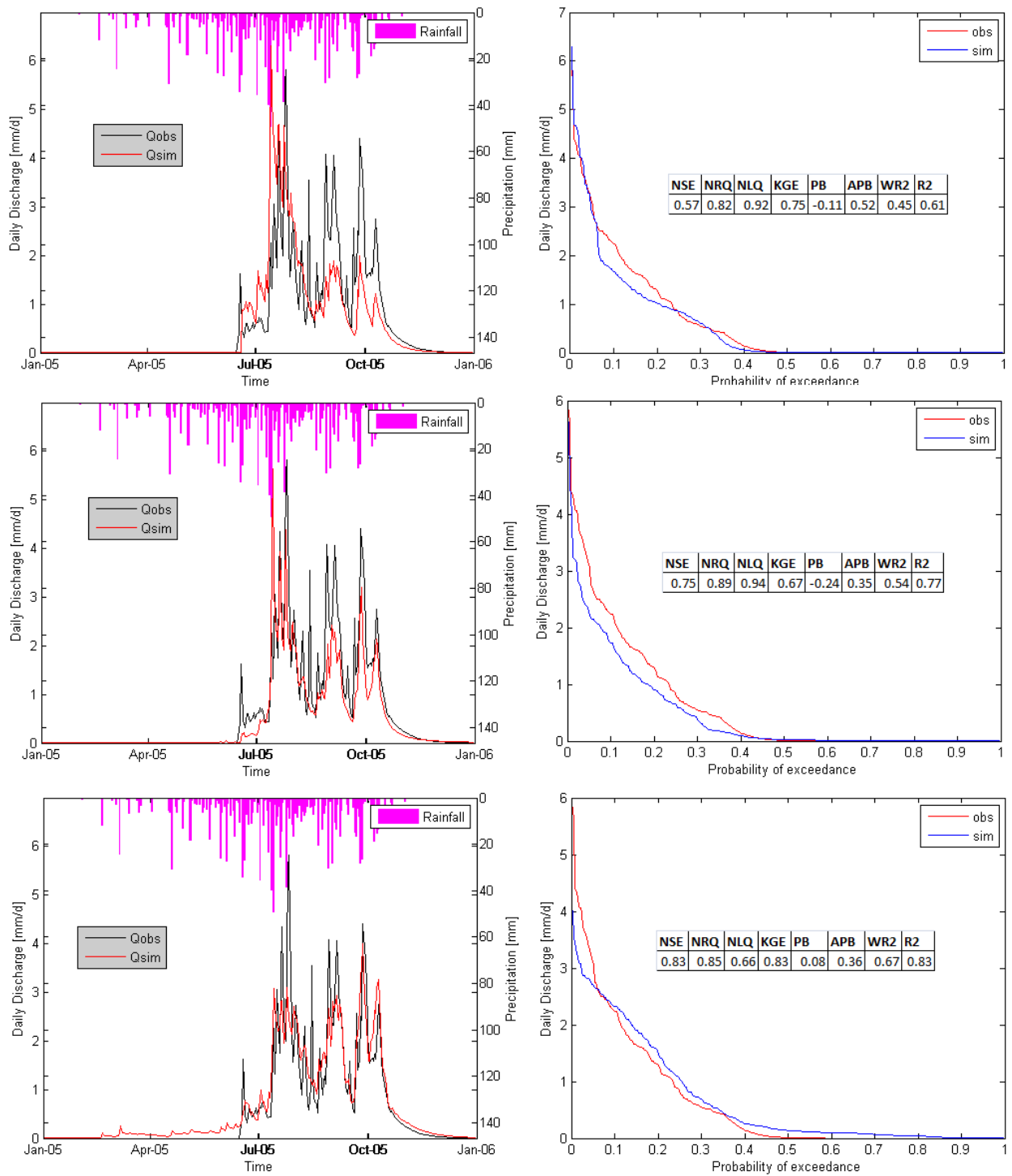


Fig.C- 12: Compared hydrographs, flow duration curves and criteria of performance for MODHYPMA, GR4J & HBV: Validation of Saramanga catchment (BENIN), 1 360 km<sup>2</sup>.

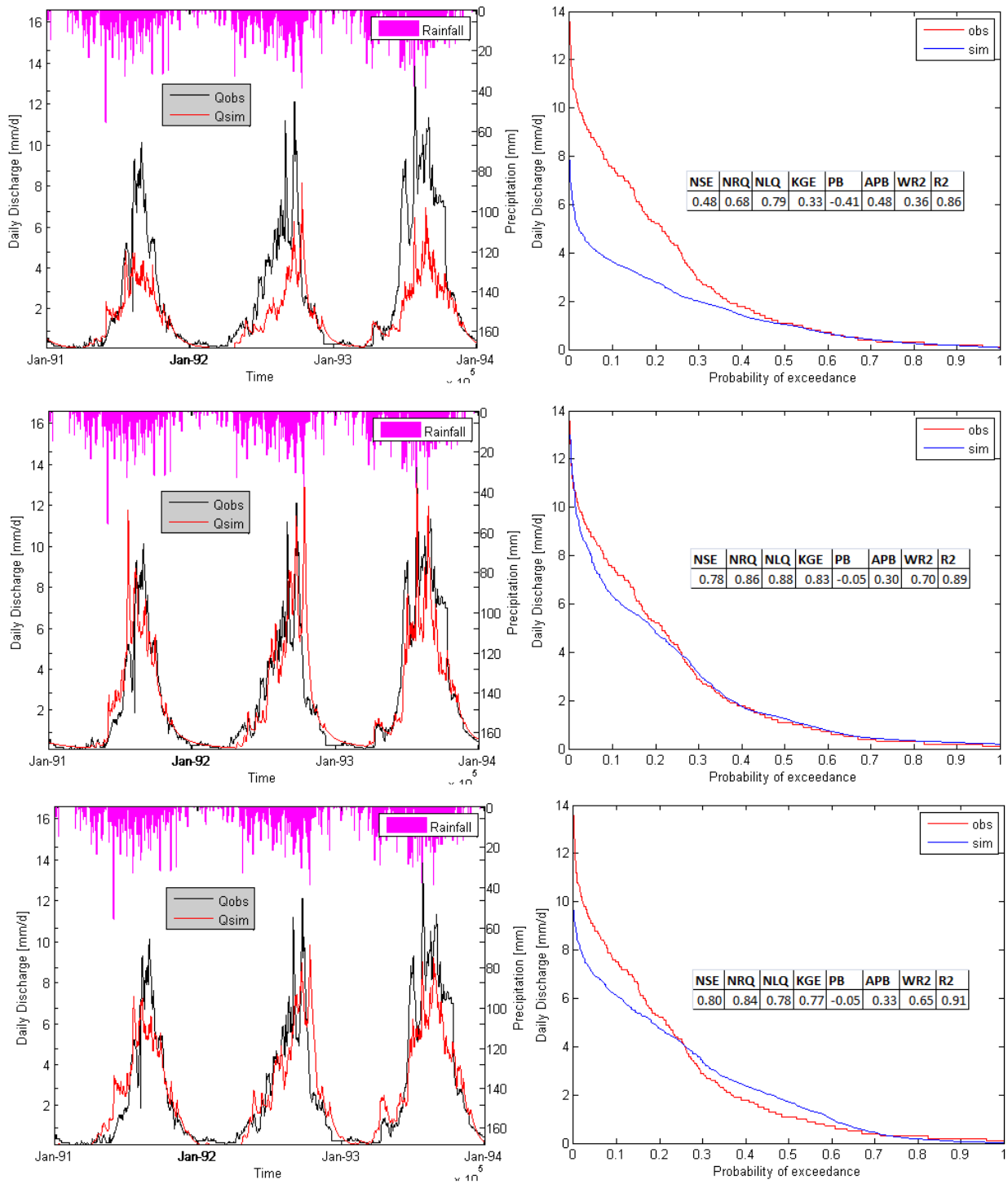


Fig.C- 13: Compared hydrographs, flow duration curves and criteria of performance for MODHYPMA, GR4J & HBV: Calibration of Sore catchment (BENIN), 1 711 km<sup>2</sup>.

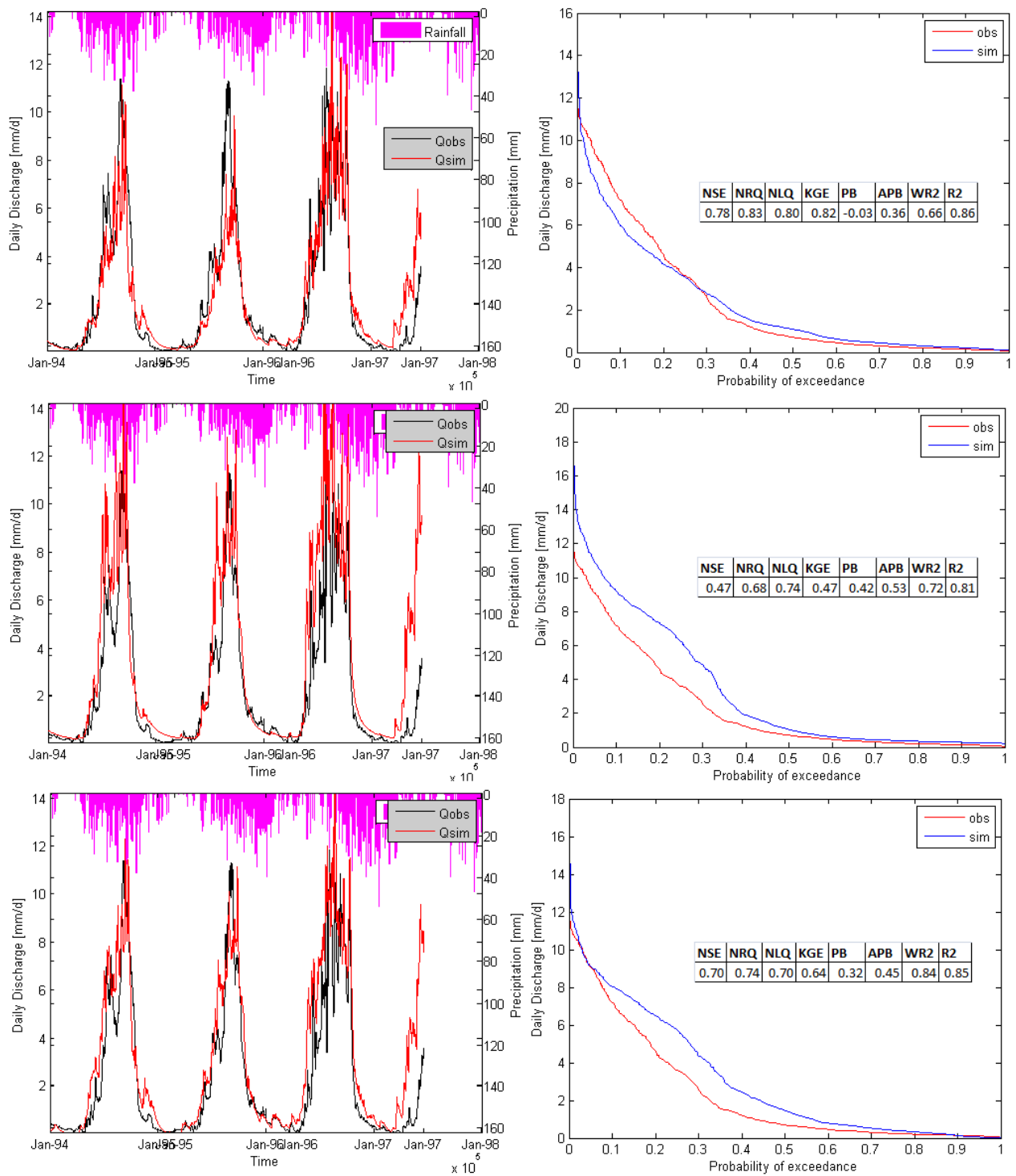


Fig.C- 14: Compared hydrographs, flow duration curves and criteria of performance for MODHYPMA, GR4J & HBV: Validation of Sore catchment (ETHIOPIA), 1 711 km<sup>2</sup>.

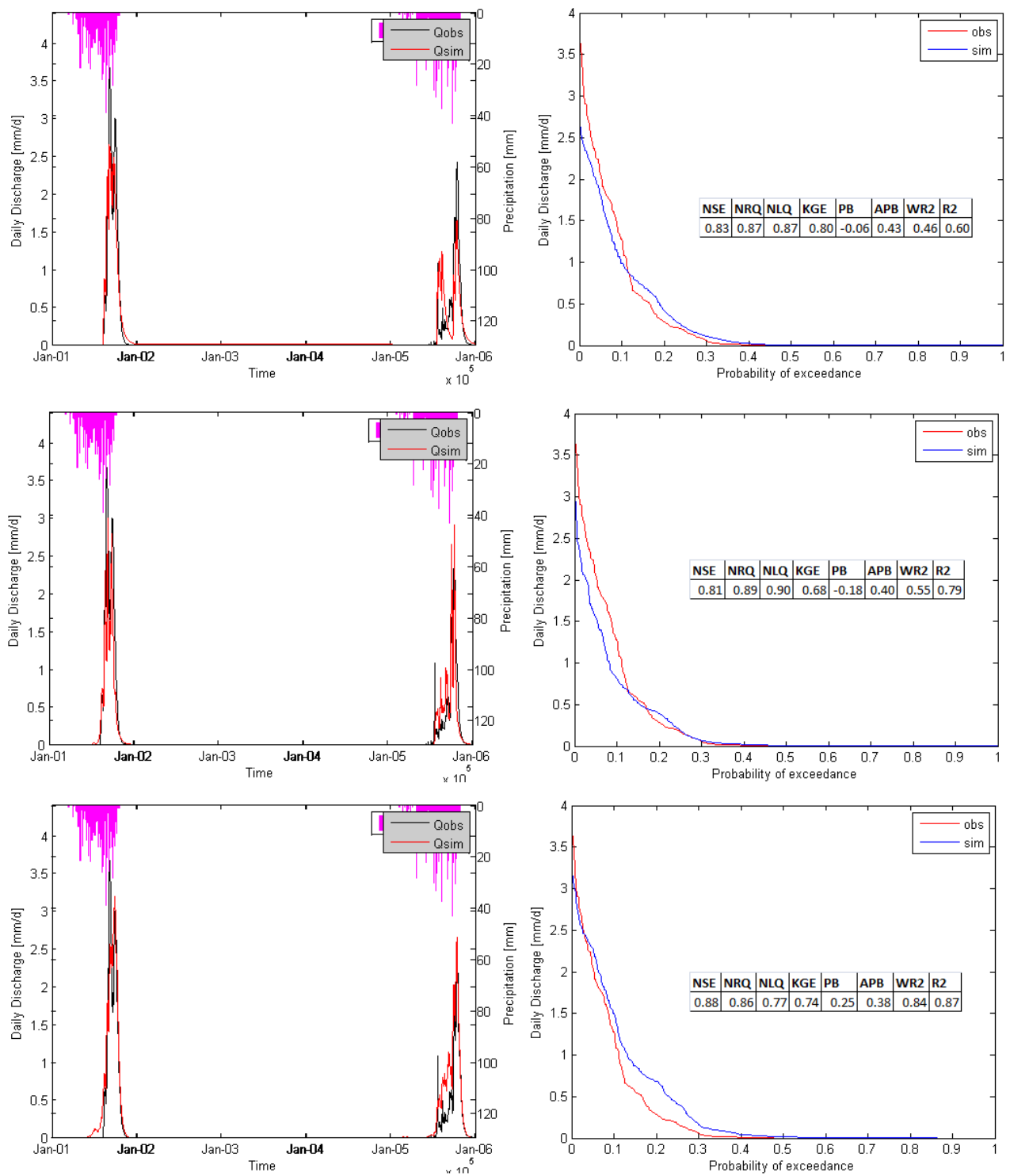


Fig.C- 15: Compared hydrographs, flow duration curves and criteria of performance for MODHYPMA, GR4J & HBV: Calibration of Barérou catchment (BENIN), 2 134 km<sup>2</sup>.

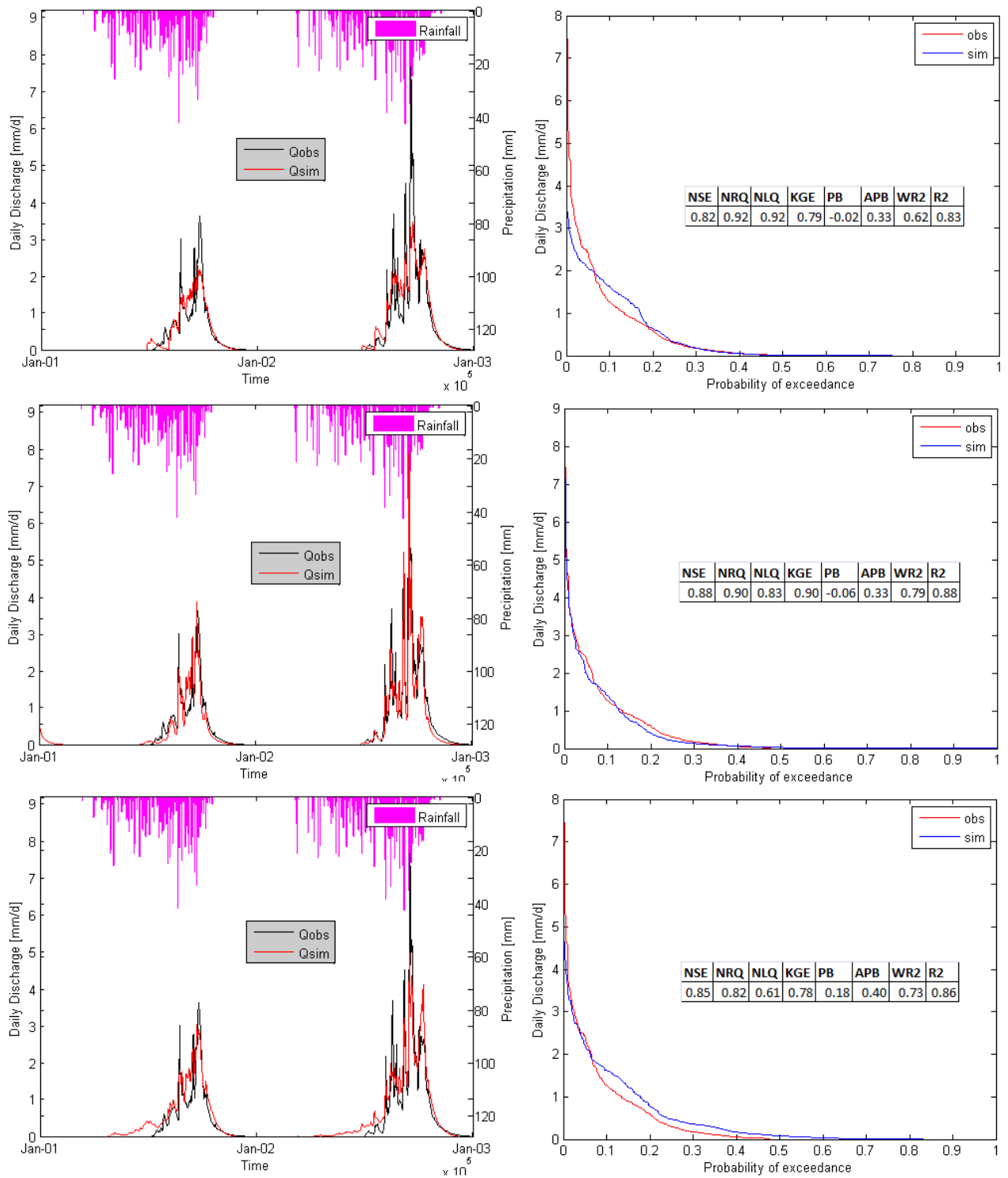


Fig.C- 16: Compared hydrographs, flow duration curves and criteria of performance for MODHYPMA, GR4J & HBV: Calibration of Côte 238 catchment (BENIN), 3 060 km<sup>2</sup>.

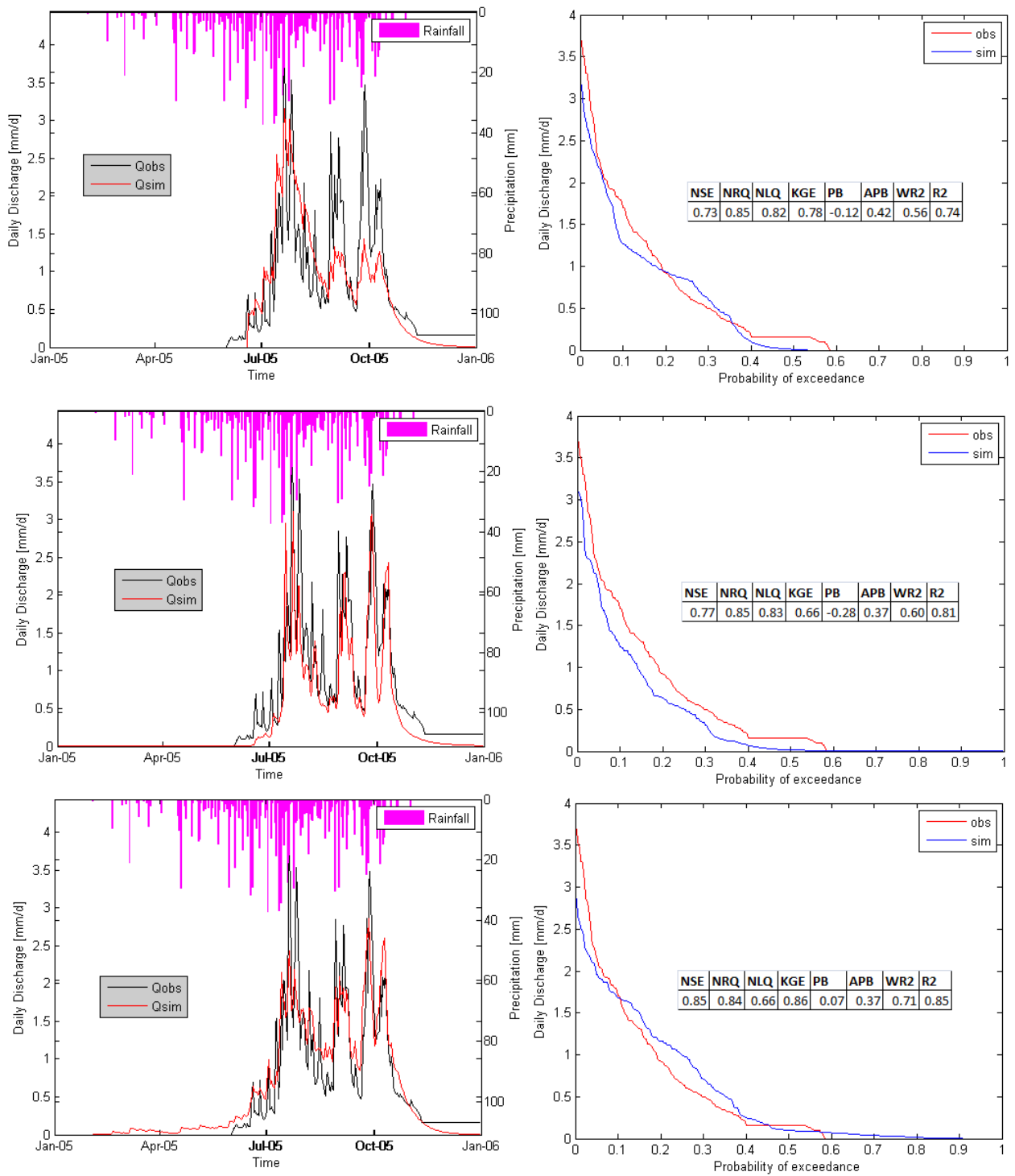


Fig.C- 17: Compared hydrographs, flow duration curves and criteria of performance for MODHYPMA, GR4J & HBV: Validation of Côte 238 catchment (BENIN), 3 060 km<sup>2</sup>.

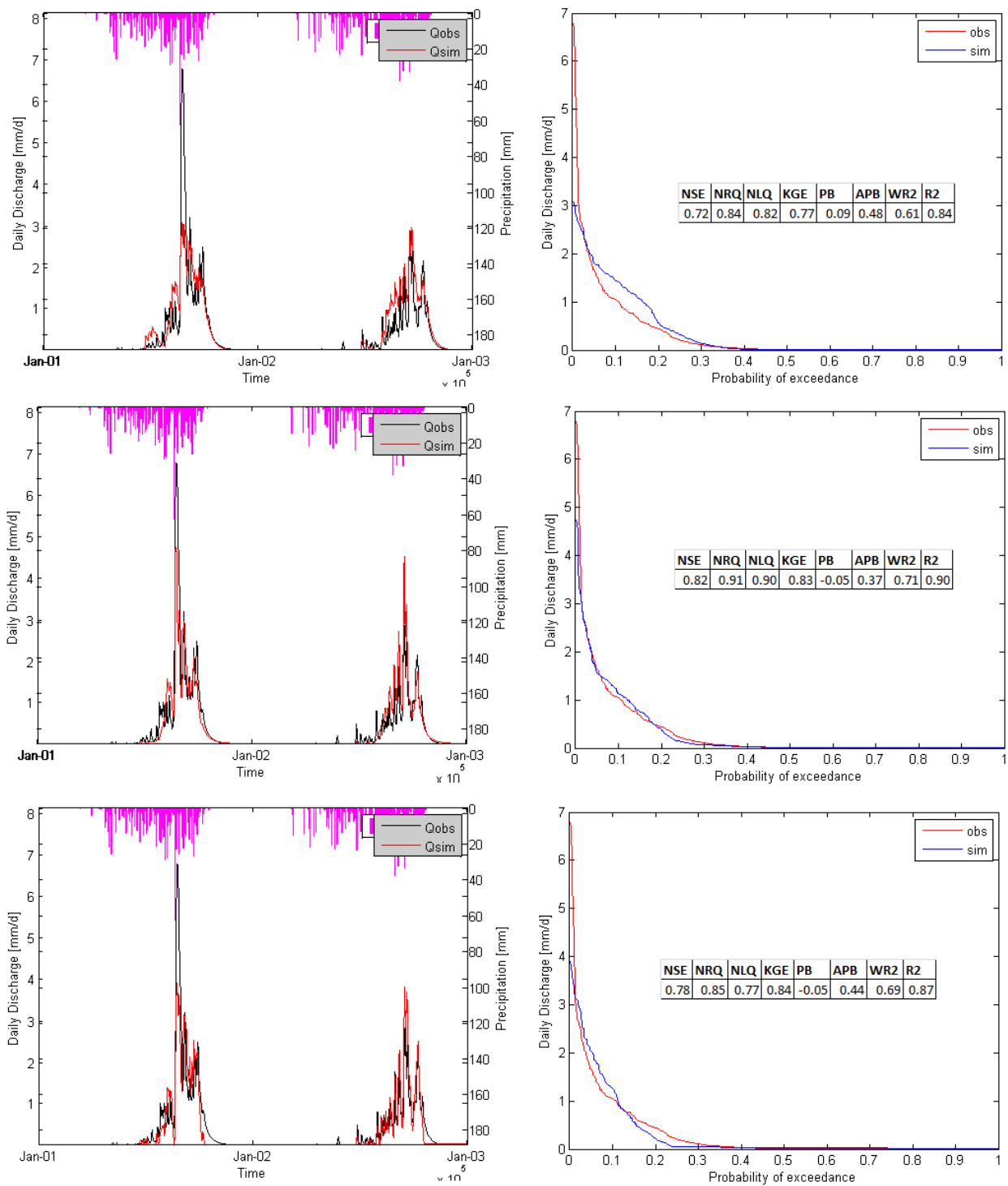


Fig.C- 18: Compared hydrographs, flow duration curves and criteria of performance for MODHYPM, GR4J & HBV: Calibration of Aval Sani catchment (BENIN), 3 279 km<sup>2</sup>.

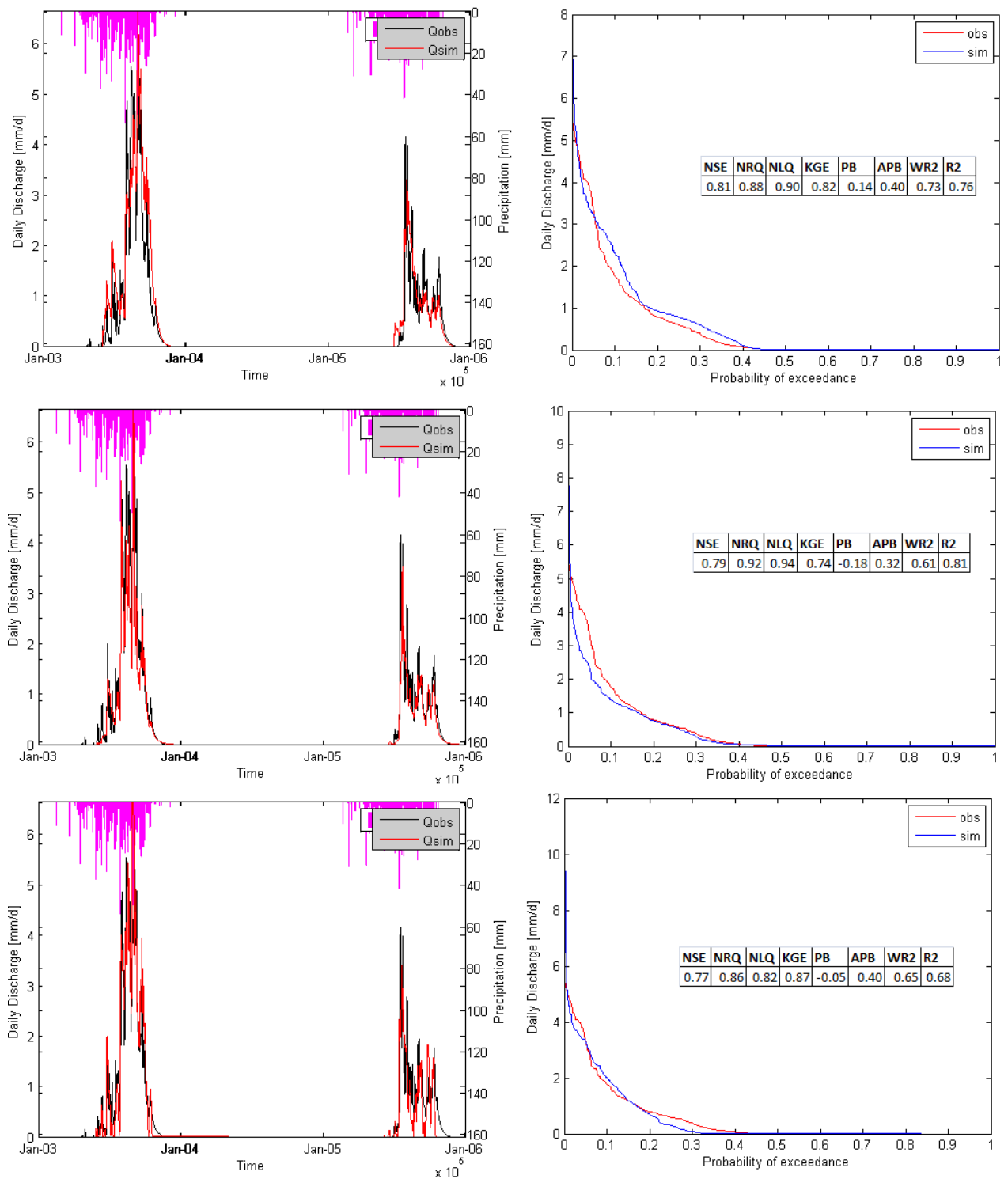


Fig.C- 19: Compared hydrographs, flow duration curves and criteria of performance for MODHYPMA, GR4] & HBV: Validation of Aval Sani catchment (BENIN), 3 279 km<sup>2</sup>.

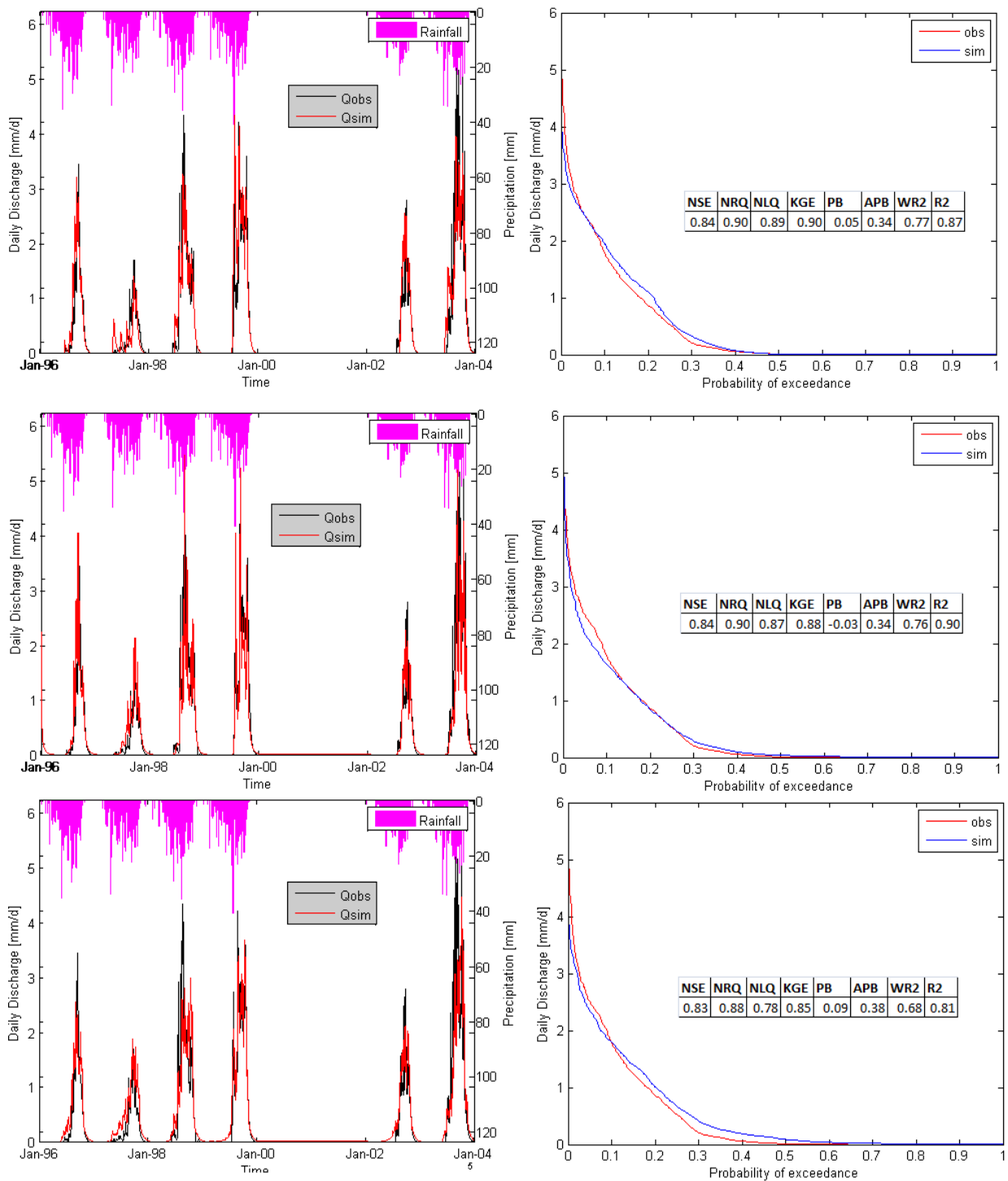


Fig.C- 20: Compared hydrographs, flow duration curves and criteria of performance for MODHYPMA, GR4J & HBV: Calibration of Savè catchment (BENIN), 23 491 km<sup>2</sup>.

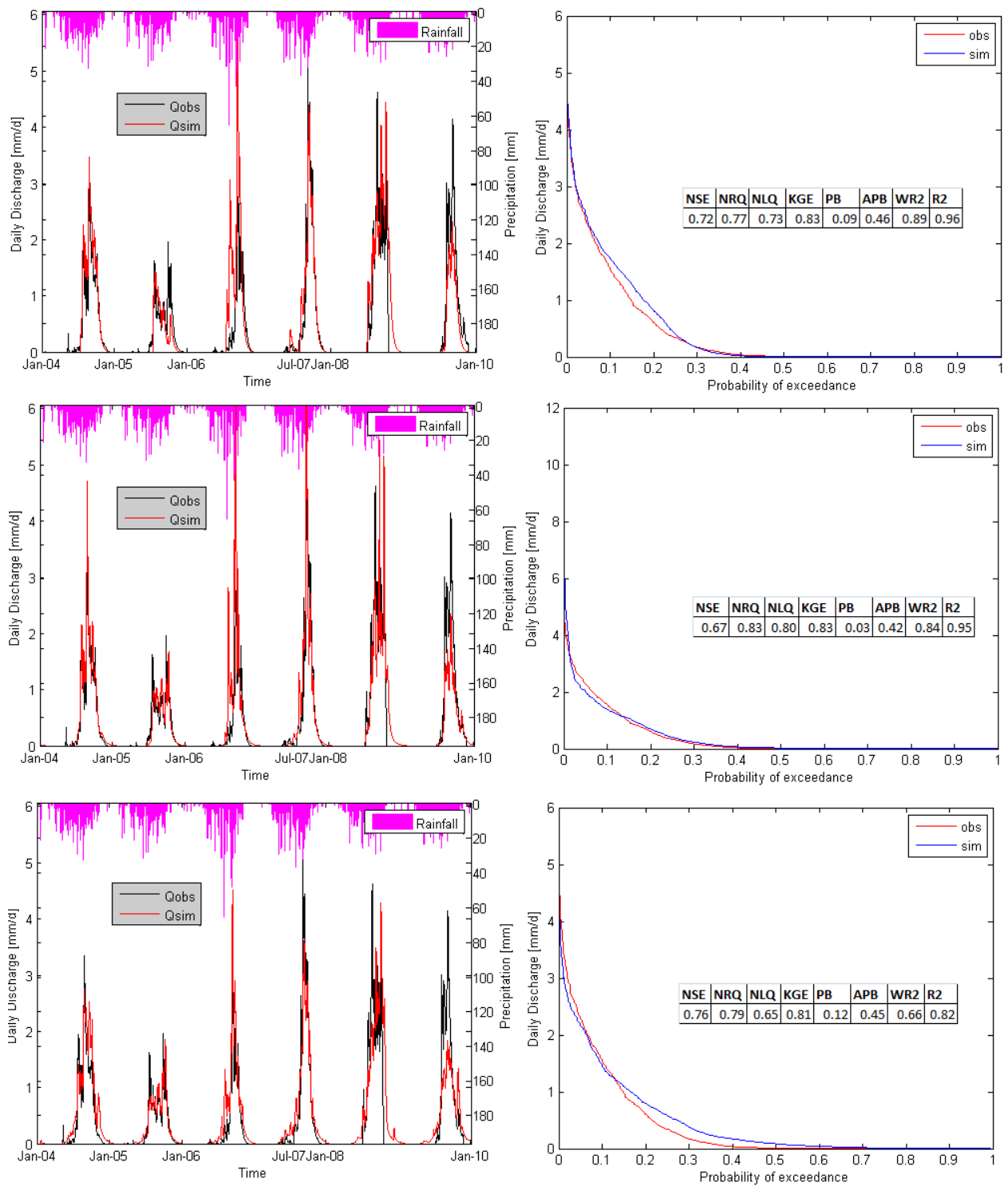


Fig.C- 21: Compared hydrographs, flow duration curves and criteria of performance for MODHYPMA, GR4J & HBV: Validation of Savè catchment (BENIN), 23 491 km<sup>2</sup>.

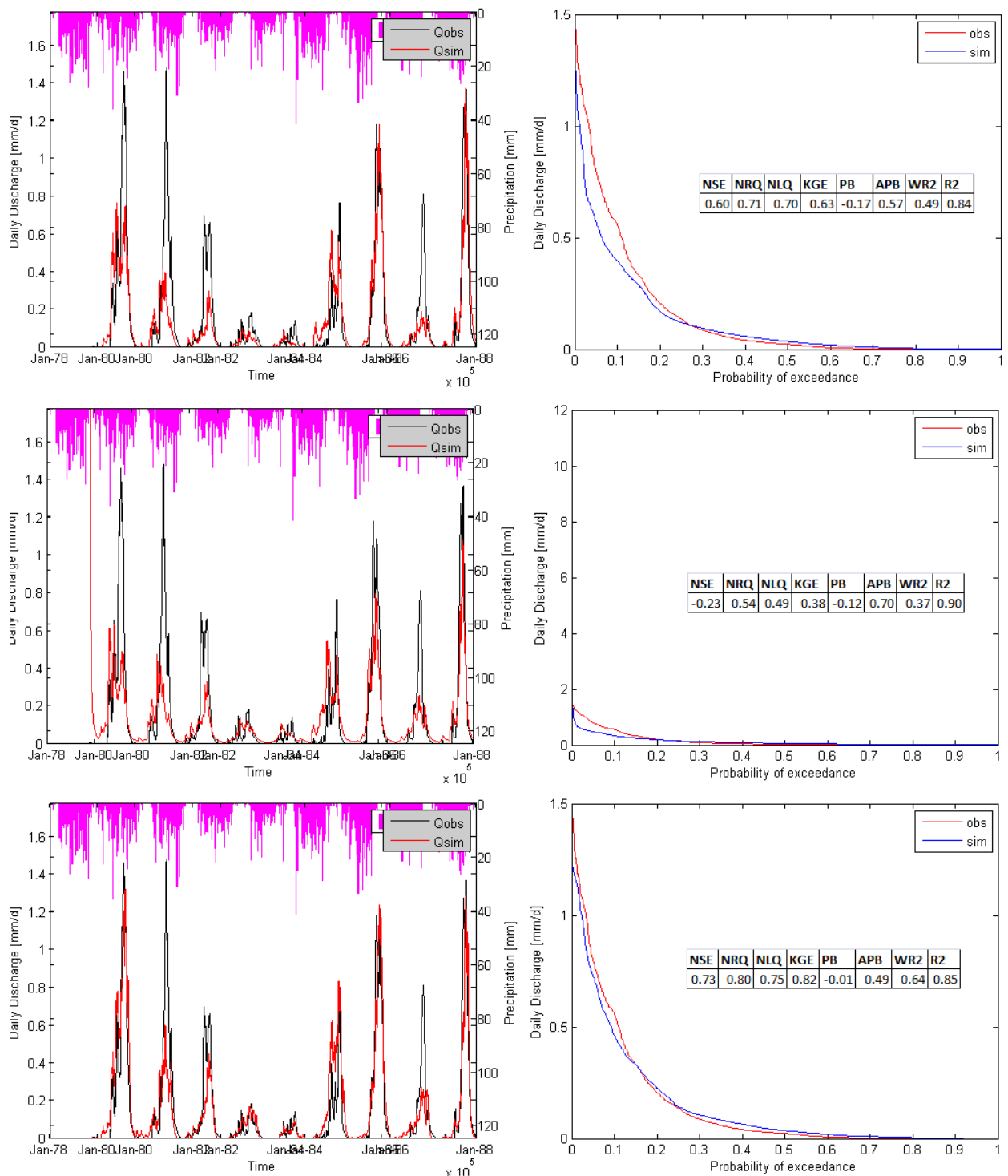


Fig.C- 22: Compared hydrographs, flow duration curves and criteria of performance for MODHYPMA, GR4J & HBV: Calibration of Mbasso catchment (CÔTE D'IVOIRE), 74 900 km<sup>2</sup>.

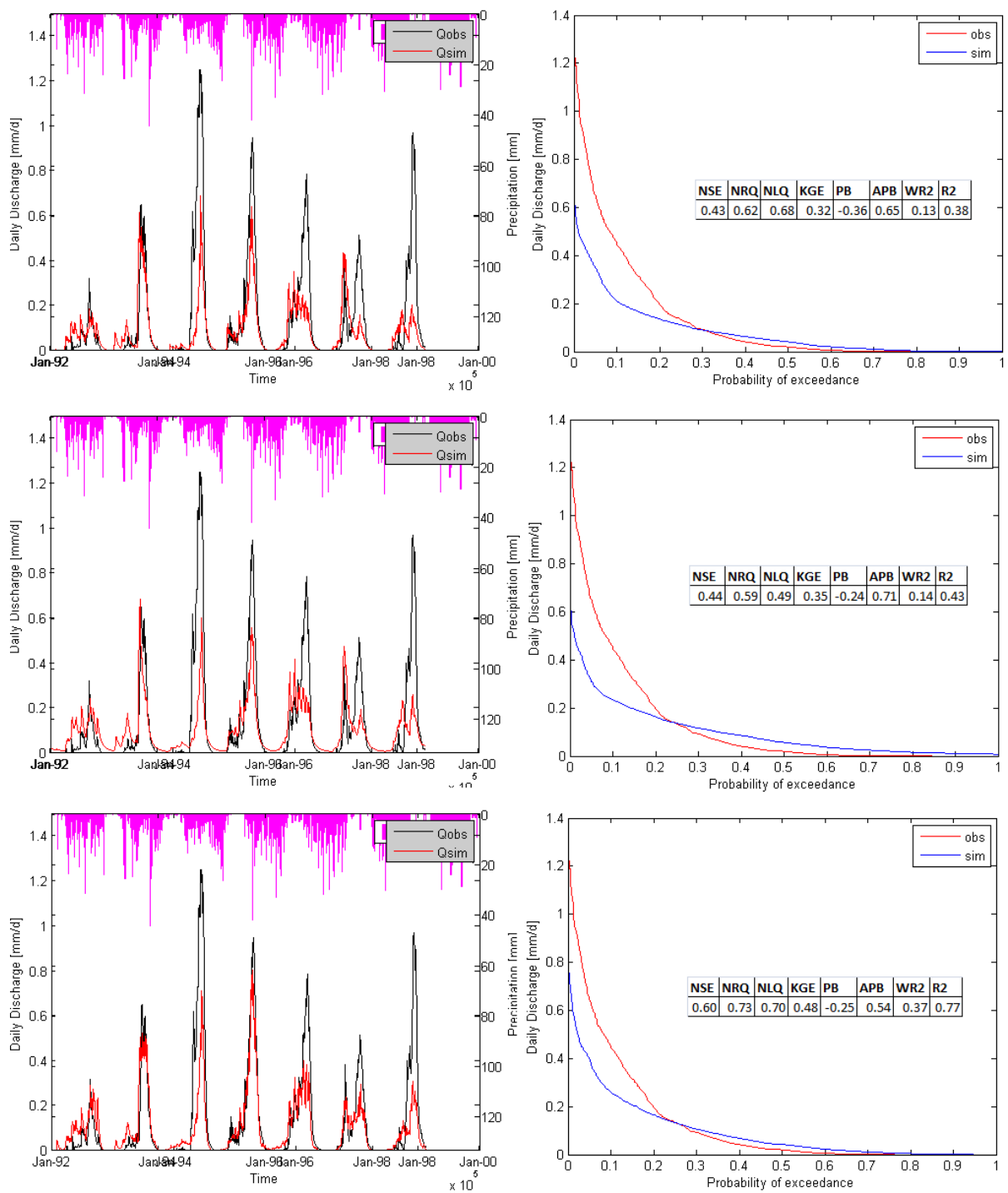


Fig.C- 23: Compared hydrographs, flow duration curves and criteria of performance for MODHYPMA, GR4J & HBV: Validation of Mbasso catchment (CÔTE D'IVOIRE), 74 900 km<sup>2</sup>.

## APPENDIX D. SENSITIVITY AND UNCERTAINTY ANALYSES RESULTS

<i>Fig.D- 1: The dotted plot map of the parameters versus Nash criterion for discharge simulation on Lookout Creek catchment (USA), 62 km<sup>2</sup> .....</i>	167
<i>Fig.D- 2: 90% confidence interval of daily runoff due to parameter uncertainty calculated by GLUE method with threshold of 0.6 on Lookout Creek catchment (USA), 62 km<sup>2</sup>.....</i>	167
<i>Fig.D- 3: The dotted plot map of the parameters versus Nash criterion for discharge simulation on Le Léguer catchment (FRANCE), 260 km<sup>2</sup> .....</i>	168
<i>Fig.D- 4: 90% confidence interval of daily runoff due to parameter uncertainty calculated by GLUE method with threshold of 0.6 on Le Léguer catchment (FRANCE), 260 km<sup>2</sup>.....</i>	168
<i>Fig.D- 5: The dotted plot map of the parameters versus Nash criterion for discharge simulation on Donga Pont catchment (BENIN), 587 km<sup>2</sup> .....</i>	169
<i>Fig.D- 6: 90% confidence interval of daily runoff due to parameter uncertainty calculated by GLUE method with threshold of 0.6 on Donga Pont catchment (BENIN), 587 km<sup>2</sup>.....</i>	169
<i>Fig.D- 7: The dotted plot map of the parameters versus Nash criterion for discharge simulation on Sani catchment (BENIN), 745 km<sup>2</sup> .....</i>	170
<i>Fig.D- 8: 90% confidence interval of daily runoff due to parameter uncertainty calculated by GLUE method with threshold of 0.6 on Sani catchment (BENIN), 745 km<sup>2</sup>.....</i>	170
<i>Fig.D- 9: The dotted plot map of the parameters versus Nash criterion for discharge simulation on Donga Affon catchment (BENIN), 1 308 km<sup>2</sup>.....</i>	171
<i>Fig.D- 10: 90% confidence interval of daily runoff due to parameter uncertainty calculated by GLUE method with threshold of 0.6 on Donga Affon catchment (BENIN), 1 308 km<sup>2</sup> ..</i>	171
<i>Fig.D- 11: The dotted plot map of the parameters versus Nash criterion for discharge simulation on Saramanga catchment (BENIN), 1 360 km<sup>2</sup> .....</i>	172
<i>Fig.D- 12: 90% confidence interval of daily runoff due to parameter uncertainty calculated by GLUE method with threshold of 0.6 on Saramanga catchment (BENIN), 1 360 km<sup>2</sup>.....</i>	172
<i>Fig.D- 13: The dotted plot map of the parameters versus Nash criterion for discharge simulation on Sore catchment (ETHIOPIA), 1 711 km<sup>2</sup>.....</i>	173
<i>Fig.D- 14: 90% confidence interval of daily runoff due to parameter uncertainty calculated by GLUE method with threshold of 0.6 on Sore catchment (ETHIOPIA), 1 711 km<sup>2</sup> .....</i>	173
<i>Fig.D- 15: The dotted plot map of the parameters versus Nash criterion for discharge simulation on Barérou catchment (BENIN), 2 134 km<sup>2</sup>.....</i>	174
<i>Fig.D- 16: 90% confidence interval of daily runoff due to parameter uncertainty calculated by GLUE method with threshold of 0.6 on Barérou catchment (BENIN), 2 134 km<sup>2</sup> .....</i>	174
<i>Fig.D- 17: The dotted plot map of the parameters versus Nash criterion for discharge simulation on Cote 238 catchment (BENIN), 3 060 km<sup>2</sup>.....</i>	175
<i>Fig.D- 18: 90% confidence interval of daily runoff due to parameter uncertainty calculated by GLUE method with threshold of 0.6 on Cote 238 catchment (BENIN), 3 060 km<sup>2</sup> .....</i>	175
<i>Fig.D- 19: The dotted plot map of the parameters versus Nash criterion for discharge simulation on Aval Sani catchment (BENIN), 3 279 km<sup>2</sup>.....</i>	176
<i>Fig.D- 20: The dotted plot map of the parameters versus Nash criterion for discharge simulation on Savè catchment (BENIN), 23 491 km<sup>2</sup>.....</i>	177

Fig.D- 21: 90% confidence interval of daily runoff due to parameter uncertainty calculated by GLUE method with threshold of 0.6 on Savè catchment (BENIN), 23 491 km<sup>2</sup>. .....177

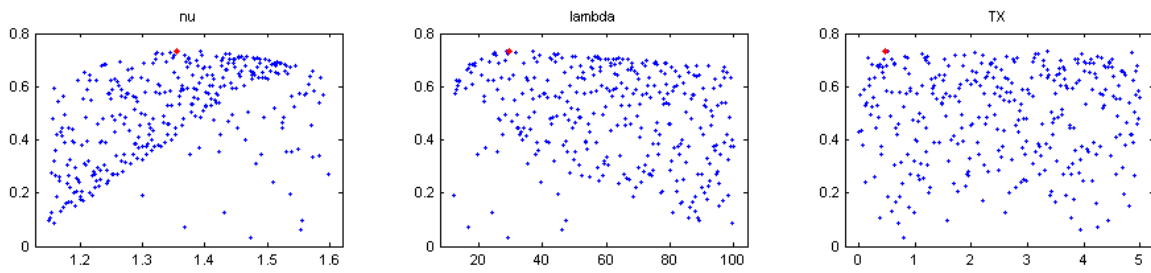


Fig.D- 1: The dotted plot map of the parameters versus Nash criterion for discharge simulation on Lookout Creek catchment (USA), 62 km<sup>2</sup>.

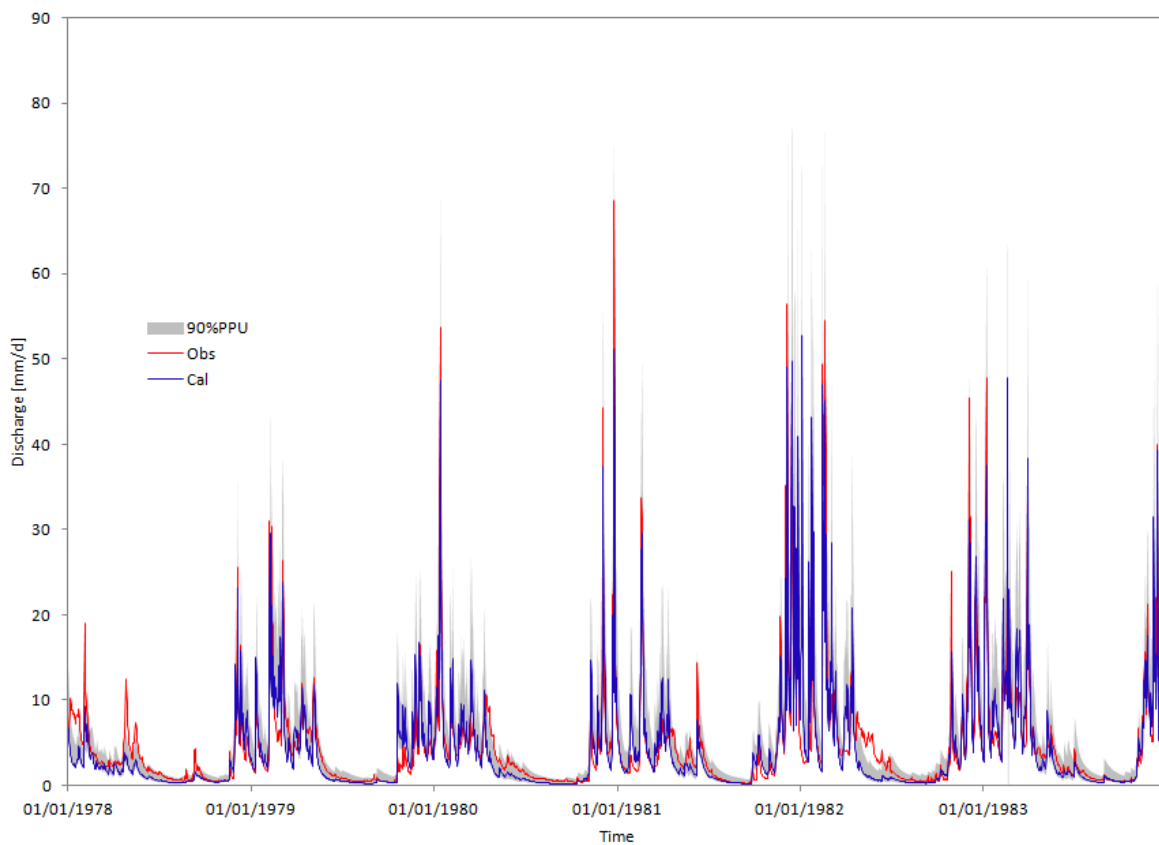


Fig.D- 2: 90% confidence interval of daily runoff due to parameter uncertainty calculated by GLUE method with threshold of 0.6 on Lookout Creek catchment (USA), 62 km<sup>2</sup>.

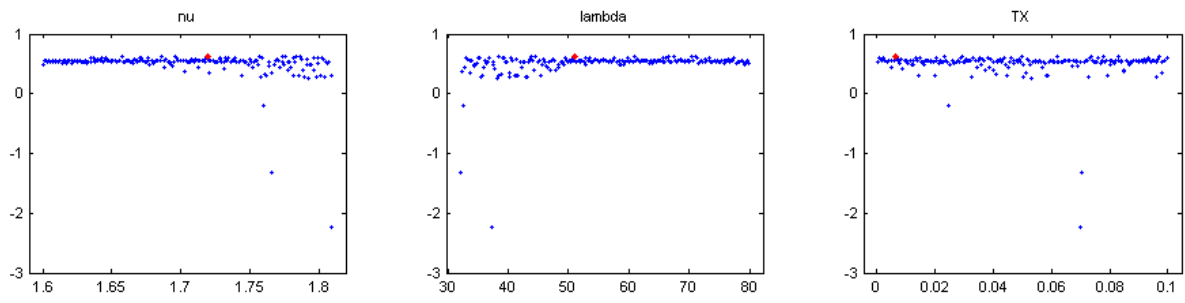


Fig.D- 3: The dotted plot map of the parameters versus Nash criterion for discharge simulation on Le Léguer catchment (FRANCE), 260 km<sup>2</sup>.

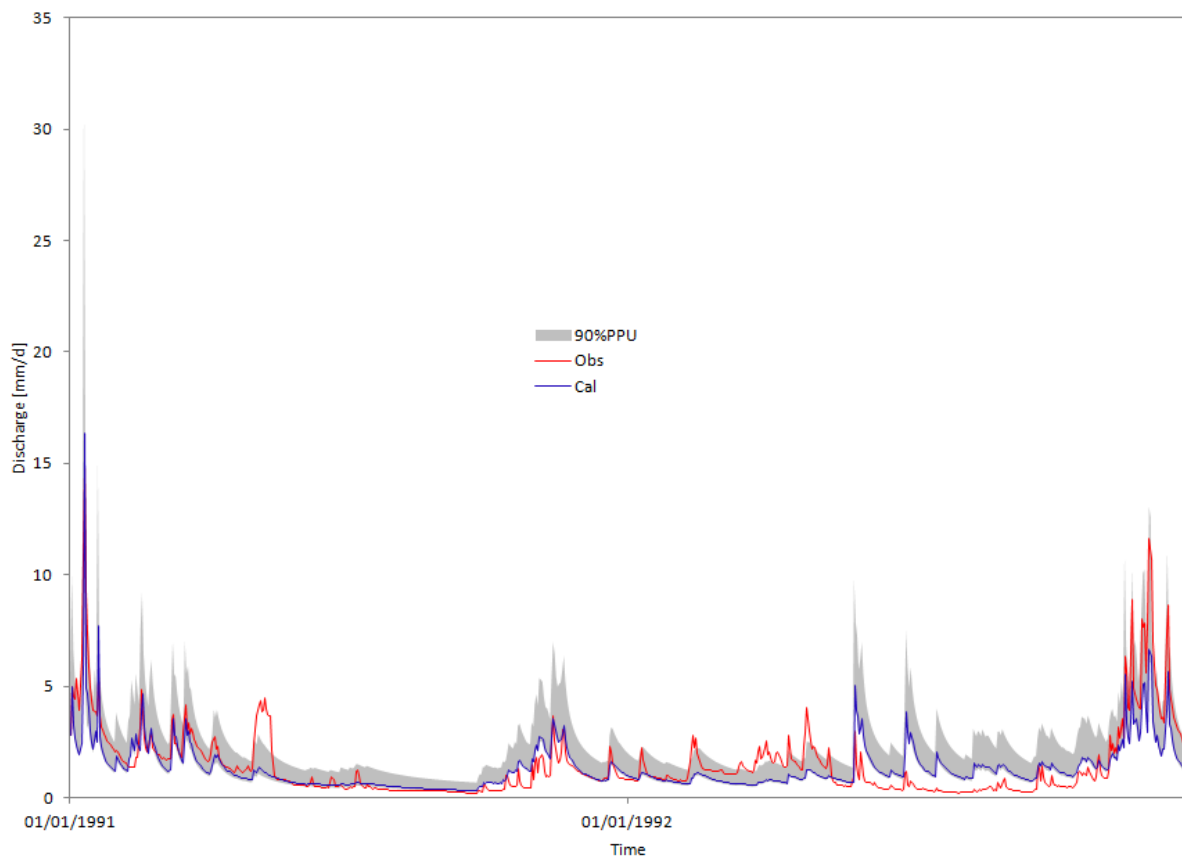


Fig.D- 4: 90% confidence interval of daily runoff due to parameter uncertainty calculated by GLUE method with threshold of 0.6 on Le Léguer catchment (FRANCE), 260 km<sup>2</sup>.

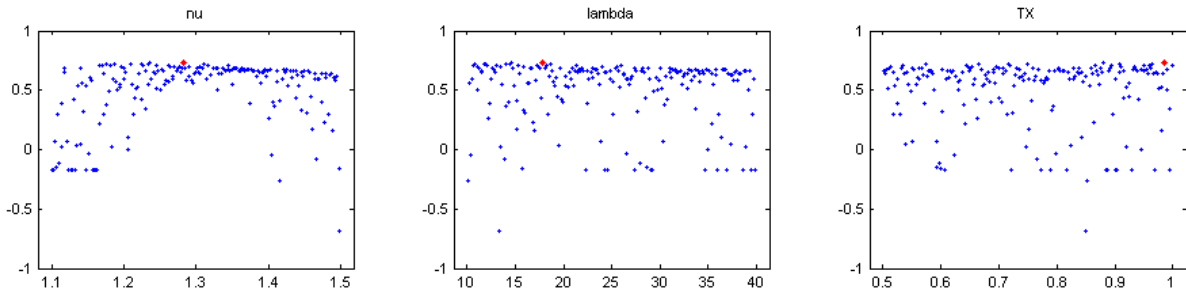


Fig.D- 5: The dotted plot map of the parameters versus Nash criterion for discharge simulation on Donga Pont catchment (BENIN), 587 km<sup>2</sup>.

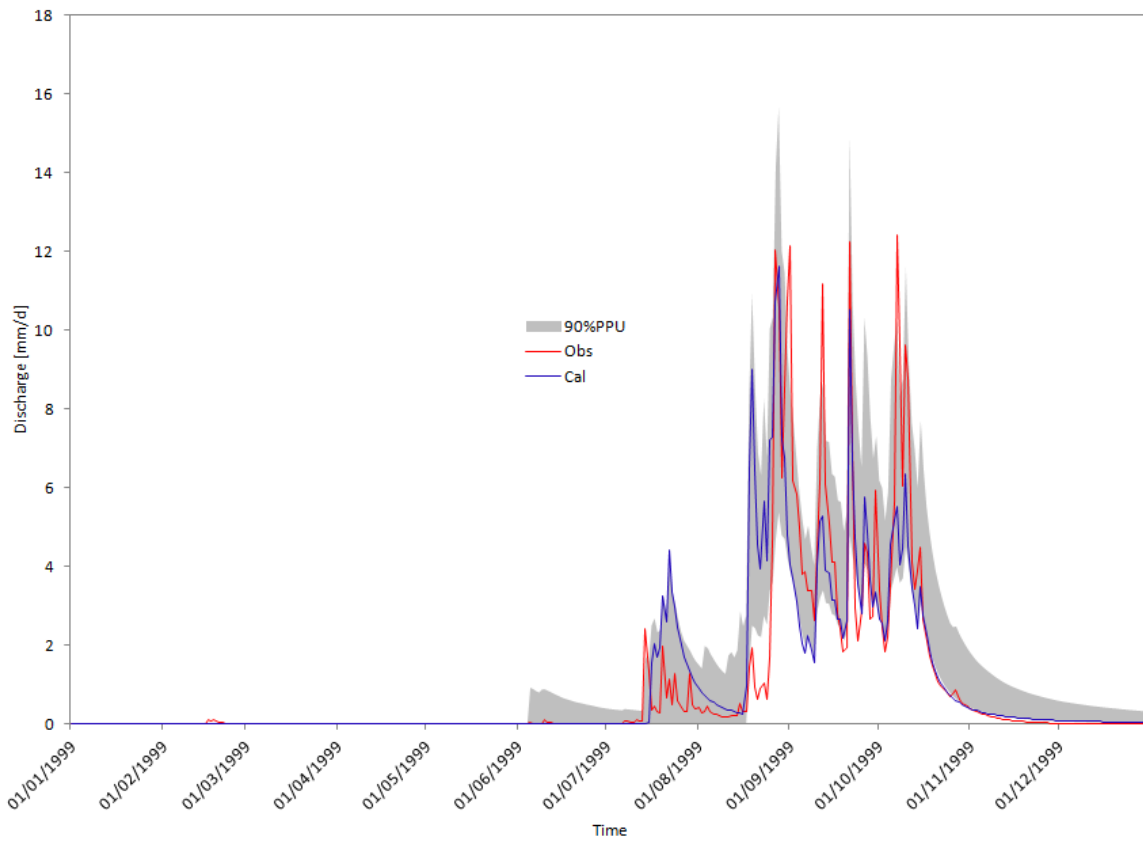


Fig.D- 6: 90% confidence interval of daily runoff due to parameter uncertainty calculated by GLUE method with threshold of 0.6 on Donga Pont catchment (BENIN), 587 km<sup>2</sup>.

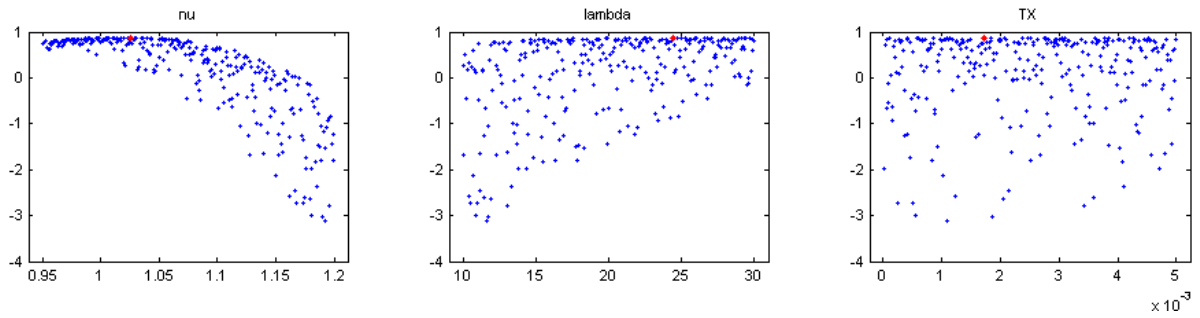


Fig.D- 7: The dotted plot map of the parameters versus Nash criterion for discharge simulation on Sani catchment (BENIN), 745 km<sup>2</sup>.

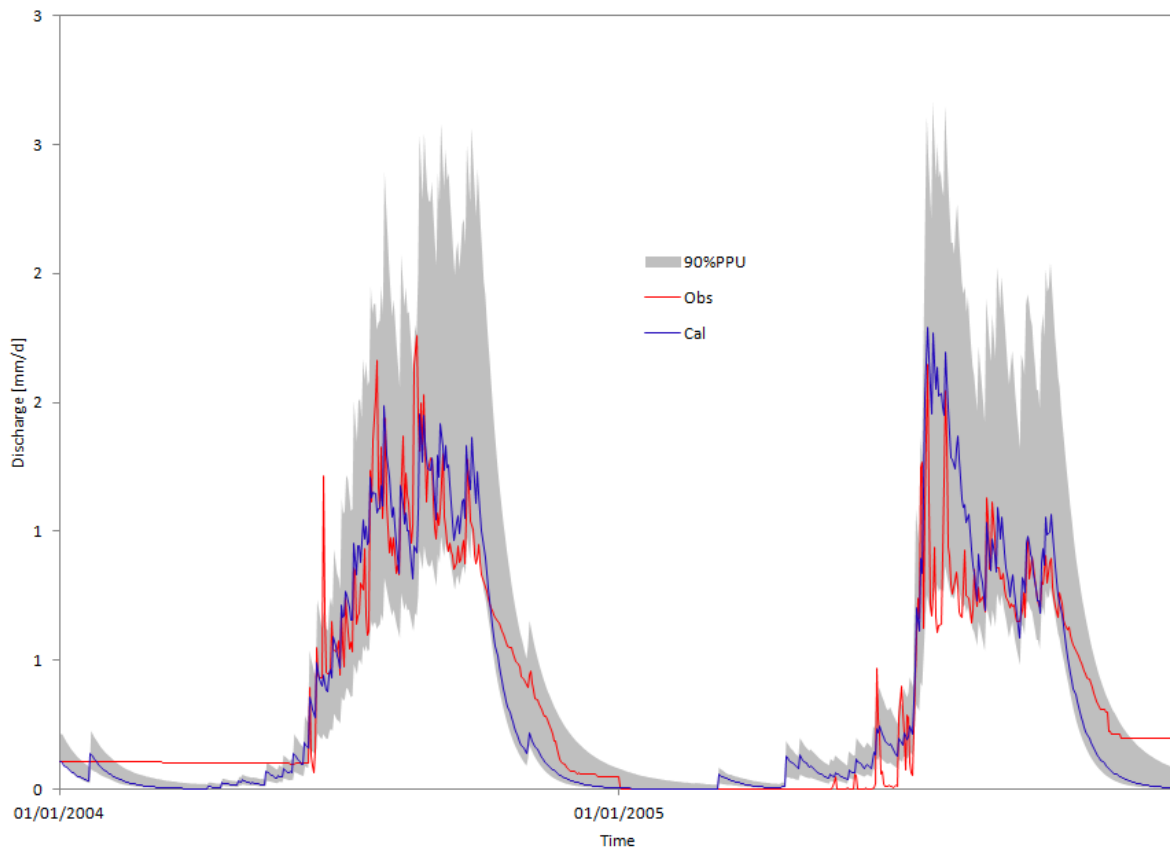


Fig.D- 8: 90% confidence interval of daily runoff due to parameter uncertainty calculated by GLUE method with threshold of 0.6 on Sani catchment (BENIN), 745 km<sup>2</sup>.

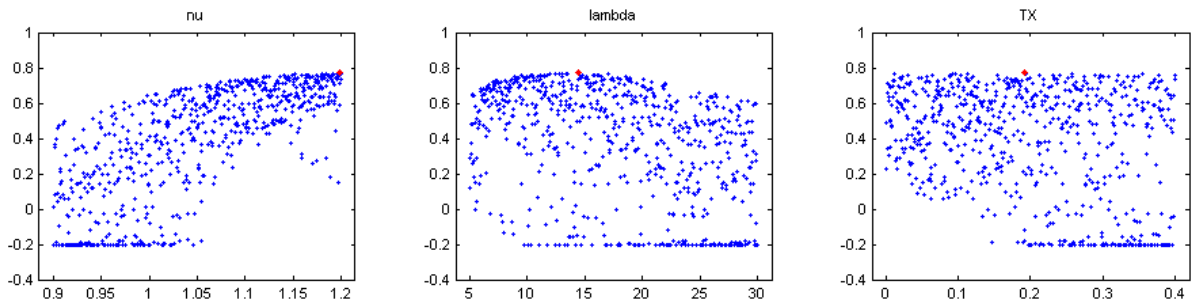


Fig.D- 9: The dotted plot map of the parameters versus Nash criterion for discharge simulation on Donga Affon catchment (BENIN), 1 308 km<sup>2</sup>.

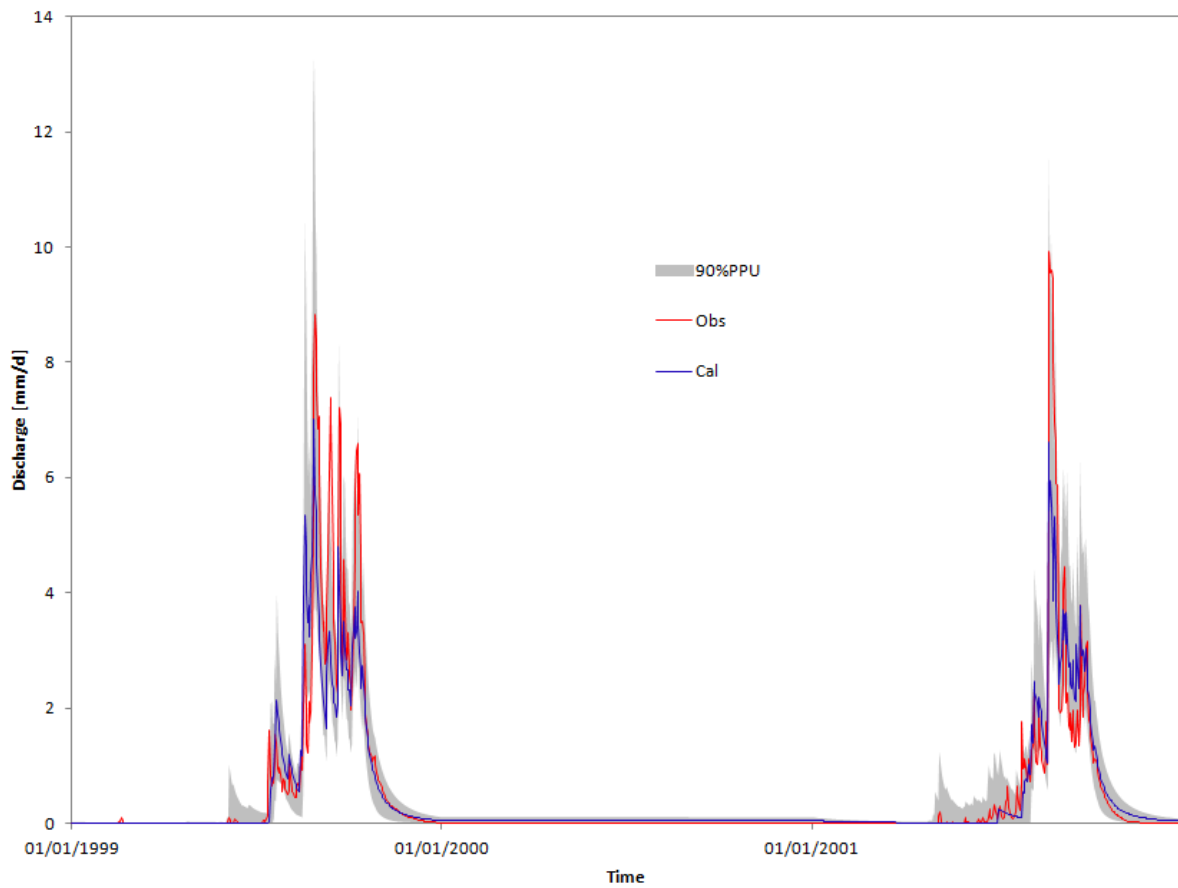


Fig.D- 10: 90% confidence interval of daily runoff due to parameter uncertainty calculated by GLUE method with threshold of 0.6 on Donga Affon catchment (BENIN), 1 308 km<sup>2</sup>.

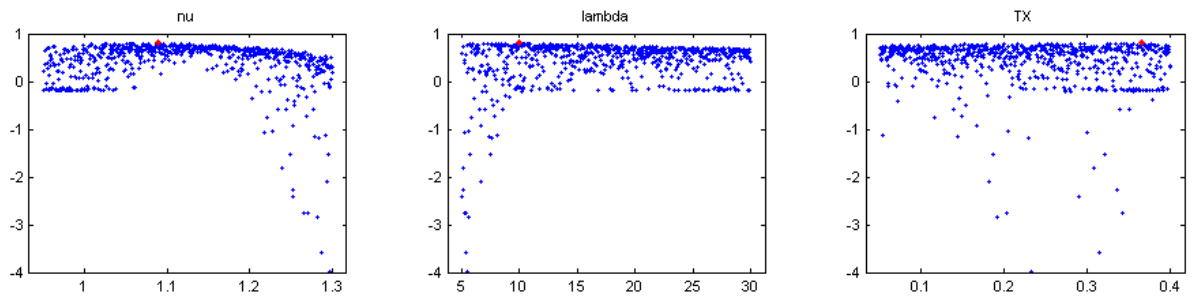


Fig.D- 11: The dotted plot map of the parameters versus Nash criterion for discharge simulation on Saramanga catchment (BENIN), 1 360 km<sup>2</sup>.

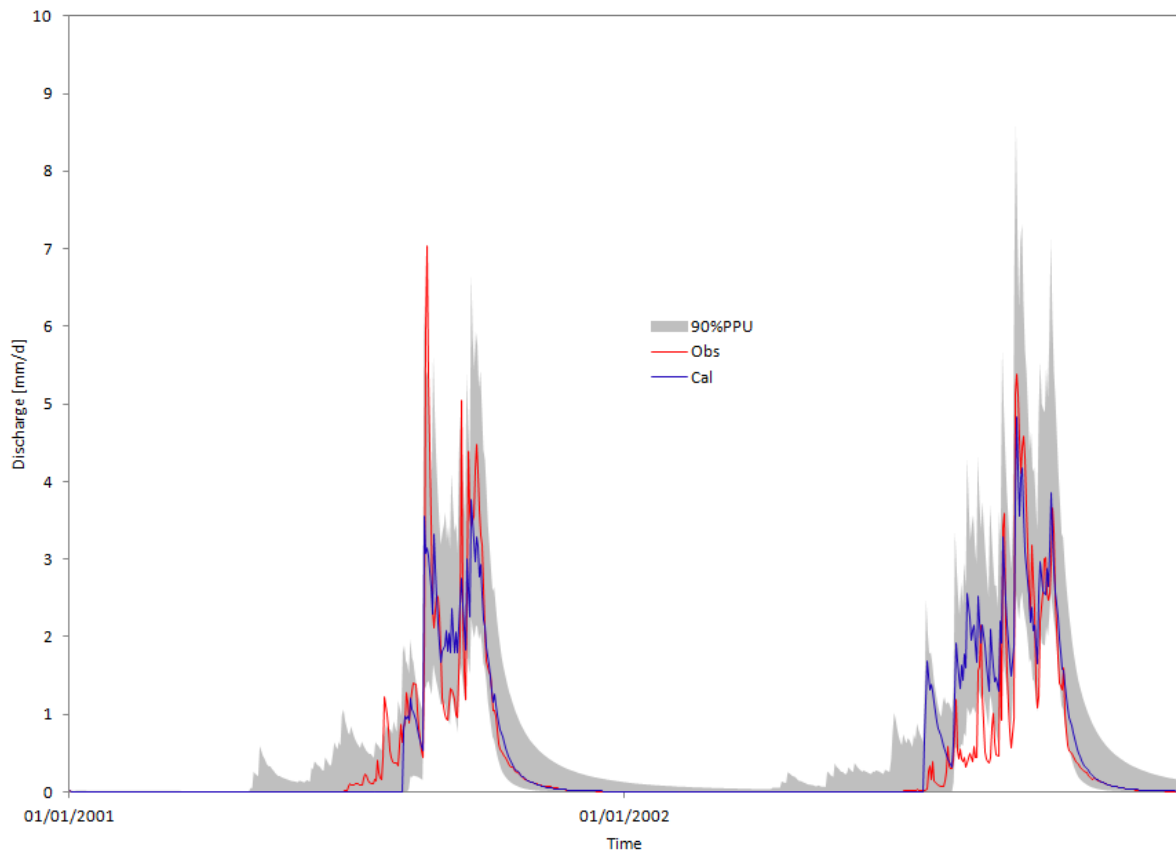


Fig.D- 12: 90% confidence interval of daily runoff due to parameter uncertainty calculated by GLUE method with threshold of 0.6 on Saramanga catchment (BENIN), 1 360 km<sup>2</sup>.

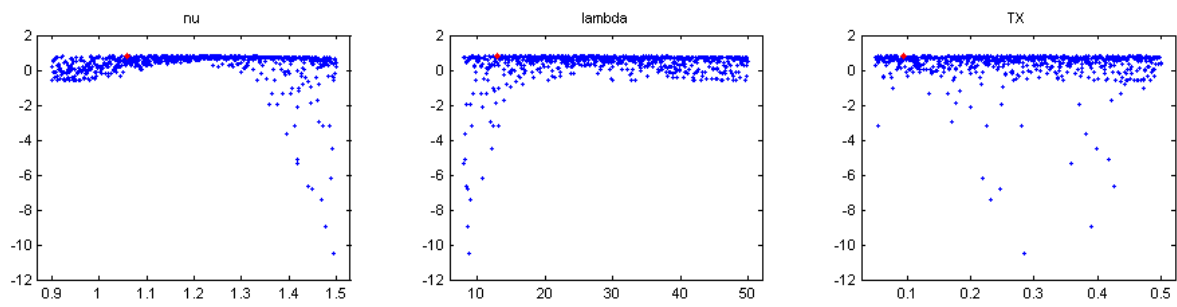


Fig.D- 13: The dotted plot map of the parameters versus Nash criterion for discharge simulation on Sore catchment (ETHIOPIA), 1 711 km<sup>2</sup>.

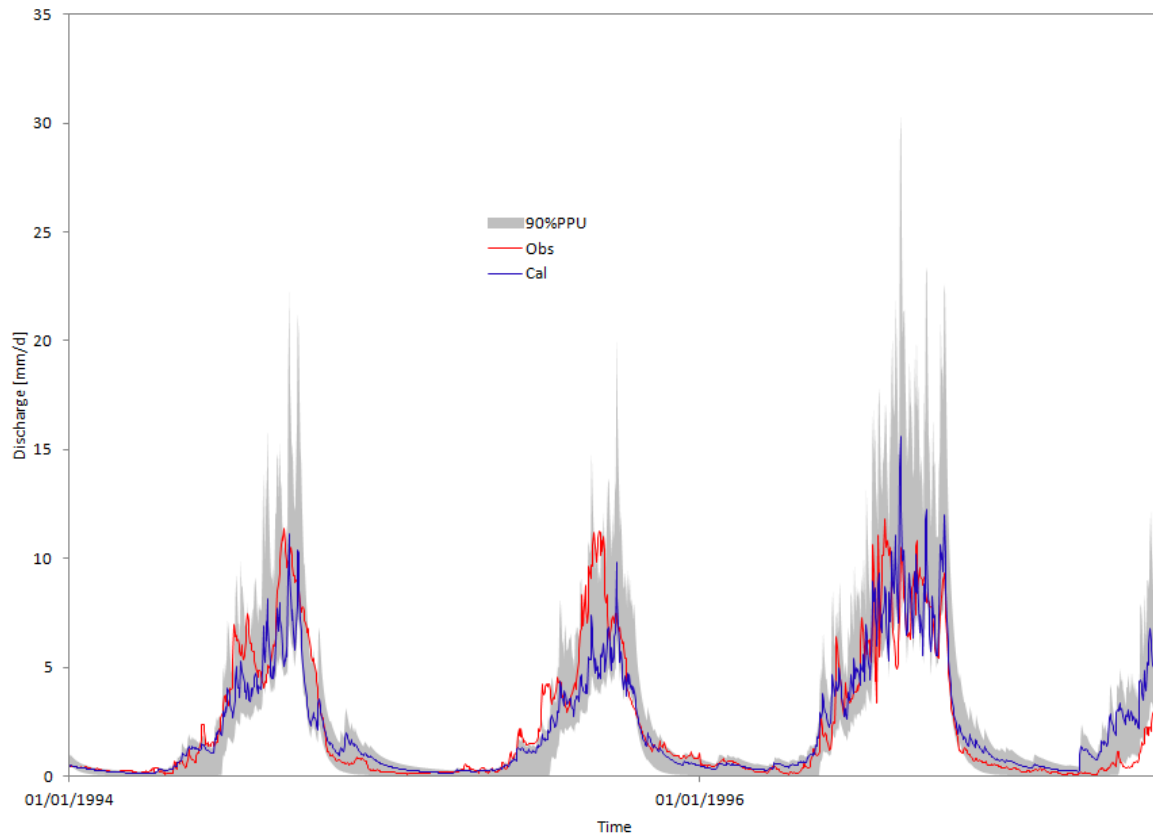


Fig.D- 14: 90% confidence interval of daily runoff due to parameter uncertainty calculated by GLUE method with threshold of 0.6 on Sore catchment (ETHIOPIA), 1 711 km<sup>2</sup>.

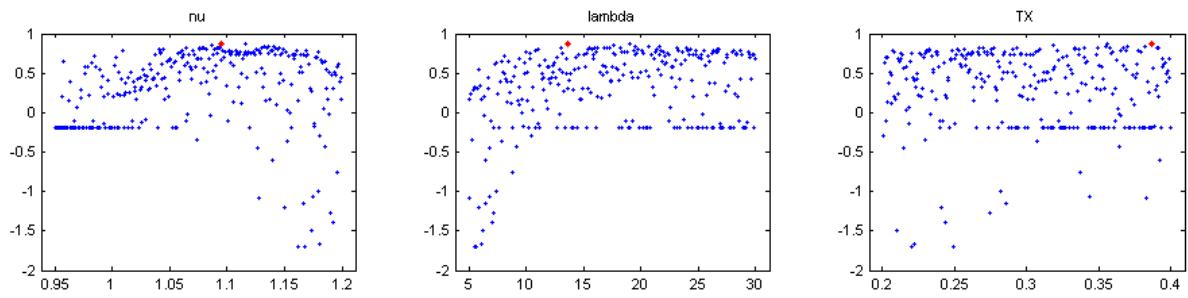


Fig.D- 15: The dotted plot map of the parameters versus Nash criterion for discharge simulation on Barérou catchment (BENIN), 2 134 km<sup>2</sup>.

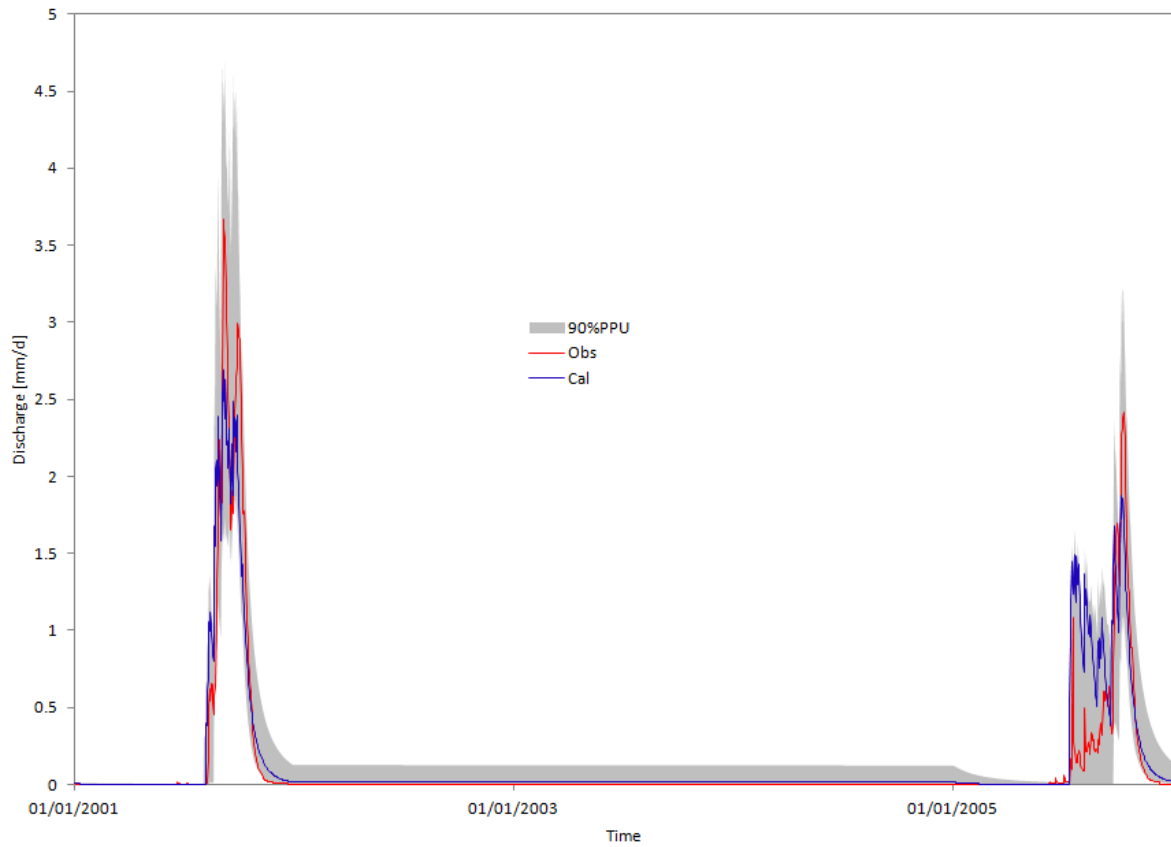


Fig.D- 16: 90% confidence interval of daily runoff due to parameter uncertainty calculated by GLUE method with threshold of 0.6 on Barérou catchment (BENIN), 2 134 km<sup>2</sup>.

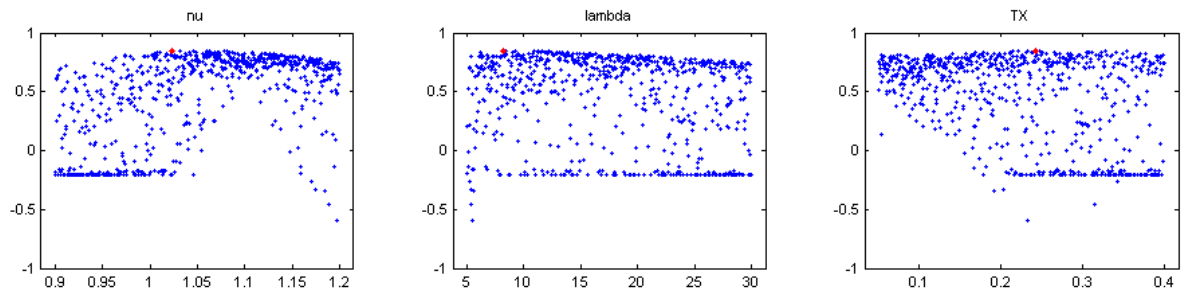


Fig.D- 17: The dotted plot map of the parameters versus Nash criterion for discharge simulation on Cote 238 catchment (BENIN), 3 060 km<sup>2</sup>.

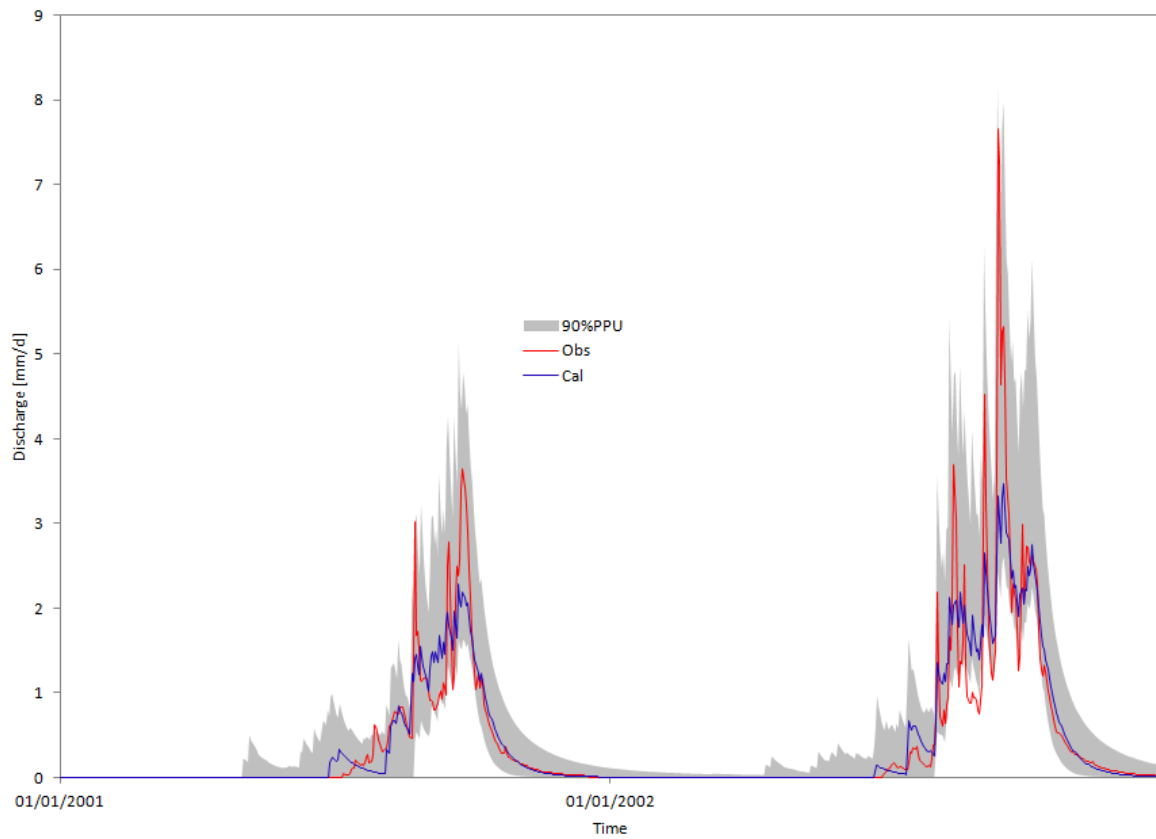


Fig.D- 18: 90% confidence interval of daily runoff due to parameter uncertainty calculated by GLUE method with threshold of 0.6 on Cote 238 catchment (BENIN), 3 060 km<sup>2</sup>.

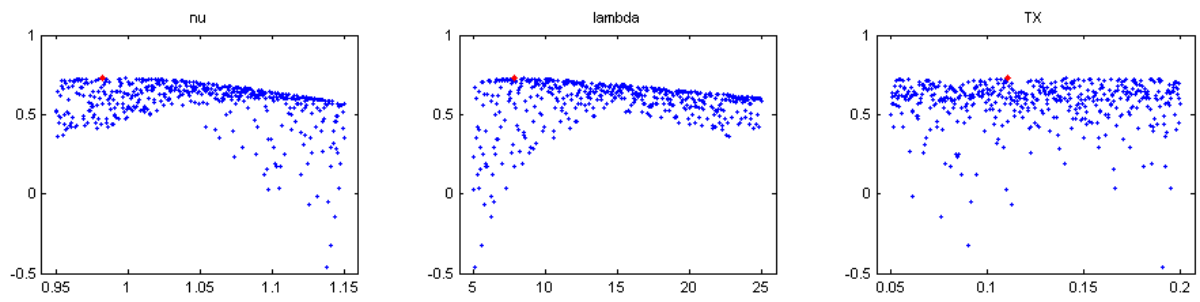
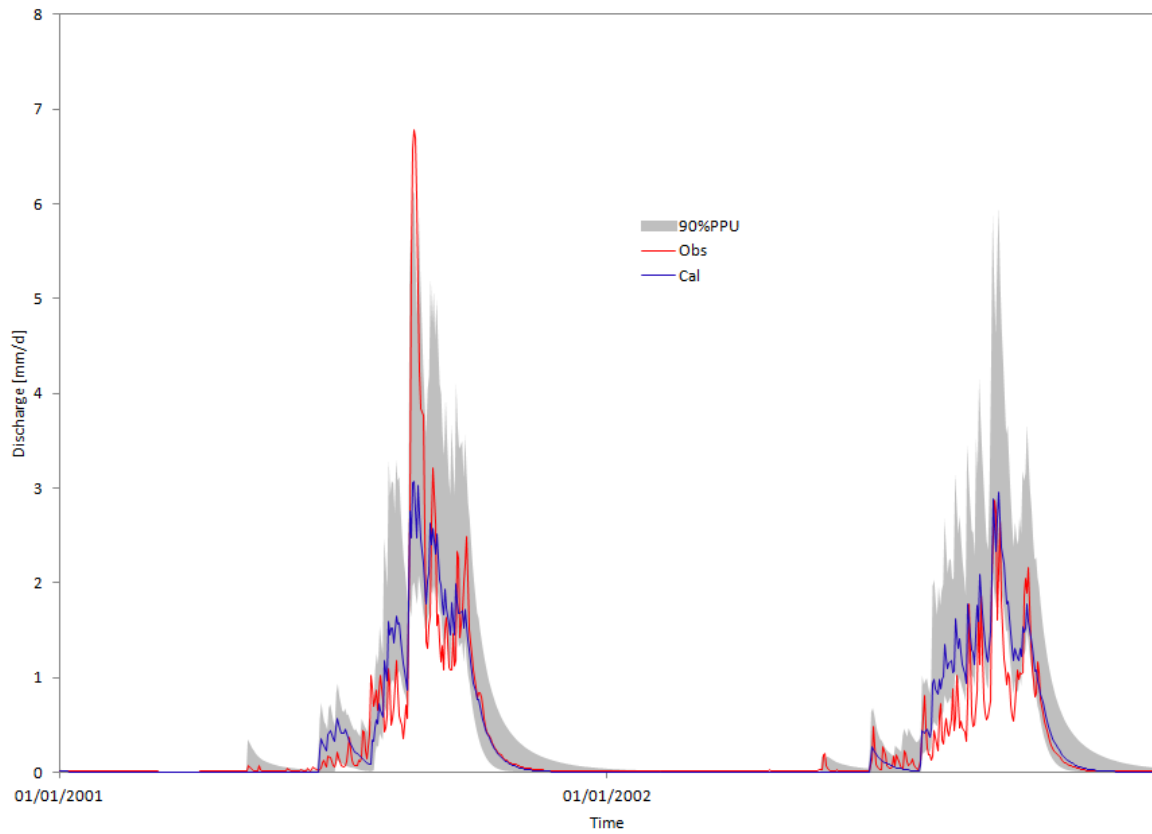


Fig.D- 19: The dotted plot map of the parameters versus Nash criterion for discharge simulation on Aval Sani catchment (BENIN), 3 279 km<sup>2</sup>.



90% confidence interval of daily runoff due to parameter uncertainty calculated by GLUE method with threshold of 0.6 on Aval Sani catchment (BENIN), 3 279 km<sup>2</sup>.

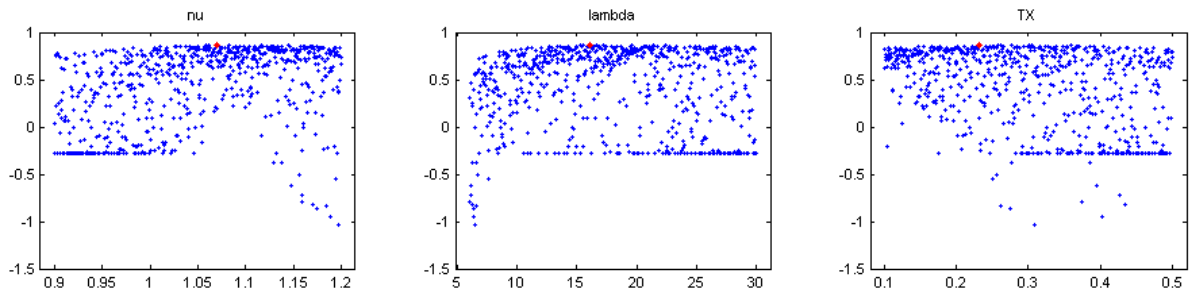


Fig.D- 20: The dotted plot map of the parameters versus Nash criterion for discharge simulation on Savè catchment (BENIN), 23 491 km<sup>2</sup>.

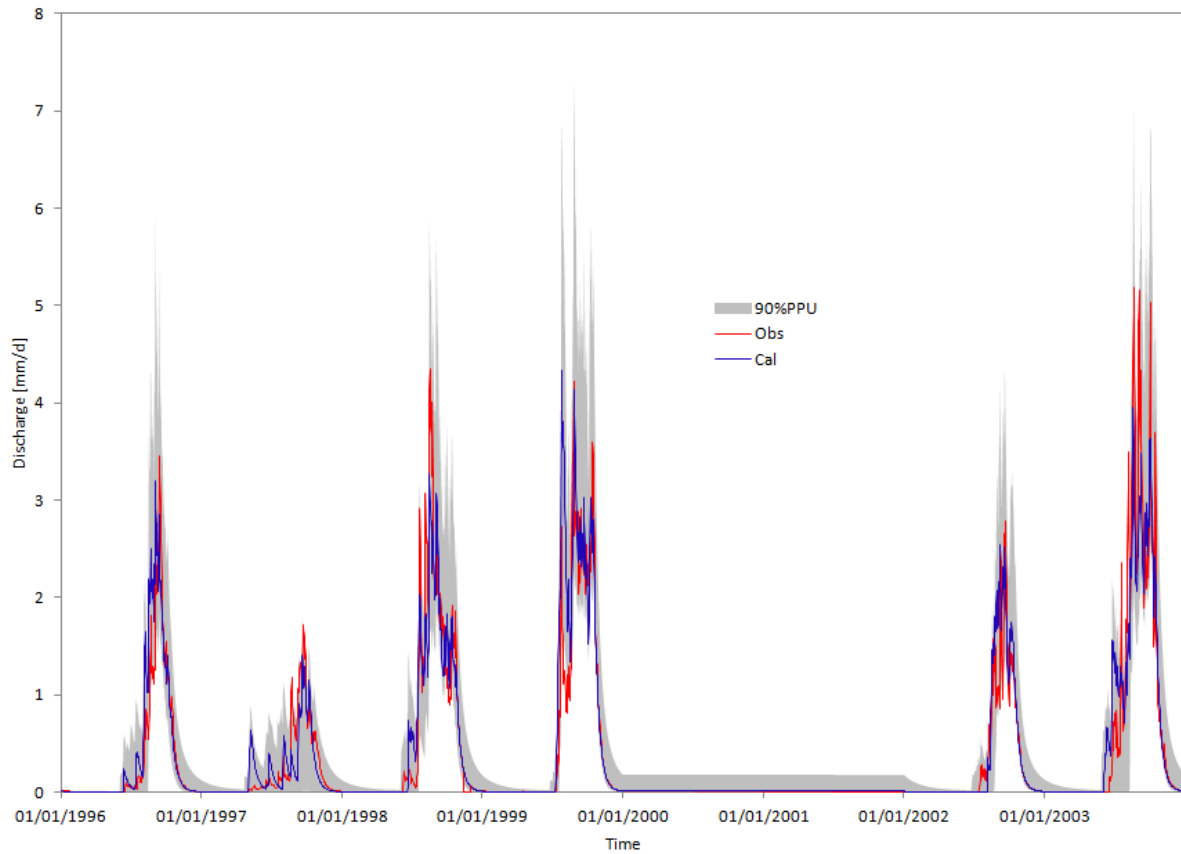


Fig.D- 21: 90% confidence interval of daily runoff due to parameter uncertainty calculated by GLUE method with threshold of 0.6 on Savè catchment (BENIN), 23 491 km<sup>2</sup>.

## PUBLICATIONS

1- The article entitled: “*An Ensemble Approach Modelling to Assess Water Resources in the Mékrou Basin, Benin*” was published on 8th July, 2015.

2- The article entitled: “*Influence of the uncertainties related to the Random Component of Rainfall Inflow in the Ouémé River Basin (Benin, West Africa)*” was published on 15th May, 2015.

3-The article entitled “*Improvement and comparative assessment of a new hydrological modelling approach to catchments in Africa and the USA*” was submitted in May, 2015 to the **Hydrological Sciences Journal**.

**PUBLICATION 1**

**PUBLICATION 2**

**ARTICLE SUBMITTED TO THE *HYDROLOGICAL SCIENCES*  
*JOURNAL***

